NOTICE

AVIS

Canada

UNIVERSITY OF ALBERTA

FRAME METHODS FOR ANALYSIS OF REINFORCED CONCRETE
TWO-WAY SLABS

BY

MICHAEL N. MULENGA　　　　Ⓒ

A Thesis submitted to the Faculty of Graduate Studies and Research
in partial fulfillment of the requirements for the degree of DOCTOR
OF PHILOSOPHY

IN

STRUCTURAL ENGINEERING

DEPARTMENT OF CIVIL ENGINEERING

EDMONTON, ALBERTA

SPRING 1993

The author has granted an irrevocable non-exclusive licence allowing the National Library of Canada to reproduce, loan, distribute or sell copies of his/her thesis by any means and in any form or format, making this thesis available to interested persons.

L'auteur a accordé une licence irrévocable et non exclusive permettant à la Bibliothèque nationale du Canada de reproduire, prêter, distribuer ou vendre des copies de sa thèse de quelque manière et sous quelque forme que ce soit pour mettre des exemplaires de cette thèse à la disposition des personnes intéressées.

The author retains ownership of the copyright in his/her thesis. Neither the thesis nor substantial extracts from it may be printed or otherwise reproduced without his/her permission.

L'auteur conserve la propriété du droit d'auteur qui protège sa thèse. Ni la thèse ni des extraits substantiels de celle-ci ne doivent être imprimés ou autrement reproduits sans son autorisation.

Canada

UNIVERSITY OF ALBERTA

RELEASE FORM

NAME OF AUTHOR: MICHAEL N. MULENGA

TITLE OF THESIS: FRAME METHODS FOR ANALYSIS OF

REINFORCED CONCRETE TWO-WAY SLABS

DEGREE: DOCTOR OF PHILOSOPHY

YEAR THIS DEGREE GRANTED: SPRING 1993

PERMANENT ADDRESS

Dept of Civil Engineering

University of Zambia

P.O Box 32379

Lusaka , ZAMBIA
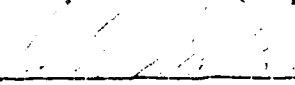
Date: ____Dec   17 , 1992____

THE UNIVERSITY OF ALBERTA
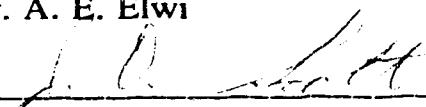
FACULTY OF GRADUATE STUDIES AND RESEARCH

The undersigned certify that they have read, and recommend to the Faculty of Graduate Studies and Research for acceptance, a thesis entitled FRAME METHODS FOR ANALYSIS OF REINFORCED CONCRETE TWO-WAY SLABS submitted by MICHAEL N. MULENGA in partial fulfillment of the requirements for the degree of DOCTOR OF PHILOSOPHY in STRUCTURAL ENGINEERING.

_____
Dr. S. H. Sjmmonds (Supervisor)

_____
Dr. J. G. MacGregor

_____
Dr. A. E. Elwi

_____
Dr. J. D. Scott

_____
Dr. M. G. Faulkner

_____
Dr. R. E. Loov (External Examiner)

DATE: December 16, 1992

DEDICATION

To my wife, Lumba; son, Mwimba and daughter, Mutinta, for
making it all worthwhile.

ABSTRACT

Present North American codes contain two simplified design procedures for regular two-way slab systems subjected to gravity loading. It is shown that these two methods may give significantly different design moments for some geometries. These code procedures are evaluated by using a non-linear finite element analysis program, NISA80. The effects of geometry, reinforcement densities and layout on the behaviour of slabs without beams is addressed. New recommendations for the transverse distribution of design moments at critical sections for these slabs are presented.

It is shown that the code procedures can be replaced with an analysis utilizing a standard elastic plane frame program, using direct stiffness formulation and prismatic members. Approximate stiffnesses for the members in such an analysis are presented.

ACKNOWLEDGEMENT

Table of contents

List of Tables

List of figures

List of symbols

α	Beam to slab stiffness ratio for use in determining I_{eff}
a	Depth of the Whitney's rectangular compression stress block
α_1	Beam to slab stiffness ratio in the longitudinal direction
α_2	Beam to slab stiffness ratio in the transverse direction
A_c	Gross concrete cross sectional area for columns
α_c	Ratio of column stiffness below the slab to the sum of flexural stiffnesses of the design strip
A_{cef}	Effective concrete area
α_{cs}	Column to slab stiffness ratio
α_{ec}	Ratio of column stiffnesses above and below the slab to the sum of flexural stiffnesses of the slab and beam
A_g	Gross concrete cross sectional area for slabs
A_s	Area of reinforcement in the tension zone
β_t	Factor for modification of lateral distribution of moments
c_1	Column dimension in the longitudinal direction
c_2	Column dimension in the transverse direction
d	Effective depth to tension reinforcement in the slab
$\Delta\varepsilon$	Incremental strain
ΔM	Difference between centreline and design moment at the exterior support
$\Delta\sigma$	Incremental stress
E'_s	Tangent modulus of reinforcement after yield
E_B	Tangent modulus in direction parallel to crack
E_c	Initial tangent modulus of concrete

ε_{co}	Strain at peak compressive stress for concrete
E_{col}	Young's modulus of concrete in columns
ε_{cr}	Strain at cracking for concrete
ε_{μ}	Strain at end of first slope in the tri-linear concrete curve
ε_{max}	Maximum strain for concrete in tension
E_s	Young's modulus of reinforcement
e_{sc}	Eccentricity of the critical section from column centreline
E_{sec}	$\sigma_{cu}/\varepsilon_{cu}$=ultimate strength/ultimate strain
E_{slb}	Young's modulus of concrete in the slab
f'_c	Cylinder compressive strength of concrete, at 28 days
f'_t	Tensile strength of concrete
f_{cR}	Cracking stress in concrete
f_{so}	Concrete stress due to tension softening
f_{sT}	Average tensile stress across crack after cracking
γ	Ratio of effective to gross moment of inertia of columns
γ_f	Fraction of total unbalanced moment assigned to flexure
G_f	Cracking energy in concrete
G_o	Initial shear modulus of concrete, $E_c/2(1+\nu_o)$
γ_v	Fraction of total unbalanced moment assigned to eccentricity of shear
h	Slab thickness
I_{eff}	Effective moment of inertia of a column for use in the PEFM
I_g	Gross moment of inertia of a column
K	A constant based on experimental study used in computing G_f
K_b	Prismatic beam stiffness
K_{ec}	Equivalent column stiffness as computed for the EFM
K_s	Prismatic slab stiffness

K_{sb}	Slab-beam stiffness as computed for the EFM
K_t	Torsional member stiffness as computed for the EFM
l'_{col}	Column length, from slab centreline to inflection point
l_1	Longitudinal centre to centre span length of a panel
l_2	Width of a design strip
λ_m	Load factor
l_n	Clear span in a design strip
l_t	Length of the torsional member
μ	A factor for stress level at which slopes change in the tri-linear stress-strain curve
M'_u	Ultimate negative moment capacity of a section
M_1	Design Moment at the exterior support
M_2	Design Moment at midspan of the exterior span
M_3	Design Moment at the interior support of the exterior span
M_{cl}	Moment at the centroid of the exterior column
M_{des}	Design moment at the face of the column support
M_e	Design moment at the exterior support (Section 1)
M_e^+	Positive design moment in the exterior span (Section 2)
M_i	Design moment at the first interior support (Section 3)
M_o	Total static moment for a design strip
M_u	Ultimate positive moment capacity of a section
N	Number (odd) of integration points over the slab depth
v_o	Initial Poisson's ratio
r, s, t	Local axes of an element
R_ε	Ratio of strain to the ultimate strain ($\varepsilon/\varepsilon_{cu}$)
σ_A	Maximum principal stress (negative)
σ_B	Minimum principal stress (negative)

σ_{cu} Ultimate strength from the failure envelope, for concrete

ΣK_c Sum of top and bottom column stiffnesses for a joint

V Reaction at the end of each slab-beam member (No moment gradient)

V' Reaction at the end of each slab-beam member

W_f Factored load on a slab

W_u Ultimate load capacity of the slab

Chapter 1

Introduction

1.1 General Background

Two-way reinforced concrete slab systems are three-dimensional structures consisting of a continuous structural slab reinforced to resist flexure in two or more directions and supporting walls or columns. Frequently, the structural slab is stiffened with either beams spanning between columns or the addition of drop panels or column capitals. Live loading may be applied over the entire slab surface or only over portions of the surface (pattern loading). Furthermore, cracking of the concrete with increasing load and time dependent effects such as creep and shrinkage, even under service loading, cause the stiffness of the different elements of the slab system to change, resulting in a non-linear response. Thus, an exact analysis of reinforced concrete slab systems is not practical.

On the other hand, two-way reinforced concrete slabs are generally lightly reinforced so that sections are highly ductile. Since such slabs are also highly statically indeterminate, this ductility permits a considerable amount of moment redistribution. Therefore, it may be argued that an exact determination of the moment field for selection of flexural reinforcement for strength is not necessary. However, the distribution of the flexural reinforcement selected will affect the distribution of cracking of the concrete which will directly affect the nature of the moment

redistribution, the load-deflection response and hence the overall serviceability of the slab. Furthermore, the moment fields for flexural reinforcement are also used to determine the moment transfer between the slab and supports, a condition that may govern the design of slabs without beams. For these reasons, an examination of possible moment fields and their effect on the behaviour of slab systems is warranted.

In practice, many slab systems consist of a continuous slab supported on columns arranged in more or less straight lines to form essentially rectangular panels. Live loads may be considered uniformly distributed over the surface area. Such regular slab systems have been successfully designed by dividing the structure in each direction into strips or frames centered on the column lines and bounded laterally by the centrelines of panels on each side. These strips or frames are then analyzed as two-dimensional structures for the purpose of determining bending moments at critical sections, located at either midspans or at faces of supports. Moments derived from this analysis are then distributed laterally across the strip in accordance with preset rules. These moments are also used to determine the magnitude of the unbalanced moment that must be transferred between the slab and the supporting columns. In this manner, the complex three-dimensional analysis of reinforced concrete slab systems is simplified considerably to that of a two-dimensional frame.

It is this simplified approach for the design of regular slab systems that forms the basis for the Direct Design Method (DDM) and the Equivalent Frame Method (EFM) that are the two analytical

methods contained in North American design codes (A23.3-M84, ACI 318-89).

These methods are based primarily on experience, supplemented by elastic analyses and laboratory tests of a limited number of slab geometries. The development of these procedures predates widespread availability of digital computers and the ability to perform non-linear analyses of such complex structures.

Application of the EFM is sufficiently time consuming that it is impractical as a hand solution even when using approximate tabulated distribution parameters. For many slab geometries, the DDM and the EFM do not give the same results. In an attempt to simplify the DDM further, new rules were developed to determine the unbalanced moment at exterior supports. For slabs without beams, the magnitude of the unbalanced moment at the exterior support for determining shear capacity based on these rules does not always lead to reasonable results.

Developments in the field of non-linear finite element techniques permit a new evaluation of these methods and an examination of the feasibility of supplementing or replacing them with a procedure that uses any of the multitude of two-dimensional elastic frame analysis programs that are now available.

1.2   Objectives and scope

The main purpose of this study is to develop a more simple but realistic procedure of analysis and design of regular reinforced concrete two-way slab systems subjected to static gravity loading. Specific objectives are:

(a)   To evaluate the valid and limitations of the DDM and EFM for predicting desig oment fields.

(b)   To examine the possibility of replacing these methods with a two-dimensional elastic frame analysis, using prismatic members with appropriate stiffnesses.

To evaluate the DDM and the EFM, solutions obtained using these methods, for a limited number of slab geometries, are compared to solutions obtained using the non-linear finite element program, NISA80. The possibility of using a standard elastic frame analysis with appropriate stiffnesses is evaluated by comparing design moments obtained using standard elastic plane frame analysis to those obtained using the finite element procedure and existing code procedures.

1.3   Outline of Thesis

Chapter 2 contains a description of the code procedures, DDM and EFM, and their limitations. Solutions obtained using these procedures are compared in Chapter 3, for a limited number of slab geometries. The finite element program, NISA80, is described in Chapter 4. Solutions obtained using this program are discussed in Chapter 5. Chapter 6 contains a comparison of solutions obtained using the code procedures (DDM and EFM) to those obtained using NISA80. Recommendations on the stiffness factors for use in the Prismatic Equivalent Frame Method (PEFM), solutions obtained using this procedure and comparisons with the code procedures and

NISA80 (for slabs without beams) are presented in Chapter 7. A summary of the major conclusions and recommendations is given in Chapter 8.

Chapter 2

Simplified Methods of Analysis

2.1 Introduction

The provisions for the design of continuous two-way slab systems are essentially identical in both North American building codes (A23.3, Canada; ACI 318, USA). Both codes indicate that the analysis of continuous two-way slab systems may be based on any procedure that satisfies equilibrium and geometric compatibility with the supports. The design must ensure that the design strength at each section be equal to or greater than that required by the factored loading and that specified serviceability requirements are met. No other details or guidelines are given for this general condition but the clause is used to justify analyses based on elastic plate theory, numerical approximations such as finite difference and finite element methods and upper and lower bound theorems of plasticity.

In contrast, for the case of regular continuous slab systems, when analysis can be represented adequately by use of orthogonal two-dimensional frames and the loading is restricted to uniformly distributed gravity loading, both codes contain the simplified procedures, Direct Design Method (DDM) and Equivalent Frame Method (EFM), each presented in considerable detail.

The DDM is presented as a complete design procedure with sufficient detail to obtain the design moment at each section

7

required to select flexural reinforcement and the unbalanced moments for the design of the slab-column connections. The EFM, on the other hand, presents only a means of assigning stiffnesses to members and the load patterns to be used when analyzing the two-dimensional elastic frame so as to better represent the three-dimensional slab system. For lateral distribution of the resulting moments at critical sections, it refers to the DDM.

At the time the DDM and the EFM were formulated, the only practical method for solving two-dimensional frames was the method of moment distribution. Since the availability of digital computers, the usual procedure for analyzing such structures is the use of matrix structural analysis, generally based on the direct stiffness method. Computer programs using this method for analyzing frames consisting of prismatic members are available to all practising engineers. The design method using such programs will be referred to as the Prismatic Equivalent Frame Method (PEFM). A major objective of this study is to replace the DDM and EFM, for the analysis of plane frames, with a procedure based on the PEFM using appropriate member stiffnesses to approximate the behaviour of continuous three-dimensional slab systems.

2.2 Description of Simplified Methods

Full details of the specified code requirements, explanatory notes and examples of use of DDM and EFM are given in CPCA (1985). Only the essence of the methods is given here for convenience of the reader and to facilitate later discussion.

Although differing significantly in details of calculation, the DDM and the EFM have much in common. Both methods tacitly assume that an adequate analysis can be obtained by modelling the slab system as a series of orthogonal two-dimensional one storey frames, that is, design moments at any part of the slab can be obtained by considering the structure to be made up of a wide beam and supporting columns. This simplified structure is referred to as the design strip. An interior design strip is shown in Fig 2.1, where dimensions in the direction along the strip are designated with subscript 1 and those perpendicular to the direction of the strip with subscript 2.

Both methods define the same critical sections for determining design moments, essentially the face of supports and at each midspan. The clear span or distance between critical sections for negative moments is designated by the subscript n.

For distributing design moments at critical sections laterally across the design strip, both methods make use of column and middle strips. Definitions of column and middle strips, are clearly shown in Fig 2.2.

While an essential part of the DDM, both methods make use a total factored static moment, M_o, that is computed for each span as:

$$M_o = \frac{w_f l_2 l_n^2}{8}$$

(2.1)

When the PEFM is used to analyze the design strip, the above definitions for design strips, critical sections and static moment will be used.

Since all simplified methods use approximate representations of the actual structure, some limitations on the geometry and loading are required. These limitations are examined following presentation of the features unique to each method.

2.2.1 Equivalent Frame Method (EFM)

The EFM considers the slab design strip and columns above and below to be a two-dimensional frame that can be analyzed elastically. The slab design strip between column centrelines is referred to as a slab-beam element. Columns are assumed fixed at their far ends. The stiffness assigned to the columns and slab-beam members are selected to represent the behaviour of the three-dimensional slab system.

As mentioned ea 'er, it was assumed that the analysis of the simplified frame would be performed manually using the moment distribution method. Hence, based on the stiffnesses specified, values for fixed end moments and parameters for determining distribution and carry-over factors can be computed. For computer application, the same parameters can be utilized with a slope-deflection formulation.

For computing these quantities for slab-beam elements, the moment of inertia outside of joints, column capitals or brackets is based on the gross concrete area, taking into account variation in

concrete dimensions that may occur along the axis, say due to drop panels. For the region between the center of the column and the face of the column, bracket or capital, the moment of inertia is taken as the moment of inertia of the slab-beam at the face of the column, bracket or capital, divided by the quantity $(1-c_2/l_2)^2$.

It was realized that in a real slab structure, loading a single panel results in moments in adjacent panels of the design strip even if an infinitely rigid column is provided. That is, rotation of the boundary between adjacent slab panels can occur even when rotation of the column is prevented. This permits moments to leak around the column, a condition that can not be accounted for directly in a two-dimensional analysis. To approximate this condition, an equivalent column with stiffness smaller than that of the actual column is defined. This is accomplished by assuming the equivalent column consists of the actual columns above and below the slab-beam plus an attached torsional member on each side of the column that extends to the edge of the design strip (see Fig 2.3). The torsional member is assumed to have a constant cross section throughout its length. The section to be used is defined in detail in terms of the slab thickness, transverse beam (if any) and effective column width. The flexibility (inverse of stiffness) of the equivalent column is defined as:

$$\frac{1}{K_{ec}} = \frac{1}{\Sigma K_c} + \frac{1}{K_t}$$

(2.2)

When computing K_c, the moment of inertia of a column outside the joint is based on the gross concrete dimensions. The moment of inertia of the column from top to bottom of the slab-beam is assumed to be infinite.

The stiffness of the attached torsional members, K_t, is computed as:

$$K_t = \Sigma \frac{9E_{cs}C}{l_2(1-\frac{c_2}{l_2})^3}$$

(2.3)

where the summation relates to the transverse spans on each side of the column. C is the section parameter evaluated by dividing the cross section into separate rectangular parts and summing, as given in Eqn 2.4:

$$C = \Sigma \left(1 - 0.63\frac{x}{y}\right) \frac{x^3 y}{3}$$

(2.4)

where x is the shorter dimension of a component rectangle and y is the longer dimension. Where beams are provided between supports, as shown in Fig 2.4, K_t defined above is increased by the ratio of the moment of inertia of the slab with the beam to the moment of inertia of the slab without such beam, as given below:

$$K_{ta} = K_t \frac{I_{sb}}{I_s}$$

(2.5)

For a slab-beam member with drop panels at each end, there could be as many as six unique concrete cross sections. Similarly, for a column with a tapered capital there would be three sections with different but constant cross sections and one section with a variable cross section. Theoretically, it is possible to determine values for the fixed end moments, stiffness factors (as defined by moment distribution) and carry-over factors using any of the classical elastic methods, such as the moment-area theorems. For even the most simple slab, a manual determination of these quantities is not practical. Attempts (Misic and Simmonds, 1970), have been made to tabulate approximate values of these quantities in terms of dimensionless ratios which significantly reduces the computational effort involved, but it is still far greater than could be justified in practice. Hence, application of the EFM, as defined in the code, can only be accomplished by a computer program that is written especially to handle non-prismatic members with the cross sections specified.

The EFM considers pattern loading explicitly when the ratio of the factored live load to the factored dead load exceeds 0.75. Loading patterns to obtain maximum moments at various critical sections are specified, however, in no case may the design moments be taken to be less than those for the case of full factored loads on all spans.

When using the EFM, member lengths are defined in terms of the intersections of member centrelines and so the moments computed are at the ends of the members. However, the location of

the critical sections for negative moments for different conditions are specified in detail but, with no provision as to how the moment at the critical section is to be computed.

The procedures used in textbooks (Ferguson et al., 1988; Wang and Salmon, 1979) is to draw a free body diagram of the beam-slab element and to reduce the centreline moment to the critical section by the area under the shear force diagram between these two sections. Using the distance between the member end and the critical section equal to $c_i/2$ and the shear force at the end of the slab-beam member obtained from the EFM solution, considering the difference in end moments in the span, as V', the design moment at the critical section may be expressed as:

$$M_{des} = M_d - \left(V' \frac{c_1}{2} - w_f \frac{l_2 c_1^2}{8} \right)$$ (2.6)

For normal column sizes, V' is less than V (neglecting the difference in end moments), but the maximum difference is of the order of 5%. Use of V instead of V' implies more reduction in moment at the exterior support. The procedure of Eqn 2.6 will be referred to as the equilibrium method for the rest of the study.

However, Corley and Jirsa (1970), in the code background paper to the ACI, on the Equivalent Frame Method, used a simplified equation, by neglecting the second term in the reduction, as follows:

$$M_{des} = M_d - V \cdot \frac{c_1}{2}$$
(2.7)

For small column sizes, the differences in the design moments obtained using Eqn 2.7 compared to Eqn 2.6 is small.

2.2.2 Direct Design Method (DDM)

The complexity of the EFM precludes its use as a manual procedure for the design of slab systems. However, it was realized that many slab geometries encountered in practice could be analyzed very simply and quickly with only a minimal amount of manual computation. This is the purpose of the DDM.

For each span of the design strip, the factored static moment, M_o, given by Eqn 2.1, is computed. Fractions of this moment are assigned to the various critical sections in that span. At each critical section, the design moment is proportioned between the column and the two half middle strips on either side for an interior design strip.

For interior spans, 65% of M_o is assigned to the negative moment at critical sections located at faces of the supports and 35% to the positive moment at midspans. For exterior spans, the portion of M_o depends on the degree of fixity at the exterior support.

While the EFM is unchanged since its introduction, the DDM has undergone a series of changes. Simmonds (1962) showed that moments in exterior panels are sensitive to the flexural stiffness of

the exterior columns. Initially, the DDM (ACI, Feb., 1970) used a set of coefficients for determining the design moments in interior spans and expressions involving the parameter α_c for moments in exterior spans, where α_c is the ratio of the sum of flexural stiffnesses of exterior columns below the slab, to the flexural stiffness of the design strip. During the period of discussion of the code revisions, Gamble (1970) suggested expressions for moments in exterior spans be in terms of α_{ec} (defined in Eqn 2.8) which were adopted by ACI 318-71 and A23.3-73. However, manual computation of α_{ec} is tedious which resulted in the replacement of expressions for moment in exterior panels by a table of coefficients (ACI 318-77; A23.3-M84). In this study, the term DDM is used generically when a distinction between versions is not required. When referring to the 1971 version that utilizes α_{ec}, the term DDM' is used while the version involving the table of coefficients is referred to as DDM-84.

The term α_{ec} is defined as:

$$\alpha_{ec} = \frac{K_{ec}}{(K_s + K_b)} \tag{2.8}$$

where K_{ec} is the stiffness of the equivalent column defined by Eqn 2.2, for the exterior column and, (K_s+K_b) is the stiffness of the slab-beam member in the exterior span. To enable manual computation of these quantities, member stiffnesses are computed

assuming members are prismatic with a cross section equal to that outside the region of the joint or drop panel.

Applying the moment distribution method to the exterior spans and assuming the first interior support does not rotate, results in a balanced moment at the exterior support of $1/(1+1/\alpha_{ec})$ times the fixed end moment for the exterior column. Consistent with the assumed end moment for interior spans, namely 0.65 M_O, this results in a design moment of:

$$M_e = \left(\frac{0.65}{1 + \dfrac{1}{\alpha_{ec}}} \right) M_o \qquad (2.9)$$

Using a similar format, the design moment at the face of the first interior support, with a maximum value of 0.75 M_O when there is no restraint at the exterior column, is given by the expression:

$$M_i = \left(0.75 - \frac{0.10}{1 + \dfrac{1}{\alpha_{ec}}} \right) M_o \qquad (2.10)$$

From the total panel moment and these expressions for negative moments, the positive design moment, taken at midspan is:

$$M_e^+ = \left(0.63 - \frac{0.28}{1 + \dfrac{1}{\alpha_{ec}}} \right) M_o \qquad (2.11)$$

These expressions were replaced in 1984 (DDM-84) by Table 2.1.

When the ratio of unfactored dead load to unfactored live load is less than 2.0, pattern loading must be considered by either ensuring that column stiffnesses above and below are greater than specified minima or by increasing positive moments by a factor that is a function of the column stiffnesses provided.

Clauses for the DDM permit modifying the design moment at any critical section by up to 10% as long as the total static moment, M_o, is maintained in each span. For nearly equal spans and loading, the negative moments on opposite faces of an interior column could be adjusted so that they are equal. For purposes of designing the connection for interior columns, a minimum unbalanced moment equal to approximately 85% of the difference in fixed end moments of the adjacent spans obtained by considering dead load on both spans and 50% of live load on the longer span, is specified. When using Table 2.1, the moment to be transferred at an exterior column for slabs without edge beams is specified as the nominal flexural capacity of the reinforcement in the column strip at this location.

2.2.3 Prismatic Equivalent Frame Method (PEFM)

It is proposed that when using the PEFM, the same two-dimensional frame defined for the EFM be used. The only difference is in the determination of the stiffness values.

By assuming all members have constant cross sections over their length (prismatic), based on concrete dimensions of the

member outside of the joint, any prismatic two-dimensional elastic frame program can be used. Consistent with usual slab analysis, axial deformations may be suppressed. To account for leakage of moments around stiff columns, the stiffness of the column can be modified by a factor thereby eliminating the need to attach torsional members. The determination of this factor and the validity of the solutions is the major objective of this study.

2.3 Limitations for use of Simplified Methods

The most obvious limitation for use of the DDM, EFM or PEFM is that the assumption on which they are based, namely that an adequate analysis can be obtained by considering the three-dimensional slab system as a series of parallel two-dimensional frames, is valid. A second limitation is that, when distributing moments laterally across the design strip, using a set of rules, the geometry not deviate too far from the geometry on which the rules are based.

Virtually all the laboratory tests and analytical studies on which the DDM and EFM are based were performed on specimens containing square panels and square columns. In most cases, the specimens contained nine panels arranged in three bays by three bays to form a square slab system. While it was understood that the design provisions would also apply to slabs with less regular geometry, it was felt necessary to specify limitations to the geometries for which the recommendations could be used.

The DDM was intended to be very simple to use and so its use is restricted to simple common configurations. The EFM, while more complex in execution, was intended to permit a wider range of application.

The limitations given for the DDM and how they apply to the EFM are now examined. The limitations for use of the DDM as given by A23.3-M84, Clause 13.6 are:

1   There shall be a minimum of three continuous spans in each direction.

2   Panels shall be rectangular with a ratio of longer to shorter span, centre-to-centre of supports within a panel of not greater 2.

3   Successive span lengths centre-to-centre of supports in each direction shall not differ by more than one-third of the longer span.

4   Columns may be offset a maximum of 10% of the span (in the direction of offset) from either axis between centre lines of successive columns.

5   All loads shall be due to gravity only and uniformly distributed over entire panel. The factored live load shall not exceed 3 times the factored dead load.

6   For a panel with beams between supports on all sides, the relative stiffness of beams in two, perpendicular directions $\alpha_1 l_2^2 / \alpha_2 l_1^2$ shall not be less than 0.2 nor greater than 5.0.

7   Moment redistribution, as permitted by clause 8.4, shall not be applied to slab systems designed by the Direct Design Method (see Clause 13.6.7).

Clause 8.4 specifies..."negative moments calculated by elastic analysis at the supports of continuous flexural members for any assumed loading arrangement may each be increased or decreased by not more than (30-50 c/d) per cent, but not more than 20%, and the modified negative moments shall be used for calculation of the moments at sections within the spans". For slab systems, the effective value is 20%.

Limitations 2 and 6 are to ensure two-way behaviour in a panel. Thus, they must be satisfied by all slabs designed as two-way slabs using provisions of Chapter 13 in the design codes. When limitation 2 is not satisfied, slabs with no beams tend to act as one-way slabs in the long direction whereas slabs with beams, even if limitation 6 is satisfied, tend to act as one-way slabs spanning in the short direction. When limitation 6 is not satisfied, one-way behaviour occurs and the slab tends to span perpendicular to the stiffer beams. Obviously, the transition from complete two-way action to one-way action, as the panels become more rectangular, is a gradual one. Hence the values given in limitations 2 and 6 marking the transition from two-way action to one-way action are arbitrary but tend to be generous in defining two-way behaviour.

Limitation 4 is to ensure that the basic assumption that a design based on a series of orthogonal design strips analyzed as two-dimensional frames is adequate. Again this limit is arbitrary but applies to all methods where this assumption is used.

Limitations 1, 3 and 5 are included to ensure that the coefficients for determining moments at the critical sections contained in the DDM are valid. Since the factors considered by these limitations can be considered explicitly by an elastic frame analysis, these limitations do not apply to the EFM or PEFM.

For approximately equal spans, the maximum negative moment at the central support for a two span strip is approximately 25% greater than negative moments at supports when there are more than two spans. Thus, this condition is precluded for the DDM by limitation 1 as the coefficients are based on there being three or more approximately equal spans. This also explains the reason for limitation 3. Similarly, limitation 5 is to ensure that the provisions for pattern loading are adequate. Again the absolute values in these limitations are somewhat arbitrary as the coefficients are based on equal spans and uniform loading on all spans, and become less reliable as the geometry and loading deviates from this condition.

Limitation 7 was not included in the original version and its later inclusion is not clear since it is difficult to argue that the coefficients used in the DDM are equivalent to an elastic frame analysis of continuous flexural members. Furthermore, the DDM specifically states that moments at the critical sections can be

modified by 10% provided the total factored static moment in each span is maintained. The possibility of modifying design moments is not addressed in the EFM. This can be interpreted as either no modification is permitted, an unlikely interpretation, or the general redistribution of moments up to 20% for continuous flexural members analyzed by elastic frame analysis permitted by Clause 8.4 is applicable. Obviously, if the latter interpretation is chosen, there can be very large differences in design moments obtained by different designers for the same slab system when using the EFM.

2.4   Lateral Distribution of Design Moments

Once design moments have been obtained at the critical sections, they are distributed laterally across the design strip. Within the provisions of the DDM, the portion of the design moment at each critical section to be assigned to the column strip is specified. The remainder of the design moment is assigned to the two half middle strips in proportion to their widths. When beams are present, more of the total moment at the critical section is assigned to the column strip. Rules are also given to proportion the column strip moment between the beam and the slab.

The rules for distributing design moments laterally across the design strip were obtained from averaging moments obtained from elastic analyses of square panels using solutions based on finite difference analyses. These rules are certainly reasonable for slabs satisfying all of the limitations given for the use of the DDM.

The EFM permits the same rules to be used if limitation 6 is satisfied. This is curious because, as argued previously, this limitation is required to ensure two-way action and as such is equally applicable for the validity of considering analysis of orthogonal design strips, a basic assumption of the EFM. For consistency, one would expect that limitations 2 and 4 would also need being satisfied. By implication, the EFM would permit the lateral distribution rules to be used if limitations 1, 3 and 5 are not satisfied.

It is also highly questionable whether the rules for uniformly distributed loading would be ar licable if concentrated live loads were considered within the scope of the EFM.

2.5   General Observations

The DDM and EFM contained in the North American building codes for the analysis of regular slab systems are characterized by the depth of detail provided both in the limitations for their use and the means of execution.

European building codes also contain references to simplified methods for regular slab systems but, in contrast, provide very little detailed guidance. While use of elastic analysis of design strips is permitted, nothing approaching the complexity and detail of the EFM is given. This implies that some deviation from the strict limitations or distribution rules for the DDM and EFM are reasonable for some applications based on the designer's experience.

Since 1973, both ACI 318 and A23.3 have contained the clause "For gravity loads, a slab system, including the slab and beams (if any) between supports and supporting columns or walls forming orthogonal frames, may be designed by either the DDM or the EFM". The term "orthogonal frame" is not defined but limitation 4 for the DDM indicates a maximum column offset of 10% of the span (in the direction of the offset) from either axis between centre lines of successive columns. The only restriction for use of the EFM is the term "orthogonal frame".

In this thesis, limitation 4 is taken as the limit in defining orthogonal frames. It is understood that the concept of EFM might be applied for frames not meeting this limitation but it is also understood that when this is done, considerable judgement is required by the designer to arrive at the distribution of final design moments to ensure both strength and serviceability requirements. A discussion of this judgement is outside the scope of this study.

The same limitation for the definition of orthogonal frame will also be used when considering the PEFM.

Table 2.1: Design moment coefficients for the exterior span (DDM-84)*

Case →	1	2	3	4	5
Ratio of M_o	Exterior edge unrestrained	slab with beams between all supports	Slab without beams between interior supports		Exterior edge fully restrained
			Without edge beam	With edge beam	
Interior negative moment	0.75	0.70	0.70	0.70	0.65
Positive moment	0.66	0.59	0.53	0.50	0.35
Exterior negative moment	0	0.16	0.26	0.30	0.65

* From CSA Standard, CAN3-A23.3-M84, Clause 13.6.3.3
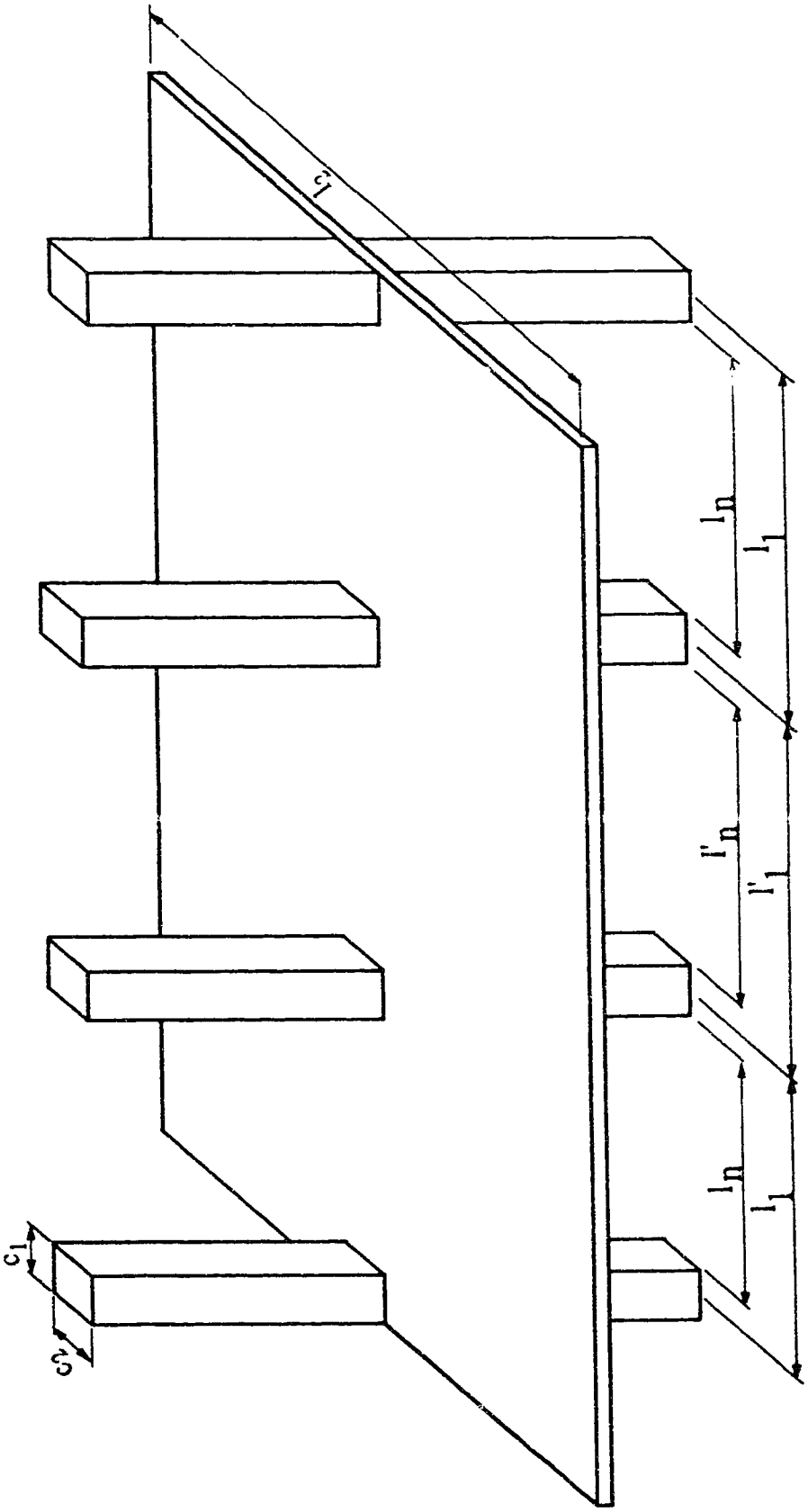
Fig 2.1: Interior design strip
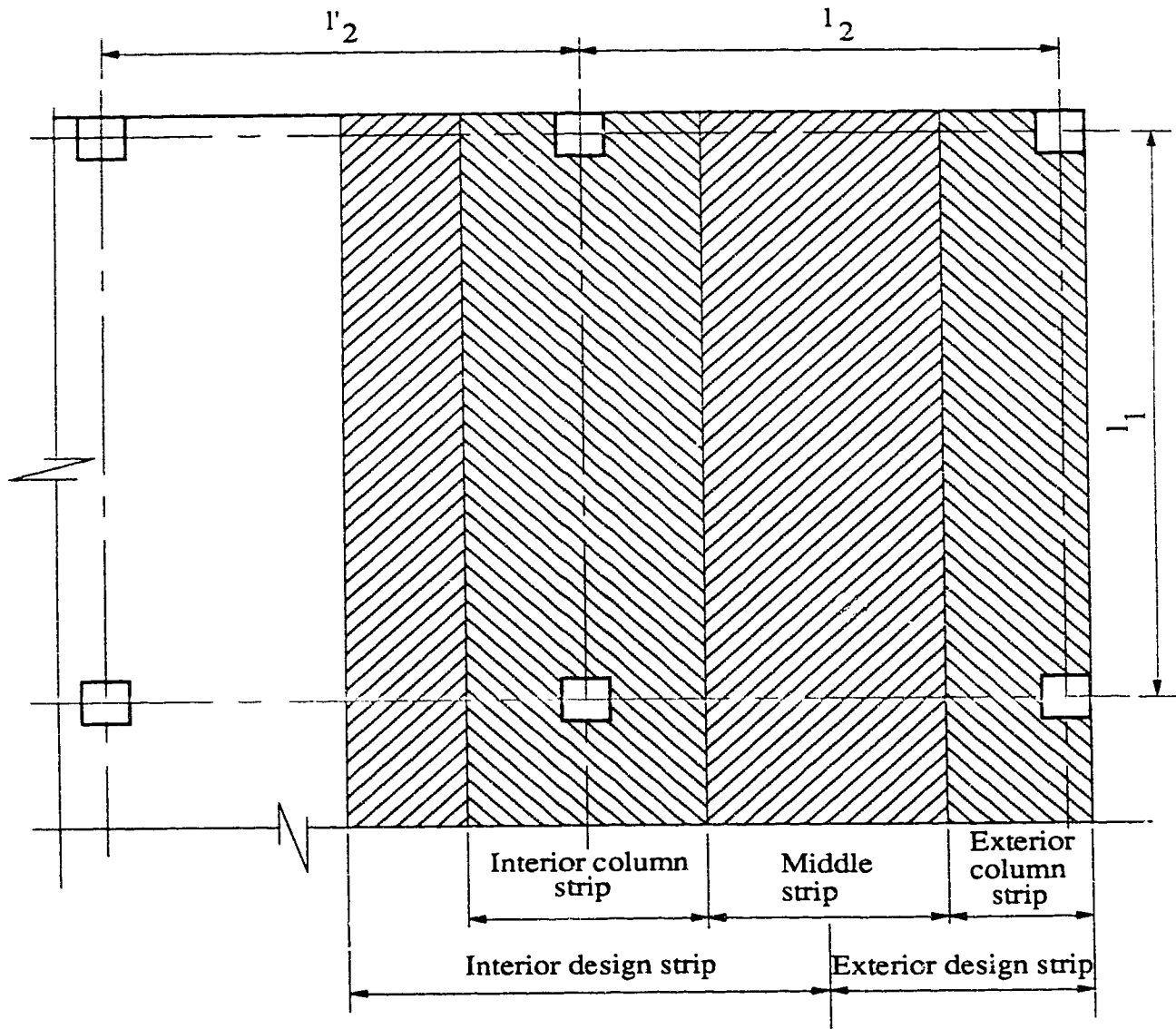
Fig 2.2: Definition of design strips

Slab member (K_s)

Actual Column above (K_{ca})

Attached
Torsional member
(K_t)

Actual Column below
(K_{cb})

Slab member (K_s)
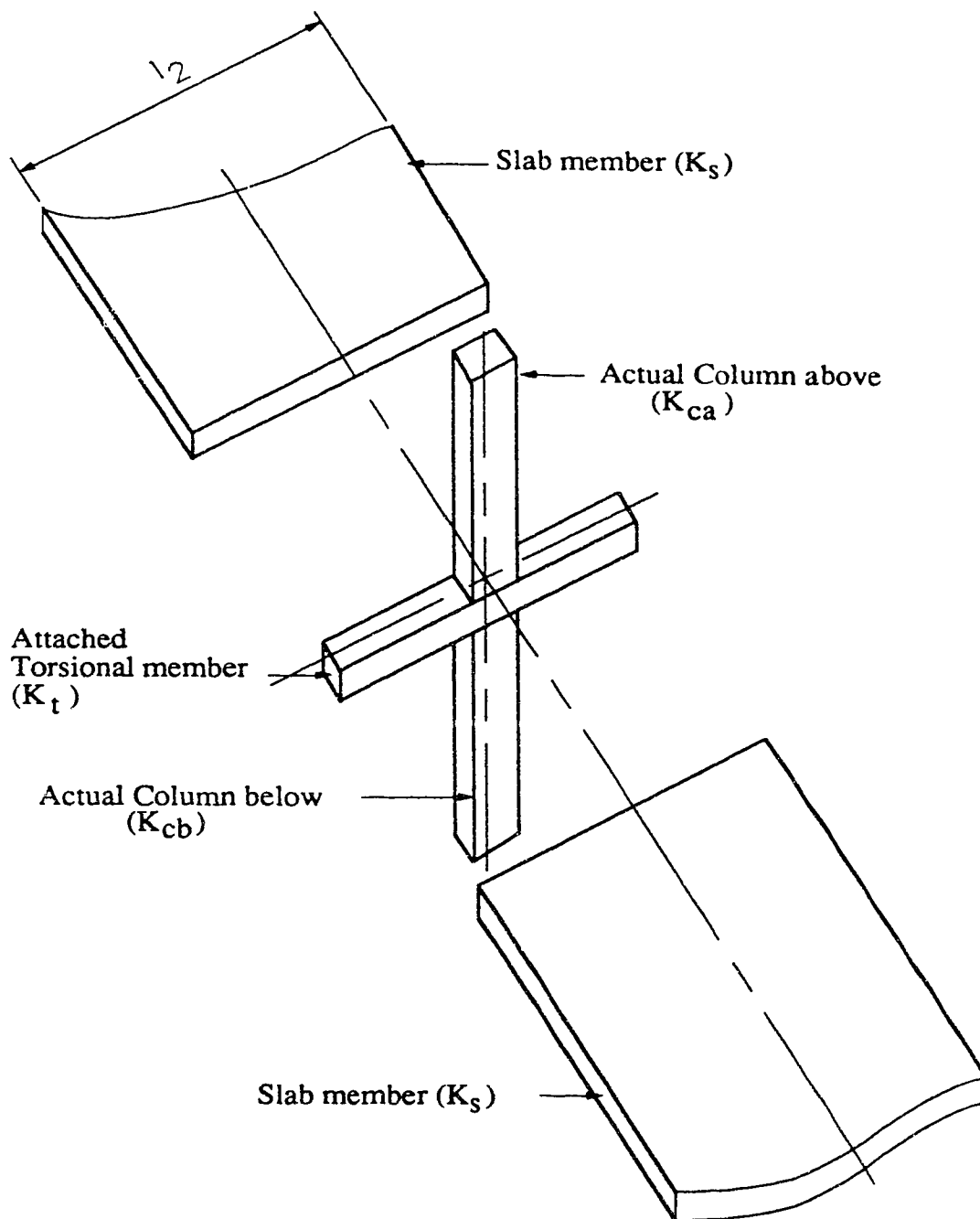
Fig 2.3: Slab-Column Joint (EFM)
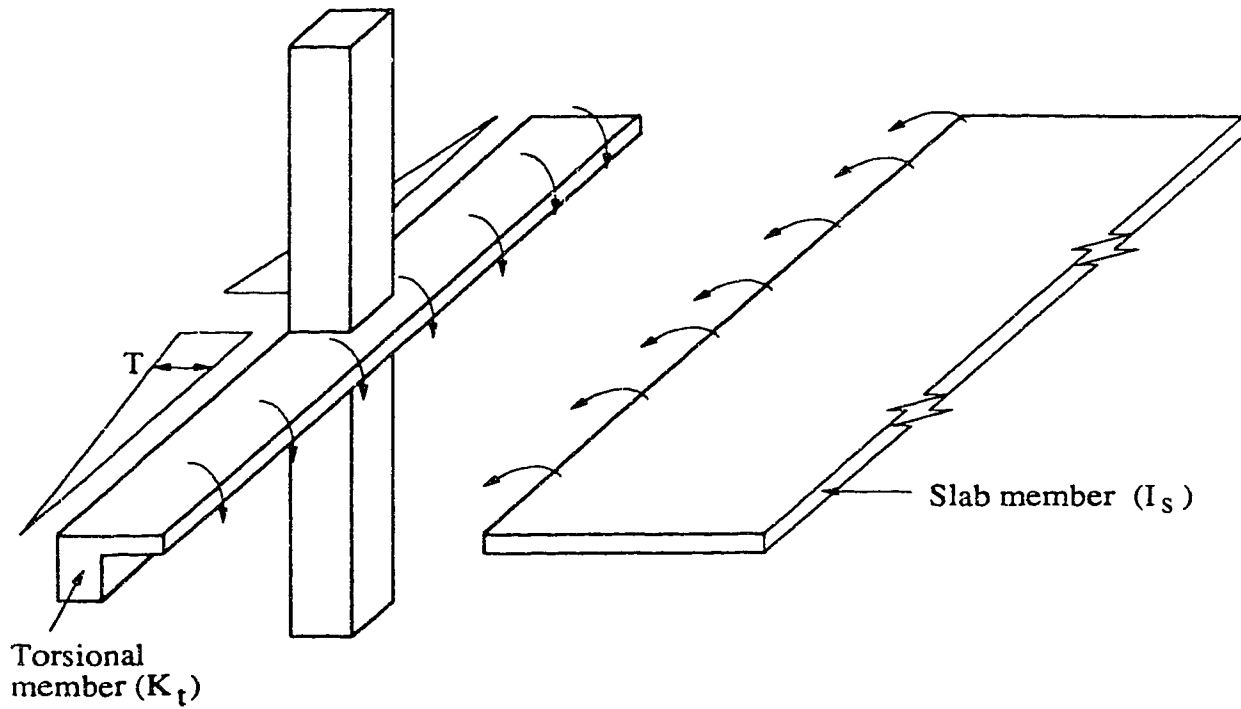
(a) Slab without longitudinal beam

Torsional
member (K_t)

Slab member (I_s)

Slab-beam member (I_{sb})

Torsional
member (K_{ta})
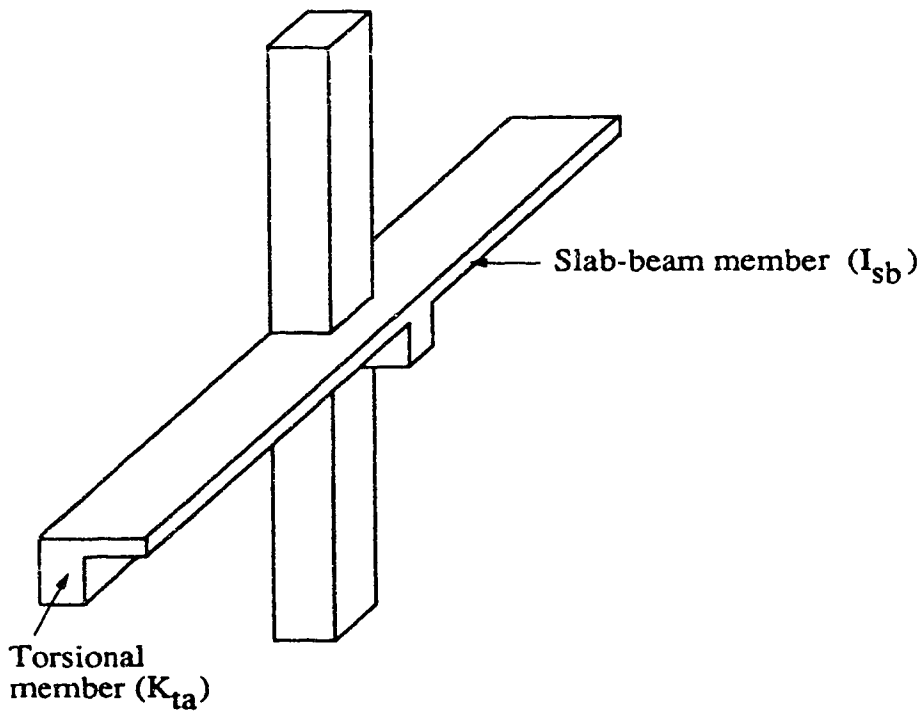
(b) Slab with longitudinal beam

Fig 2.4: Torsional member and restraint at exterior support

Chapter 3

Comparison of DDM and EFM

3.1 Introduction

The Direct Design Method (DDM) and Equivalent Frame Method (EFM) use similar design strips for the analysis of slabs but differ significantly in the manner design moments are obtained at the critical sections. To evaluate the significance of these differences, design moments obtained using each method are compared for a limited number of geometries.

While such comparisons will indicate the magnitude of the differences in solution between the methods, they do not permit a direct evaluation of the accuracy of either method. They will, however, indicate the sensitivity of the methods to changes in geometry which may lead to conclusions regarding limitations to the range of geometry for which their application is valid. Both the DDM and EFM satisfy equilibrium in the sense that, as a minimum, they provide the total factored static moment for each span. Since the methods do not evaluate moment intensities between critical sections, they are upper bound solutions for the slab systems they represent.

Data for the comparisons were obtained using the comput. program, SLAB, written specially for this purpose. This program is described in the next section.

3.2 Program SLAB

Program SLAB is written specifically to implement the provisions of DDM-84, DDM' and EFM as contained in the A23.3 and ACI 318 building codes. The program is written in Fortran 77 and can run on any IBM personal computer or compatible. A description of the input and output is given in Appendix A.

3.2.1 Scope of program

The program is capable of analyzing either an interior or exterior design strip in slabs with or without beams. The number of spans along the design strip is limited to 9. Beams are specified by entering the overall depth and the web width. Drops and column capitals may also be specified.

The program considers only uniformly distributed gravity loading applied over the full panel. The unfactored dead and live loads are input and then factored loading is computed using the load factors associated with the building code specified. Exterior wall loading may be input as an unfactored line load with the corresponding eccentricity of the load from the centreline of the exterior column. The effects of pattern loading are taken into account consistent with the provisions of the design method specified.

To obtain centreline moments and shear forces at the exterior supports, cantilever spans measured from the centreline of the exterior support to the edge of slab are considered. For exterior design strips, transverse cantilevers, in addition to the longitudinal ones, are required.

When analysis by the EFM is carried out, variations in cross sectional properties along the member to be used in determining the stiffness and carry-over factors are considered using the method of column analogy. A slope deflection formulation is used to obtain the unknown joint displacements. These displacements are then used to obtain centreline moments. Centreline moments are reduced to faces of the column supports by considering equilibrium of each span (Eqn 2.6). The resulting moments are also expressed as ratios of the total static moment, M_O, for that span.

At supports without beams, a moment-shear transfer analysis, for each code design procedure, is carried out. Output includes the factored shear force, the unbalanced moment at the centroid of the shear critical area and the component of the total unbalanced moment that is assigned to eccentricity of shear. The component of shear stresses corresponding to uniform shear force and moment transfer are output separately in addition to their sum. The allowable shear stress is also output.

3.3 Geometry and designation of design strips

To compare moments obtained using different methods for frequently encountered slab geometries, solutions were obtained for a typical interior design strip of a typical storey. The slab is of constant thickness, 200 mm, and the panels on either side of the column centrelines have the same transverse spans resulting in the design strip having constant width in all spans. Columns of length 3.5 m exist above and below the slab and are fixed at their ends, as shown in Fig 3.1. When varying the panel aspect ratio, the longer

span in the panel is taken as equal to 7.0 m. These dimensions were considered to be representative for the type of slab systems under consideration.

The definitions for obtaining stiffnesses for use with the EFM, the computation of α_{ec} for use in DDM' and the coefficients in Table 2.1 for DDM-84, are functions of geometry only and are independent of loading. Hence the distribution of moments obtained using the simplified code procedures will not vary because of changes in the magnitude of loading or the dead to live load ratio, except for those conditions when pattern loading governs. For this reason, the primary variables refer to geometry and are column aspect ratio (C), panel aspect ratio (P) and successive span length ratio (S). Other variables are the beam to slab stiffness ratio and dead to live load ratio.

To facilitate discussion, each design strip is designated in terms of the variables, as follows:

<primary identification> <panel aspect ratio or span ratio> <column aspect ratio> <unfactored dead to live load ratio> (<beam to slab stiffness ratio or edge beam width>).

For primary identification, single letters corresponding to the first letter of the primary variables are used except when beams are provided. When beams are provided, PE is used for panels with edge beams and PB for panels with beams between all supports. Panel aspect ratio is defined as l_1/l_2 and span ratio as l_1/l'_1 (Fig 3.2). Column aspect ratio is designated by a letter, as defined in Table 3.1. To eliminate use of decimal points in the designation, all numerical ratios, except beam to slab stiffness ratio, are presented as integers

obtained by multiplying the ratios by 10. Therefore, P10B20 refers to a series where panel aspect ratio is the primary variable, the panel has no beams, the panel is square ($l_1/l_2 = 1.0$), the exterior column is square with dimensions 500 mm by 500 mm, and the unfactored dead to live load ratio is 2.0. PB20B5(1.5) is a design strip where panel aspect ratio is the primary variable, the panel has beams between all supports, a panel aspect ratio of 2.0, has an exterior column of size B, a load ratio of 0.5 and a beam to slab stiffness ratio of 1.5.

The reader should note that when the l_1/l_2 or l_1/l'_1 ratios are 0.75 and 1.33, respectively, the numbers designating panel aspect ratio or span ratio are 7 and 13, respectively. Similarly, a load ratio of 0.33 is designated as 3.

All design strips consist of three spans except the S series, which has five spans (Fig 3.2). For all strips, loading, including pattern loading, is assumed to be uniformly distributed gravity loading and so placed that the design strips are also symmetric about the transverse centreline of the most interior span. This reduces the number of critical sections for which critical moments are reported to 5 and 8, for 3 and 5 span design strips, respectively. Critical sections for a 3 span interior design strip are shown in Fig 3.3.

3.4 Presentation and comparison of results

Design moments for the various series were obtained using the DDM-84, DDM' and EFM. All results are presented without adjustments to moments permitted by the codes. The presentation

and discussion of results are distinquished by the primary variables. For each series, moment ratios for the DDM-84 are included, even though they do not vary, to facilitate comparisons.

3.4.1 Exterior column size and shape (C series).

The purpose of the C series is to evaluate the increase in the design moment at the critical section located at the face of the exterior column (Section 1), due to increase in the exterior column stiffness. Hence the design strips consist of square panels and square interior columns of size B. To change the stiffness of the exterior column, both the area and aspect ratio are varied. Design moments at critical sections are presented as ratios of the total static moment, M_O, for each design strip in Table 3.2. The variation of M_e/M_O at Section 1 is also plotted in Fig 3.4.

It is seen from Table 3.2 that the effect of changing the stiffness of the exterior column has a significant effect only on moments in the exterior span. There is close agreement between design moments in the interior span, obtained for the different design procedures.

When the DDM' is used as the design procedure, moments at the face of the exterior support increase as the stiffness of the exterior support increases (α_{ec} increases), as expected. When the EFM is used, design moments at Section 1 are consistently lower than those obtained for the DDM'. For square columns, the design moments from the EFM are about 80% for smaller size columns and about 75% for the larger ones, compared to moments obtained from the DDM'. However, for a given column size, as the stiffness of the

column is varied by increasing the column aspect ratio. the same increase in design moments is not observed. and for larger column sizes, the design moment actually decreases.

3.4.2 Panel aspect ratio (P series)

Moments obtained at the various critical sections are presented in Table 3.3. It is observed that major differences in the design moments occur in the exterior span. Moments in the interior span are essentially the same. The variation of M_e/M_o with panel aspect ratio is plotted in Fig 3.5. For $l_1/l_2=1.0$, the DDM' gives a moment that is 20% greater. It is seen that as the width of the design strip is reduced (l_1/l_2 increases), the design moment at Section 1 increases for both the DDM' and EFM, but at a slightly lower rate for the DDM' so that when the aspect ratio is equal to 2.0, the difference is approximately 7%. On the other hand, as the width of the design strip is increased from the square panel, while both methods give reduced moments, the rate of change for the EFM is very much greater so that at l_1/l_2 of 0.5, the DDM' gives a moment that is 6.3 times that for the EFM.

At the interior support (Section 3), the DDM' shows reducing support moment as the panel aspect ratio increases whereas the EFM shows reducing moment as the panel departs from the square one. In both cases, however, the change in moment ratio is less than 4% from 0.7.

The coefficient for the design moment at the face of the exterior column used in DDM-84 was obtained as a reasonable lower value for the moment obtained using the EFM, for a number of slab

geometries. Hence, it is not surprising that there is close agreement between DDM-84 and EFM, for strip P10B20 (square panel, square columns and small live load) in Fig 3.5.

In the interior span, there is close agreement between moments given by the different procedures, although the EFM gives slightly lower negative moments and higher positive ones, as the panel geometry departs from the square one.

To evaluate the possible effects of pattern loading, solutions for the P series were also obtained for a load ratio of 0.5 and are also shown in Table 3.3. Pattern load effects may be observed for panel aspect ratios less than 1.0, in the exterior span for the DDM', and the interior for the EFM. For a panel aspect ratio of 0.5, positive moment increases due to pattern loads are 26 and 8% for the DDM' and EFM, respectively.

For square panels with square columns, reducing the dead to live load ratio from 2.0 to 0.33 does not affect the EFM moments.

3.4.3 Panel aspect ratio for slabs with edge beams (PE series)

The purpose of the PE series is to investigate the effect of varying the edge beam size on the design moments. This was accomplished by varying the width of the edge beam stem while maintaining a total depth of beams at 500 mm. Results are presented for a load ratio of 2.0 so that pattern loads do not govern.

Design moments from the three design procedures are presented in Table 3.4. Again major differences are observed in the exterior span, where the EFM consistently gives lower exterior support moments compared to the DDM', especially for panel aspect

ratios less than 1.0. However, as the edge beam size increases, agreement gets better, especially for panel aspect ratios greater than 1.0.

In the interior spans, there is close agreement between the DDM' and the EFM. As the edge beam size increases and panel aspect ratio reduces, the EFM gives lower design moments at the support and higher positive moments. The maximum difference in design moment ratios at Section 1 is about 7%.

3.4.4 Panel aspect ratio for slabs with beams (PB series)

For this series, 500 mm by 500 mm columns (size B) and a constant beam width of 400 mm were chosen. However, beam depths were varied to give beam to slab stiffness ratios ranging from 0.5 to 4.0, as shown in Table 3.5. Beam sizes were the same for both longitudinal and transverse beams. The load ratio was kept at 0.5.

Moment ratios at the critical sections are presented in Table 3.6. Major differences in the design moments between the DDM' and EFM are observed in the exterior span, for panel aspect ratios less than 1.0. Fig 3.6 shows the variation of exterior support moment with panel aspect ratio, for selected beam to slab stiffness ratios. It is observed that the DDM' and EFM give similar moment ratios, for panel aspect ratios greater than 1.0. For panel aspect ratios less than 1.0, agreement in design moments between the DDM' and EFM improves as the beam to slab stiffness ratio increases.

In the interior span, the EFM shows lower negative and higher positive moments, as the panel aspect ratio departs from 1.0, but the differences with the DDM' are generally less than 5%.

Pattern load effects occur for panel aspect ratios less than 1.0, for both procedures. For the DDM', pattern load effect are greater for smaller beam sizes and reduces with increasing beam size. For the EFM, pattern load effects are smaller than for the DDM' and occur for larger beam sizes and a panel aspect ratio of 0.5.

3.4.5 Span ratio for slabs without beams (S series)

The purpose of the S series is to examine the effect of interior column rotation on the design moments. Thus, a flexible column (size B), was selected for both exterior and interior columns. The width of each design strip was maintained at 7.0 m. Load ratios of 2.0 and 0.5 were used. The lower load ratio is used to study the effect of pattern loads on the design moments.

Ratios of the design moments to the total panel static moment for a load ratio of 2.0, when pattern loads need be considered, are presented in Table 3.7a. Similarly, moment ratios for a load ratio of 0.5 (pattern load effect), are presented in Table 3.7b. Some of the design strips considered are outside the successive span limitation specified for the DDM', but are included in the tables for comparison. These strips are marked with an asterisk (*). A negative sign in front of a moment ratio indicates a moment different in sign than is usually associated with that critical section.

From Table 3.7a, it seen that for the case of all panels loaded, there is reasonable agreement between the DDM' and EFM for those

strips that satisfy the successive span limitations for the DDM'. For strips outside this limitation, there is little change in the moment ratios for the DDM' but major changes for the EFM moment ratios. Also, for this case the EFM may give a change in sign for positive moment sections in the short spans, and at the face of the exterior support, for $l_1/l'_1 = 0.5$. Again, there appears to be a greater variation in the moment ratios obtained from various methods for panels aspect ratio less than 1.0.

From Table 3.7b (load ratio of 0.5), major differences between the methods exist even for those strips which satisfy the successive span limitations, when pattern loads are considered. Since some of these differences result in a change in sign, both the minimum and maximum moment ratios at each design section are tabulated for the EFM. For the DDM', moment ratios are tabulated for the exterior span only, although pattern load effects were observed for positive moments at Sections 5 and 8.

The variation of M_e/M_o with span ratio is presented in Fig 3.7. It can be observed that for span ratios greater than about 1.25, the DDM' and EFM exterior support moment remains about 0.32 M_o and, the DDM-84 gives a lower bound to these values, independent of the span ratio. Change in load ratio causes differences in exterior support moments for the EFM only, where for a load ratio of 2.0 and span ratios less than about 0.60, the EFM assigns positive moments at faces of exterior supports. However, for a load ratio of 0.5, considering maximum moments only, a negative moment is obtained.

For all design strips, including those falling within the successive span ratio limitation for the DDM', analyses using the EFM indicate that there is a reversal in sign for moments at some midspans in the shorter spans and for the design moment at the face of the exterior support. Thus, while the geometries for these strips are not extreme, the interpretation of the results from the EFM are not clear. Commercial programs for the design of slab systems, such as ADOSS (1991), that purportedly use the EFM as the basis for determining design moments, do not complete the design, but print a message indicating the reversal in design moment and suggesting the design be completed by hand. It is not clear what this means, unless it implies the use of the DDM'.

3.5   Discussion of differences between DDM' and EFM

The results presented in Section 3.4, show that significant differences in design moments obtained using DDM' and EFM occur primarily in the exterior span when successive spans are equal and in all spans when pattern loads govern. The reasons for these differences is explored in this section. An examination of the code procedures suggests that there are three possibilities for the observed differences:

(a)   The difference in defining the member stiffnesses.

(b)   The DDM' does not utilize a full moment distribution procedure in that only the exterior joint is released.

(c)   Differences in the moment reduction procedures.

The DDM' computes member stiffnesses based on centreline dimensions and assuming members are prismatic while the EFM takes into account the stiffening effect at joints and variations in member cross sections over their lengths. While a value for α_{ec} is generally not computed when using the EFM, the stiffness values required to compute α_{ec} (as defined in DDM') are computed as part of the procedure and so a comparable value of α_{ec} is readily obtained. Comparing corresponding values of α_{ec} provides a convenient means of evaluating differences in stiffness values between the DDM' and EFM. Similarly, a comparison of centreline moments is a convenient means of assessing the partial moment distribution inherent in the DDM'. This requires determining the moment at the member centreline which corresponds to the implicit reduction in moment to the critical section for the DDM'.

For the DDM', the design moment at the exterior support is given by Eqn 2.9, as:

$$M_e = \left(\frac{0.65}{1 + \dfrac{1}{\alpha_{ec}}} \right) M_o$$

(3.1)

Assuming the same c_1 for both exterior and first interior supports, Eqn 3.1 becomes:

$$M_e = \left(\frac{0.65}{1 + \dfrac{1}{\alpha_{ec}}} \right) w_f \frac{(l_1 - c_1)^2 l_2}{8} = \left(\frac{1}{1 + \dfrac{1}{\alpha_{ec}}} \right) w_f \frac{(l_1 - c_1)^2 l_2}{12}$$

(3.2)

By analogy, the centreline moment at the exterior support. M_{cl}, is expressed as:

$$M_{cl} = \left(\frac{1}{1 + \frac{1}{\alpha_{ec}}}\right) M_F \approx \left(\frac{0.667}{1 + \frac{1}{\alpha_{ec}}}\right) M_1 \qquad (3.3)$$

where

$$M_1 = w_f \frac{l_1^2 l_2}{8} \quad \text{and} \quad M_F = 0.667 \, M_1 \qquad (3.4)$$

The ratio of this moment to the centre to centre static moment, M_1, may be expressed as:

$$\frac{M_d}{M_1} = \left(\frac{0.667}{1 + \frac{1}{\alpha_{ec}}}\right) \qquad (3.5)$$

Then, the change in moment between the centreline moment and the design moment, ΔM, is:

$$\Delta M = \left(\frac{1}{1 + \frac{1}{\alpha_{ec}}}\right) \frac{w_f l_2}{12} \left[l_1^2 - (l_1 - c_1)^2\right] \qquad (3.6)$$

or

$$\Delta M = \left(\frac{1}{1 + \frac{1}{\alpha_{ec}}}\right) \left[\frac{V c_1}{3} - \frac{w_f l_2 c_1^2}{12}\right] \qquad (3.7)$$

where $\quad V = w_f \dfrac{l_1 l_2}{2}$ $\qquad\qquad\qquad$ (3.8)

For the EFM, centreline moments are obtained directly from the frame analysis, and may be expressed as ratios of the static moment, M_1. Centreline moments are reduced to design moments by using Eqn 2.6.

The stiffness parameters, the stiffness ratio α_{ec}, the moment ratio M_{cl}/M_1 and the moment reduction ratio, $\Delta M/M_1$, for the DDM' and EFM, at the exterior support, are presented in Tables 3.8 to 3.12. For the DDM', the ratio M_{cl}/M_1 is presented as M_e/M_o instead of using Eqn 3.5, as the difference is only 3%.

For slabs without beams, equal successive span lengths, load ratio of 2.0 (no pattern loads), but with varying exterior column size and aspect ratios, and variable panel aspect ratios, parameters are given in Tables 3.8 and 3.9. For these slabs, differences in the ratio α_{ec} computed for each of the DDM' and EFM is small, generally less than 4%. This would suggest that, for such slabs, consideration of variation in cross-sections when computing stiffnesses can not account for the differences in design moments between the procedures. Similarly, values of the moment ratios M_{cl}/M_1 obtained for the two methods agree closely, usually within 6%, but can be as large as 17% for small values of α_{ec}. Again, considering the assumptions made in obtaining M_{cl} for the DDM', these differences can not account for the observed differences in design moments, which means that the approximation in the moment distribution for the DDM' is valid.

However, the $\Delta M/M_1$ ratios obtained at Section 1 for the EFM are of the order of 180 to 400% of those obtained for the DDM', much greater than the differences in taking V as V'. This difference in ΔM may be responsible for the differences in design moments between the DDM' and the EFM. For all panel aspect ratios, the reductions for the DDM' are essentially constant whereas for the EFM, the reductions decrease significantly, for panel aspect ratios less than 1.0. Similar differences are observed at other critical sections and the differences in $\Delta M/M_1$ correspond to the design moment ratios. For the design strip P5B20, with small l_1/l_2, the design moment for the DDM' is 6.3 times that for the EFM, even though the M_{c1} for the EFM is actually 1.2 times larger. This difference is due to the reduction, which is almost as large as M_{c1} for the EFM.

For slabs with either edge beams or beams between all supports (Tables 3.10 and 3.11), the values of α_{ec} computed for the EFM are larger, accounting for the effects of infinite stiffness over the depth of the beam at the ends of the columns. For beams of usual dimensions, the difference is less than 20% but can be as high as 40% for very stiff beams ($\alpha_1=4.0$). Despite these differences, the ratios of centreline moments are similar, indicating that differences in the moment distribution procedures have little effect. The differences in design moments, as for slabs without beams, can be attributed to the amount of the moment reductions. For the DDM', these are nearly constant for all panel aspect ratio, but for the EFM they are greater, especially for small values of panel aspect ratios.

however, the differences are not as drastic as for slabs without beams.

For the S series, comparisons are presented in Table 3.12, for a load ratio of 2.0 (no pattern loads). Considering the successive span limitation (0.75 to 1.33) for the DDM', the stiffness ratios α_{ec} computed for the two procedures are exactly the same. There is als a reasonable agreement (14 to 16% difference) in centreline moment ratios. For l_1/l'_1 ratios less than 0.75, the exterior beam-slab member gets relatively stiffer compared to the exterior column and the EFM gives much lower centreline moments. Thus, the effect of moment distribution becomes important. The smaller M_{cl} at the exterior support leads to smaller value of V' which, in turn, leads to less reduction in moment for the EFM. For example, with a span ratio of 0.5 and panel aspect ratio of 0.5 (S5B20), the EFM reduction is only 2.3 times the DDM' reduction compared to 4.0 times for design strip P5B20.

For a load ratio of 0.5 and for the case of full factored load on all spans, the centreline moment ratios and reductions are the same as for the load ratio of 2.0, tabulated in Table 3.12. When pattern loads are considered, the EFM results in reversal of sign at some critical sections, as discussed previously, and so centreline and moment reduction ratios are not tabulated.

3.6 Summary

A comparison of design moment ratios obtained using the DDM' and EFM shows that, for spans of equal length in the design strip, large differences in these moments occur primarily in the

exterior span and that the differences increase significantly as the panel aspect ratio, l_1/l_2, is decreased from 1.0. The differences in moment ratios are also dependent, but to a lesser degree, on the size and aspect ratio of the exterior column.

The DDM' computes moments directly at the critical section. To obtain moments at the column centreline requires some assumption. Similarly, the EFM computes moments at the column centreline and requires an assumption to reduce these moments to the critical section. Obtaining centreline moments for the DDM' by using the same proportions of M_1 as used for M_0 at the critical sections results in centreline moments that agree closely with the centreline moments obtained for the EFM. This would indicate that the procedure for reducing the centreline moment for the EFM errs by providing too large a reduction, especially for small l_1/l_2 ratios. On the other hand, had centreline moment for the DDM' been obtained by applying all of the difference between M_1 and M_0 to the negative support moments instead of proportionately, the ΔM for the DDM' would have been much larger, approaching the ΔM obtained for the EFM, but this would also result in larger centreline moments than obtained for the EFM.

The only way to resolve which method gives the better set of design moments is to obtain these moments independently, using a method that realistically models the actual reinforced concrete slab behaviour. Since laboratory testing of a sufficient number of slabs is not feasible, solutions obtained from a non-linear finite element program are used to evaluate the code design procedures. These solutions would also permit an evaluation of the rules for lateral

distribution of the moments at the critical sections. The results obtained from such a study and the evaluation of the code procedures are presented in Chapter 5.

Table 3.1: Column designation and geometric properties

Column Designation	c_1 mm	c_2 mm	c_1/c_2	Area mm^2	Moment of Inertia $mm^4 \times 10^9$
A	354	707	0.50	250000	2.604
B	500	500	1.00	250000	5.208
C	612	408	1.50	250000	7.813
D	707	354	2.00	250000	10.416
E	500	750	0.67	375000	7.813
F	612	612	1.00	375000	11.718
G	750	500	1.50	375000	17.578
H	866	433	2.00	375000	23.437
I	500	1000	0.50	500000	10.416
J	707	707	1.00	500000	20.833
K	866	577	1.50	500000	31.249
L	1000	500	2.00	500000	41.666
M	750	1000	0.75	750000	35.156
N	866	866	1.00	750000	46.873
O	1000	750	1.25	750000	62.500
P	1225	612	2.00	750000	93.750
Q	1000	1000	1.00	1000000	83.333
R	1400	1400	1.00	1960000	320.130

Note: Dimensions of columns computed from pre-selected areas and c_1/c_2 ratios

Table 3.2: Design moment ratios for C series (square panels without beams)

Method	Section 1			Section 2			Section 3			Section 4			Section 5		
	D	D'	E	D	D'	E	D	D'	E	D	D'	E	D	D'	E
A_c=250000 mm^2															
C10A20	0.260	0.242	0.212	0.530	0.526	0.523	0.700	0.713	0.737	0.650	0.650	0.673	0.350	0.350	0.327
C10B20	0.260	0.316	0.263	0.530	0.494	0.504	0.700	0.701	0.728	0.650	0.650	0.663	0.350	0.350	0.337
C10C20	0.260	0.358	0.285	0.530	0.476	0.497	0.700	0.695	0.726	0.650	0.650	0.657	0.350	0.350	0.343
C10D20	0.260	0.386	0.295	0.530	0.464	0.493	0.700	0.691	0.727	0.650	0.650	0.654	0.350	0.350	0.346
A_c=375000 mm^2															
C10E20	0.260	0.344	0.291	0.530	0.482	0.493	0.700	0.697	0.723	0.650	0.650	0.661	0.350	0.350	0.339
C10F20	0.260	0.381	0.307	0.530	0.466	0.487	0.700	0.691	0.722	0.650	0.650	0.656	0.350	0.350	0.344
C10G20	0.260	0.415	0.314	0.530	0.451	0.484	0.700	0.686	0.725	0.650	0.650	0.651	0.350	0.350	0.349
C10H20	0.260	0.438	0.314	0.530	0.441	0.483	0.700	0.683	0.730	0.650	0.650	0.648	0.350	0.350	0.352
A_c=500000 mm^2															
C10I20	0.260	0.368	0.315	0.530	0.472	0.483	0.700	0.693	0.718	0.650	0.650	0.659	0.350	0.350	0.341
C10J20	0.260	0.421	0.328	0.530	0.448	0.478	0.700	0.685	0.723	0.650	0.650	0.652	0.350	0.350	0.348
C10K20	0.260	0.450	0.328	0.530	0.436	0.478	0.700	0.681	0.730	0.650	0.650	0.648	0.350	0.350	0.352
C10L20	0.260	0.470	0.316	0.530	0.428	0.480	0.700	0.678	0.738	0.650	0.650	0.645	0.350	0.350	0.355
A_c=750000 mm^2															
C10M20	0.260	0.456	0.352	0.530	0.434	0.466	0.700	0.680	0.723	0.650	0.650	0.650	0.350	0.350	0.350
C10N20	0.260	0.472	0.343	0.530	0.427	0.468	0.700	0.677	0.730	0.650	0.650	0.647	0.350	0.350	0.353
C10O20	0.260	0.487	0.330	0.530	0.420	0.472	0.700	0.675	0.740	0.650	0.650	0.645	0.350	0.350	0.355
C10P20	0.260	0.507	0.302	0.530	0.411	0.480	0.700	0.672	0.758	0.650	0.650	0.642	0.350	0.350	0.358

													$A_c=1000000$ mm^2		
C10Q20	0.260	0.502	0.343	0.530	0.414	0.464	0.700	0.673	0.742	0.650	0.650	0.646	0.350	0.350	0.354
C10R20	0.260	0.560	0.302	0.530	0.389	0.466	0.700	0.664	0.792	0.650	0.650	0.645	0.350	0.350	0.354

Table 3.3: Design moment ratios for P series (slabs without beams)

	Section 1			Section 2			Section 3			Section 4			Section 5		
Method	D	D'	E	D	D'	E	D	D'	E	D	D'	E	D	D'	E
							Load ratio=2.0								
P5B20	0.260	0.209	0.033	0.530	0.540	0.646	0.700	0.718	0.675	0.650	0.650	0.647	0.350	0.350	0.353
P7B20	0.260	0.270	0.180	0.530	0.514	0.522	0.700	0.708	0.716	0.650	0.650	0.660	0.350	0.350	0.340
P10B20	0.260	0.316	0.263	0.530	0.494	0.504	0.700	0.701	0.728	0.650	0.650	0.663	0.350	0.350	0.337
P13B20	0.260	0.406	0.361	0.530	0.455	0.463	0.700	0.688	0.713	0.650	0.650	0.646	0.350	0.350	0.354
P20B20	0.260	0.510	0.475	0.530	0.411	0.418	0.700	0.672	0.688	0.650	0.650	0.635	0.350	0.350	0.365
							Load ratio=0.5								
P5B5	0.260	0.209	0.033	0.666	0.679	0.646	0.700	0.718	0.675	0.650	0.650	0.647	0.350	0.350	0.381
P7B5	0.260	0.270	0.180	0.646	0.626	0.552	0.700	0.708	0.716	0.650	0.650	0.660	0.350	0.350	0.348
P10B5	0.260	0.316	0.263	0.530	0.494	0.504	0.700	0.701	0.728	0.650	0.650	0.663	0.350	0.350	0.337
P13B5	0.260	0.406	0.361	0.530	0.455	0.463	0.700	0.688	0.713	0.650	0.650	0.646	0.350	0.350	0.354
P20B5	0.260	0.510	0.475	0.530	0.411	0.418	0.700	0.672	0.688	0.650	0.650	0.635	0.350	0.350	0.365
							Load ratio=0.33								
P10B3	0.260	0.316	0.263	0.536	0.499	0.504	0.700	0.701	0.728	0.650	0.650	0.663	0.350	0.354	0.337

Note: Only maximum moments are presented for the EFM at load ratios 0.5 and 0.33

Table 3.4: Design moment ratios for PE series (slabs with edge beams)

Design Strip Procedure	Section 1			Section 2			Section 3			Section 4			Section 5		
	D	D'	E	D	D'	E	D	D'	E	D	D'	E	D	D'	E
PE5B20(200)	0.300	0.252	0.106	0.500	0.522	0.617	0.700	0.711	0.659	0.650	0.650	0.635	0.350	0.350	0.365
PE7B20(200)	0.300	0.316	0.251	0.500	0.494	0.526	0.700	0.701	0.696	0.650	0.650	0.650	0.350	0.350	0.350
PE10B20(200)	0.300	0.363	0.331	0.500	0.474	0.481	0.700	0.694	0.707	0.650	0.650	0.655	0.350	0.350	0.345
PE13B20(200)	0.300	0.444	0.420	0.500	0.439	0.443	0.700	0.682	0.693	0.650	0.650	0.641	0.350	0.350	0.359
PE20B20(200)	0.300	0.531	0.514	0.500	0.401	0.407	0.700	0.668	0.672	0.650	0.650	0.633	0.350	0.350	0.367
PE5B20(300)	0.300	0.332	0.224	0.500	0.487	0.571	0.700	0.699	0.634	0.650	0.650	0.616	0.350	0.350	0.384
PE7B20(300)	0.300	0.397	0.357	0.500	0.459	0.488	0.700	0.689	0.668	0.650	0.650	0.636	0.350	0.350	0.364
PE10B20(300)	0.300	0.440	0.426	0.500	0.441	0.448	0.700	0.682	0.679	0.650	0.650	0.644	0.350	0.350	0.356
PE13B20(300)	0.300	0.500	0.484	0.500	0.415	0.421	0.700	0.673	0.669	0.650	0.650	0.635	0.350	0.350	0.365
PE20B20(300)	0.300	0.559	0.547	0.500	0.389	0.396	0.700	0.664	0.658	0.650	0.650	0.631	0.350	0.350	0.369
PE5B20(400)	0.300	0.374	0.287	0.500	0.469	0.546	0.700	0.692	0.620	0.650	0.650	0.605	0.350	0.350	0.395
PE7B20(400)	0.300	0.436	0.408	0.500	0.442	0.469	0.700	0.683	0.654	0.650	0.650	0.629	0.350	0.350	0.371
PE10B20(400)	0.300	0.475	0.469	0.500	0.425	0.432	0.700	0.677	0.666	0.650	0.650	0.638	0.350	0.350	0.362
PE13B20(400)	0.300	0.523	0.516	0.500	0.405	0.412	0.700	0.670	0.659	0.650	0.650	0.632	0.350	0.350	0.368
PE20B20(400)	0.300	0.570	0.562	0.500	0.384	0.393	0.700	0.662	0.653	0.650	0.650	0.630	0.350	0.350	0.370
PE5B20(500)	0.300	0.394	0.316	0.500	0.460	0.535	0.700	0.689	0.614	0.650	0.650	0.601	0.350	0.350	0.392
PE7B20(500)	0.300	0.453	0.431	0.500	0.435	0.460	0.700	0.680	0.648	0.650	0.650	0.626	0.350	0.350	0.374
PE10B20(500)	0.300	0.490	0.488	0.500	0.419	0.426	0.700	0.675	0.660	0.650	0.650	0.636	0.350	0.350	0.364
PE13B20(500)	0.300	0.532	0.528	0.500	0.401	0.408	0.700	0.668	0.655	0.650	0.650	0.631	0.350	0.350	0.369
PE20B20(500)	0.300	0.574	0.567	0.500	0.383	0.391	0.700	0.662	0.651	0.650	0.650	0.630	0.350	0.350	0.370

Table 3.5 :Cross sectional properties for slabs with beams (PB series)

Design Strip	l_2 (m)	α_1 values for $b_w = 400$ mm						
		0.50 d (mm)	1.00 d (mm)	1.50 d (mm)	2.00 d (mm)	2.50 d (mm)	3.00 d (mm)	4.00 d (mm)
PB5B5(α_1)	7.00	374.0	458.6	516.9	562.8	601.4	635.0	692.1
PB7B5(α_1)	7.00	374.0	458.6	516.9	562.8	601.4	635.0	692.1
PB10B5(α_1)	7.00	374.0	458.6	516.9	562.8	601.4	635.0	692.1
PB13B5(α_1)	5.25	343.5	421.4	475.0	516.9	552.2	582.9	635.0
PB20B5(α_1)	3.50	304.6	374.0	421.3	458.6	489.8	516.9	562.8

Table 3.6: Design moment ratios for PB series (slabs with beams between all supports)

Design Strip Procedure	Section 1			Section 2			Section 3			Section 4			Section 5		
	D	D'	E	D	D'	E	D	D'	E	D	D'	E	D	D'	E
PB5B5 (0.5)	0.160	0.287	0.155	0.757	0.597	0.588	0.700	0.706	0.668	0.650	0.650	0.613	0.412	0.412	0.387
PB7B5 (0.5)	0.160	0.352	0.296	0.742	0.526	0.502	0.700	0.696	0.700	0.650	0.650	0.633	0.385	0.385	0.367
PB10B5 (0.5)	0.160	0.398	0.372	0.604	0.459	0.460	0.700	0.689	0.708	0.650	0.650	0.641	0.358	0.358	0.359
PB13B5 (0.5)	0.160	0.442	0.420	0.590	0.440	0.441	0.700	0.682	0.699	0.650	0.650	0.637	0.350	0.350	0.363
PB20B5 (0.5)	0.160	0.488	0.471	0.590	0.420	0.420	0.700	0.675	0.689	0.650	0.650	0.636	0.350	0.350	0.364
PB5B5 (1.0)	0.160	0.294	0.175	0.649	0.613	0.580	0.700	0.705	0.666	0.650	0.650	0.609	0.426	0.426	0.391
PB7B5 (1.0)	0.160	0.360	0.313	0.590	0.551	0.495	0.700	0.695	0.697	0.650	0.650	0.630	0.406	0.406	0.370
PB10B5 (1.0)	0.160	0.405	0.387	0.590	0.456	0.454	0.700	0.688	0.704	0.650	0.650	0.639	0.350	0.350	0.361
PB13B5 (1.0)	0.160	0.451	0.437	0.590	0.436	0.435	0.700	0.681	0.694	0.650	0.650	0.635	0.350	0.350	0.365
PB20B5 (1.0)	0.160	0.507	0.496	0.590	0.412	0.411	0.700	0.672	0.681	0.650	0.650	0.633	0.350	0.350	0.367
PB5B5 (1.5)	0.160	0.276	0.161	0.677	0.586	0.586	0.700	0.708	0.667	0.650	0.650	0.612	0.402	0.402	0.388
PB7B5 (1.5)	0.160	0.342	0.301	0.622	0.509	0.500	0.700	0.697	0.699	0.650	0.650	0.633	0.369	0.369	0.363
PB10B5 (1.5)	0.160	0.388	0.376	0.590	0.463	0.458	0.700	0.690	0.707	0.650	0.650	0.641	0.350	0.350	0.359
PB13B5 (1.5)	0.160	0.435	0.425	0.590	0.443	0.439	0.700	0.683	0.697	0.650	0.650	0.636	0.350	0.350	0.364
PB20B5 (1.5)	0.160	0.493	0.485	0.590	0.418	0.415	0.700	0.674	0.685	0.650	0.650	0.634	0.350	0.350	0.366
PB5B5 (2.0)	0.160	0.256	0.143	0.590	0.612	0.594	0.700	0.711	0.669	0.650	0.650	0.616	0.412	0.412	0.385
PB7B5 (2.0)	0.160	0.321	0.285	0.590	0.541	0.507	0.700	0.701	0.702	0.650	0.650	0.636	0.385	0.385	0.364
PB10B5 (2.0)	0.160	0.368	0.362	0.590	0.472	0.464	0.700	0.693	0.710	0.650	0.650	0.643	0.350	0.350	0.357
PB13B5 (2.0)	0.160	0.415	0.410	0.590	0.451	0.446	0.700	0.677	0.701	0.650	0.650	0.638	0.350	0.350	0.362
PB20B5 (2.0)	0.160	0.475	0.471	0.590	0.425	0.419	0.700	0.677	0.690	0.650	0.650	0.635	0.350	0.350	0.365

Table 3.6 (Cont'd)

Design Strip Procedure	Section 1			Section 2			Section 3			Section 4			Section 5		
	D	D'	E	D	D'	E	D	D'	E	D	D'	E	D	D'	E
PB5B5 (2.5)	0.160	0.238	0.126	0.757	0.528	0.602	0.700	0.713	0.671	0.650	0.650	0.621	0.350	0.350	0.385
PB7B5 (2.5)	0.160	0.301	0.269	0.742	0.500	0.513	0.700	0.704	0.704	0.650	0.650	0.639	0.350	0.350	0.361
PB10B5 (2.5)	0.160	0.348	0.347	0.604	0.480	0.470	0.700	0.691	0.713	0.650	0.650	0.646	0.350	0.350	0.354
PB13B5 (2.5)	0.160	0.396	0.396	0.590	0.459	0.450	0.700	0.689	0.705	0.650	0.650	0.640	0.350	0.350	0.360
PB20B5 (2.5)	0.160	0.458	0.458	0.590	0.433	0.424	0.700	0.680	0.694	0.650	0.650	0.637	0.350	0.350	0.363
PB5B5 (3.0)	0.160	0.221	0.110	0.649	0.547	0.609	0.700	0.716	0.672	0.650	0.650	0.625	0.350	0.350	0.384
PB7B5 (3.0)	0.160	0.283	0.254	0.590	0.508	0.520	0.700	0.706	0.707	0.650	0.650	0.642	0.350	0.350	0.358
PB10B5 (3.0)	0.160	0.330	0.334	0.590	0.488	0.475	0.700	0.699	0.716	0.650	0.650	0.648	0.350	0.350	0.352
PB13B5 (3.0)	0.160	0.378	0.382	0.590	0.467	0.455	0.700	0.692	0.709	0.650	0.650	0.643	0.350	0.350	0.357
PB20B5 (3.0)	0.160	0.442	0.445	0.590	0.440	0.429	0.700	0.682	0.698	0.650	0.650	0.638	0.350	0.350	0.362
PB5B5 (4.0)	0.160	0.193	0.082	0.677	0.547	0.622	0.700	0.720	0.675	0.650	0.650	0.633	0.350	0.350	0.383
PB7B5 (4.0)	0.160	0.252	0.228	0.622	0.521	0.531	0.700	0.711	0.710	0.650	0.650	0.648	0.350	0.350	0.352
PB10B5 (4.0)	0.160	0.298	0.309	0.590	0.502	0.485	0.700	0.704	0.721	0.650	0.650	0.653	0.350	0.350	0.347
PB13B5 (4.0)	0.160	0.346	0.357	0.590	0.481	0.464	0.700	0.697	0.714	0.650	0.650	0.647	0.350	0.350	0.353
PB20B5 (4.0)	0.160	0.412	0.421	0.590	0.453	0.437	0.700	0.687	0.705	0.650	0.650	0.642	0.350	0.350	0.358

Table 3.7a: Design moment ratios for S series (full factored load on all spans)

DESIGN STRIP Procedure	Section 1			Section 2 (positive)			Section 3			Sectio 4		Section 5 (positive)		Section 6		Section 7		Section 8 (positive)	
	D	D'	E	D	D'	E	D	D'	E	D'	E	D'	E	D'	E	D'	E	D'	E
S5B20*	0.260	0.209	-.138	0.530	0.540	0.038	0.700	0.718	2.062	0.650	0.559	0.350	0.479	0.650	0.484	0.650	1.627	0.350	-.627
S7B20	0.260	0.270	0.123	0.530	0.514	0.441	0.700	0.708	0.996	0.650	0.600	0.350	0.439	0.650	0.522	0.650	0.785	0.350	0.215
S10B20	0.260	0.316	0.260	0.530	0.494	0.500	0.700	0.701	0.739	0.650	0.683	0.350	0.358	0.650	0.601	0.650	0.613	0.350	0.387
S13B20	0.260	0.316	0.288	0.530	0.494	0.542	0.700	0.701	0.627	0.650	0.898	0.350	0.162	0.650	0.777	0.650	0.535	0.350	0.465
S15B20*	0.260	0.316	0.294	0.530	0.494	0.551	0.700	0.701	0.602	0.650	1.070	0.350	0.004	0.650	0.921	0.650	0.518	0.350	0.482
S20B20*	0.260	0.316	0.301	0.530	0.494	0.561	0.700	0.701	0.576	0.650	1.910	0.350	-.774	0.650	1.638	0.650	0.498	0.350	0.502

Table 3.7b: Design moment ratios for S series (pattern loads)

DESIGN STRIP Procedure	Section 1			Section 2 (positive)			Section 3			Sectio 4		Section 5 (positive)		Section 6		Section 7		Section 8 (positive)	
	D'	E_{min}	E_{max}	D'	E_{min}	E_{max}	D'	E_{min}	E_{max}	E_{min}	E_{max}	E_{min}	E_{max}	E_{min}	E_{max}	E_{min}	E_{max}	E_{min}	E_{max}
S5B5*	0.209	-.472	0.054	0.665	-.622	0.462	0.718	0.619	2.077	0.073	0.559	0.119	0.479	0.018	0.484	0.195	1.627	-.949	0.249
S7B5	0.270	-.189	0.156	0.618	-.002	0.495	0.708	0.424	0.997	0.121	0.600	0.073	0.439	0.061	0.522	0.244	0.785	-.172	0.412
S10B5	0.316	-.216	0.288	0.494	0.090	0.542	0.701	0.219	0.627	0.200	0.683	-.003	0.403	0.134	0.601	0.139	0.613	0.012	0.421
S13B5	0.316	-.049	0.288	0.494	0.129	0.542	0.701	0.120	0.627	0.306	0.898	-.203	0.384	0.236	0.777	0.064	0.535	0.084	0.465
S15B5*	0.316	-.042	0.294	0.494	0.139	0.551	0.701	0.125	0.603	0.291	1.070	-.352	0.358	0.209	0.922	0.045	0.518	0.102	0.482
S20B5*	0.316	-.033	0.301	0.505	0.153	0.561	0.701	0.057	0.576	0.306	1.913	-1.408	0.190	0.170	1.669	0.018	0.498	0.127	0.502

D'=DDM', E_{min}=EFM (Minimum moments), E_{max}=EFM (Maximum moments)

Table 3.8: Differences between DDM' and EFM for C series (Square panels)

Method		DDM'						EFM					
Property		ΣK_c	K_s+K_b	K_{ec}	α_{ec}	M_{cl}/M_1	$\Delta M/M_1$	ΣK_c	K_{sb}	K_{ec}	α_{ec}	M_{cl}/M_1	$\Delta M/M_1$
Strip		(N-mm x 10^{10})						(N-mm x 10^{10})					
C10A20		16.30	7.30	4.32	0.59	0.242	0.024	18.90	7.48	4.49	0.60	0.286	0.085
C10B20		32.60	7.30	6.91	0.95	0.316	0.045	37.82	7.48	7.12	0.95	0.349	0.122
C10C20		48.91	7.30	8.98	1.23	0.358	0.061	56.70	7.48	9.17	1.23	0.392	0.151
C10D20		65.20	7.30	10.70	1.46	0.386	0.076	75.60	7.48	10.90	1.46	0.421	0.175
C10E20		48.91	7.30	8.21	1.12	0.344	0.049	56.73	7.54	8.41	1.12	0.374	0.123
C10F20		73.35	7.30	10.30	1.41	0.381	0.065	85.10	7.54	10.50	1.41	0.412	0.152
C10G20		110.03	7.30	12.90	1.77	0.415	0.086	128.00	7.54	13.10	1.74	0.447	0.187
C10H20		146.70	7.30	15.10	2.07	0.449	0.105	170.20	7.54	15.32	2.03	0.471	0.215
C10I20		65.20	7.30	9.52	1.30	0.368	0.056	70.17	7.61	9.72	1.28	0.396	0.124
C10J20		130.40	7.30	13.50	1.84	0.421	0.083	151.00	7.61	13.70	1.80	0.450	0.177
C10K20		195.60	7.30	16.48	2.26	0.450	0.108	226.90	7.61	16.67	2.20	0.480	0.216
C10L20		260.81	7.30	19.01	2.60	0.470	0.128	302.50	7.61	19.20	2.53	0.500	0.249
C10M20		220.06	7.30	17.16	2.35	0.456	0.095	255.30	7.74	17.34	2.23	0.480	0.189
C10N20		293.41	7.30	19.29	2.64	0.472	0.113	340.30	7.74	19.47	2.52	0.496	0.217
C10O20		391.23	7.30	21.78	2.98	0.487	0.132	453.80	7.74	21.94	2.83	0.512	0.249
C10P20		586.80	7.30	25.92	3.55	0.520	0.165	680.70	7.74	26.11	3.37	0.535	0.302
C10Q20		521.65	7.30	24.82	3.40	0.502	0.137	605.10	7.87	24.99	3.18	0.523	0.250
C10R20		2004.00	7.30	45.66	6.25	0.575	0.207	2324.00	8.37	45.81	5.47	0.569	0.343

Table 3.9: Differences between DDM' and EFM for P series (Rectangular panels)

Method	DDM'						EFM					
Property	ΣK_c	K_s+K_b	K_{ec}	α_{ec}	M_{cl}/M_1	$\Delta M/M_1$	ΣK_c	K_{sb}	K_{ec}	α_{ec}	M_{cl}/M_1	$\Delta M/M_1$
Strip	(N-mm x 10^{10})						(N-mm x 10^{10})					
P5B20	32.60	14.60	6.91	0.47	0.209	0.056	37.82	15.30	7.12	0.47	0.251	0.226
P7B20	32.60	9.74	6.91	0.71	0.270	0.050	37.82	10.04	7.12	0.71	0.305	0.158
P10B20	32.60	7.30	6.91	0.95	0.316	0.045	37.82	7.48	7.12	0.95	0.349	0.122
P13B20	32.60	5.48	9.11	1.66	0.406	0.057	37.82	5.65	9.48	1.68	0.438	0.126
P20B20	32.60	3.65	13.20	3.63	0.510	0.072	37.82	3.82	14.00	3.66	0.540	0.131

Table 3.10: Differences between DDM' and EFM for PE series (Rectangular panels)

Method	DDM'						EFM					
Property	ΣK_c	K_s+K_b	K_{ec}	α_{ec}	M_{cl}/M_1	$\Delta M/M_1$	ΣK_c	K_{sb}	K_{ec}	α_{ec}	M_{cl}/M_1	$\Delta M/M_1$
Strip	(N-mm x 10^{10})						(N-mm x 10^{10})					
PE5B20(200)	32.55	14.61	9.22	0.63	0.252	0.068	53.38	15.27	10.36	0.68	0.309	0.232
PE7B20(200)	32.55	9.74	9.22	0.95	0.316	0.059	53.38	10.04	10.36	1.03	0.368	0.162
PE10B20(200)	32.55	7.30	9.22	1.26	0.363	0.051	53.38	7.48	10.36	1.39	0.411	0.125
PE13B20(200)	32.55	5.48	11.81	2.16	0.444	0.063	53.38	5.65	13.75	2.43	0.491	0.129
PE20B20(200)	32.55	3.65	16.32	4.47	0.531	0.075	53.38	3.82	20.27	5.31	0.576	0.133
PE5B20(300)	32.55	14.61	15.26	1.05	0.332	0.090	53.38	15.27	18.67	1.22	0.403	0.240
PE7B20(300)	32.55	9.74	15.26	1.57	0.397	0.074	53.38	10.04	18.67	1.86	0.460	0.168
PE10B20(300)	32.55	7.30	15.26	2.09	0.440	0.062	53.38	7.48	18.67	2.50	0.496	0.129

	ΣKc	Ks+Kb	Kec	αec	Mcl/M1	ΔM/M1	ΣKc	Ksb	Kec	αec	Mcl/M1	ΔM/M1
PE13B20(300)	32.55	5.48	18.23	3.33	0.500	0.071	53.38	5.65	23.31	4.13	0.553	0.132
PE20B20(300)	32.55	3.65	22.54	6.17	0.559	0.079	53.38	3.82	30.83	8.07	0.607	0.134
PE5B20(400)	32.55	14.61	19.83	1.36	0.374	0.102	53.38	15.27	25.98	1.70	0.456	0.245
PE7B20(400)	32.55	9.74	19.83	2.04	0.436	0.081	53.38	10.04	25.98	2.59	0.505	0.171
PE10B20(400)	32.55	7.30	19.83	2.72	0.475	0.067	53.38	7.48	25.98	3.47	0.536	0.131
PE13B20(400)	32.55	5.48	22.53	4.11	0.523	0.074	53.38	5.65	30.83	5.46	0.578	0.133
PE20B20(400)	32.55	3.65	26.01	7.12	0.570	0.081	53.38	3.82	37.73	9.88	0.619	0.135
PE5B20(500)	32.55	14.61	22.43	1.54	0.394	0.107	53.38	15.27	30.63	2.01	0.479	0.247
PE7B20(500)	32.55	9.74	22.43	2.30	0.453	0.084	53.38	10.04	30.63	3.05	0.525	0.172
PE10B20(500)	32.55	7.30	22.43	3.07	0.490	0.069	53.38	7.48	30.63	4.10	0.553	0.132
PE13B20(500)	32.55	5.48	24.80	4.53	0.532	0.075	53.38	5.65	35.23	6.24	0.588	0.134
PE20B20(500)	32.55	3.65	27.67	7.58	0.574	0.081	53.38	3.82	41.32	10.82	0.624	0.135

Table 3.11: Differences between DDM' and EFM for PB Series (Rectangular panels)

Method	DDM'						EFM					
Property	ΣK_c	$K_s + K_b$	K_{ec}	α_{ec}	M_{cl}/M_1	$\Delta M/M_1$	ΣK_c	K_{sb}	K_{ec}	α_{ec}	M_{cl}/M_1	$\Delta M/M_1$
Strip	(N-mm x 10^{10})						(N-mm x 10^{10})					
PB5B5(0.5)	32.60	21.96	17.30	0.79	0.287	0.078	47.50	23.43	20.75	0.89	0.348	0.234
PB7B5(0.5)	32.60	14.61	17.30	1.18	0.352	0.065	47.50	15.41	20.75	1.35	0.406	0.184
PB10B5(0.5)	32.60	10.96	17.30	1.58	0.398	0.056	47.50	11.47	20.75	1.81	0.447	0.127
PB13B5(0.5)	32.60	8.22	17.48	2.13	0.442	0.063	46.23	8.40	20.76	2.47	0.491	0.129
PB20B5(0.5)	32.60	5.48	16.54	3.02	0.488	0.069	44.68	5.38	19.17	3.57	0.537	0.131
PB5B5(1.0)	32.60	29.20	24.11	0.83	0.294	0.080	51.33	33.72	33.01	0.98	0.364	0.235

	32.60	19.48	24.11	1.64	0.360	0.067	51.33	22.18	33.01	1.36	0.421	0.165
PB7B5(1.0)	32.60	19.48	24.11	1.64	0.360	0.067	51.33	22.18	33.01	1.36	0.421	0.165
PB10B5(1.0)	32.60	14.60	24.11	1.65	0.405	0.057	51.33	16.51	33.01	2.00	0.461	0.127
PB13B5(1.0)	32.60	10.96	24.87	2.27	0.451	0.064	49.58	12.09	33.67	2.79	0.506	0.129
PB20B5(1.0)	32.60	7.30	25.80	3.53	0.507	0.072	47.50	7.74	34.31	4.43	0.559	0.132
PB5B5(1.5)	32.60	36.52	26.99	0.74	0.276	0.075	54.26	44.14	40.30	0.91	0.353	0.234
PB7B5(1.5)	32.60	24.34	26.99	1.11	0.342	0.064	54.26	29.03	40.30	1.39	0.411	0.164
PB10B5(1.5)	32.60	18.25	26.99	1.48	0.388	0.055	54.26	21.61	40.30	1.87	0.451	0.127
PB13B5(1.5)	32.60	13.71	27.68	2.02	0.435	0.061	52.13	15.83	40.58	2.56	0.495	0.129
PB20B5(1.5)	32.60	9.12	28.54	3.13	0.493	0.070	49.58	10.23	40.76	3.98	0.549	0.131
PB5B5(2.0)	32.60	43.81	28.53	0.65	0.256	0.070	56.76	54.54	45.45	0.83	0.339	0.233
PB7B5(2.0)	32.60	29.21	28.53	0.98	0.321	0.060	56.76	35.87	45.45	1.27	0.397	0.163
PB10B5(2.0)	32.60	21.90	28.53	1.30	0.368	0.052	56.76	26.71	45.45	1.70	0.438	0.126
PB13B5(2.0)	32.60	16.44	29.09	1.77	0.415	0.059	54.26	19.56	45.19	2.31	0.482	0.128
PB20B5(2.0)	32.60	10.95	29.82	2.72	0.475	0.067	51.33	12.53	44.75	3.57	0.537	0.131
PB5B5(2.5)	32.60	51.12	29.47	0.58	0.238	0.065	59.00	64.93	49.47	0.76	0.325	0.232
PB7B5(2.5)	32.60	34.08	29.47	0.86	0.301	0.056	59.00	42.70	49.47	1.16	0.383	0.163
PB10B5(2.5)	32.60	25.55	29.47	1.15	0.348	0.049	59.00	31.79	49.47	1.56	0.425	0.126
PB13B5(2.5)	32.60	19.17	29.94	1.56	0.396	0.056	56.17	23.28	48.70	2.09	0.469	0.127
PB20B5(2.5)	32.60	12.78	30.53	2.39	0.458	0.062	52.87	14.92	47.63	3.19	0.525	0.130
PB5B5(3.0)	32.60	58.43	30.09	0.52	0.221	0.060	61.07	75.29	52.80	0.70	0.311	0.231
PB7B5(3.0)	32.60	38.95	30.09	0.77	0.283	0.056	61.07	49.51	52.80	1.07	0.370	0.162
PB105(3.0)	32.60	29.21	30.09	1.03	0.330	0.047	61.07	36.86	52.80	1.43	0.413	0.125
PB13B5(3.0)	32.60	21.91	30.48	1.39	0.378	0.053	57.91	27.00	51.55	1.91	0.456	0.127
PB20B5(3.0)	32.60	14.60	30.98	2.12	0.442	0.062	54.26	17.30	49.92	2.89	0.513	0.129

	ΣKc	Ks+Kb	Kec	αec	Mcl/M1	ΔM/M1	ΣKc	Ksb	Kec	αec	Mcl/M1	ΔM/M1
PB5B5(4.0)	32.60	73.05	30.85	0.42	0.193	0.052	64.84	95.88	58.25	0.61	0.289	0.229
PB7B5(4.0)	32.60	48.70	30.85	0.63	0.252	0.047	64.84	63.05	58.25	0.92	0.347	0.161
PB10B5(4.0)	32.60	36.52	30.85	0.84	0.298	0.042	64.84	46.95	58.25	1.24	0.391	0.124
PB13B5(4.0)	32.60	27.39	31.14	1.14	0.346	0.049	61.07	34.37	56.13	1.63	0.434	0.126
PB20B5(4.0)	32.60	18.25	31.50	1.73	0.412	0.058	56.76	22.02	53.51	2.43	0.491	0.128

Table 3.12: Differences between DDM' and EFM for S series (Full factored load on all spans)

Method	DDM'						EFM					
Property	ΣK_c	$K_s + K_b$	K_{ec}	α_{ec}	M_{cl}/M_1	$\Delta M/M_1$	ΣK_c	K_{sb}	K_{ec}	α_{ec}	M_{cl}/M_1	$\Delta M/M_1$
Strip	(N-mm x 10^{10})						(N-mm x 10^{10})					
S5B20*	32.60	14.60	6.91	0.47	0.209	0.056	53.38	15.27	7.12	0.47	0.029	0.131
S7B20	32.60	10.95	6.91	0.71	0.270	0.047	53.38	10.04	7.12	0.71	0.245	0.144
S10B20	32.60	7.30	6.91	0.95	0.316	0.045	53.38	7.48	7.12	0.95	0.346	0.122
S13B20	32.60	7.30	6.91	0.95	0.316	0.045	53.38	7.48	7.12	0.95	0.375	0.127
S15B20*	32.60	7.30	6.91	0.95	0.316	0.045	53.38	7.48	7.12	0.95	0.381	0.128
S20B20*	32.60	7.30	6.91	0.95	0.316	0.045	53.38	7.48	7.12	0.95	0.388	0.129
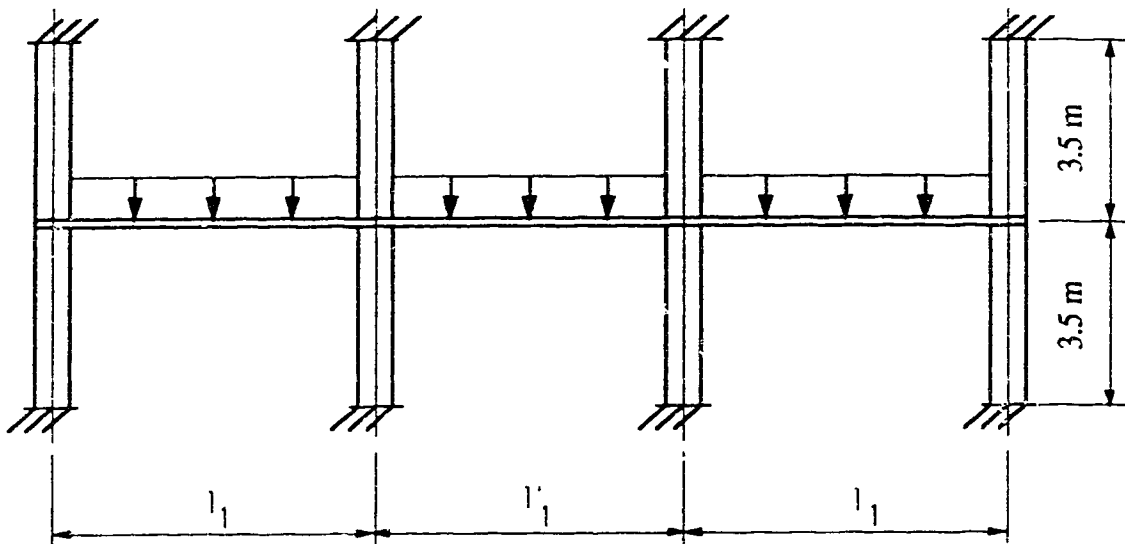
Fig 3.1: Design strip geometry for C and P series
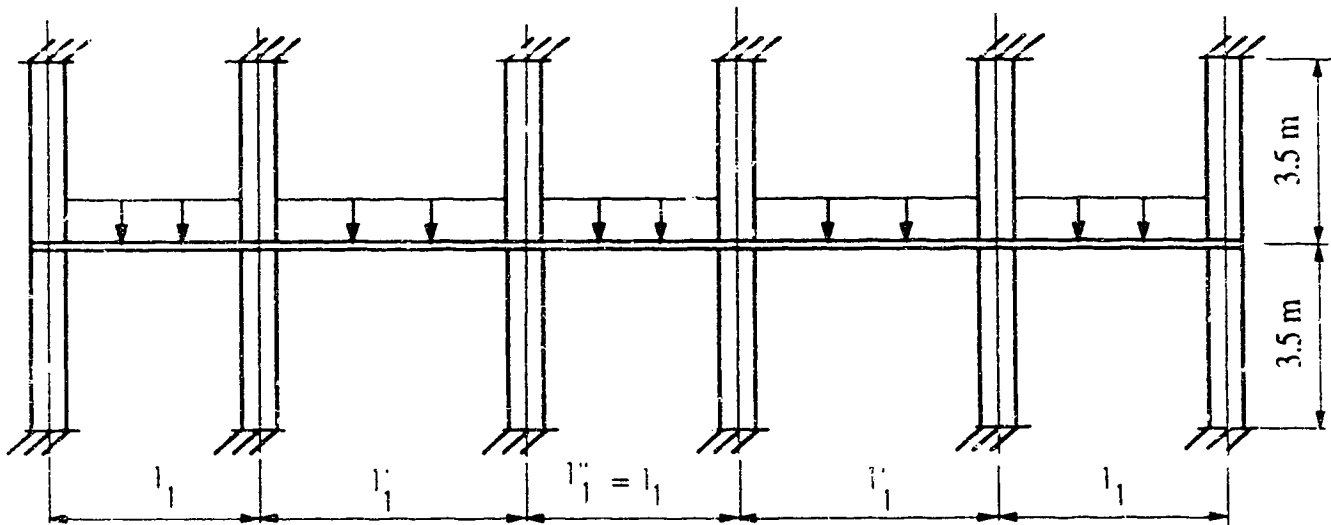

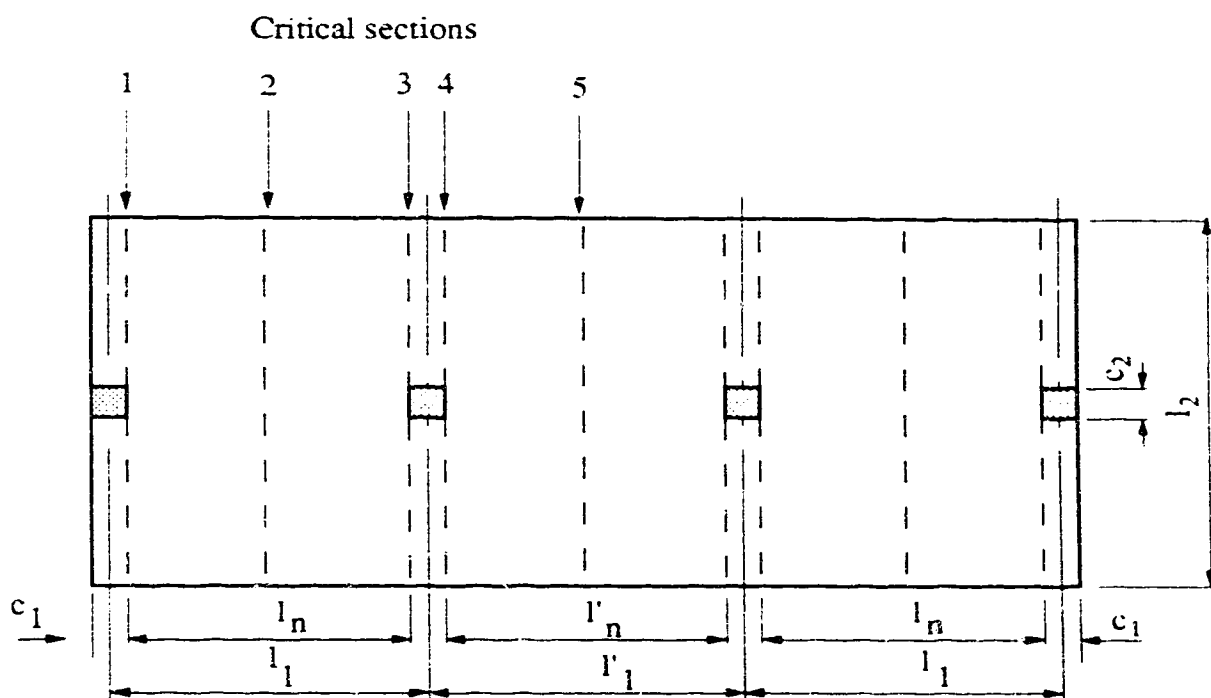Fig 3.2: Design strip geometry for S series

Critical sections

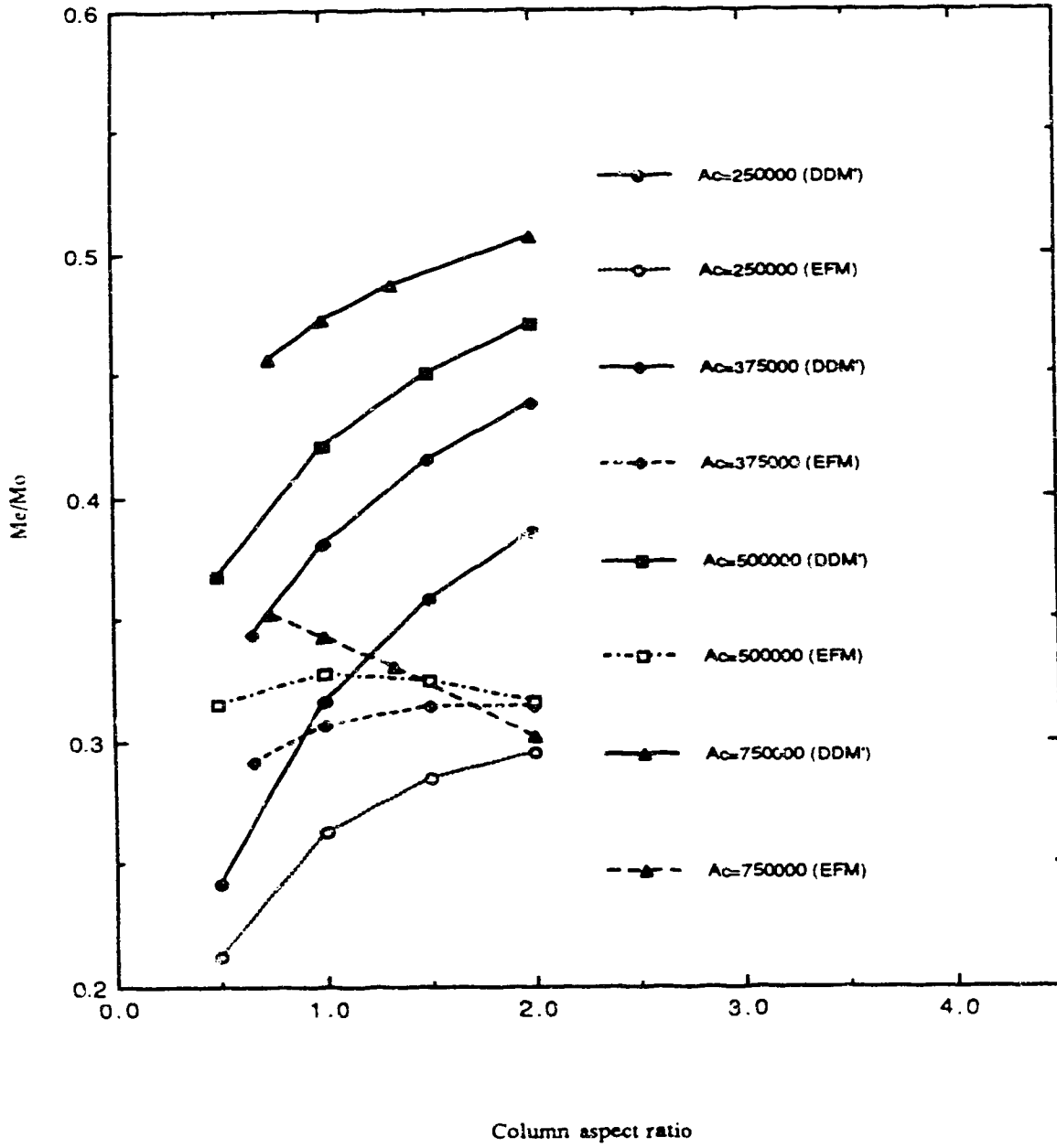Fig 3.3: Critical sections for a 3 span interior design strip

Fig 3.4: Exterior support moment ratio vs Column aspect ratio
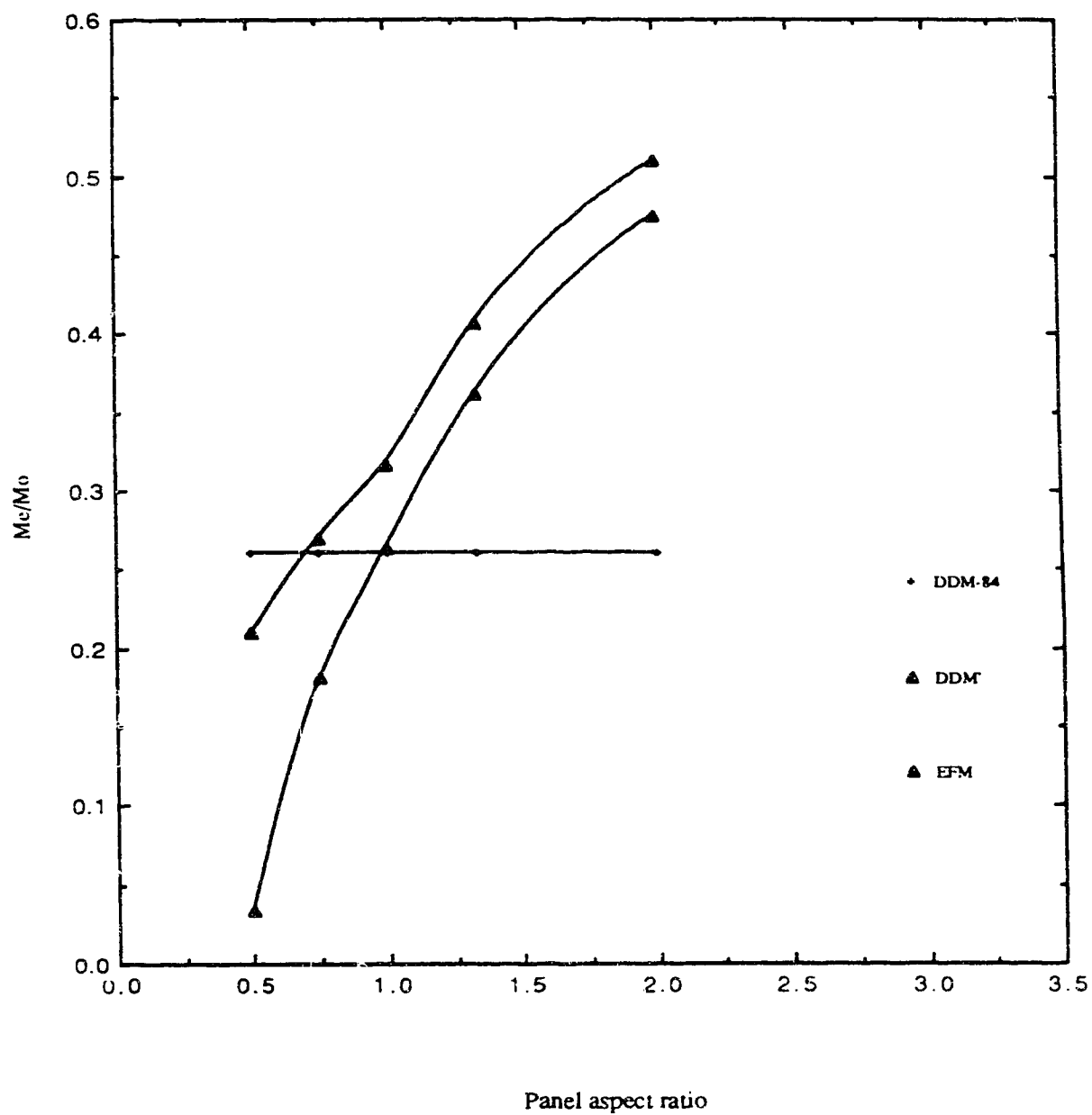
Fig 3.5: Exterior support moment ratio vs Panel aspect ratio
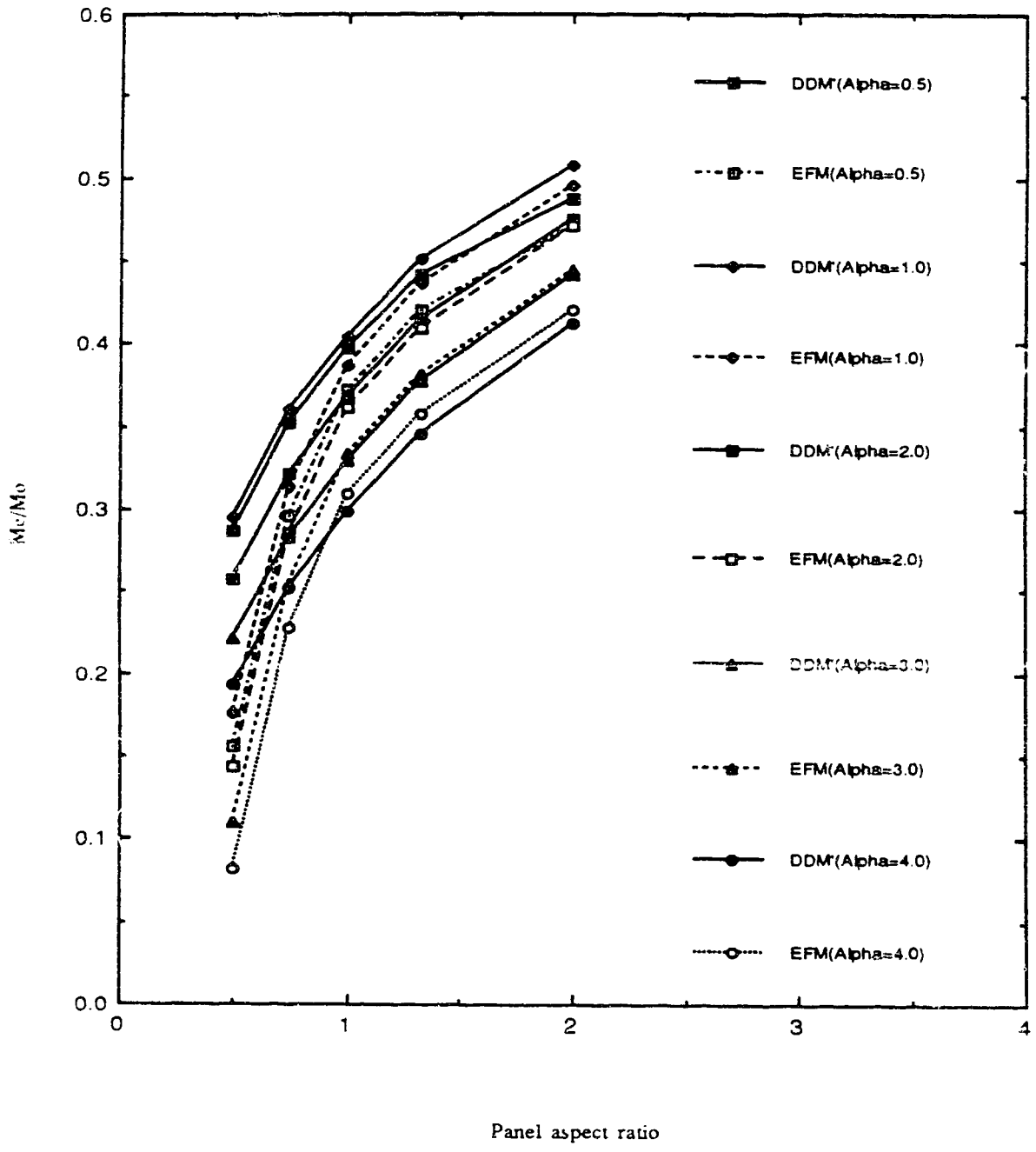
Fig 3.6: Exterior support moment ratio vs Panel aspect ratio (PB series)
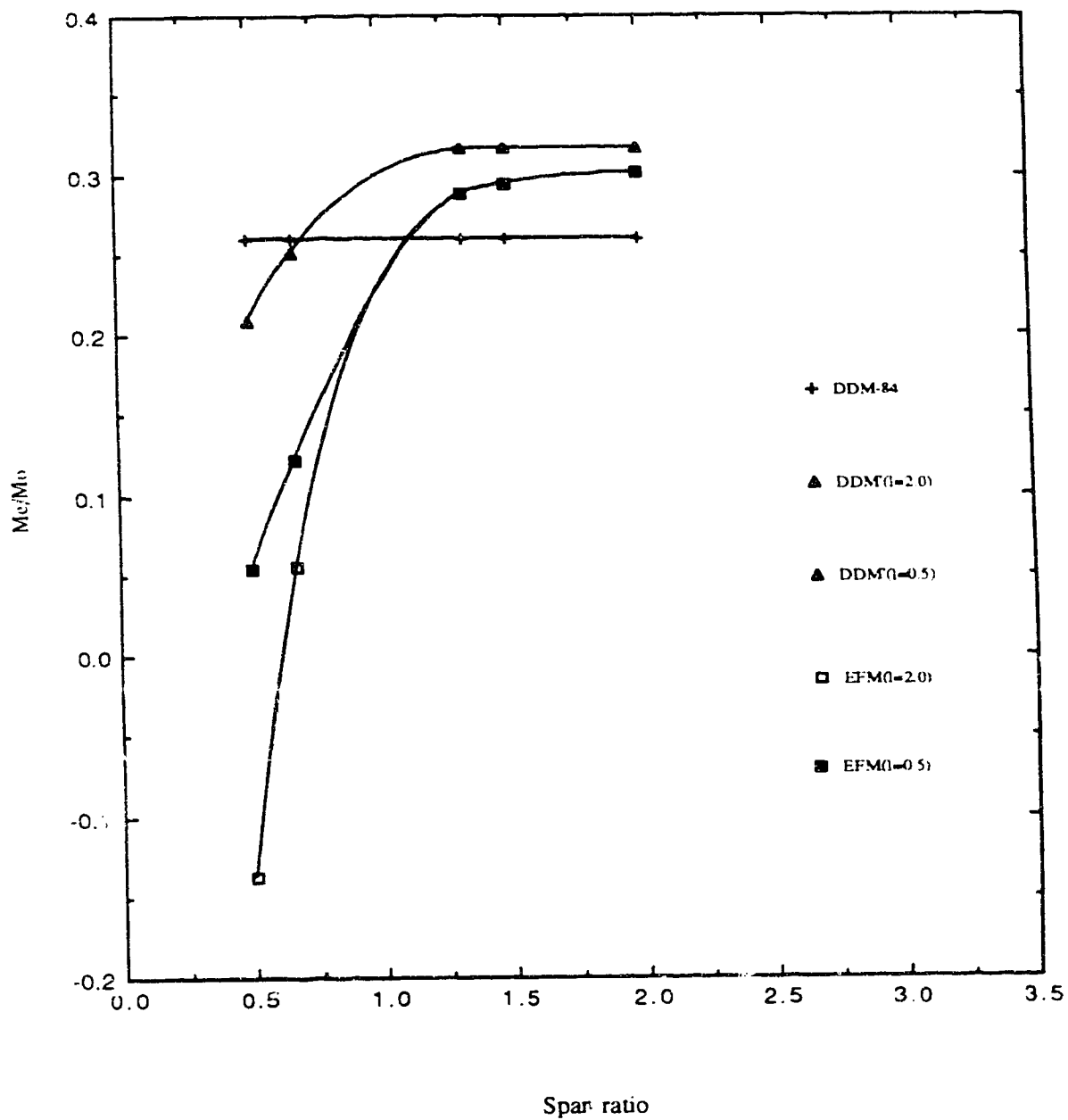
Fig 3.7: Exterior support moment ratio vs Span ratio

Chapter 4

Finite Element Analysis of Reinforced Concrete

4.1 Introduction

Modelling of reinforced concrete is very complex because the interaction between cracked concrete and reinforcement is highly non-linear. This is especially true for lightly reinforced slabs. Further, to adequately represent the composite behaviour in a prototype slab requires a large number of elements. Thus at the present time, non-linear finite element analyses are generally used only for very important structures or as a research tool. As a research tool, it can provide the much needed data on behaviour of reinforced concrete two-way slab systems, in the absence of laboratory test data.

As the main aims of this study are to examine the validity and limitations of code procedures, the use of a non-linear finite element analysis is appropriate. However, the program chosen should be able to model non-linear geometric and material behaviour. As pointed out by other researchers (Hu and Schnobrich, 1990; Massicotte et al., 1988), the reinforced concrete model adopted should have, among other ingredients, tension stiffening, tension softening, reinforcement representation, crack formulation and the shear retention phenomenon.

For these reasons, the locally available program NISA80 (Stegmüller, 1983) with the reinforced concrete material model implemented by Massicotte et al. (1988) was chosen for this study.

69

4.2   The Finite Element Program, NISA80

NISA80 is a non-linear incremental finite element structural analysis program, written in Fortran 77. The program was initially developed at the Institut für Baustatik at Stuttgart University, Germany but was later modified at the University of Alberta to apply to various problems.

NISA80 incorporates a degenerated three-dimensional (3-D) plate-shell element (Ramm, 1977) having five degrees of freedom at each node (three displacements and two rotations). The 3-D degenerated-plate-shell element is shown in Fig 4.1. The displacement at any node in the element is defined as a function of the mid-plane displacements and rotations. Independent interpolation functions (for each degree of freedom) are used to allow for shear deformations and membrane forces.

For solution strategy, the program permits use of either the Load Control Method or the Modified Constant Arc Length Method (CALM) introduced by Ramm (1980). Either the Standard Newton-Raphson (SNR) or Modified Newton-Raphson (MNR) iteration technique can be used. It is possible to change both the solution strategy and the iteration technique before restarting the solution after any specified load or time steps.

The element can be used with nine to sixteen nodes per element; the higher the number, the better the convergence. Therefore, the sixteen node element with a 4X4 gaussian integration rule over the element plane was adopted.

Total stresses, forces and moments at any gauss point are obtained by using Simpson's integration rule over the thickness. Thus, over the total depth, concrete is divided into an even number intervals of equal thickness to give an odd number of equally spaced integration points. Reinforcement is represented as sheets of uniform thicknesses located at certain relative depths in the slab but have unidirectional properties in form of a linear, bi-linear or multi-linear stress-strain curve. The reinforcement has compatible strains with the surrounding concrete.

4.3   The Reinforced Concrete Model by Massicotte

The characteristics and assumptions of the model are as follows:

(a)   It is an Hypo-elastic Incremental model.

(b)   It is developed for plane stress conditions.

(c)   Concrete remains isotropic up to cracking or crushing.

(d)   After cracking, concrete is orthotropic.

(e)   Two cracks can form at a point in two different directions.

(f)   After cracking or crushing, stress undergoes strain softening and the tangent modulus in the failure direction is set to zero.

(g)   If crushing occurs at a point, failure is assumed to have occured in all directions.

(h)   For any stress condition, concrete can unload and reload from any point on the stress-strain curve, thus allowing for cyclic loading.

The failure envelope for concrete in compression, tension or combination of the two stress states is shown in Fig 4.2a. Fig 4.2b shows the stress versus the equivalent uniaxial strain for concrete in compression. The tri-linear tension softening curve proposed by Massicotte, based on studies by Gopalaratranan and Shah (1985) and Bazant and Oh (1983), is shown in Fig 4.3. Fig 4.4 shows the various stages in the tension stiffening model. Detailed information about the concepts used in formulating the model may be found in the report by Massicotte et al. (1988).

The model requires 18 concrete material properties or parameters and the stress-strain curve for the reinforcement. The values used are those recommended by Massicotte except as noted in the following section.

4.4 Evaluation of material properties

Massicotte et al. were interested in analysis of simply supported square and rectangular reinforced concrete panels loaded both axially and transversely. The material model has been verified by laboratory tests of such panels (Aghayere and MacGregor, 1988, 1990a; Ghoneim and MacGregor, 1992). All specimens had top and bott reinforcement mats running in each of the two orthogonal directions.

The major differences between these simply supported single panels and column supported two-way slab systems are:

For two-way slabs;

(a) Reinforcement may exist on only one face of an element.

(b) Reinforcing ratios are much smaller.

(c)   Reinforcement may not be continuous between elements and reinforcement ratios may vary from element to element.

(d)   No in-plane loads are applied to the slabs (In the panel specimens, in-plane loads were found to delay the onset of cracking, increased moment capacity and magnified moments due to P-Δ effects).

(e)   Two-way slabs deform in double curvature (Panel specimens deform in single curvature).

(f)   Lower concrete strengths are used.

To determine whether these differences would influence the values of concrete material properties that should be used in the analysis of two-way slab systems. a preliminary study was undertaken.

4.5   Preliminary study

Slabs used in this study were one-way slabs simply supported at both ends (SS), fixed at one end and simply supported at the other (FS) and fixed at both ends (FF). The SS slabs were intended to assess the load-deflection response while the FS and FF slabs were intended to show how the model behaved when moment redistribution took place. Four elements, of the same size, were used for the SS and FF series while five were used for the FS series. All test slabs were 1 m width and 6 m long. The slabs were reinforced as shown in Fig 4.5. Reinforcement was represented with a bi-linear stress-strain relationship with a yield stress of 400 MPa

and Youngs modulus, E_s, of 200000 MPa. After yield, the tangent modulus, E'_s, was 2000 MPa.

The CALM was selected as the solution strategy and the MNR as the iteration technique. A constant tolerance of 0.01 on displacement was used and the maximum number of iterations was specified at 30.

4.5.1 Concrete Tensile Strength

The first run was to compare the load-deflection response of a simply supported one-way slab obtained using NISA80 and the Massicotte material model with that obtained using the provisions of A23.3-M84. The simply supported structure was selected because of the unique load-moment relationship and that the effective stiffness specified by the code should be most reliable for this support tion. When computing the ultimate moment capacity, material reduction factors ϕ_c and ϕ_s were taken as 1.0. For the finite element solution, the material properties were those recommended by Massicotte et al. (1988).

The load-deflection response for the simply supported one-way slab using a concrete strength of 30 MPa, a thickness of 200 mm (effective depth=170 mm) and reinforced for a factored load of 13.5 kPa is shown in Fig 4.6. It is seen that the finite element solutions agree well up to and including the cracking region but that above this load are less stiff and only reach approximately two thirds of the expected ultimate load. Increasing the number of integration points over the depth of the slab from 5 to 9 did not improve the solution. Calculating fracture energy based on the area

under the tension softening curve gave values lower than the accepted minimum value of 5 N/m in the literature. The significance of fracture energy values is discussed in detail in Section 4.5.3.

In performing these runs, a value for the concrete tensile strength, f'_t, of $0.33\sqrt{f'_c}$, as recommended by Massicotte was used. Tensile strength has been observed to have a very important effect on the behaviour of thin members in flexure. Balakrishnan and Murray (1986) proposed a value of $0.6f_r$, where f_r is the modulus of rupture of concrete. Raphael (1984) proposed a value of $0.73f_r$. These values correspond to $0.36\sqrt{f'_c}$ and $0.44\sqrt{f'_c}$ (assuming the CSA code value of $0.60\sqrt{f'_c}$ for f_r), respectively.

Therefore larger values for tensile strength ($0.40\sqrt{f'_c}$, $0.45\sqrt{f'_c}$ and $0.50\sqrt{f'_c}$) and the number of integration points (5 to 11) over the depth were tried. The resulting load-deflection responses are shown in Figs 4.7 to 4.9. From Fig 4.7, a value of $0.40\sqrt{f'_c}$ for f'_t gave very good results while higher values, Figs 4.8 and 4.9, tended to overestimate the ultimate moment capacity. It can also be seen that beyond a certain number of integration points, the solution does not change. Therefore, a value of $0.40\sqrt{f'_c}$ was selected for f'_t in all further runs. The Australian Code (AS3600-1988) also uses this value to calculate the characteristic principal tensile stress of concrete.

4.5.2 Number of integration points over the depth of the slab, N

Having selected a value for the concrete tensile strength, it was then considered important to determine the minimum number

of integration points that could be used to model the concrete, as increasing this number increases the computer time and cost for a solution. The number chosen has to be sufficiently large to permit obtaining realistic ultimate moment capacities and allow moment redistribution after cracking. Also permit integration through the depth using Simpson's Rule, the number chosen must be an odd integer. Factors expected to affect the choice of N include the amount of reinforcement, the concrete strength and the depth of the member.

It was thought that, in order to obtain meaningful values of ultimate strength, the maximum thickness of each interval must be less than the depth of the concrete compression zone at ultimate, c. Since the depth of the Whitney rectangular stress block for concrete, a, is less than the concrete compression zone at ultimate, a reasonable number for N is:

$$N = \frac{h}{a} \quad \text{(raised to the nearest odd number)} \qquad (4.1)$$

h = Depth of slab element

a = Depth of Whitney's rectangular compression
    block

To verify this approach for the minimum value of N, a parametric study was undertaken using the SS, FS and FF supported one-way slabs shown in Fig 4.5. Concrete strengths of 20 and 30 MPa were used. Reinforcement ratios were in the range 0.005 to 0.015. Whenever top reinforcement was used, it was of the same

quantity as the bottom reinforcement, for ease of evaluation of load carrying capacities. Strip designations are of the form SS20.005: slab is simply supported at both ends, concrete strength is 20 MPa and the reinforcement density is 0.005.

While the finite element program produces complete load-deflection plots for each case, an assessment of the reliability is limited to how well they predict the ultimate load obtained using ultimate strength theory based on Whitney stress block with $\phi_c=\phi_s=1.0$. Based on principles of equilibrium (virtual work), the ultimate load in terms of the ultimate moment capacities for the different support conditions are;

(i) SS series, $w_u = \dfrac{8\,M_u}{l^2}$
$$(4.2)$$

(ii) FS series, $w_u = \dfrac{2\,M_u}{l^2}\left(1+\sqrt{1+\dfrac{M'_u}{M_u}}\right)^2$
$$(4.3)$$

(iii) FF series, $w_u = \dfrac{16\,M_u}{l^2}$
$$(4.4)$$

where $w_u=$ Ultimate load capacity of the slab

   $M_u=$ Positive moment capacity of a section

   $M'_u=$ Negative moment capacity of a section

Data for the SS series is presented in Table 4.2 and the load-deflection curves in Figs. 4.10a to c and Figs. 4.11a to c. For both concrete strengths, the load carrying capacity was reached with the minimum required number of integration points, for all reinforcement ratios.

For FS series, data and load-deflection responses are presented in Table 4.3 and Figs 4.12a to c and 4.13a to c. All specimens reached the predicted capacities, except FS20.010, which reached the capacity with the next higher number of integration points. These slabs also indicated redistribution of moments.

Data for the FF series is presented in Table 4.4. The load-deflection responses are given in Figs 4.14a to c and 4.15a to c. All specimens except FF20.010, reached the predicted load capacities. By increasing N to the next higher value, the predicted load capacity for FF20.010 was reached.

It would appear that Eqn 4.1 is a reasonable lower limit for a range of concrete strengths and reinforcement ratios. However, if the computed value of N is very close to the next odd integer value, ie 4.84 for FS20.010 and 4.94 for FF20.010, the value of N should be increased by one increment. On the other hand, when the number of integration points is very large, N obtained from Eqn 4.1 is conservative.

In order to take into account the low reinforcement ratios in some portions of the slab, the number of integration points for the prototype slab was selected as 11.

4.5.3 Tension Stiffening parameters, E_1 and E_2

The fracture energy, G_f, is the product of the area under the tension softening curve of concrete and the width of the fracture process zone, w_c, usually taken as 2 to 3 times the maximum size of aggregate used in a reinforced concrete structure under consideration (Bazant and Oh, 1983). Values for fracture energy for normal strength concrete reported in the literature range from 50 to 200 N/m (Bangash, 1989; Balakrishnan and Murray, 1986; Darwin, 1985). In this study, the width of the fracture process zone was taken to be 3 times the aggregate size.

The tri-linear tension softening curve as implemented in NISA80, is defined by three slopes E_c, E_1 and E_2 and by the parameters μ and f_t. The values recommended by Massicotte were $E_c = 3320\sqrt{f'_c} + 6900$, $E_1 = -E_c/6$, $E_2 = -E_c/33$, $f_t = 0.33\sqrt{f'_c}$ and $\mu = 0.33$.

Computed values of G_f based on Massicotte's recommendations were found to be lower than 50 N/m. To increase the fracture energy and to stabilize later solutions, it was decided to increase the area under the tension softening curve. Based on the study in section 4.5.1, the value of f_t was increased to $0.40\sqrt{f'_c}$ and values of E_c and μ were retained as being acceptable values (Balakrishnan and Murray, 1984; Rots et al., 1984; Schnobrich, 1990).

From Fig 4.3, the values of E_1 and E_2 can be expressed as

$$E_1 = -\frac{(1-\mu)f'_t}{(\varepsilon_\mu - \varepsilon_{cr})}$$

(4.5)

and

$$E_2 = - \frac{\mu f'_t}{(\varepsilon_{max} - \varepsilon_{\mu})} \qquad (4.6)$$

where $\quad \varepsilon_{cr} = \frac{f'_t}{E_c}$

There is limited information on the value of ε_{max} for bi-linear descending branch models. Damjanic and Owen (1984) proposed values of 5 to $10\varepsilon_{cr}$ for shear type cracking and 20 to $25\varepsilon_{cr}$ for flexural type cracking. Since slab analysis is a flexural type cracking problem, a maximum strain in concrete of $20\varepsilon_{cr}$ was selected. Darwin (1985) recommended the following relationship for ε_{μ}:

$$\varepsilon_{\mu} = \frac{1}{9}(2\varepsilon_{max} + 7\varepsilon_{cr}) \qquad (4.7)$$

Based on these expressions, new values computed for E_1 and E_2 are shown in Table 4.1, for different values of concrete strength. The revised values for E_1 and E_2 were incorporated in the computer code to replace the constant values used by Massicotte.

Using the revised tension softening curve slopes, values of G_f for 15 and 20 mm aggregate sizes and concrete strength of 30 MPa, are 49.4 and 65.9 N/m, which correspond to the lower range of values reported in the literature. Use of the new tension softening curve slopes also reduced numerical instability problems in the runs discussed in Chapter 5.

4.5.4 Shear Retention Factor

For slabs without beams, shear retention is important in the vicinity of the column supports. In order to account for shear retention, the reduced shear modulus is often adopted in reinforced concrete material models.

The reduced shear modulus approach, better known as shear retention, was first introduced by Hand, Pecknold and Schnobrich (1972). Shear retention improves the cracking representation and removes some of the numerical difficulties after cracking caused by singularity of the composite material constitutive matrix. The shear retention factor is defined as the ratio of G_{cr}/G_o where G_{cr} is the effective shear modulus after cracking and G_o is the shear modulus before cracking.

Hand et al. (1972) used a constant value of 0.40 in their analyses. Hand et al. (1972) and Gerstle (1981) found that solutions were not sensitive to the value of the shear retention factor adopted. Lin and Scordelis (1975), Ivangi (1981), Razagpur and Ghali (1982) used a constant value of 0.25 as more sophisticated assumptions were found to be unwarranted. Foriborz and Schnobrich (1986) recommended a minimum value of 0.2. Hu and Schnobrich (1988) compared solutions of three test panels using constant values of 0.25 and 0.50 and obtained better convergence with a value of 0.25.

In the material model by Massicotte et al. (1988), the shear modulus after cracking, G_{cr} is reduced progressively, as a function of the stress at the crack. When the average normal stress at the crack reaches zero, at the end of the tension stiffening curve, the

crack is assumed fully open and G_r assumes G_{min} equal to 0.1 of the initial shear modulus.

Based on the above literature review, the factor for minimum shear modulus was increased to 0.25 so that G_{cr} is now given by:

$$G_{cr} = \frac{E_B}{4}\left(\frac{f_sT}{f_{cr}} + 1\right) \geq G_{min}{=}0.25G_o \qquad (4.8)$$

4.6 Additional modifications to NISA80

Trial runs on the main study design strip indicated that modifications were required to obtain information relevant to the study. These included a means of obtaining moments at required critical sections and increasing the number of reinforcement layers to represent all the reinforcement patterns in the test slabs.

4.6.1 Number of reinforcement layers

In the previous version of the program, only 8 different layers (densities) of reinforcement could be defined for all of the slab elements used. This number is inadequate to present the various reinforcement layouts in a continuous column supported two-way slab system. The reinforcement arrays in the program were adjusted to allow any number of reinforcement layers to be defined.

4.6.2 Summing of moments using D3SUMM

To obtain the total moments at critical sections in the slab structure reported in Chapter 5, it is necessary to sum moments

across the slab at selected sections. NISA80 only gives moment intensities at the gauss points and so, a subroutine D3SUMM was written to provide the sums.

This subroutine was written specially for square or rectangular plate shell elements using the 4x4 gauss integration rule over the element plane. The procedure used is described in Appendix B.

Table 4.1: Tension softening curve parameters (Revised)

f'_c (MPa)	E_c (MPa)	f'_t (MPa)	E_1	E_2
20	21747.5	1.79	-3434.0	-490.5
25	23500.0	2.00	-3710.7	-530.1
30	25084.4	2.19	-3960.9	-565.8
35	26541.4	2.37	-4191.0	-598.7
40	27897.5	2.53	-4405.1	-629.3

$$f'_t = 0.40\sqrt{f'_c}$$

Table 4.2: SS Series (h=250 mm, d=219.4 mm)

Property Strip	ρ	a (mm)	N	M_u (kN-m)	W_u (Pred.) (kN/m^2)	W_u(NISA) (kN/m^2)
SS20.005	0.005	25.81	9	90.64	20.14	20.69
SS20.010	0.010	51.16	5	169.81	37.74	36.89
SS20.015	0.015	77.42	5	237.74	52.83	53.29
SS30.005	0.005	17.20	15 (13)	92.46	20.55	20.14
SS30.010	0.010	40.48	7	174.69	38.82	41.70
SS30.013	0.013	44.73	7	224.68	49.93	52.79

Note: Number in brackets is the actual N used

Table 4.3: FS Series (h=250 mm, d=219.4 mm)

Property Strip	ρ	a (mm)	N	M_u (kN-m)	W_u (Pred.) (kN/m^2)	W_u (NISA) (kN/m^2)
FS20.005	0.005	25.81	9	90.64	29.35	31.68
FS20.010	0.010	51.61	5 (7)	169.81	54.99	61.33
FS20.015	0.015	77.42	5	237.74	76.98	81.74
FS30.005	0.005	17.20	15 (13)	92.46	29.94	30.68
FS30.010	0.010	40.48	7	174.69	56.57	65.81
FS30.013	0.013	44.73	5	224.68	72.75	83.20

Note: Number in brackets is the actual N used

Table 4.4: FF Series (h=220 mm, d=189.4 mm)

Property Strip	ρ	a (mm)	N	M_u (KN-m)	W_u (Pred.) (KN/m^2)	W_u (NISA) (KN/m^2)
FF20.005	0.005	22.28	9	67.47	29.99	30.89
FF20.010	0.010	44.56	5 (7)	126.53	56.24	55.17
FF20.015	0.015	66.82	5	177.16	78.74	84.45
FF30.005	0.005	14.85	15 (13)	68.89	30.62	33.63
FF30.010	0.010	34.94	7	130.18	57.86	62.84
FF30.015	0.015	44.55	5	167.42	84.36	97.46

Note: Number in brackets is the actual N used
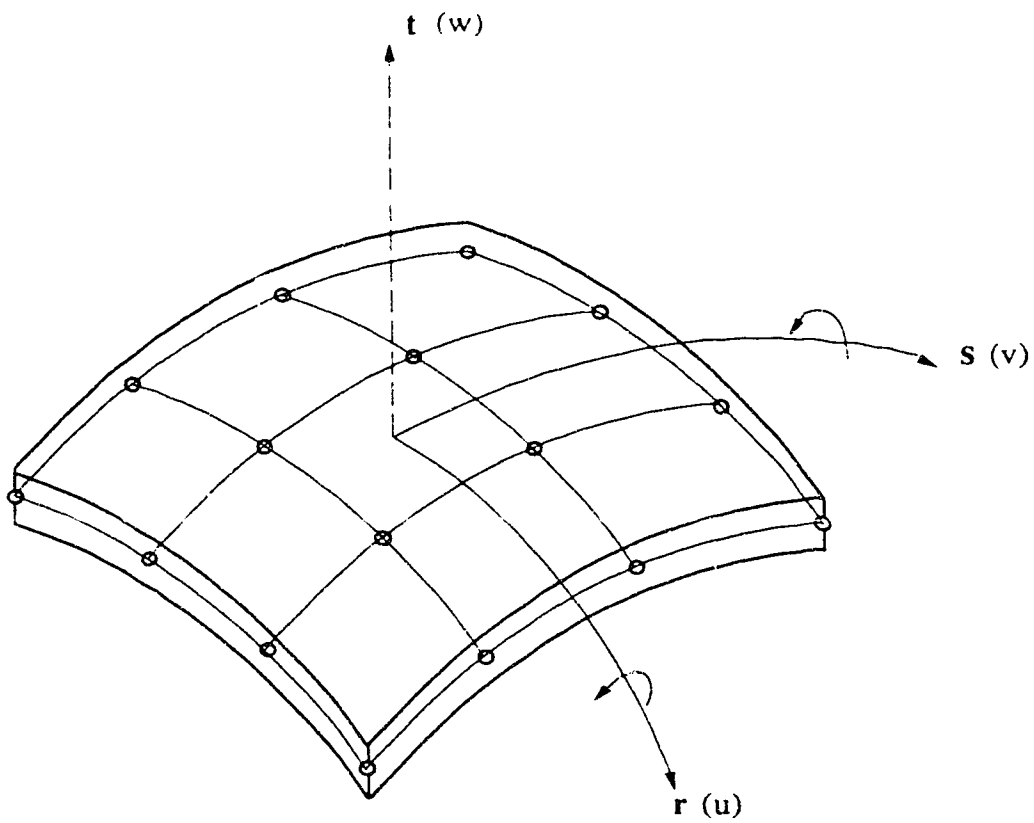
Fig 4.1: The 3-D degenerated plate-shell element (NISA80)

$$\sigma_{cu} = -\frac{1 + 3.65\,\alpha}{(1+\alpha)^2}\,f'_c$$

$$\alpha = \frac{\sigma_A}{\sigma_B}$$

(0.85f'$_c$, 0.5f$_t$)

-f'$_c$

f'$_t$
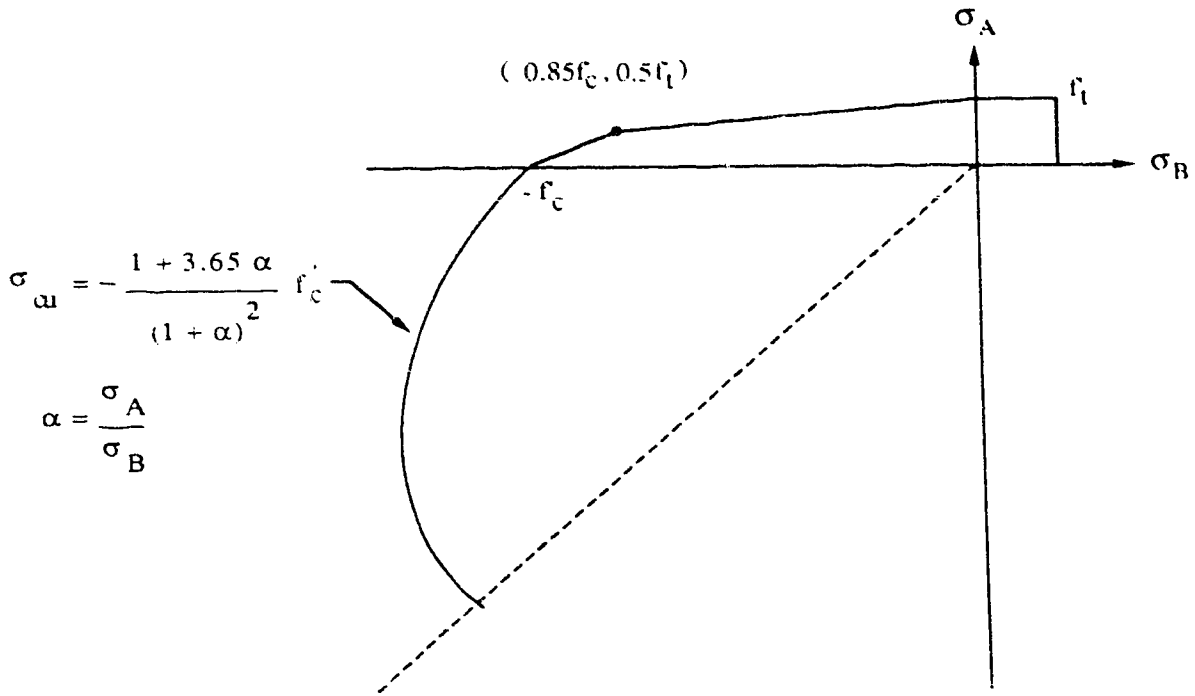
Fig 4.2a: Concrete failure envelope

Saenz-Curve

(ε_{cu},σ_{cu})

Linear strain softening

$(2E_c\dfrac{\varepsilon_{cu}^2}{\sigma_{cu}}, 0.2E_c\varepsilon_{cu})$
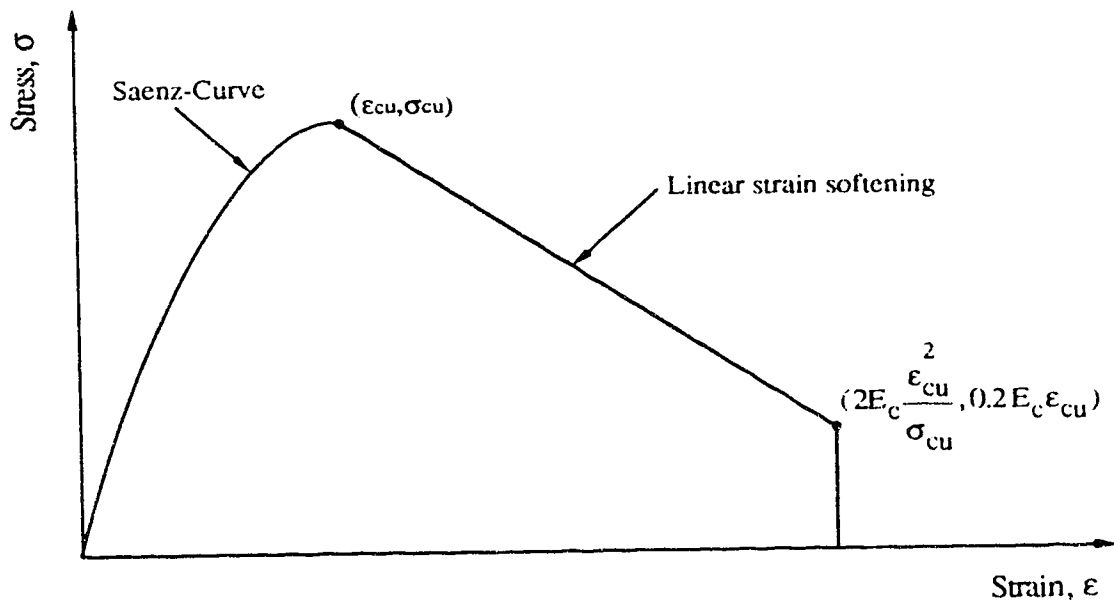
Stress, σ

Strain, ε

Fig 4.2b Stress vs Equivalent uniaxial strain for concrete in compression
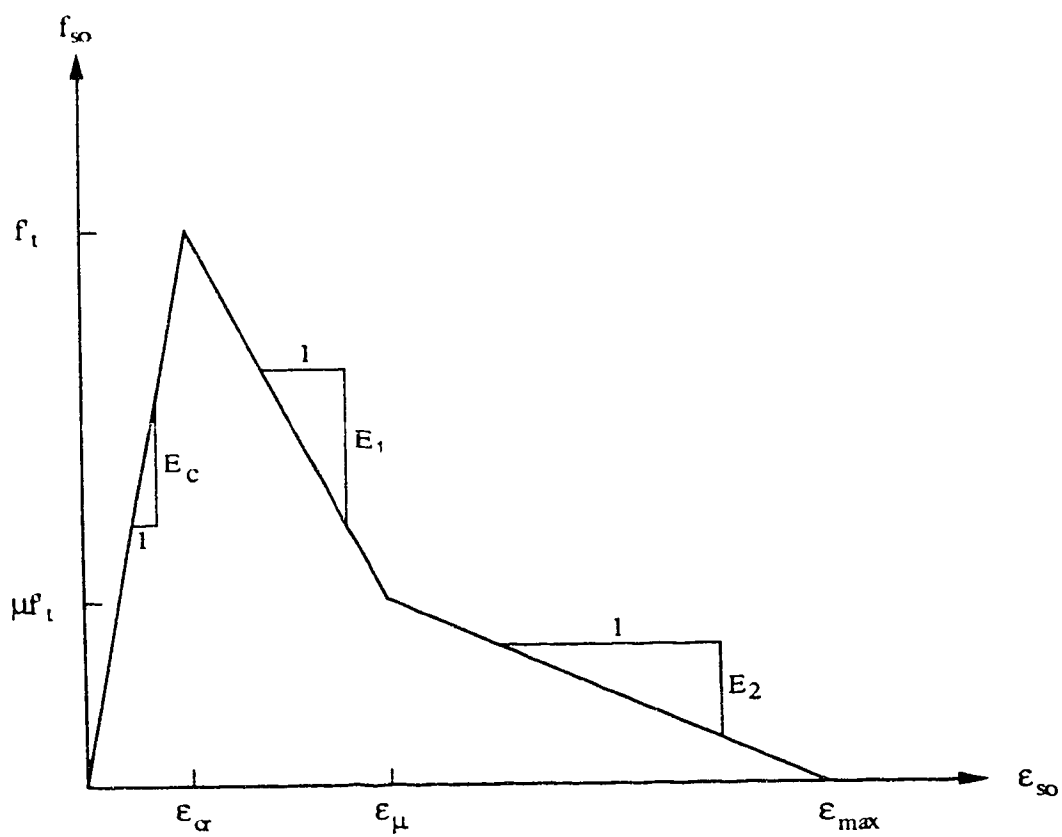
Fig 4.3: Trilinear tension softening curve for concrete
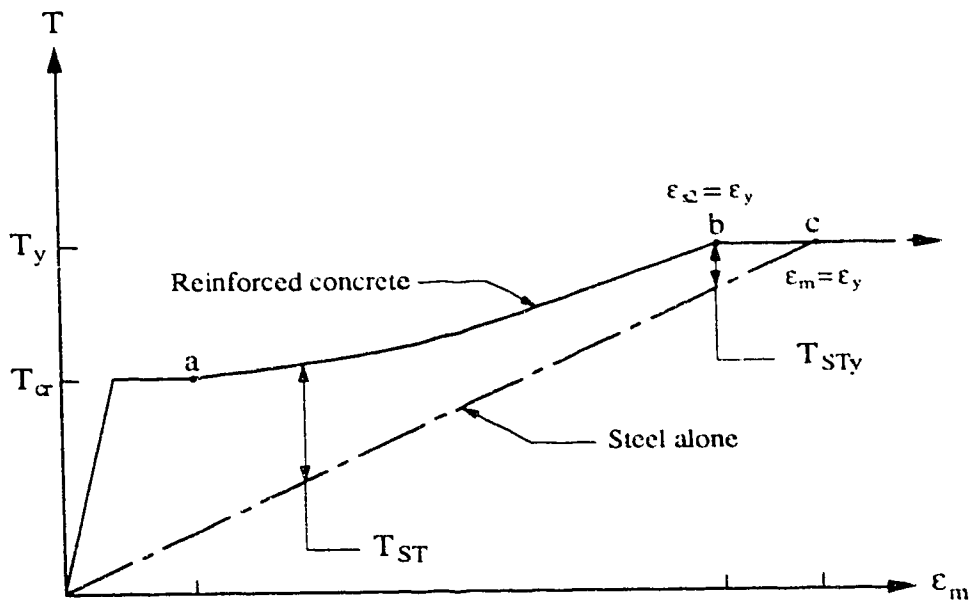
(a) Reinforced concrete member
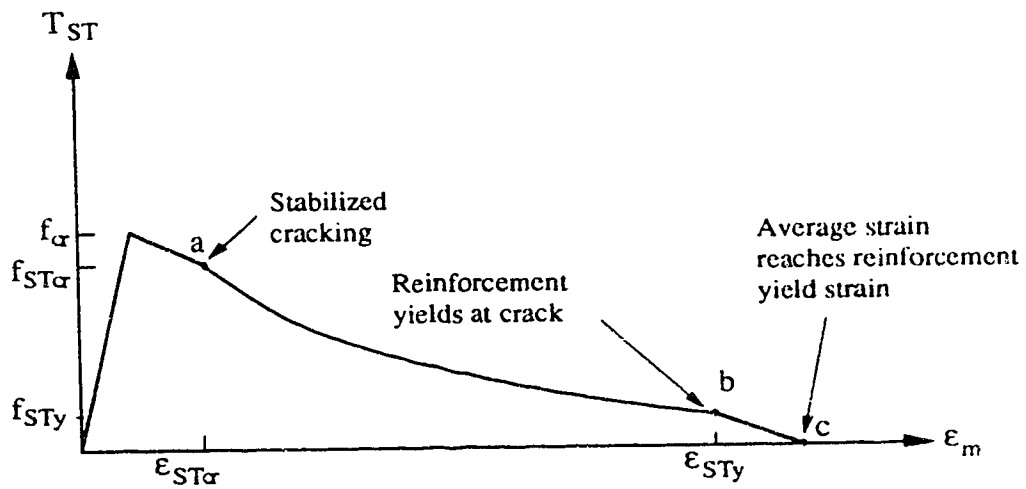
(b) Concrete contribution

Fig 4.4: Phases in tension stiffening model
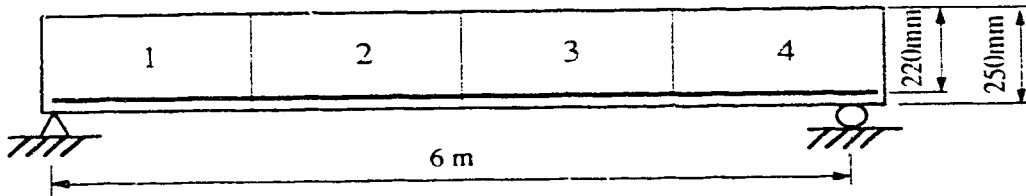
(a) Simply supported at both ends (SS)
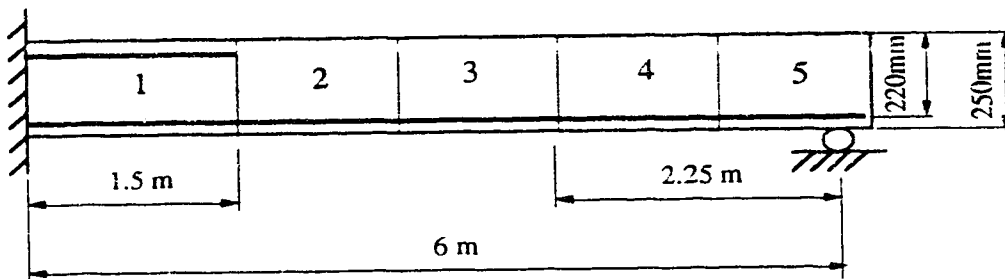
(b) Fixed at one end and simply supported at the other (FS)
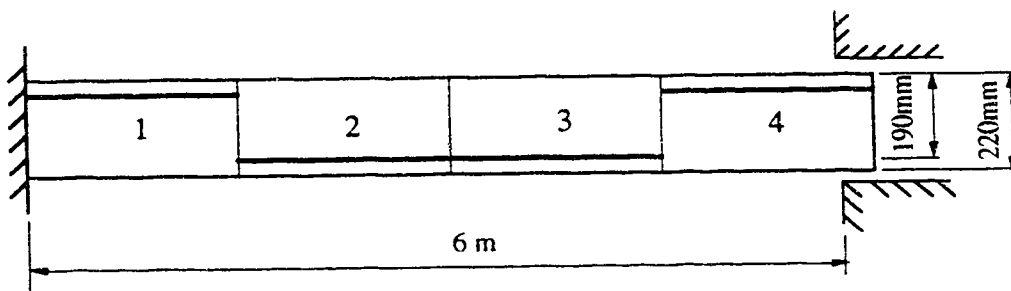
(c) Fixed at both ends (FF)

Fig 4.5: Parametric study specimens
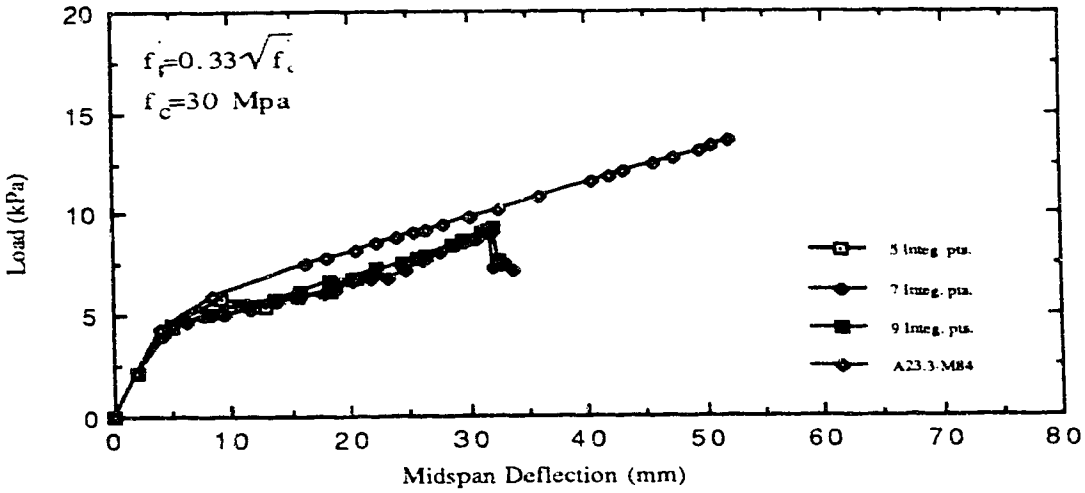
Fig 4.6: Load vs Midspan Deflection (SS)
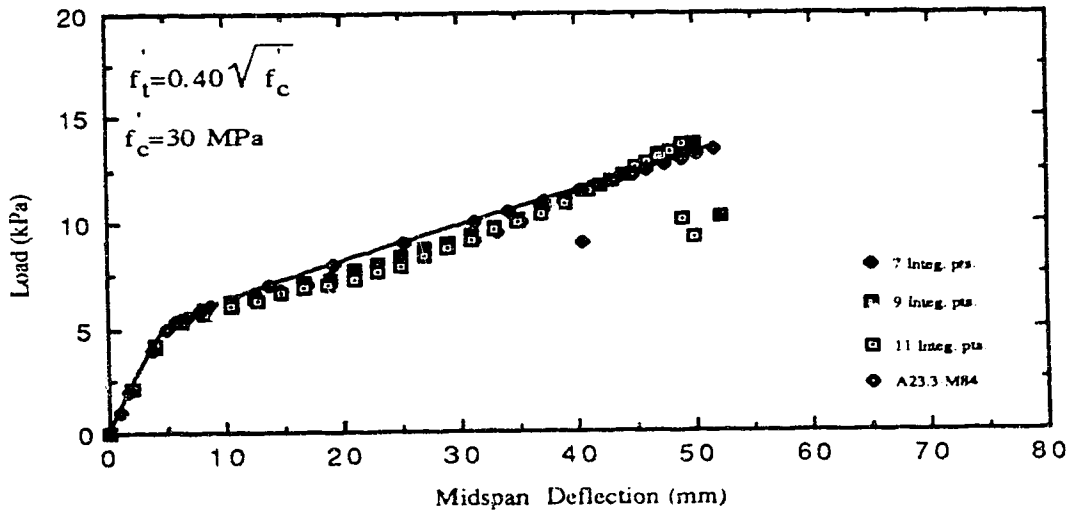
Fig 4.7: Load vs Midspan deflection (SS)
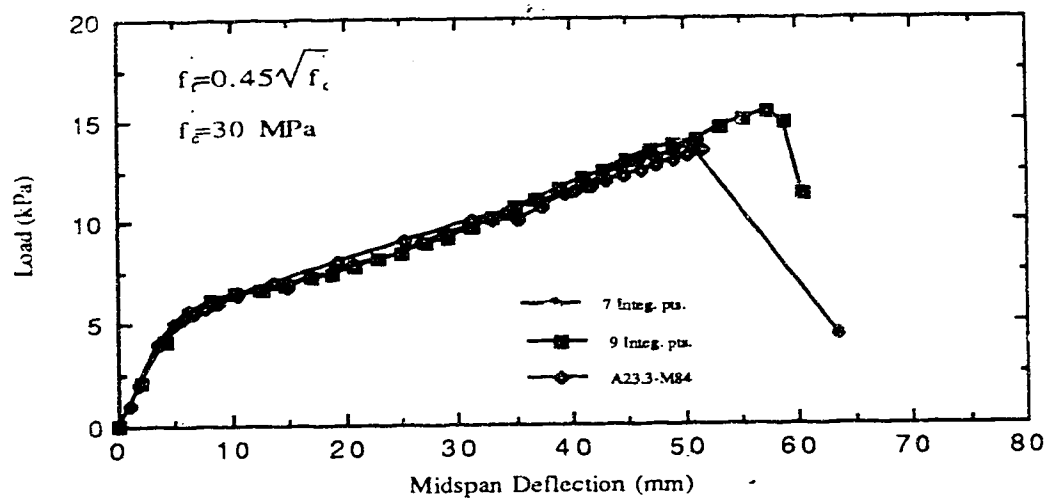
Fig 4.8: Load vs Midspan Deflection (SS)
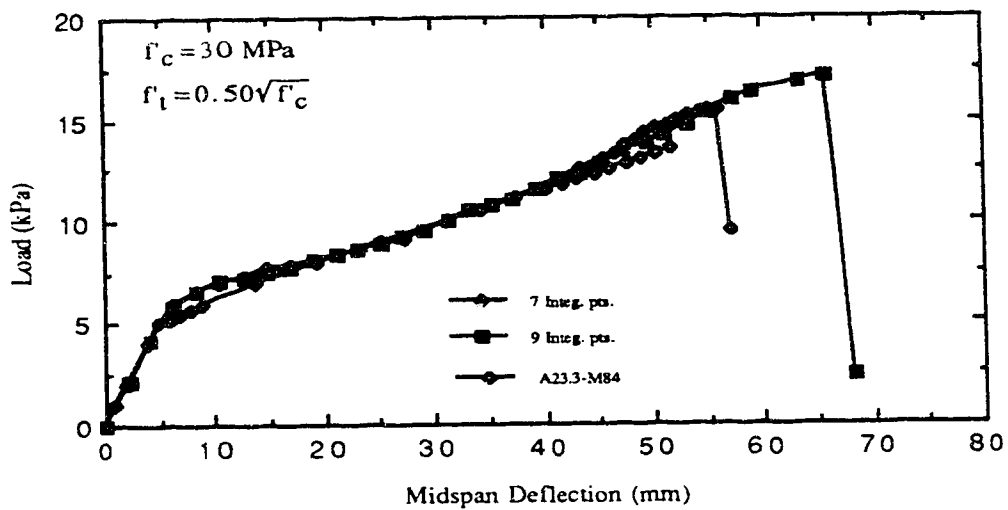
Fig 4.9: Load vs Midspan Deflection (SS)
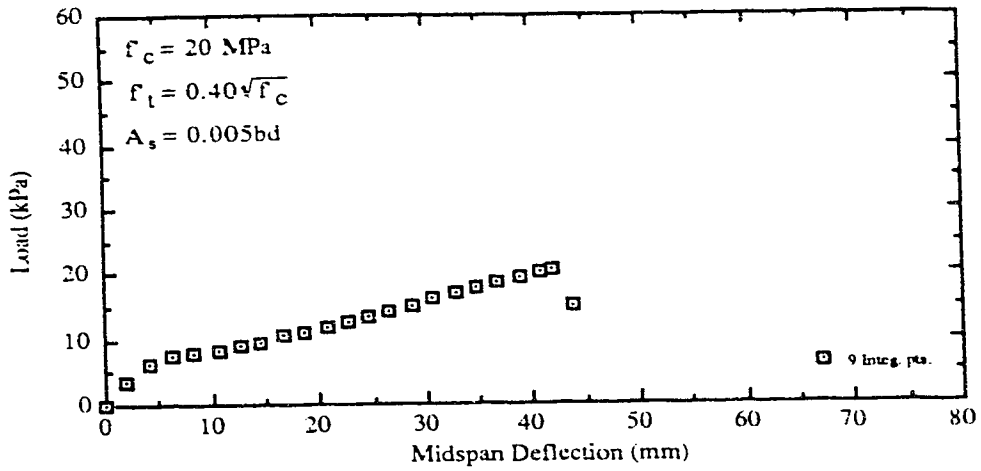
Fig 4.10a: Load vs Midspan Deflection (SS20.005)
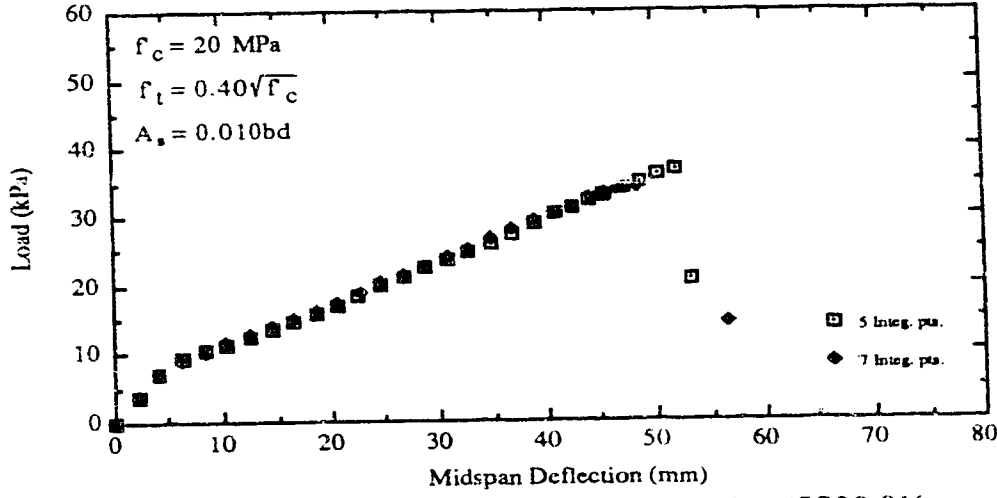
Fig 4.10b: Load vs Midspan Deflection (SS20.010)
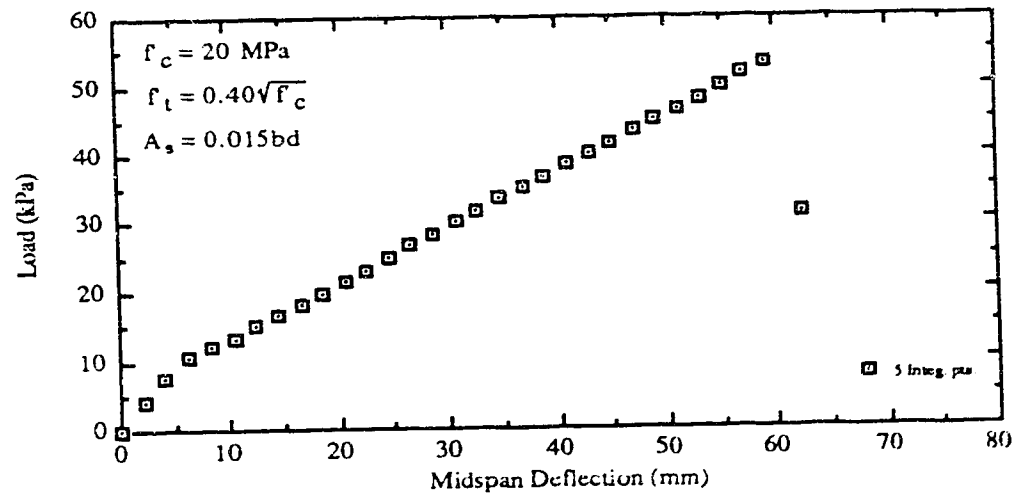
Fig 4.10c: Load vs Midspan Deflection (SS20.015)
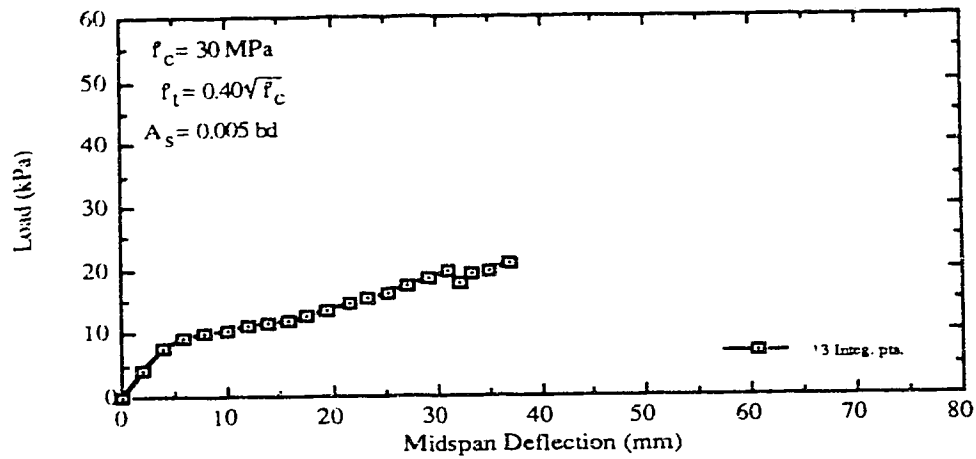
Fig 4.11a: Load vs Midspan Deflection (SS30.005)
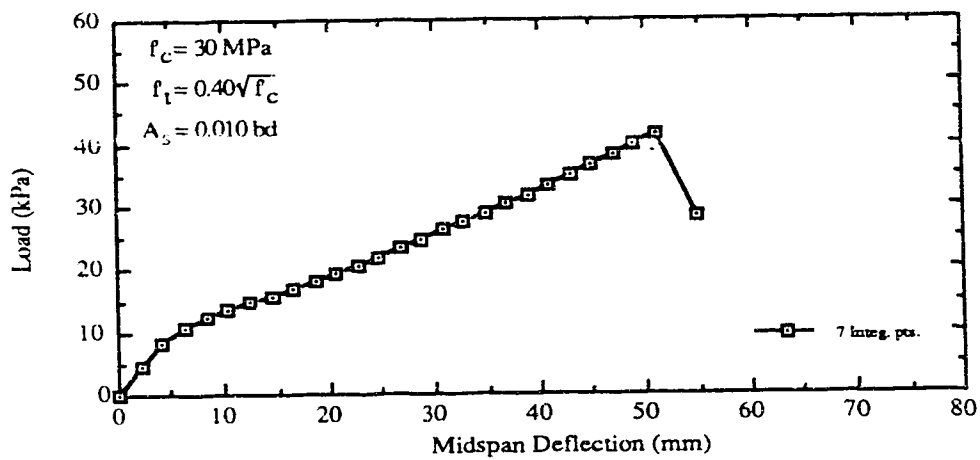
Fig 4.11b: Load vs Midspan Deflection (SS30.010)
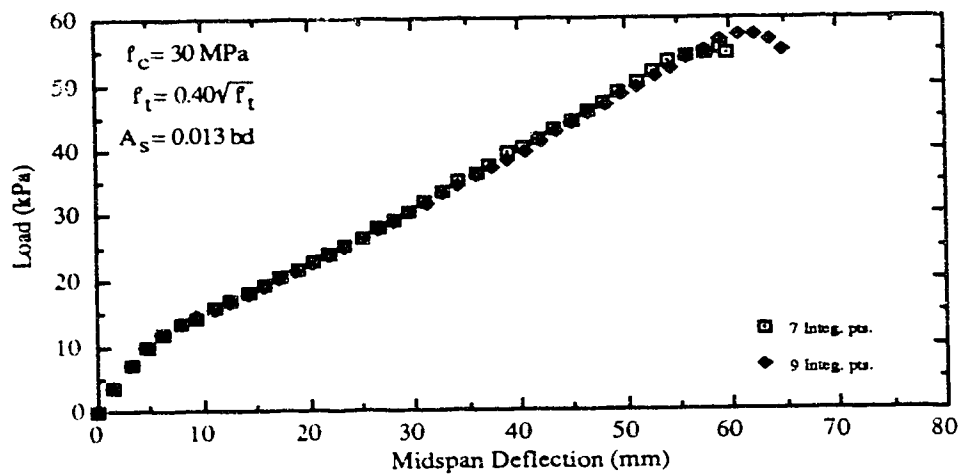
Fig 4.11c: Load vs Midspan Deflection (SS30.013)
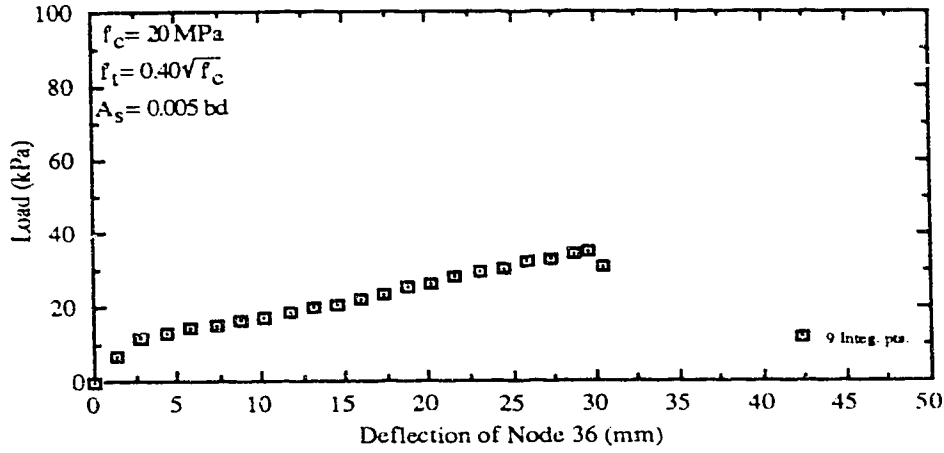
Fig 4.12a: Load vs Deflection (FS20.005)
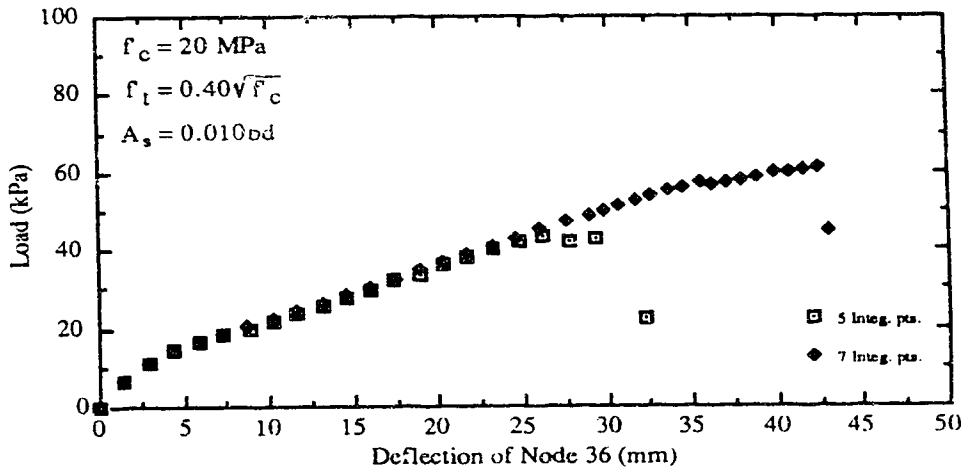
Fig 4.12b: Load vs Deflection (FS20.010)
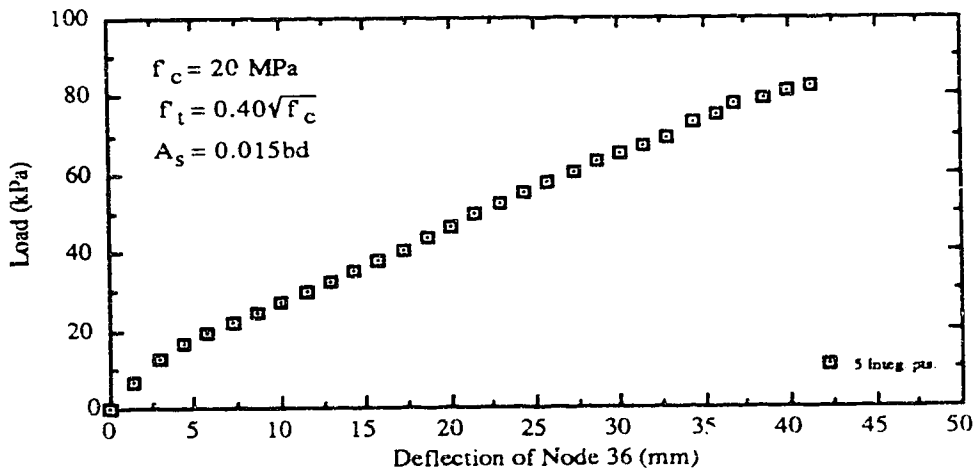
Fig 4.12c: Load vs Deflection (FS20.015)
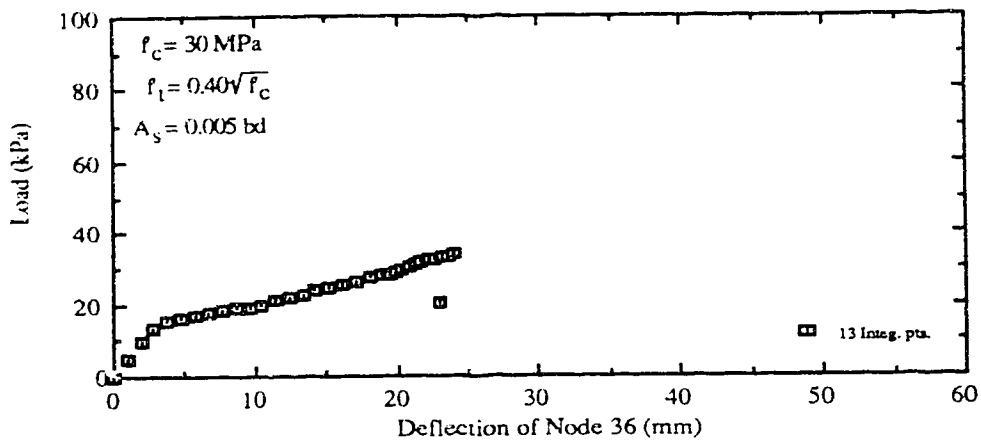
Fig 4.13a: Load vs Deflection (FS30.005)
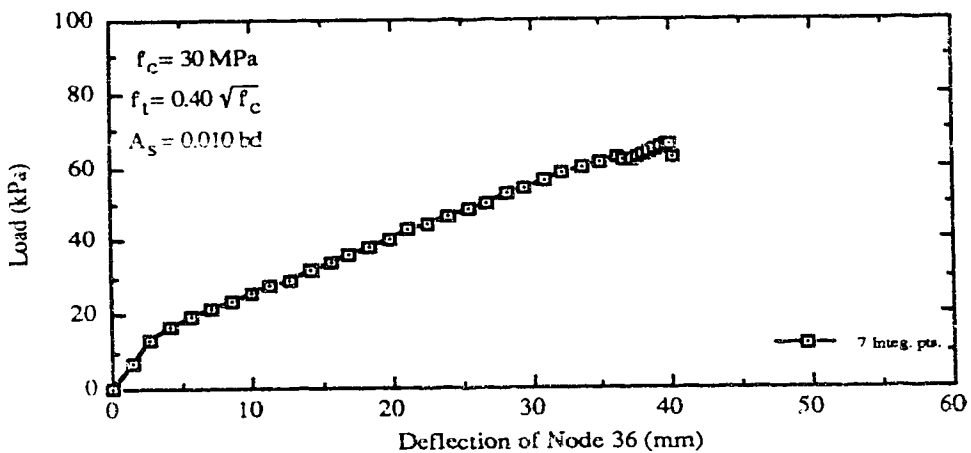
Fig 4.13b: Load vs Deflection (FS30.010)
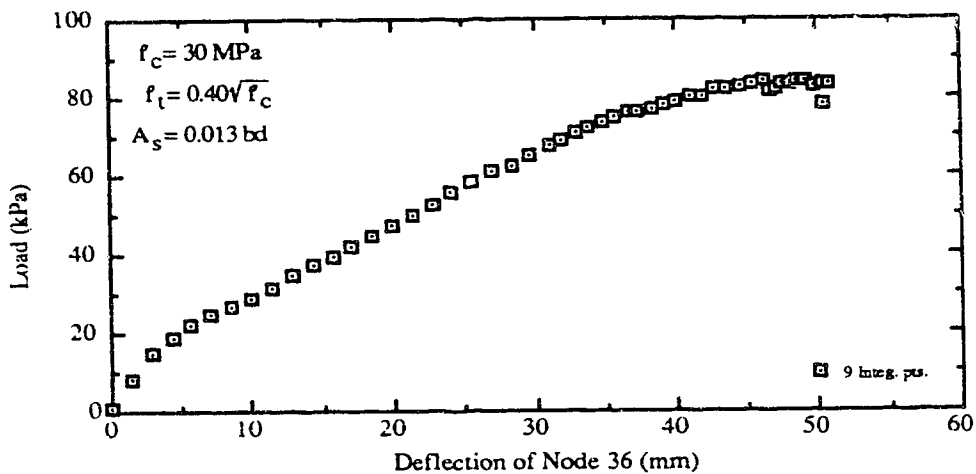
Fig 4.13c: Load vs Deflection (FS30.013)

$f_c = 20\,\mathrm{MPa}$

$f_t = 0.40\sqrt{f_c}$

$A_s = 0.005\,bd$

9 Integ. pts.
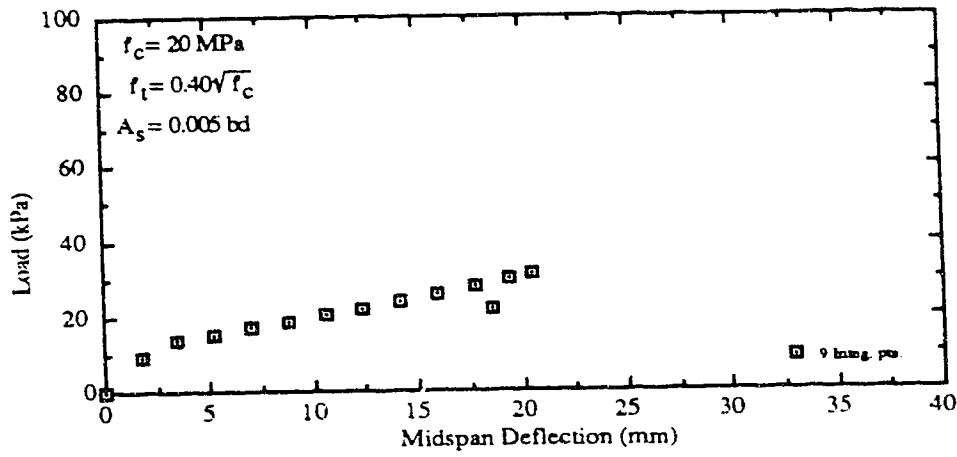
Fig 4.14a: Load vs Midspan Deflection (FF20.005)

$f_c = 20\,\mathrm{MPa}$

$f_t = 0.40\sqrt{f_c}$

$A_s = 0.010\,bd$

5 Integ. pts.

7 Integ. pts.
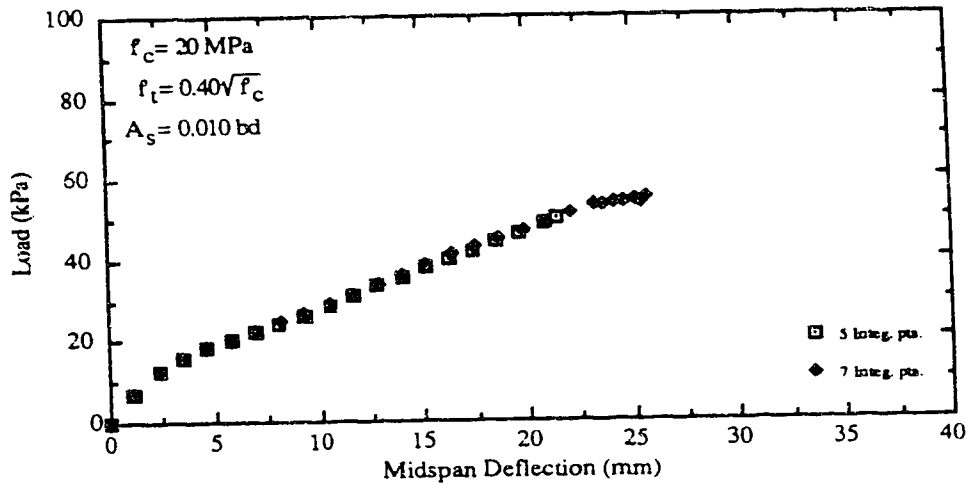
Fig 4.14b: Load vs Midspan Deflection (FF20.010)

$f_c = 20\,\mathrm{MPa}$

$f_t = 0.40\sqrt{f_c}$

$A_s = 0.015\,bd$

5 Integ. pts.
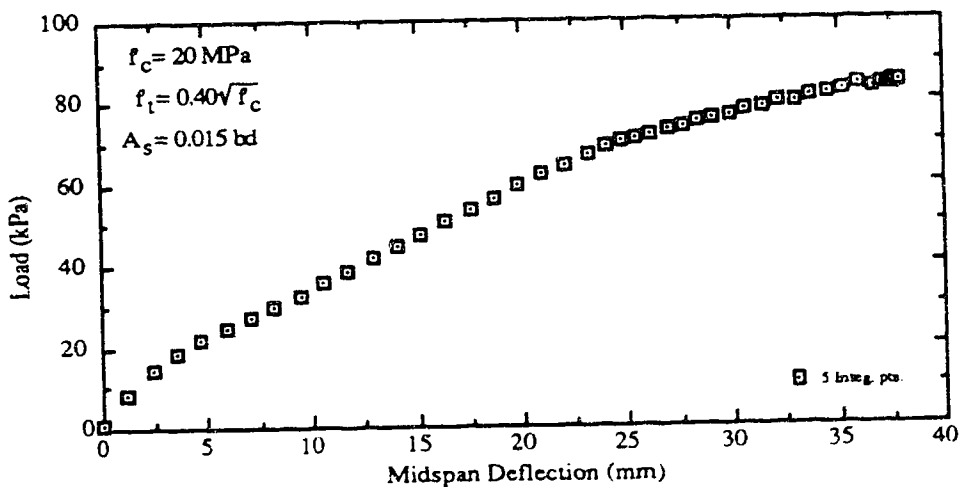
Fig 4.14c: Load vs Midspan Deflection (FF20.015)
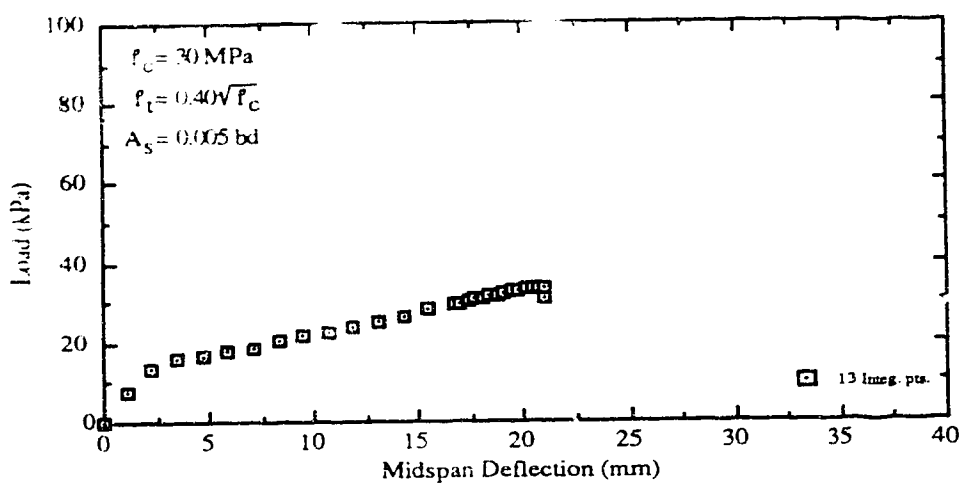
Fig 4.15a: Load vs Midspan Deflection (FF30.005)
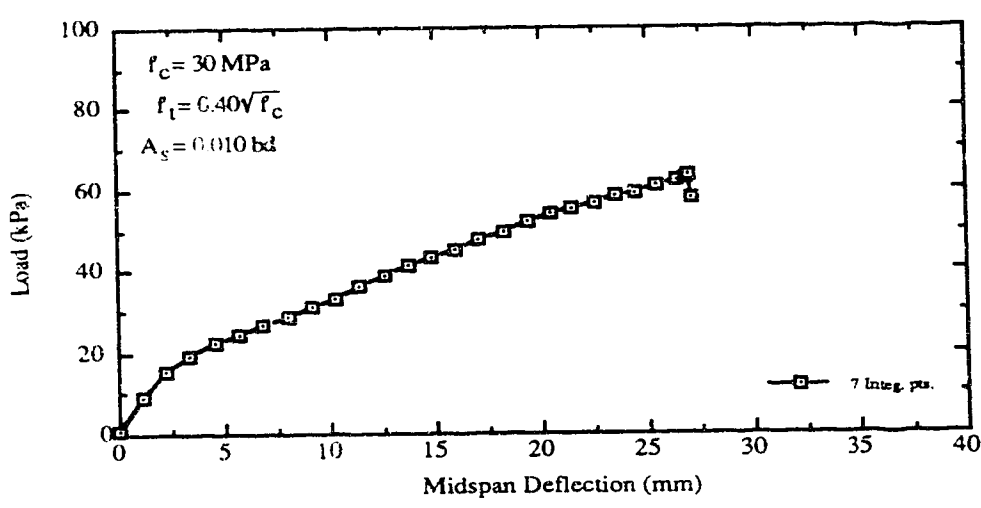
Fig 4.15b: Load vs Midspan Deflection (FF30.010)
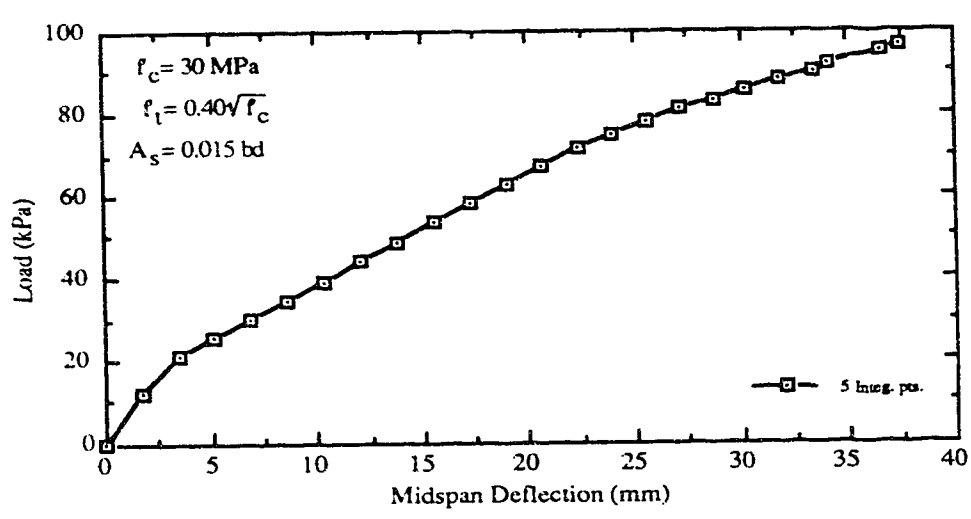
Fig 4.15c: Load vs Midspan Deflection (FF30.015)

Chapter 5

Finite Element study using NISA80

5.1 Modelling of the design strip

From Chapter 3, it was observed that solutions obtained for analysis of slab systems by the DDM' and the EFM may be different. Because of limited laboratory test data on slab systems, non-linear finite element analysis was used to provide numerical data which can be used to evaluate these procedures.

The finite element study was conducted on slabs having regular column layout to form square or rectangular panels. A typical interior design strip with 3 spans in the longitudinal direction was chosen (as shown in Fig 2.1). This choice was seen to be the minimum requirement to obtain solutions which can be compared to those from the DDM' and EFM.

Because of symmetry in both geometry and loading, only one quarter of the design strip is modelled, as shown in Fig 5.1. A typical arrangement of the slab elements is shown in Fig 5.2. In general, the maximum aspect ratio of plate-shell elements was limited to about 5.0, to reduce the number of elements as much as possible, without losing much accuracy. The number of slab elements was either 44 or 55, depending on the shape of the exterior column (Figs 5.2 and 5.3).

Columns were modelled using the 3-D beam element, which has six degrees of freedom at each node (three displacements and

99

three rotations). This beam element was chosen as it is the only element that can be coupled to the plate-shell element in NISA80.

Since the 3-D beam element is a linear element, the assigned stiffness does not change during a solution. However, this is a sufficient approximation for columns, since most of the cracking takes place in the slab and cracking that may occur in columns may be represented by reducing the column stiffnesses. Reinforcement in columns is not modelled.

Because the 3-D beam element has only two nodes at its ends, one of its ends has to be connected to one of the slab element nodes. The general arrangement of the coupling is shown in Fig 5.4.

To study the effect of column shapes on the behaviour, the slab region occupied by the actual column, shown as shaded in Figs 5.2 and 5.3, is represented by two or four slab elements that have been stiffened by increasing both the Young's modulus, E_c, and the tensile strength, f'_t. This ensures that the column cross section at the slab does not crack and remains plane during loading. The value of E_c selected was 1000 times that in the slab elements outside the column area.

Code procedures model the design strip with columns of length equal to the full storey height, fixed at the ends. In this study, inflection points are located at mid-heights of columns, to model a typical storey in a multistorey structure more realistically. Column heights were nominally 3500 mm (1750 mm from the middle surface of the slab to the inflection points at mid-column heights) but the actual heights were selected to give pre-selected

ratios of column to slab stiffness (α_{cs}). Actual column heights are given in Table 5.1.

The cutting planes to isolate the design strip are axes of zero twisting moments, zero shear and zero rotation. In order to reduce the effect of membrane forces in the slab, the only additional restraints applied to the slab are a translational restraint in the X direction, at the center of the exterior column and a translational restraint in the Y direction along the X-axis. For gross equilibrium of the resulting substructure under gravity loading only, the vertical displacements are zero at the base of the lower column stubs while the top of the upper column stubs were allowed to translate in the Z-axis only and rotate about the Y-axis only. The bottoms of the lower column stubs were prevented from translating in the other directions and could only rotate about the Y-axis. This arrangement also ensures that the exterior column deforms in double curvature at all stages of loading, with no secondary moments due to lateral displacement. The boundary conditions for each design strip are as shown in Fig 5.7.

5.2 Material properties and reinforcement layout

Concrete strength, f'_c, for all specimens was 30 MPa. NISA80 allows input of only a single value for number of layers across the depth of slab elements even though reinforcement ratios are different from element to element. For this reason, 11 layers was chosen in view of the likely low reinforcement densities in some slab elements.

Reinforcement was represented by a uni-directional, bilinear stress-strain curve, with a yield strength of 400 MPa at a strain of 0.002 and a tangent modulus of 2000 MPa, after yielding. The maximum strain was set at 0.12. Curtailment of reinforcement can not be represented within an element. Therefore, the termination of reinforcement coincides with the element boundaries.

A total of 24 reinforcement densities (thicknesses) were required to represent all the reinforcement patterns used in the slab portion of the structure. 10 densities were used for top reinforcement while 12 were used for bottom reinforcement. 2 densities were used as dummy reinforcement, in the stiffened column-slab regions. The layouts of top and bottom reinforcement are as shown in Figs 5.5 and 5.6, respectively.

5.3 Design strip variables and designation

The distribution of moments in the exterior panel is the major concern of this study. These moments are a function of the amount of rotation that takes place at the exterior column-slab connection, which is affected by the column-slab stiffness ratio, the amount of flexural reinforcement at this support and the panel geometry. From Chapter 3, it was also observed that the major differences in solutions obtained by the DDM' and EFM occured for l_1/l_2 ratios less than 1.0. Therefore, the main variables in the design strips are panel aspect ratio, l_1/l_2, exterior column size and aspect ratio, exterior column-slab stiffness ratio, α_{cs}, and amount of flexural reinforcement at the exterior column support. The

procedure for computing the column-slab stiffness ratio is described in Appendix C.

In all cases, CAN A23.3-M84 (dead and live load factors of 1.25 and 1.50, respectively) was used to obtain the reinforcement quantities and distribution. The slab was reinforced for a service load of 7.2 kPa (4.8 kPa Dead and 2.4 kPa Live Load), corresponding to a load ratio of 2.0 in Chapter 3. The longer center to center dimension of each panel and the slab thickness were maintained at 7000 and 200 mm, respectively.

The designation used in this study is of the form; *N <panel aspect ratio> <column aspect ratio> <column-slab stiffness ratio> <portion of M_0 for reinforcement at exterior support>*, where N stands for series geometry for which solutions using the program NISA80 were obtained. For the sake of brevity in the designation, panel aspect ratio is given as an integer obtained by multiplying the panel aspect ratio by 10. The exterior column sizes, represented by letters, and the corresponding column to slab stiffness ratios are presented in Table 5.1. These sizes correspond to the sizes in Table 3.1 but with defined dimensions rather than cross sectional areas. Size C in this Table 5.1 is redefined as 350x350 mm. For all design strips, interior columns are square and of size either 350 or 500 mm. For design strips with square exterior columns, interior columns are of the same size as the exterior columns. For design strips with rectangular exterior columns, interior columns are of size equal to the smaller dimension of the exterior column.

Reinforcement thicknesses at any critical section were evaluated from the moment obtained by assigning a fraction of the total static moment for that span, to the critical section. In the longitudinal direction, exterior spans were reinforced for one of 0.2, 0.3 or 0.4 M_0 at the face of the exterior column support while the face of the interior support was always designed for 0.7 M_0. The midspan of the exterior span was reinforced for 0.55, 0.50 or 0.45M_0, to satisfy the total static moment in this span, but not less than the minimum reinforcement specified in A23.3 (1989), namely 0.002A_g. The reinforcement densities in the interior spans were always evaluated for 0.70 M_0, at the support, and 0.35 M_0 at midspan, as the number of spans was limited to 3. In the transverse direction, the reinforcement densities were always evaluated for 0.65 M_0 at the support and 0.35 M_0 at midspan, simulating a typical interior design strip.

Thus, a design strip designated as N20B6.2 is from series N, having a panel aspect ratio (l_1/l_2) of 2.0, exterior column size of type B, exterior column-slab stiffness ratio of 6.0 and is reinforced for 0.2 M_0 at the face of the exterior column support.

5.4   Solution procedure and accuracy

Each design strip was subjected to uniformly distributed gravity load increments for as long as convergence could be reached. In most cases, 5 load steps were used up to self weight and an additional 5 to reach service load level.

The load control strategy was continued until convergence was difficult to achieve. All solutions were obtained using the MNR

iteration technique with the number of iterations limited to 30, for each load step. If convergence could not be reached by reducing the load step to a reasonable value, the solution strategy was changed to CALM. The tolerance was varied depending on the size of the load increment; lower values for bigger load increments and higher values for smaller ones but the minimum tolerance used was 0.01.

Each solution was monitored by checking the statical equilibrium of converged steps and also examining local failures in elements positioned in the vicinity of the critical sections. Statical equilibrium was achieved if the total panel static moment, M_0, at each load level, was satisfied within 5%. Once excessive cracking, crushing or unloading occurs in the various elements, convergence is very difficult to achieve. Even if convergence is attained, statical equilibrium, as defined above, may not be satisfied. The solution was stopped once statical equilibrium was not satisfied. In all cases, solutions beyond the service load level were obtained.

Moments at critical sections are presented as ratios of the total static moment in each span, M_0, in Tables 5.2 and 5.3, at the service and factored load levels. It can be seen that some design strips could not be loaded to the factored load level (9.6 kPa). This may be due to local failure resulting from high moment gradients at regions near the supports and the failure criterion in the concrete material model. Once concrete failure is reached in compression at a gauss point, it occurs in all directions and the capacity of that concrete layer is lost. This means that the moment capacity at that section could not be maintained until a mechanism

is formed. Therefore, it may be argued that the existing concrete material model does not represent moment redistribution well. Massicotte obtained solutions mainly for specimens that did not have such high moment gradients or require the same level of moment redistribution.

Although it was not possible to load all design strips until a full flexural mechanism was achieved, it is believed, because of the criterion used to terminate the solutions, that the results are reliable up to the maximum load reported.

5.5 Obtaining slab and column moments

Moments in the sla output from NISA80 are at gauss points and not at positions of the critical sections. Therefore, interpolation or extrapolation is required to obtain moments at these sections. The procedure for obtaining interpolated or extrapolated moments is described in Appendix B. The total moment across a critical section is obtained from these moments by using the trapezoidal rule.

Column forces are output for the 3-D beam element. These were used to confirm the total applied load on the design strip. Exterior column centreline moments were calculated by making use of the support joint shear forces and the column height. The reduction of the exterior column centreline moment to the design section, ΔM, was obtained as the difference between the centreline moment and the extrapolated moment at Section 1.

5.6 Load-Deflection response

Although the deflections at all nodes were output at each load level, load-deflection plots (Figs 5.8a to 5.28a), are presented for four nodes only, for selected design strips. These nodes are located on the edge and centreline of the design strips, at midspans between columns and are the numbered nodes in Figs 5.2 and 5.3.

Since the purpose of this series of analyses is to obtain data to evaluate the DDM' and EFM and these methods do not predict deflections, the only reason for examining the deformation response is to assist in assessing the reliability of the finite element solutions. From the deflection data, the relative magnitudes of deflections at the four nodes monitored are as expected in the prototype slab. The non-linear response indicates that some moment redistribution is taking place. It is believed that the magnitudes obtained are realistic of the short term deflection, for the slab design strips they represent.

5.7 Design moments at critical sections

For selected design strips, complete load-moment ratio plots are presented for the exterior span in Figs 5.8b to 5.28b. It is immediately apparent that the moment ratio at any critical section is also a function of the level of loading. Loads near zero correspond to the elastic solution of the uncracked plate. As the load increases, there is a redistribution of moments due to cracking and non-linear behaviour of the concrete. Since the intensity of loading is not a parameter with the DDM' and EFM, the question arises as to which is the appropriate load intensity to be used

when evaluating these methods. Since all slabs will crack due to construction and applied loads, obviously, the uncracked state is not consistent with ultimate strength design. The likely load levels for design are service and factored. For this reason, moment ratios from NISA80 are presented for all design strips only at the service load (7.2 kPa) and the factored (9.6 kPa) or the maximum reliable load reached, in Tables 5.2 and 5.3.

When selecting reinforcement, an equivalent density of reinforcement was provided at sections based on the usual theory of reinforced concrete that assumes cracked sections where concrete takes no tension and a rectangular compressive stress block. Thus, as the load level approaches ultimate load, it was expected that the moment ratios would approach the ratios of panel static moment for which reinforcement was provided (a parallel yield line pattern).

Densities of reinforcement were provided based on the material resistance factor ϕ_S of 0.85 so as to correspond more closely with the reinforcement that would be provided in a prototype slab. In NISA80, this implies a failure load of 1.18 times the factored load of 9.6 kPa. However, the computer cost to reach the failure load because of the much smaller load increments is significant. For this reason, solutions were generally stopped at load levels approximately 10% greater than the factored load. This is justified as the study is aimed at the behaviour of slabs at the service and factored load levels.

At Section 1, the reinforcement provided to resist the selected portion of M_0 was all placed in the column strip, in

accordance with the code provisions for slabs without edge beams. However, NISA80 computes the moments by integrating stresses through the thickness. For those elements in the middle strip that were not provided with flexural reinforcement, the concrete model will still provide a moment resisting capability, since the section will not be fully cracked. Thus, for lightly reinforced sections, the total moment capacity across Section 1 will be greater than the capacity based on the reinforcement provided. Since it is common practice to provide additional reinforcement along the free edge to improve serviceability, the predicted behaviour using NISA80 may in fact be closer to what actually happens. As equilibrium of the moments in the panel is satisfied, an overestimation of the moment across Section 1 will also affect the moments at the other critical sections. Furthermore, especially for rectangular panels, the reinforcement density provided in the short direction to resist positive moment, is selected to satisfy minimum reinforcement of $0.002A_g$ rather than flexural requirements. For these reasons, caution is required in interpreting specific values at factored load and only a general discussion of trends in behaviour is possible.

5.7.1 Square panels

For selected square panels, the variation of load with moment ratio are presented in Figs 5.8b to 5.17b. It may be observed that, at the uncracked stage, the distribution of the static moment in the exterior span is essentially independent of the reinforcement provided at the exterior support and only slightly affected by the difference in the column to slab stiffness ratio. As

cracking progresses due to increasing load, there is a drop in the portion of moment resisted at the supports which is compensated for by an increase in positive moment ratio at Section 2. This is attributed to the cracking of the concrete in the vicinity of columns. This effect continues until near service load, at which stage, increased cracking at the positive moment region occurs, resulting in a reduction in the portion of moment carried by Section 2.

The effect of the stiffness of the exterior column on the moments in the exterior panel should be apparent by comparing two identical strips except for the ratio of the exterior column to slab stiffness ratio. Thus, one can compare Fig 5.8b with 5.10b and 5.9b with 5.11b. It is seen that the moment ratio curves are almost identical. To properly evaluate the effect of exterior column to slab stiffness ratios on design moment ratios would require solutions for exterior columns smaller than 500 by 500 mm (Size B). However, to keep the number of elements manageable and element panel aspect ratios acceptable, design strips with smaller exterior column sizes were not analysed. It is concluded that the insensitivity of moment ratios at Section 1 to exterior column-slab stiffness ratio is because the more flexible column used (column-slab stiffness ratio of 6.0) is already stiff and doubling the stiffness ratio has minimal effect.

However, the stiffness ratios used permit evaluating the effect of reinforcement ratio on the moment ratios as the columns are sufficiently stiff to allow determination of the development of the reinforcement at Section 1. By looking at the design strips,

N10B6 and N10B12 (Figs 5.8b and 5.11b), a change in amount of reinforcement provided at the exterior support from 0.2 to 0.4 M_o, results in a variation in design moments at the exterior support from 0.27 to 0.35 M_o. The fact the moment ratio is greater than 0.2 is due to the tension in the uncracked concrete, as explained later.

The same trends may be observed for square panels with size L (1000x500) exterior columns (Figs 5.14 and 5.15). For these design strips, it may be observed that for an extremely long column and low reinforcement ratio at the exterior support (N10L6.2), the exterior column is able to rotate and cracking at Section 1 is delayed, allowing moments greater than those for which the reinforcement is provided to be carried. When the reinforcement provided at Section 1 is doubled, the maximum load reached is slightly lower than that for which the reinforcement is provided for at Section 1 indicating that the reinforcement could not be developed. When a realistic column length is used (N10L48, Figs 5.17), the rotation of the exterior column is small as the column is very stiff, so that when a low reinforcement ratio is used at the exterior support, major cracking occurs at about the self load level and the reinforcement yields. This can also be observed in Fig 5.17a, where there is sudden change in the load-deflection response at about the self weight level. However, by using twice the reinforcement ratio, the cracking is delayed, allowing loads greater than the factored to be reached and the final moment ratio at Section 1 is about 0.38.

The influence of the exterior column shape on the design moment ratios may be examined by considering design strips

having the same exterior column-slab stiffness ratio, for example design strips, N10B12, N10I12 and N10L12 in Table 5.2. There appears to be no significant difference in design moment ratios at Section 1, although the moment developed tends to increase with increasing perimeter of the exterior column. A definite conclusion can not be drawn since the columns used are stiff for the slab geometries chosen.

In the interior span, it may be observed from Table 5.2, that for all design strips, the final design moment ratios are less than 0.60 at Section 4 and more than 0.40 at Section 5. The distributions are not affected by the amount of reinforcement provided at the exterior support.

5.7.2 Rectangular panels

For rectangular panels, load-moment ratio plots are presented in Figs 5.18b to 5.28b. Figs 5.18b to 5.24b are for panel aspect ratios less than 1.0, while Figs 5.25b to 5.28b are for panel aspect ratios greater than 1.0. The general variation in moment ratios with load are different for these two cases and are discussed seperately.

For a panel aspect ratio of 0.5, it is possible to define a column as small as 350x350 mm (Size C) and still maintain reasonable element aspect ratio, except for elements located in the middle strip, which were not considered critical to the accuracy of a solution.

For panel aspect ratio of 0.5, it can be observed that the distribution of moment ratios to critical sections in the exterior

span does not change until near the service load level. The effect of the smaller exterior column stiffness on the moment ratio at Section 1 is seen by comparing the critical moment of about 0.3 M_O with exterior column size C ($\alpha_{cs}=0.83$) to the critical moment of 0.4 M_O for exterior columns with stiffness ratios of 3.0 or greater.

Beyond this load level, there are continuous drops in moment ratios at both Sections 1 and 3, while the positive moment section (Section 2) continues to take larger moment ratios. In general, it may be seen that the critical sections at the supports take less moment than the reinforcement provided at Section 1. This is because the moment capacities provided at Section 2, resulting from the provided minimum reinforcement of $0.002A_g$ are nearly as large as the total exterior panel moment, M_O. For panel aspect ratios of 0.50 and 0.75 with size B columns, the capacities are 0.97 and 0.77 M_O, respectively. Therefore, for a panel aspect ratio of 0.5, it is not surprising that the design moment ratios at the critical sections are not much influenced by the reinforcement provided at the exterior support, but by the exterior column to slab stiffness ratio and the moment capacity at Section 2. A similar but not so drastic effect is also observed for a panel aspect ratio of 0.75.

For panel aspect ratios greater than 1.0, the behaviour shown in Figs 5.25 to 5.28 is different from the above, in that minimum reinforcement at the positive critical sections does not control. For a panel aspect ratio of 1.33, the reinforcement provided at the exterior support has some effect on the final moment ratios, which ranged from 0.25 to 0.40, at Section 1 and were about 0.50 and 0.65 at Sections 2 and 3, respectively. For a panel aspect ratio of

2.0, the design moment ratios at Section 1 are essentially independent of the reinforcement provided. This is due to the relatively shorter width of the design strip, which permits some of the moment to be taken by the tension in the concrete. For this reason, the reinforcement provided at the exterior support has little effect on the final design moment ratios.

Ir the interior span, like square panels, it may be observed from Table 5.3, that for all design strips, the final design moments ratios are less than 0.60 at Section 4 and more than 0.40 at Section 5. The distributions are not affected by the amount of reinforcement provided at the exterior support. This indicates that, the design moment ratios by the codes of practice may be reasonable for the uncracked stage, but overestimate the negative moment for the service and factored load levels.

5.8   Distribution of critical moments to column and middle strips

The code transverse distribution of critical moments to column and middle strips for slabs without beams is independent of the panel aspect ratio and reinforcement provided at the critical sections. The percentage distribution of design moments at critical sections to the column strip are; 100% at exterior column supports, 75% at interior column supports and 60% at the positive moment sections.

Analyses using NISA80 were carried out for slabs without beams and moments at critical sections are presented in Tables 5.4 and 5.5, for square and rectangular panels, respectively. Percentage distributions to column and middle strips are compared

for each design strip, in Table 5.6, at the service and factored load levels only, although percentages were computed at each load level. These distributions are at positions of gauss points located closest to the critical sections, in the unstiffened portions of the slab. In general, it was observed that the distribution of moments did not change much with load increase except at higher load levels. The distributions are generally presented as ranges of percentages, pertaining to the change in amount of reinforcement provided at the exterior support.

At column support sections (Sections 1, 3 and 4), the magnitude of the moment across portions of the middle strip may be positive, resulting in the total moment being less than the portion in the column strip. For those cases, the column strip was assigned 100% of the total design moment at the section.

From Tables 5.6a and b, for square panels, practically all the moment at Section 1 goes to the column strip. At Section 2, column strip moments are in the range 50 to 56% at service and 50 to 54% at the factored load level. At section 3, regardless of the exterior column aspect ratio, stiffness ratio and reinforcement provided at the sections, column strip moments are in the range 71 to 74% at service and 68 to 72% at factored load level. At Section 4 (interior span), column strip moments are lower than those at Section 3, by about 7% for square panels with size B (500x500) exterior columns. Column strip moments are in the range 68 to 72% at service and 64 to 71% at factored load level. At Section 5 (interior span), column strip moments are in the range 57 to 61% at service and 54 to 56% at factored load level.

From the above discussion, it may be concluded that the code transverse distribution of critical moments to column strips, is adequate for square panels.

From Tables 5.6a and b, as the panel aspect ratio increases, a lesser fraction of the total moment at all sections goes to the column strip. At service load, increasing the panel aspect ratio from 1.0 to 2.0, resulted in column strip moments of approximately 100, 50, 60, 60 and 50%, at Sections 1 to 5, respectively. The amount of flexural reinforcement provided at the exterior support had minimal effect on the percentage distributed to the column strip. As the slab tends to bend primarily in one direction, the distribution at the positive moment critical sections become uniform.

Decreasing the panel aspect ratio from 1.0 to 0.5 resulted in the column strip moments of 100, 60, 100, 100 and 60% at Sections 1 to 5, respectively, at the service load level.

Similar distributions of moments were observed at the factored load level, as seen in Table 5.6b.

It is clear that the lateral distribution of moments, for slabs without beams, is a function of the panel aspect ratio. In A23.3, for slabs with beams, the distribution of moments at critical sections is a function of panel aspect ratio, presumably based on elastic solutions of rectangular panels with non-deflecting supports. The reason for not doing so for slabs without beams is not clear, but could be due to a lack of suitable data from which conclusions could be drawn since solutions for column supported slabs based on plate theory are few.

Major variations in the column strip moments occur at the negative moment critical sections. As the panel aspect ratio increases, there are sharper drops in column strip moments at the interior supports compared to the exterior ones. Thus, a new distribution of moments for slabs without beams is proposed and is presented in Table 5.7. The values in the parenthesis are the present code (A23.3) provisions for distribution to the column strip. Interpolation between values in Table 5.7 is suggested.

Table 5.1: Exterior column size, column-slab stiffness ratio and actual length

Design Strip	c_1 (mm)	c_2 (mm)	α_{cs}	Column length (mm)
N5C1	350	350	0.83	2931
N5A2	350	700	1.60	2931
N5D6	700	350	6.00	3752
N7C1	350	350	1.20	2931
N7A2	350	700	2.40	2931
N7B6	500	500	6.00	2931
N7D9	700	350	9.00	3752
N10B6	500	500	6.00	3906
N10B12	500	500	12.00	1953
N10I12	500	1000	12.00	3906
N10I24	500	1000	24.00	1953
N10L6	1000	500	6.00	31250
N10L12	1000	500	12.00	15625
N10L48	1000	500	48.00	3906
N13B9	500	500	9.00	3472
N20B12	500	500	12.00	3906

Table 5.2: Design moment ratios for square panels

Design Strip Section	SERVICE LOAD (7.20 kPa)					Load	MAXIMUM OR FACTORED LOAD				
	1	2	3	4	5		1	2	3	4	5
N10B6.2	0.306	0.537	0.621	0.595	0.405	9.60	0.281	0.524	0.671	0.581	0.419
N10B6.4	0.341	0.523	0.612	0.591	0.409	9.60	0.378	0.496	0.630	0.559	0.441
N10B12.2	0.308	0.535	0.623	0.593	0.407	9.60	0.297	0.525	0.653	0.545	0.455
N10B12.4	0.349	0.519	0.612	0.591	0.409	9.60	0.361	0.503	0.634	0.570	0.429
N10I12.2	0.353	0.530	0.586	0.614	0.386	9.30	0.368	0.521	0.591	0.596	0.404
N10I12.4	0.416	0.506	0.572	0.609	0.391	9.60	0.427	0.506	0.561	0.561	0.404
N10I24.2	0.356	0.513	0.552	0.563	0.438	7.85	0.405	0.528	0.593	0.536	0.464
N10I24.4	0.404	0.518	0.557	0.561	0.438	8.85	0.403	0.517	0.554	0.586	0.417
N10L6.2	0.342	0.517	0.624	0.578	0.422	9.60	0.333	0.526	0.624	0.532	0.468
N10L6.4	0.364	0.510	0.616	0.574	0.426	9.30	0.364	0.514	0.609	0.555	0.445
N10L12.2	0.363	0.511	0.615	0.574	0.426	8.10	0.351	0.524	0.610	0.544	0.456
N10L48.2	0.267	0.543	0.648	0.586	0.414	8.20	0.298	0.537	0.627	0.567	0.433
N10L48.4	0.399	0.498	0.605	0.570	0.430	9.60	0.382	0.503	0.613	0.552	0.448

Table 5.3: Design moment ratios for rectangular panels

Design Strip Section	SERVICE LOAD (7.20 kPa)					Load	MAXIMUM OR FACTORED LOAD				
	1	2	3	4	5		1	2	3	4	5
N5C1.2	0.283	0.543	0.631	0.614	0.386	9.60	0.242	0.624	0.510	0.501	0.499
N5C1.4	0.284	0.543	0.630	0.615	0.385	9.30	0.230	0.608	0.555	0.539	0.461
N5A2.3	0.380	0.532	0.557	0.627	0.373	9.60	0.321	0.590	0.498	0.611	0.389
N5B3.2	0.394	0.523	0.560	0.587	0.413	9.60	0.319	0.587	0.507	0.540	0.460
N5B3.4	0.395	0.506	0.594	0.588	0.412	9.60	0.320	0.560	0.560	0.542	0.485
N5D6.3	0.416	0.487	0.610	0.559	0.441	9.60	0.288	0.603	0.505	0.459	0.541
N7C1.2	0.227	0.573	0.627	0.611	0.389	7.70	0.222	0.581	0.616	0.604	0.396
N7C1.4	0.255	0.563	0.619	0.607	0.393	9.40	0.221	0.602	0.576	0.566	0.434
N7A2.3	0.308	0.553	0.586	0.644	0.356	8.60	0.279	0.580	0.5..	0.615	0.385
N7B6.2	0.311	0.537	0.615	0.594	0.406	9.60	0.261	0.584	0.572	0.531	0.469
N7B6.4	0.337	0.527	0.610	0.596	0.404	9.60	0.295	0.569	0.566	0.557	0.443
N7D9.3	0.349	0.530	0.591	0.578	0.422	9.60	0.302	0.577	0.545	0.536	0.464
N13B9.2	0.355	0.500	0.645	0.608	0.392	9.30	0.283	0.529	0.659	0.582	0.418
N13B9.4	0.387	0.489	0.636	0.605	0.395	9.60	0.370	0.498	0.633	0.583	0.417
N20B12.2	0.454	0.450	0.646	0.612	0.388	9.60	0.430	0.474	0.622	0.587	0.413
N20B12.4	0.470	0.440	0.649	0.611	0.389	9.60	0.466	0.457	0.621	0.586	0.414

Table 5.4a: Column and middl: trip moments for square panels at service load (kN-m)

Design Strip	EXTERIOR SPAN						INTERIOR SPAN			
Section	1		2		3		4		5	
	CS	MS	CS	MS	CS	MS	CS	MS	CS	MS
N10B6.2	-41.13	2.24	38.24	32.47	-52.64	-20.15	-48.51	-21.49	30.80	22.25
N10B6.4	-45.62	2.22	37.32	31.60	-52.18	-19.60	-48.58	-20.79	30.97	22.50
N10B12.2	-41.39	2.36	38.22	32.26	-53.11	-20.01	-48.40	-21.29	30.91	22.36
N10B12.4	-46.49	2.06	37.15	31.27	-52.19	-19.63	-48.33	-20.71	31.06	22.65
N10I12.2	-45.97	0.83	37.58	32.50	-48.70	-19.97	-48.22	-23.72	28.86	21.32
N10I12.4	-54.25	0.34	36.56	30.94	-48.11	-19.43	-47.96	-23.51	29.23	21.80
N10I24.2	-46.08	0.64	37.42	31.66	-49.99	-20.17	-47.45	-23.19	28.97	21.82
N10I24.4	-52.67	0.53	37.21	31.07	-42.34	-22.55	-39.93	-25.02	31.84	25.11
N10L6.2	-41.08	0.85	35.28	33.69	-49.85	-17.71	-48.47	-19.80	31.69	23.56
N10L6.4	-43.80	0.79	34.76	28.06	-49.08	-17.77	-47.82	-19.06	31.89	23.79
N10L12.2	-43.19	0.83	34.86	27.79	-49.32	-17.67	-48.12	-18.59	31.78	23.75
N10L48.2	-32.31	-1.19	37.07	30.04	-51.12	-19.30	-48.02	-20.78	31.36	22.95
N10L48.4	-46.85	-0.38	34.16	27.11	-48.30	-17.34	-47.78	-18.59	32.04	24.03

CS=Column strip, MS=Middle strip

Table 5.4b: Column and middle strip moments for square panels at factored load (kN·m)

Design Strip Section	EXTERIOR SPAN						INTERIOR SPAN			
	1		2		3		4		5	
	CS	MS	CS	MS	CS	MS	CS	MS	CS	MS
N10B6.2	-49.70	3.67	45.28	44.22	-72.22	-30.20	-59.01	-29.01	40.04	30.96
N10B6.4	-65.25	2.37	42.81	42.39	-68.29	-28.37	-55.15	-27.85	40.88	32.84
N10B12.2*										
N10B12.4	-62.48	2.70	43.63	42.50	-68.59	-28.54	-59.10	-27.79	40.66	32.59
N10I12.2*										
N10I12.4	-73.16	0.49	46.66	42.08	-60.56	-26.30	-58.62	-28.89	39.01	31.39
N10I24.2*										
N10I24.4*										
N10L6.2	-52.13	0.83	44.77	39.98	-61.98	-25.17	-51.38	-26.20	41.76	35.45
N10L6.4*										
N10L12.2*										
N10L48.2*										
N10L48.4	-59.51	0.06	43.10	38.29	-62.48	-25.00	-58.19	-24.90	41.25	34.76

CS=Column strip, MS=Middle strip

* Did not reach the factored load level

Table 5.5a: Column and middle strip moments for rectangular panels at service load (kN-m)

| Design Strip | EXTERIOR SPAN | | | | | | INTERIOR SPAN | | | |
| | 1 | | 2 | | 3 | | 4 | | 5 | |
Section	CS	MS	CS	MS	CS	MS	CS	MS	CS	MS
N5C1.2	-9.99	1.91	10.23	6.69	-20.11	2.49	-19.46	2.23	7.17	4.78
N5C1.4	-10.02	1.91	10.22	6.69	-20.08	2.49	-19.46	2.23	7.18	4.79
N5A2.3	-12.82	1.75	9.77	6.83	-17.73	2.31	-19.60	1.89	6.90	4.77
N5B3.2	-12.37	2.12	8.31	5.96	-18.08	2.49	-17.39	2.33	6.74	4.95
N5B3.4	-12.51	2.11	8.31	5.90	-18.02	2.50	-17.38	2.33	6.73	4.95
N5D6.3	-13.30	2.41	7.92	5.70	-18.09	2.90	-18.42	2.89	7.98	5.69
N7C1.2	-18.89	2.94	25.71	17.41	-37.14	-4.76	-35.50	-5.29	18.75	10.14
N7C1.4	-20.85	2.81	25.32	17.11	-36.80	-4.57	-35.35	-5.10	18.85	10.27
N7A3.3	-24.38	2.38	24.47	17.16	-33.99	-5.05	-35.45	-6.36	16.36	9.21
N7B6.2	-23.78	2.89	22.83	15.26	-35.04	-3.93	-33.58	-3.77	18.08	10.34
N7B6.4	-25.52	2.72	22.38	15.04	-34.65	-4.03	-32.91	-4.34	18.04	10.46
N7D9.3	-25.95	2.86	22.29	14.58	-34.45	-3.63	-34.37	-3.87	19.76	11.51
N13B9.2	-32.10	1.61	25.47	23.59	-37.39	-20.57	-33.47	-19.75	20.20	17.99
N13B9.4	-43.19	1.71	24.92	23.07	-36.98	-20.20	-33.44	-19.51	20.31	18.10
N20B12.2	-22.94	-5.96	14.86	14.57	-22.72	-16.05	-20.87	-15.03	12.73	12.56
N20B12.4	-24.59	-5.62	14.63	14.40	-22.53	-15.91	-20.87	-14.98	12.75	12.58

CS=Column strip, MS=Middle strip

Table 5.5b: Column and middle strip moments for rectangular panels at factored load (kN-m)

Design Strip	EXTERIOR SPAN						INTERIOR SPAN			
Section	1		2		3		4		5	
	CS	MS	CS	MS	CS	MS	CS	MS	CS	MS
N5C1.2	-10.76	1.46	16.30	10.33	-23.61	4.62	-22.63	4.36	12.29	8.32
N5AC.4*										
N5A2.3	-14.80	2.53	14.67	9.78	-21.51	3.50	-27.00	2.88	10.32	6.76
N5B3.2	-13.94	3.10	12.66	8.58	-22.64	3.71	-21.67	3.46	10.21	7.08
N5B3.4	-14.20	3.09	12.60	8.55	-22.57	3.70	-21.72	3.47	10.19	7.08
N5D6.3	-13.64	3.87	13.43	9.10	-21.32	5.01	-21.49	5.00	13.15	9.15
N7AC.2*										
N7AC.4*										
N7A3.3*										
N7B6.2	-27.46	4.41	32.78	22.23	-41.77	-5.91	-39.52	-2.23	39.52	2.23
N7B6.4	-30.45	4.17	32.14	21.63	-41.96	-5.35	-40.05	-5.78	26.81	14.79
N7D9.3	-30.84	4.51	32.22	21.07	-41.16	-5.20	-40.79	-6.11	29.34	16.53
N13B9.2*										
N13B9.4	-43.54	-2.23	31.79	31.85	-47.33	-26.60	-40.77	-25.03	27.24	25.25
N20B12.2	-26.96	-8.57	20.33	19.94	-28.61	-19.73	-25.39	-18.53	17.38	17.25
N20B124	-30.67	-8.28	19.74	19.49	-28.13	-19.56	-25.41	-18.52	17.38	17.25

CS=Column strip, MS=Middle strip

* Did not reach the factored load level

Table 5.6a: Percentage of moment in column strip at service load (NISA80)

Design strip	Section 1	Section 2	Section 3	Section 4	Section 5
N5C1	100	60	100	100	60
N5A2.3	100	59	100	100	59
N5B3	100	58	100	100	58
N5D6.3	100	58	100	100	58
N7C1	100	60	89-87	87	65
N7A3.3	100	59	87	85	64
N7B6	100	59-60	90	89-88	62-63
N7D9.3	100	60	90	90	63
N10B6	100	54-50	72	69	58
N10B12	100	54	73	69-70	58
N10I12	100	54	71	67	58-57
N10I24	100	54	71-68	67-63	57-55
N10L6	100	55	74	72	57
N10L12.2	100	56	74-73	72	57
N10L48	100-99	55-56	73-74	70-72	58-57
N13B9	95	52	65	63	53
N20B12	81	51-50	59	58	50

Table 5.6b: Percentage of moment in column strip at factored load (NISA80)

Design strip	Section 1	Section 2	Section 3	Section 4	Section 5
N5C1	100-*	61-*	100-*	100-*	60-*
N5A2.3	100	60	100	100	60
N5B3	100	60	100	100	59
N5D6.3	100	60	100	100	59
N7C1	*	*	*	*	*
N7A3.3	*	*	*	*	*
N7B6	100	60	88-89	85-87	65-64
N7D9.3	100	60	89	87	64
N10B6	100	50-51	71	67	56
N10B12	100	51	69-71	64-68	56
N10I12	*-100	*-51	*-71	*-68	*-56
N10I24	*	*	*	*	*
N10L6	100-*	53-*	71-*	66-*	54-*
N10L12	*	*	*	*	*
N10L48.4	100	53	71	70	54
N13B9	*-95	*-50	*-64	*-62	*-52
N20B12	76-79	50	59	58	50

* No factored load value available

Table 5.7: Transverse distribution of moments to the column strip for slabs without beams (%)

Location	Panel aspect ratio (l_1/l_2)		
	0.50	1.00	2.00
Exterior Column (Section 1)	100 (100)	100 (100)	80 (100)
Midspan (Sections 2, 5)	60 (60)	55 (60)	50 (60)
Interior Column (Sections 3, 4)	95 (75)	75 (75)	60 (75)

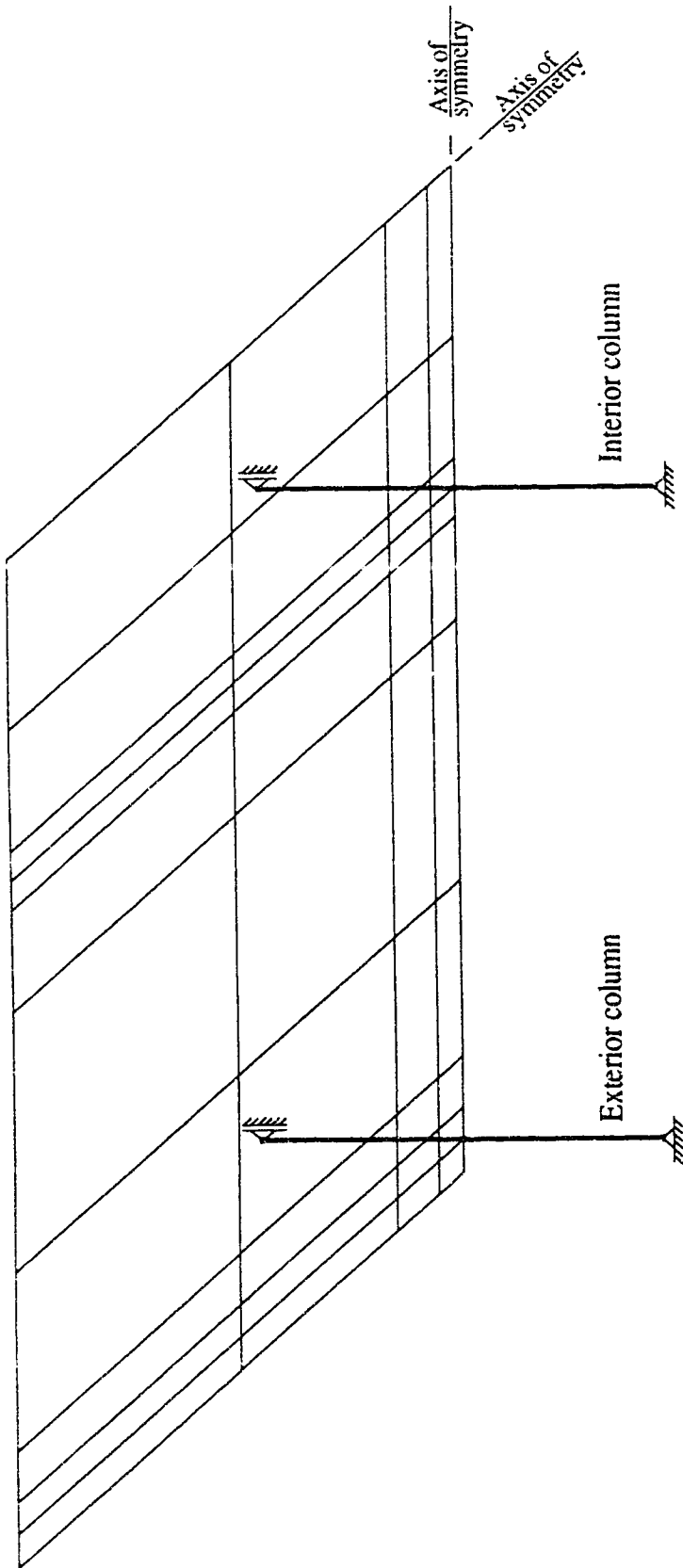Note: Values in the parenthesis are the present code provisions

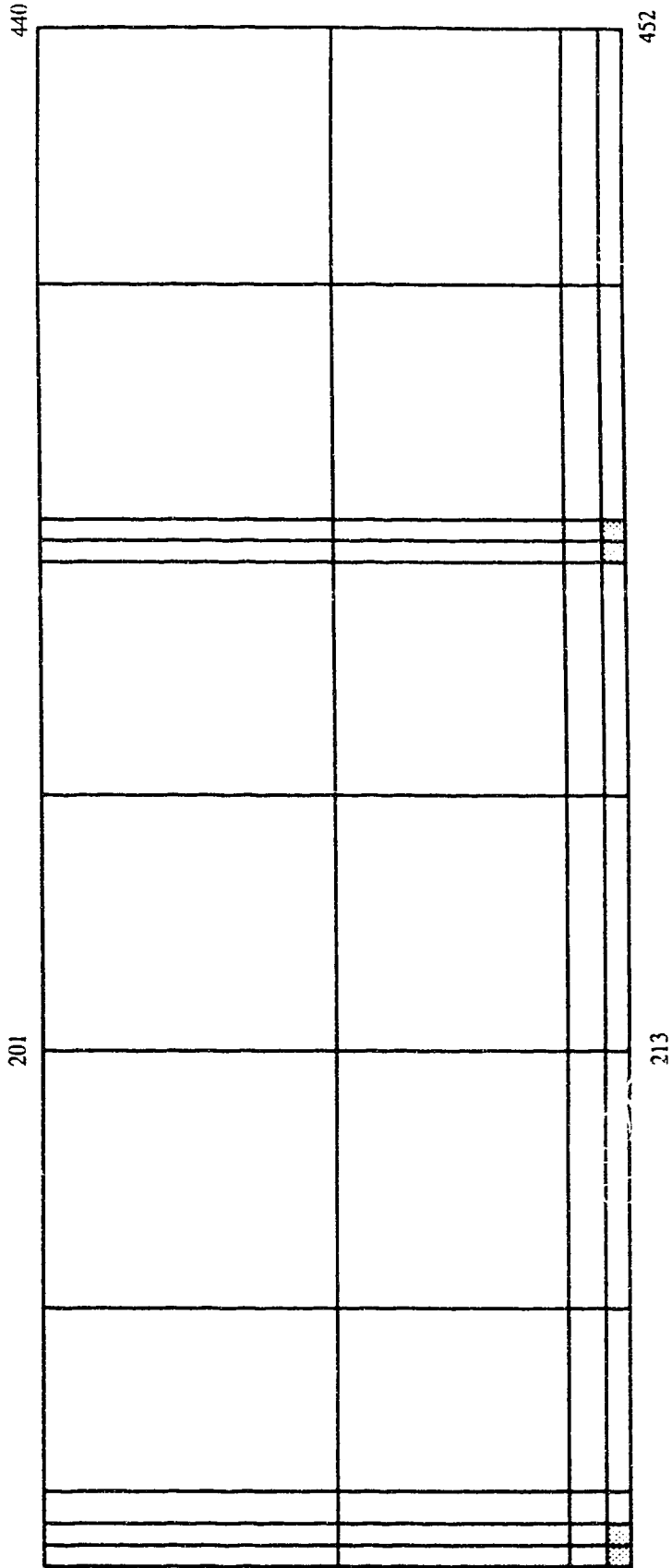Fig 5.1: Column and slab elements (one quarter of the design strip)

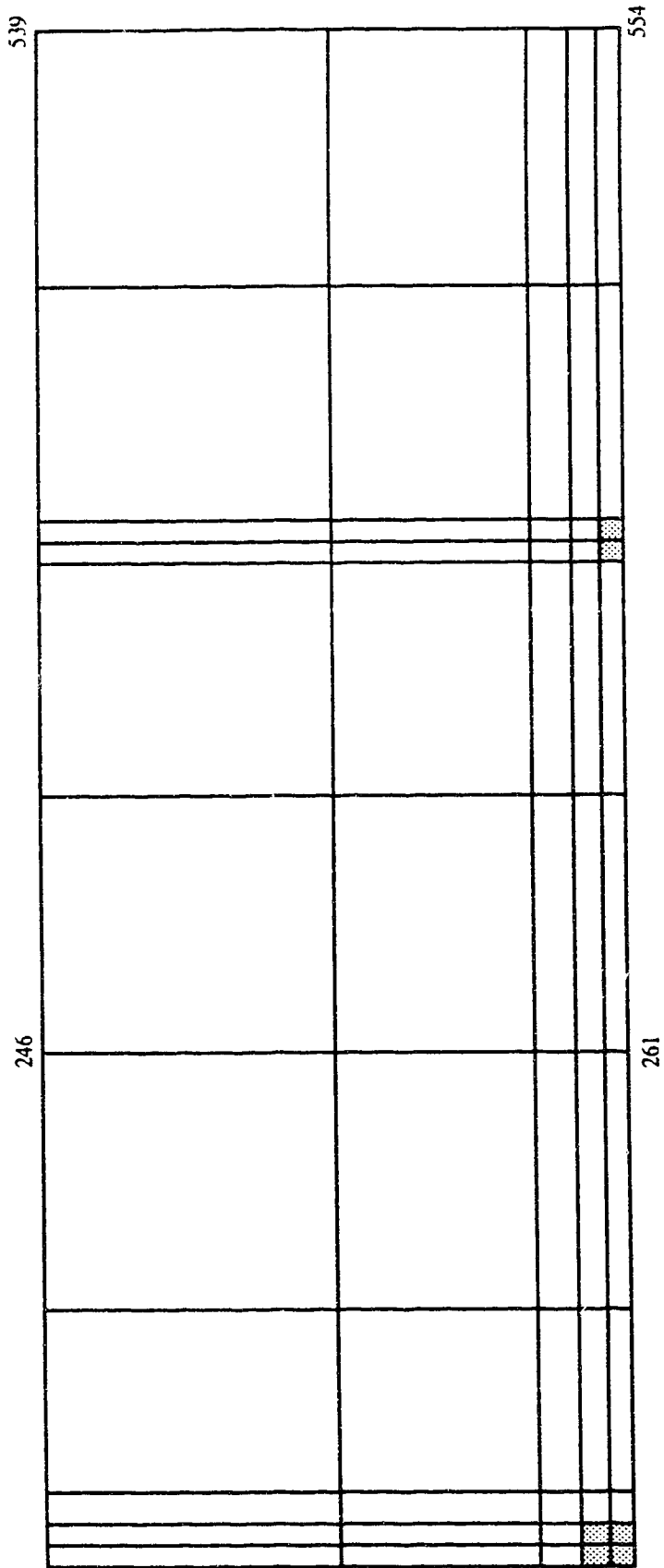Fig 5.2: Arrangement of 44 slab elements

130

Fig 5.3: Arrangement of 55 slab elements
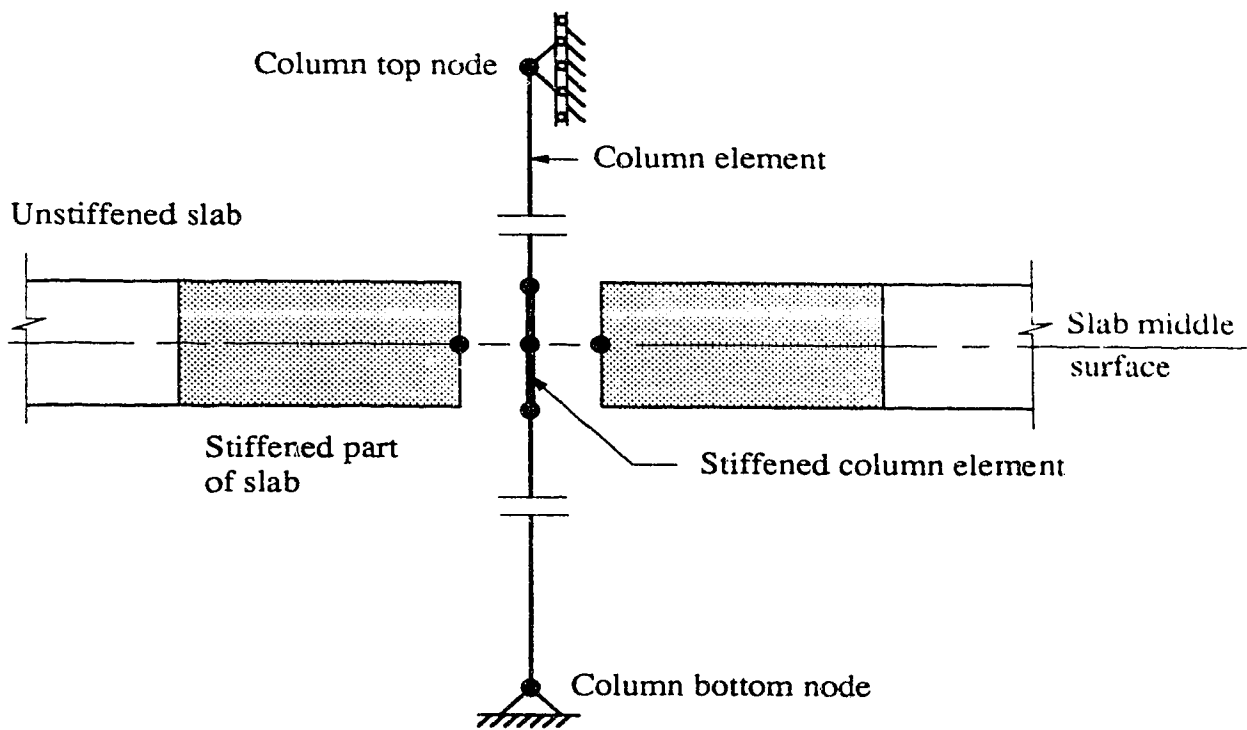
Fig 5.4: Connection between column and slab nodes
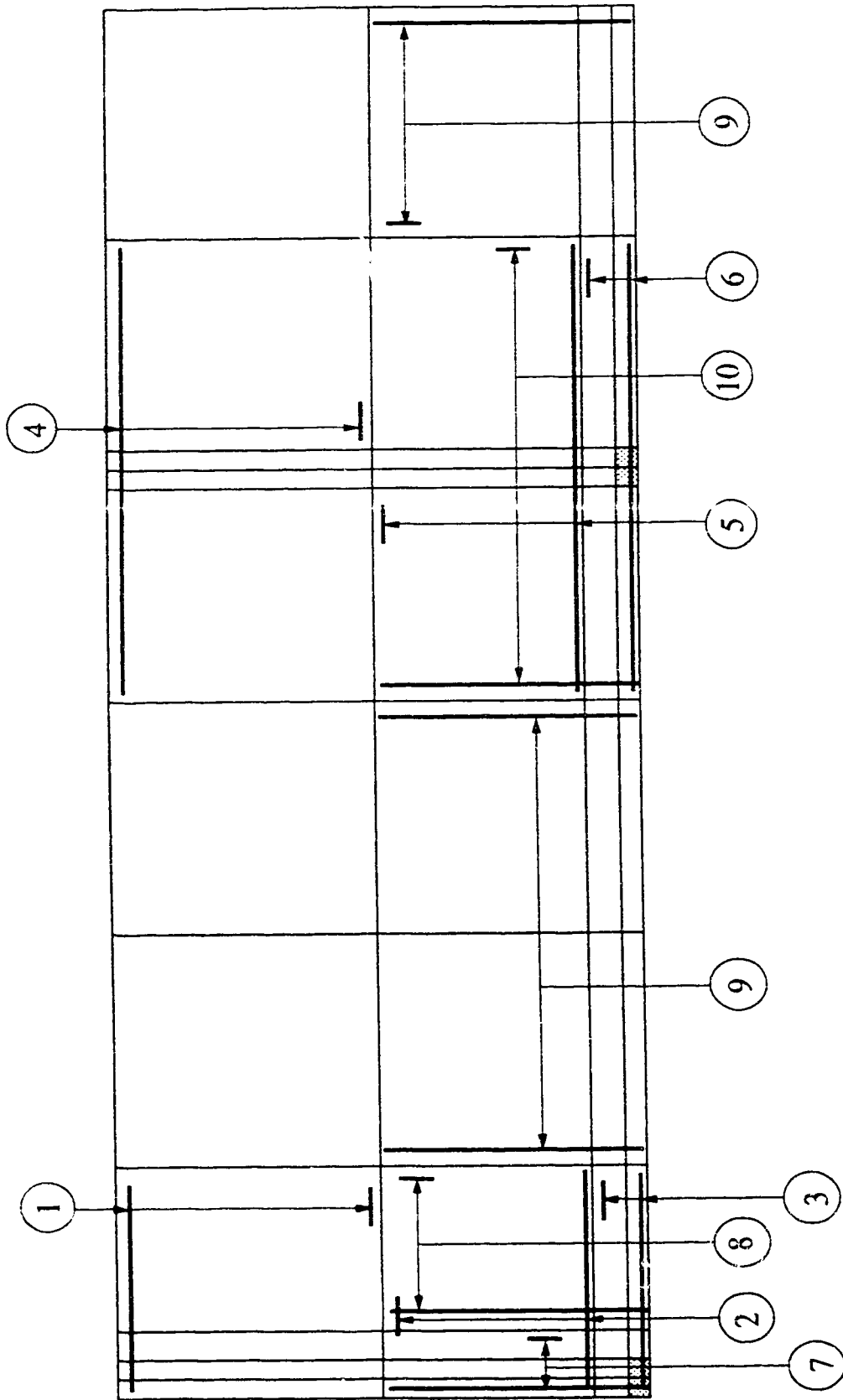
Fig 5.5: Top reinforcement layout
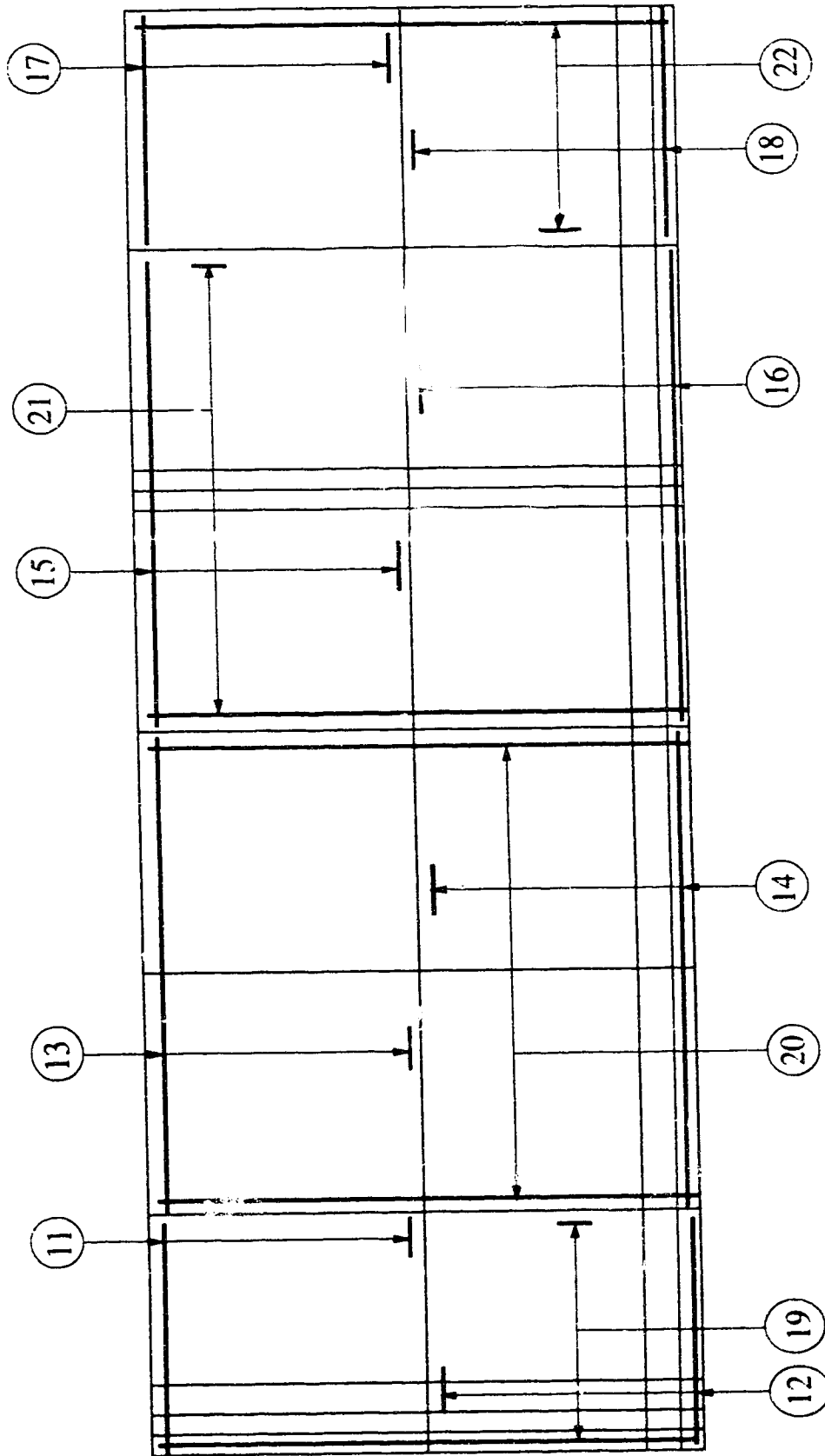
Fig 5.6: Bottom reinforcement layout

134

LEGEND

No translation along this axis

No rotation along this axis
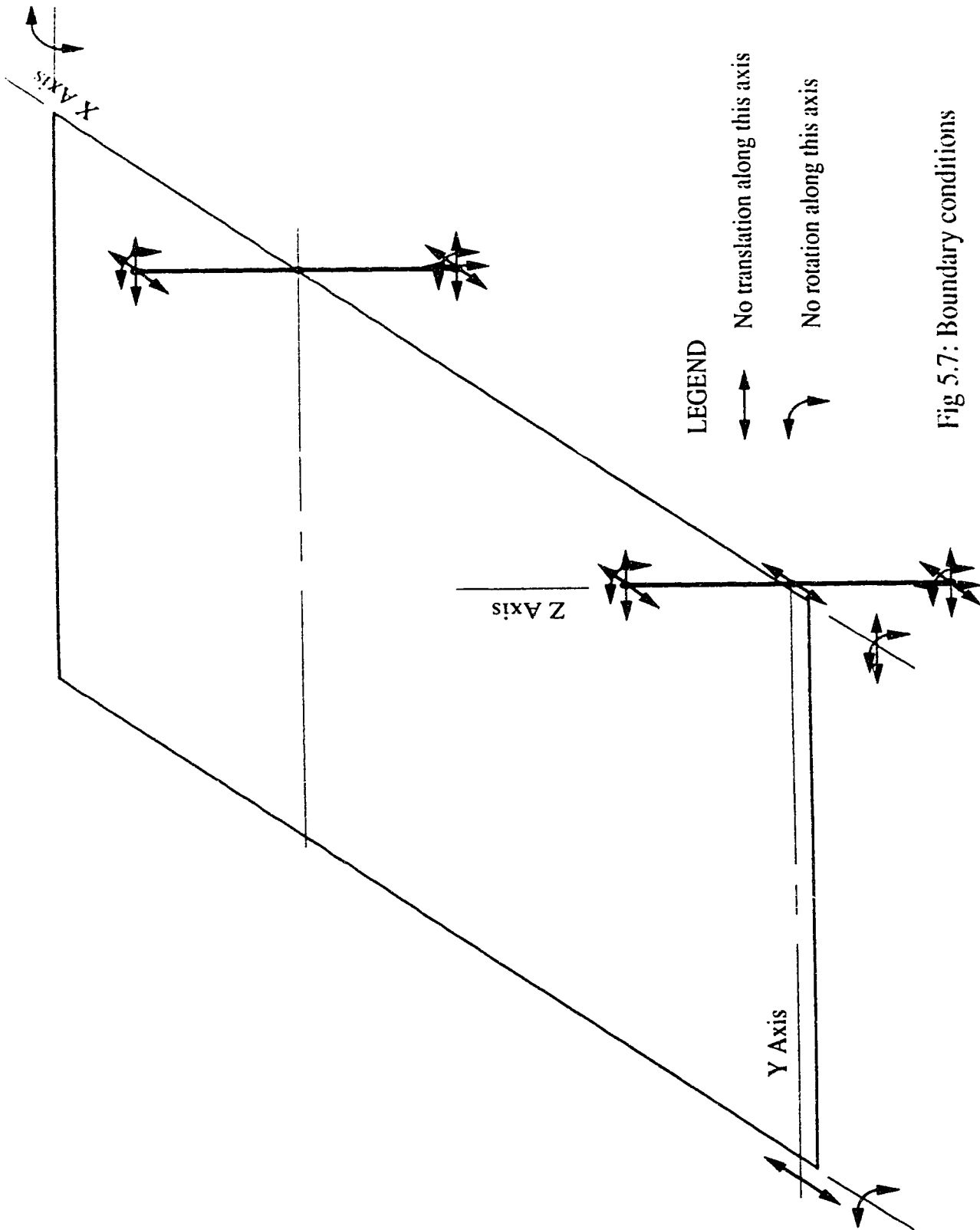
Fig 5.7: Boundary conditions

Fig 5.8a: Load vs Deflection (N10B6.2)

Fig 5.8o: Load vs Moment ratio (N10B6.2)

Fig 5.9a: Load vs Deflection (N10B6.4)

Fig 5.9b: Load vs Moment ratio (N10B6.4)

Fig 5.10a: Load vs Deflection (N10B12.2)

Fig 5.10b: Load vs Moment ratio (N10B12.2)

Fig 5.11a: Load vs Deflection (N10B12.4)

Fig 5.11b: Load vs Moment ratio (N10B12.4)
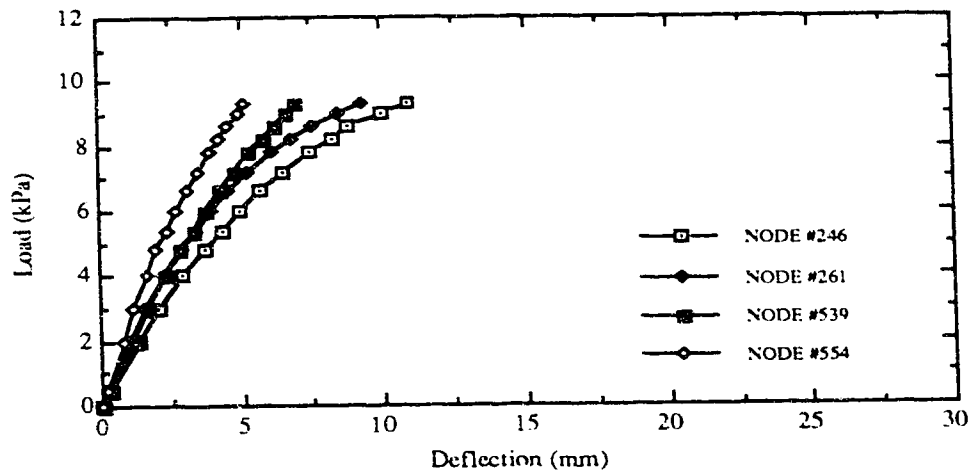
Fig 5.12a: Load vs Deflection (N10I12.2)
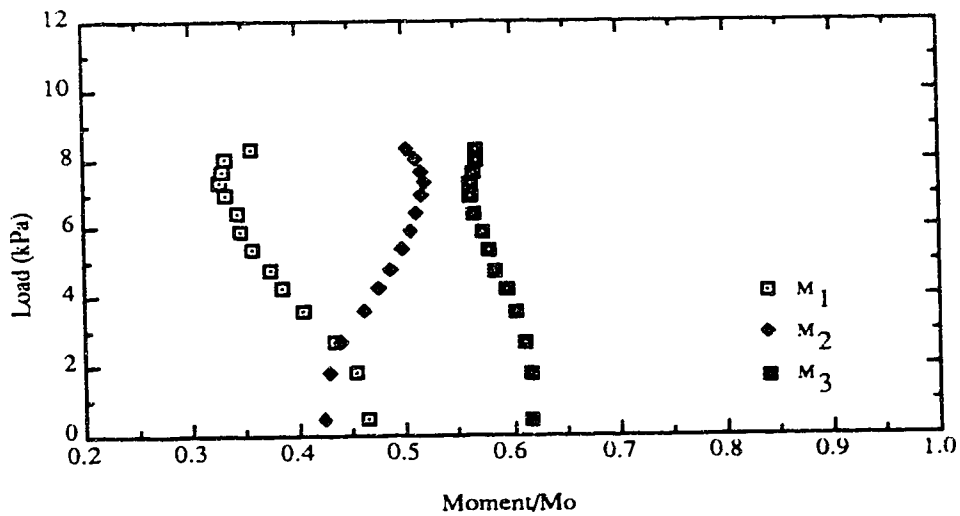
Fig 5.12b: Load vs Moment ratio (N10I12.2)
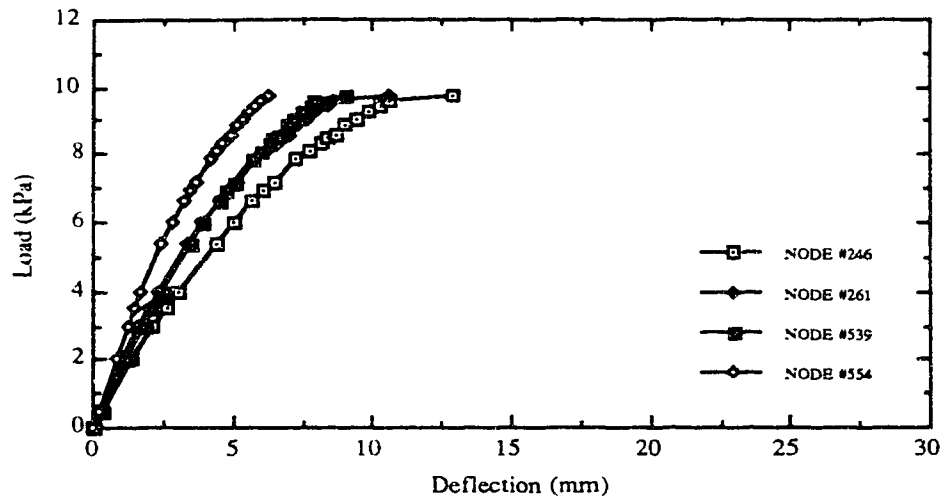
Fig 5.13a: Load vs Deflection (N10I12.4)
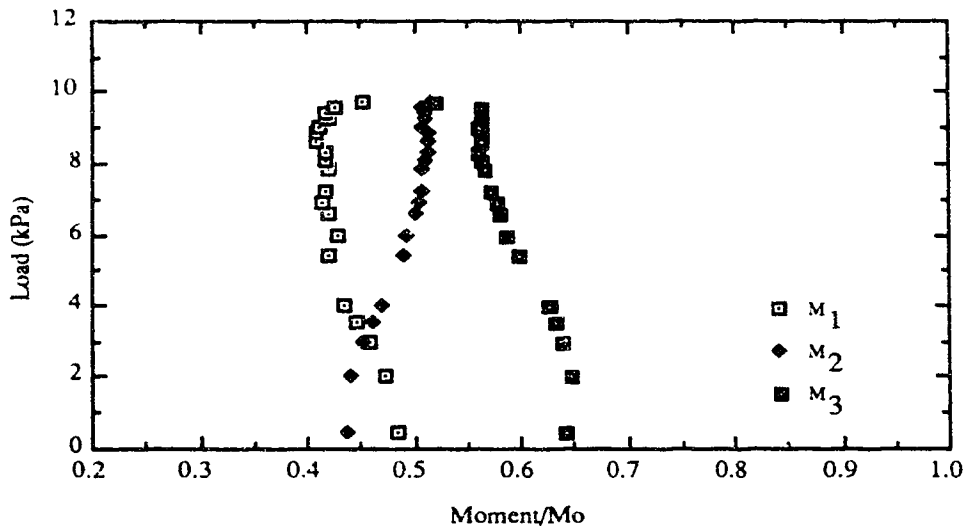
Fig 5.13b: Load vs Moment ratio (N10I12.4)
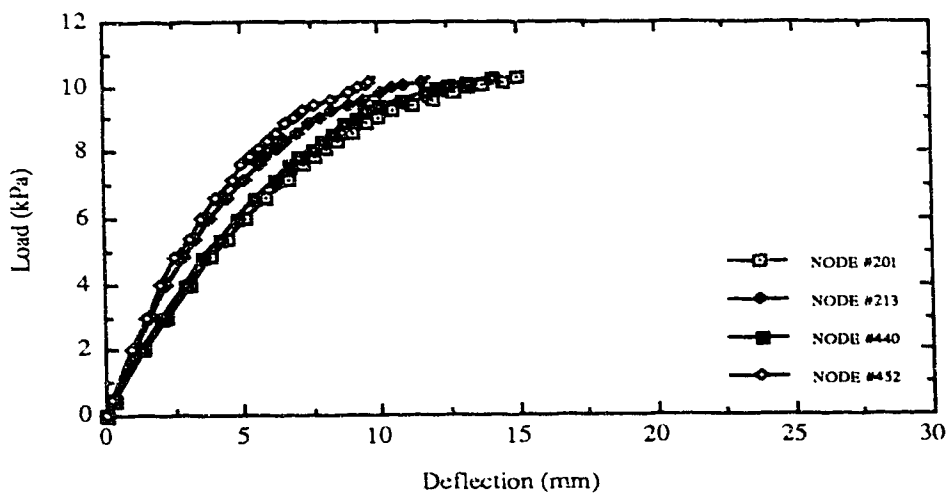
Fig 5.14a: Load vs Deflection (N10L6.2)
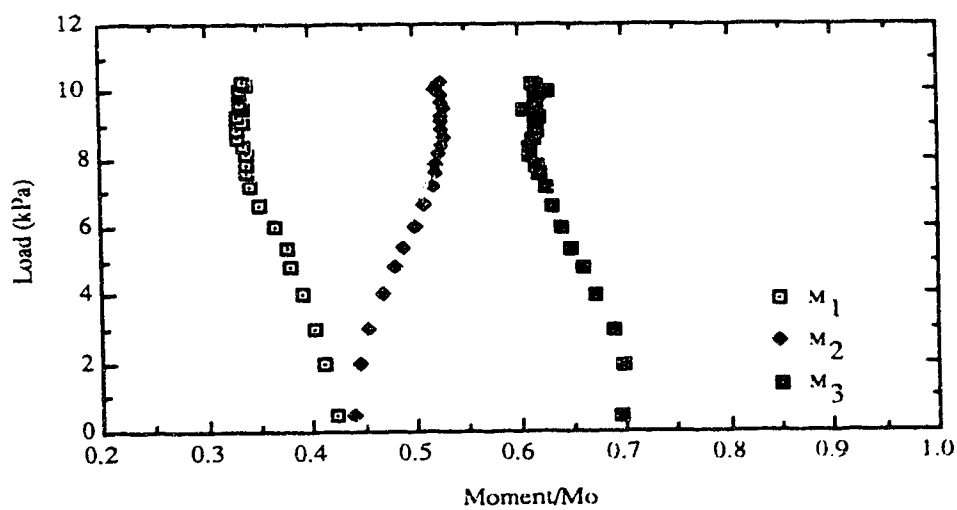
Fig 5.14b: Load vs Moment ratio (N10L6.2)
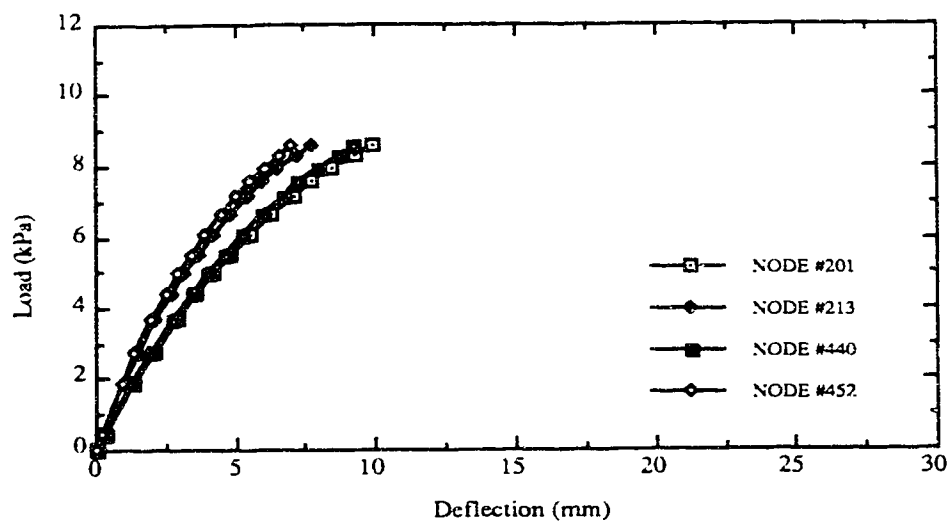
Fig 5.15a: Load vs Deflection (N10L6.4)
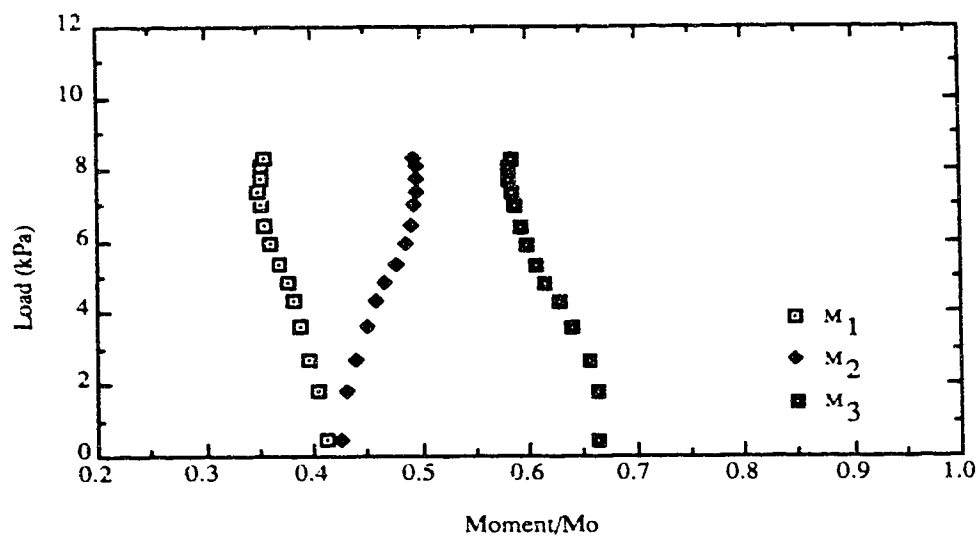
Fig 5.15b: Load vs Moment ratio (N10L6.4)
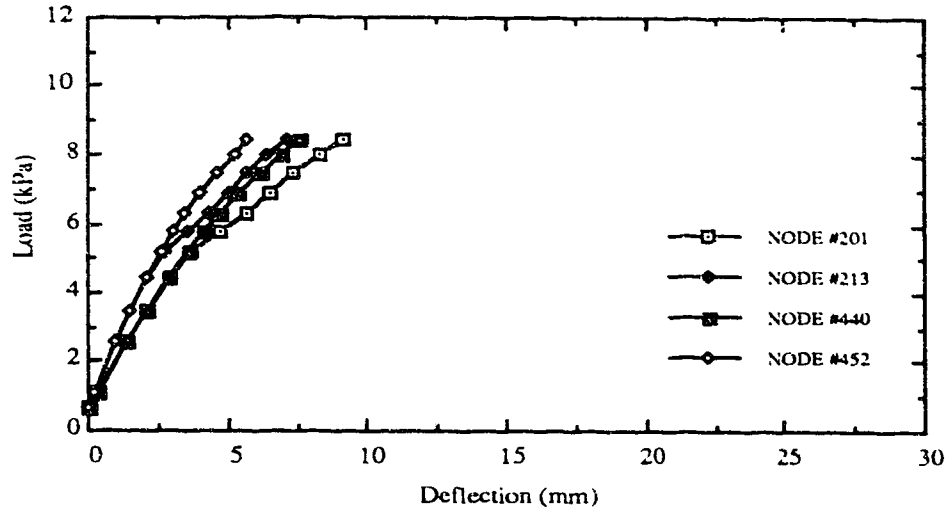
Fig 5.16a: Load vs Deflection (N10L48.2)
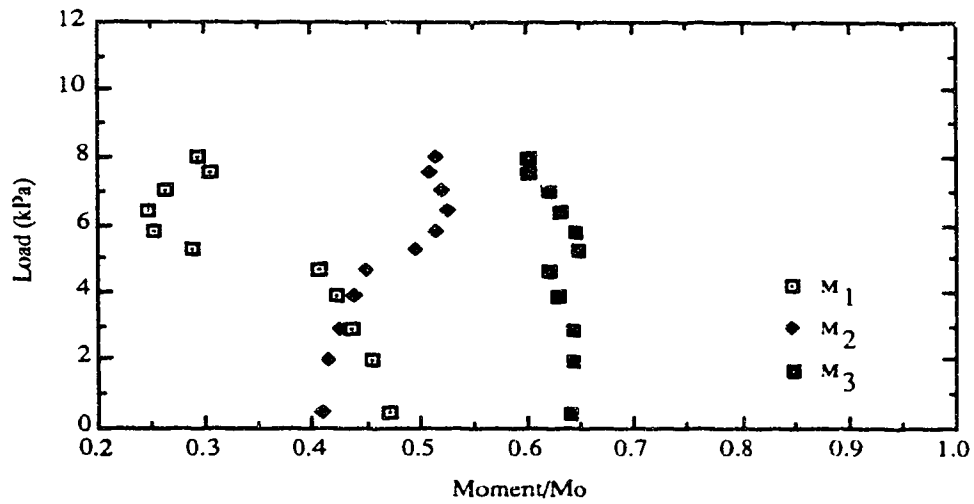
Fig 5.16b: Load vs Moment ratio (N10L48.2)
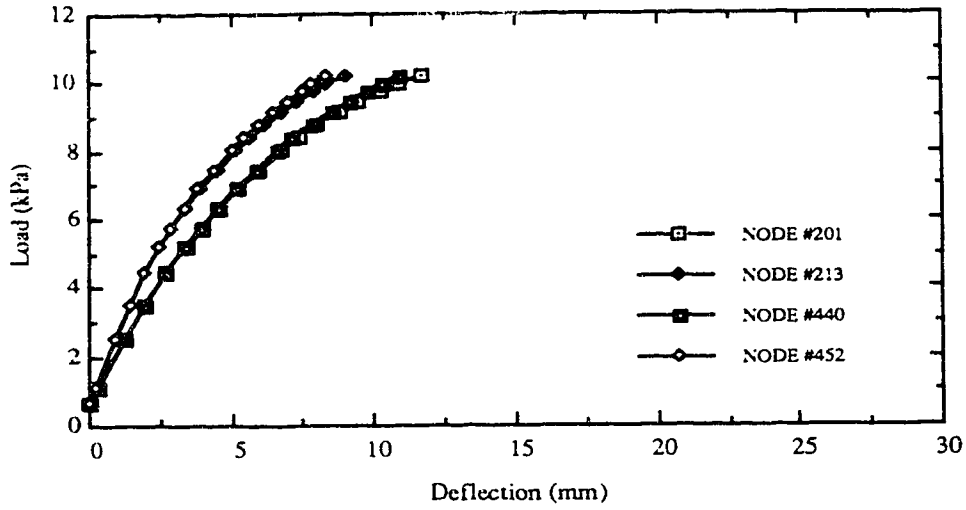
Fig 5.17a: Load vs Deflection (N10L48.4)
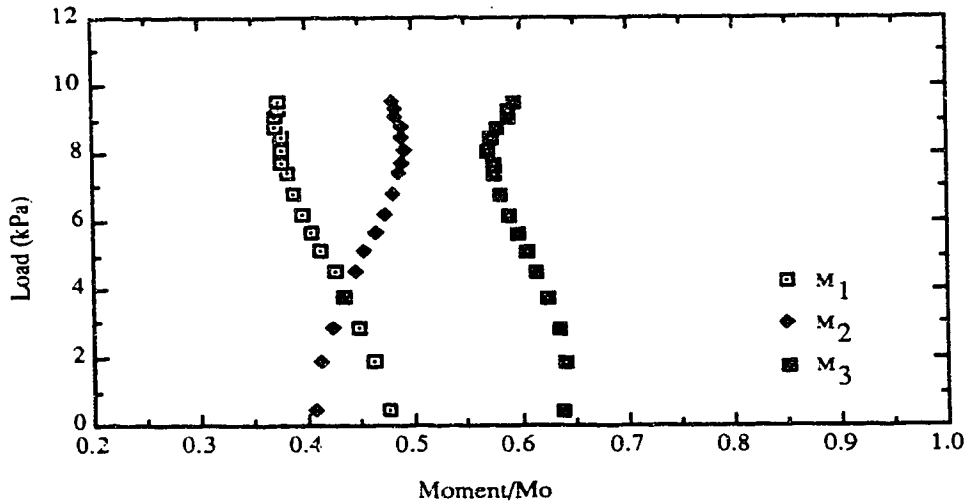
Fig 5.17b: Load vs Moment ratio (N10L48.4)
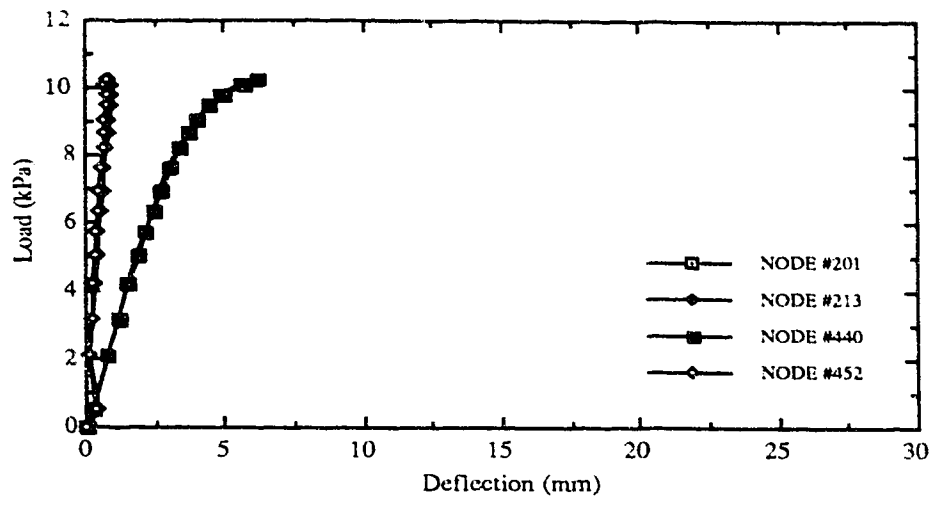
Fig 5.18a: Load vs Deflection (N5C1.2)
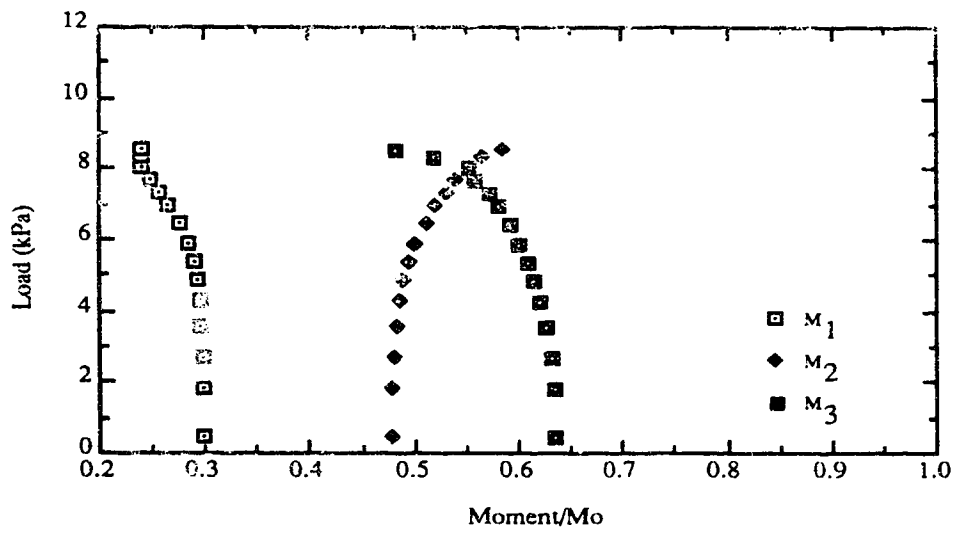
Fig 5.18b: Load vs Moment ratio (N5C1.2)
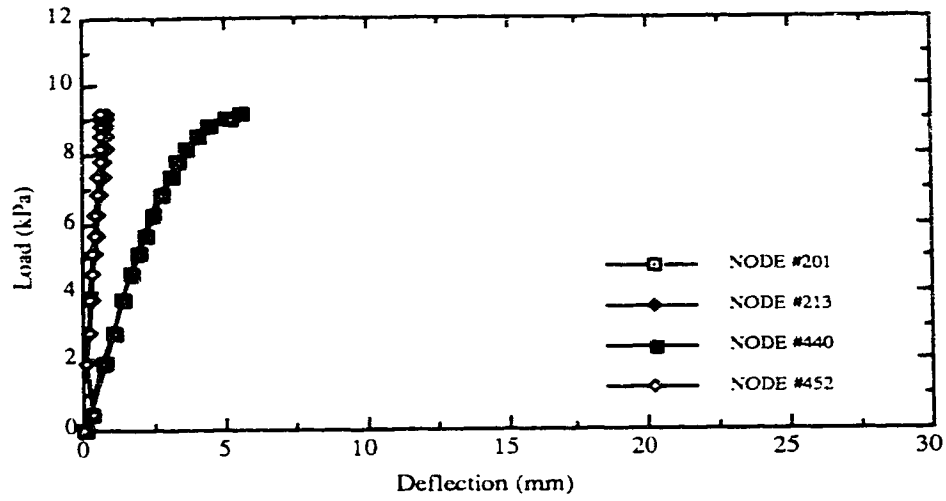
Fig 5.19a: Load vs Deflection (N5C1.4)
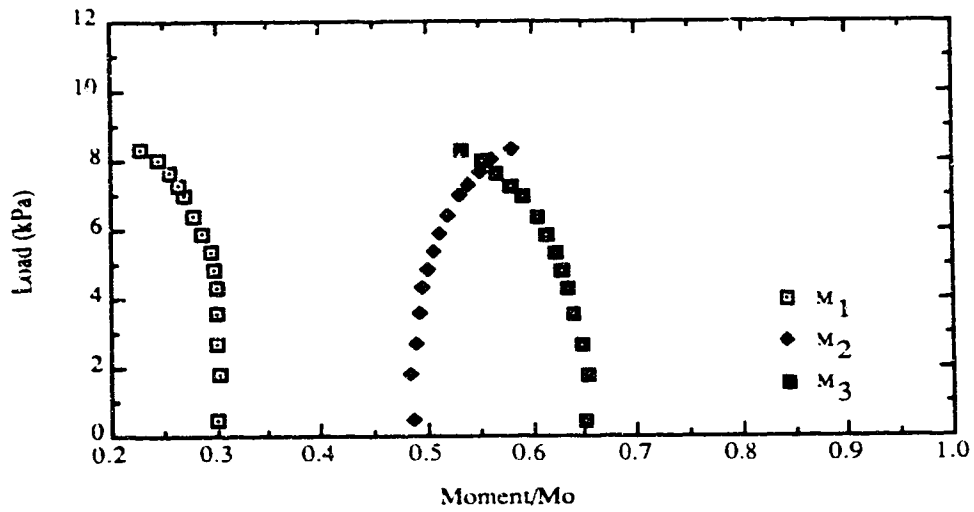
Fig 5.19b: Load vs Moment ratio (N5C1.4)
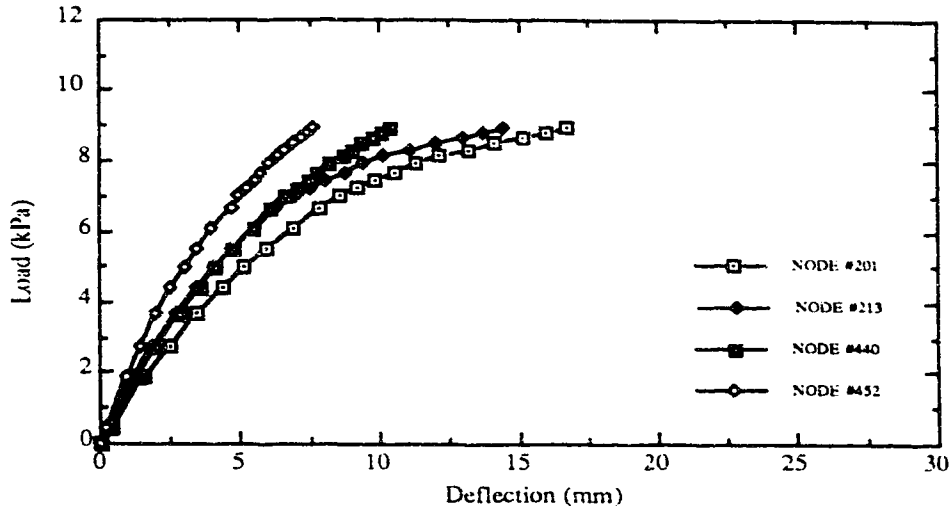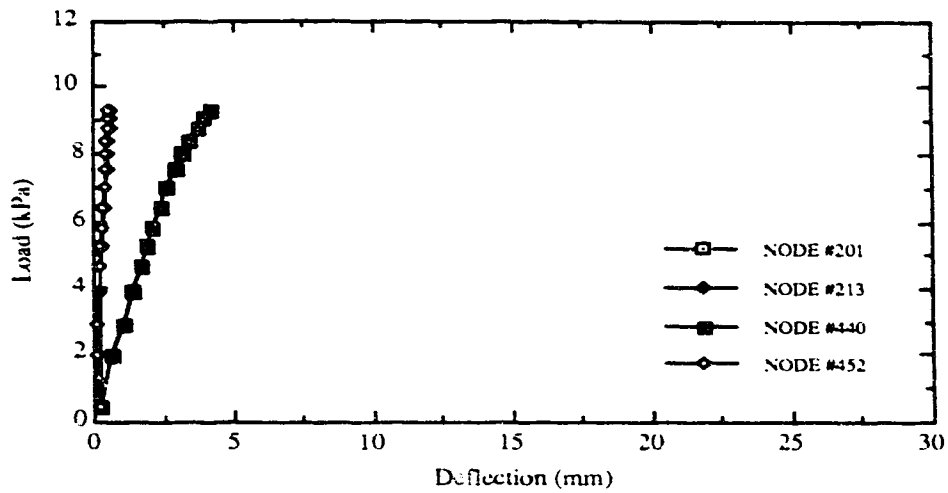
Fig 5.20a: Load vs Deflection (N5B3.2)
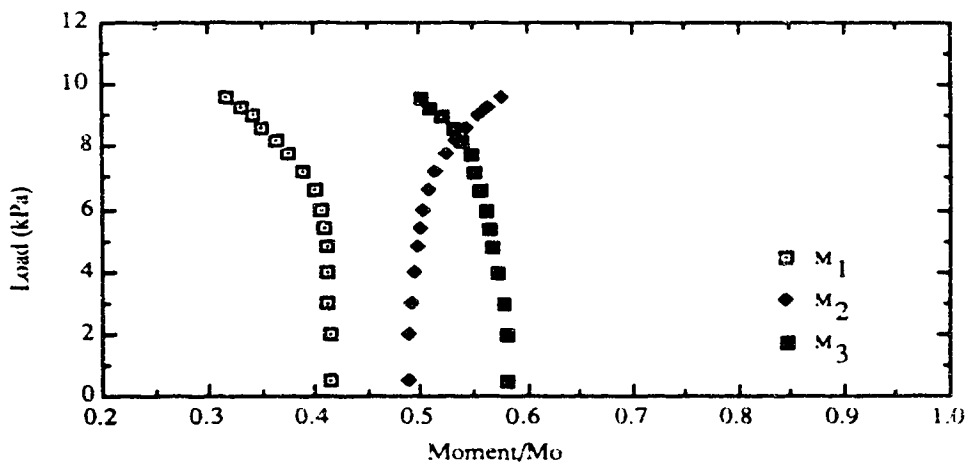
Fig 5.20b: Load vs Moment ratio (N5B3.2)
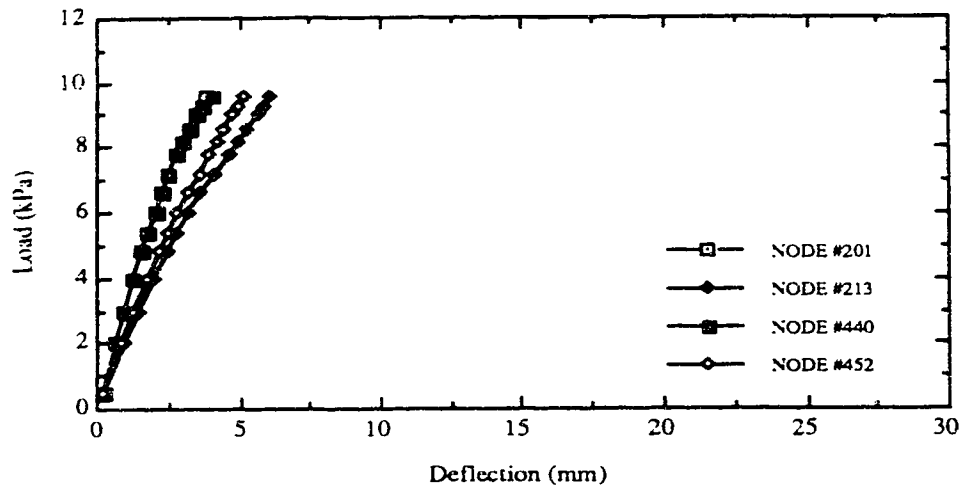
Fig 5.21a: Load vs Deflection (N5B3.4)
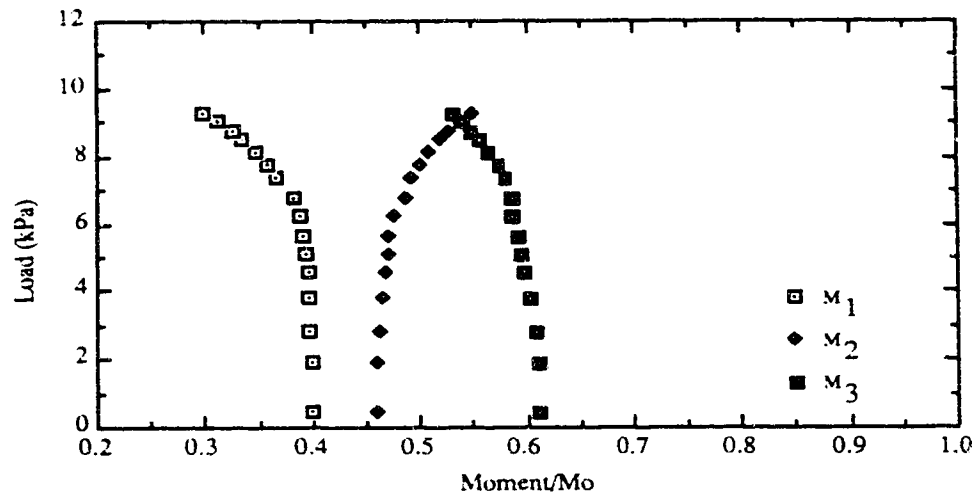
Fig 5.21b: Load vs Moment ratio (N5B3.4)
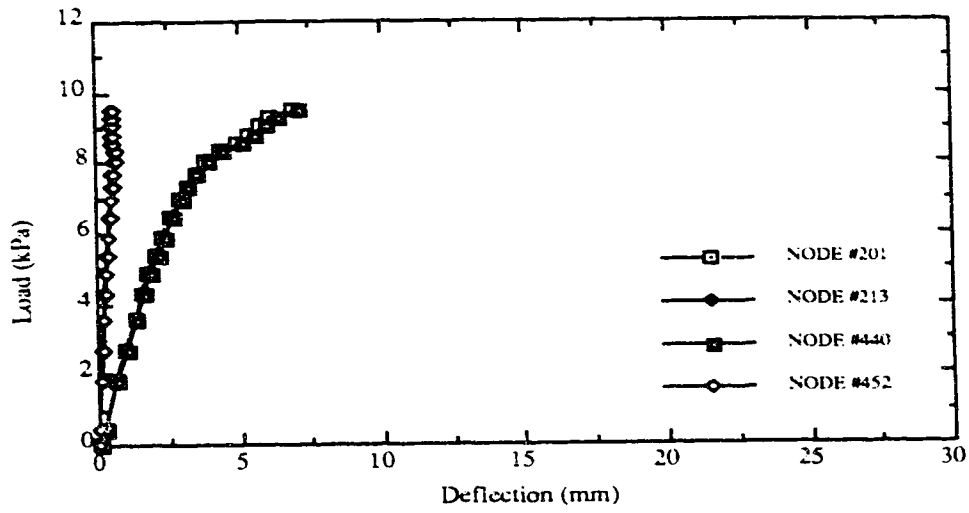
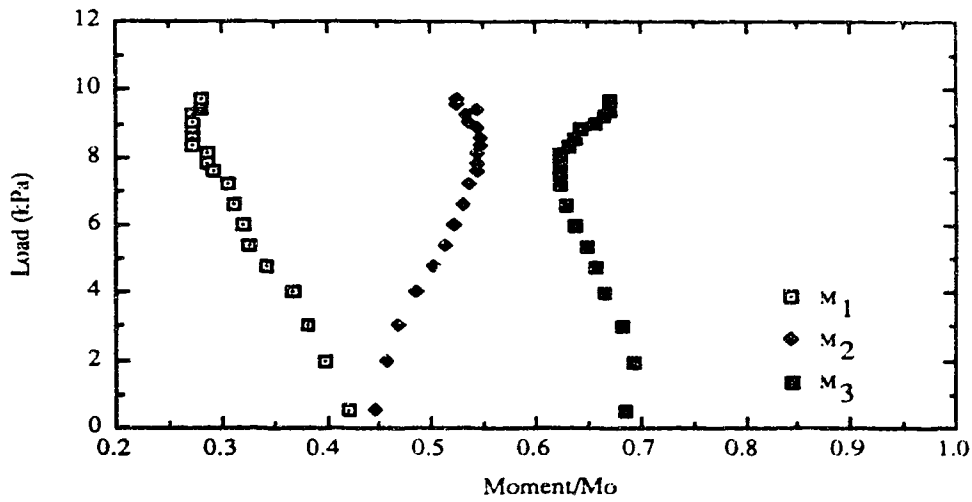Fig 5.22a: Load vs Deflection (N5D6.3)
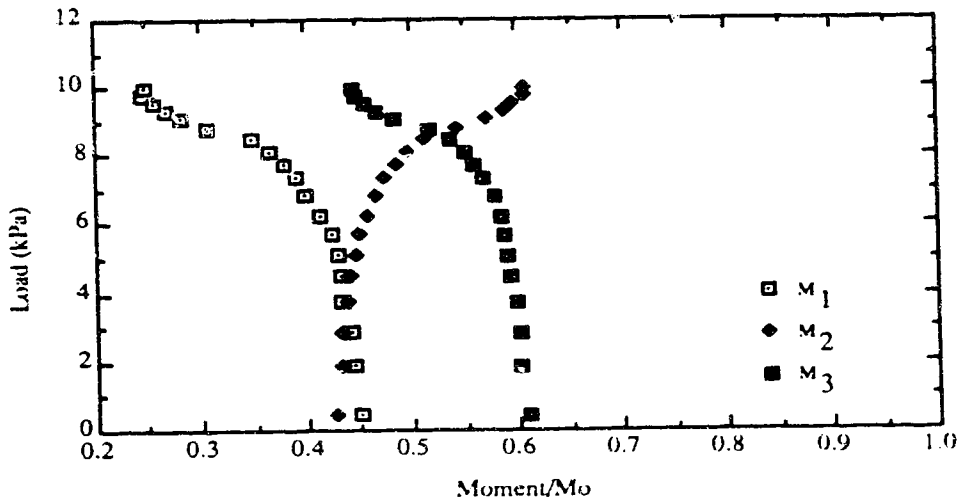
Fig 5.22b: Load vs Moment ratio (N5D6.3)
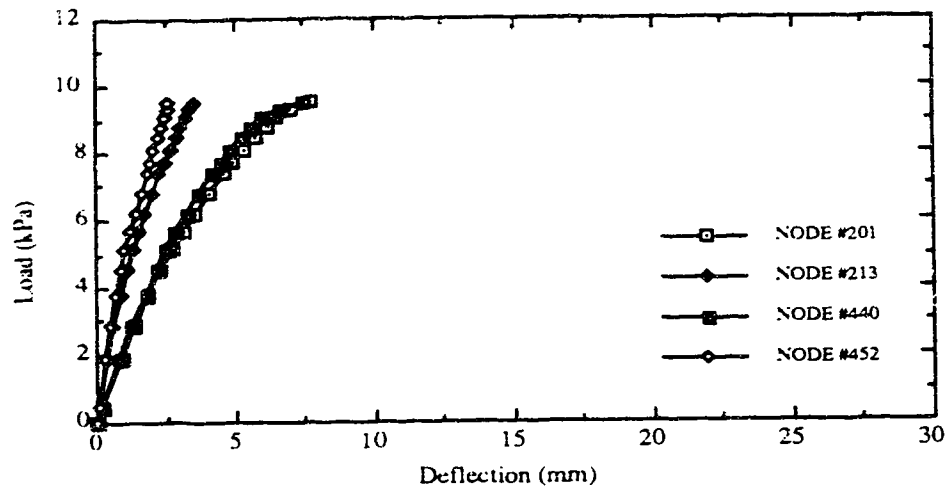
Fig 5.23a: Load vs Deflection (N7B6.2)
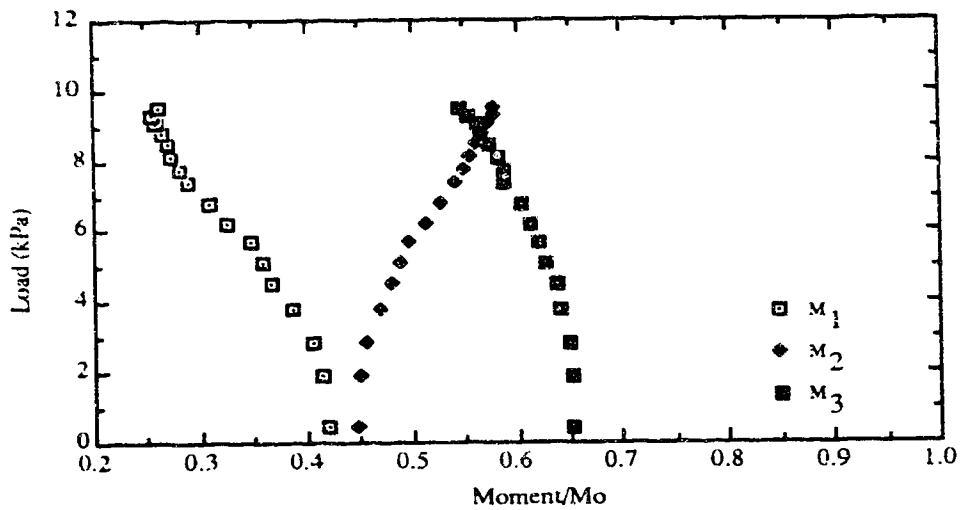
Fig 5.23b: Load vs Moment ratio (N7B6.2)

NODE #201
NODE #213
NODE #440
NODE #452
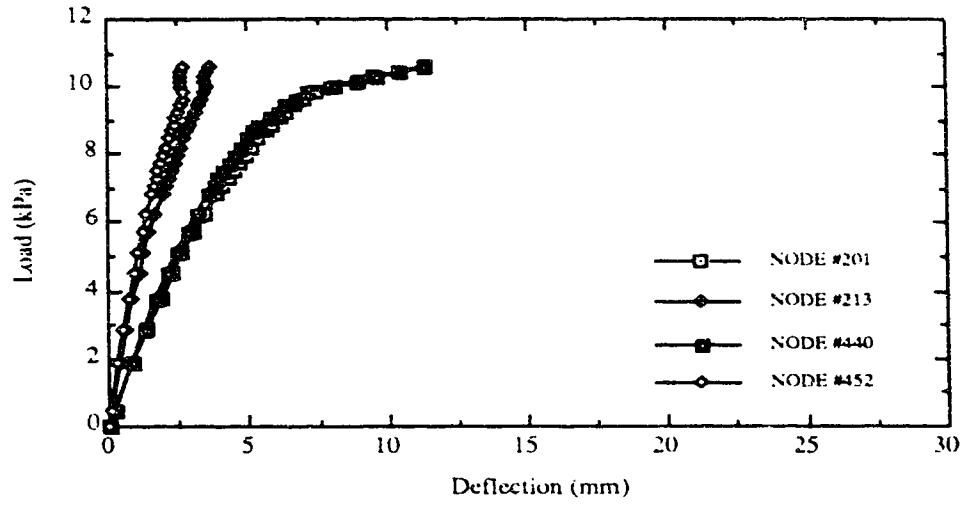
Fig 5.24a: Load vs Deflection (N7B6.4)

M_1
M_2
M_3
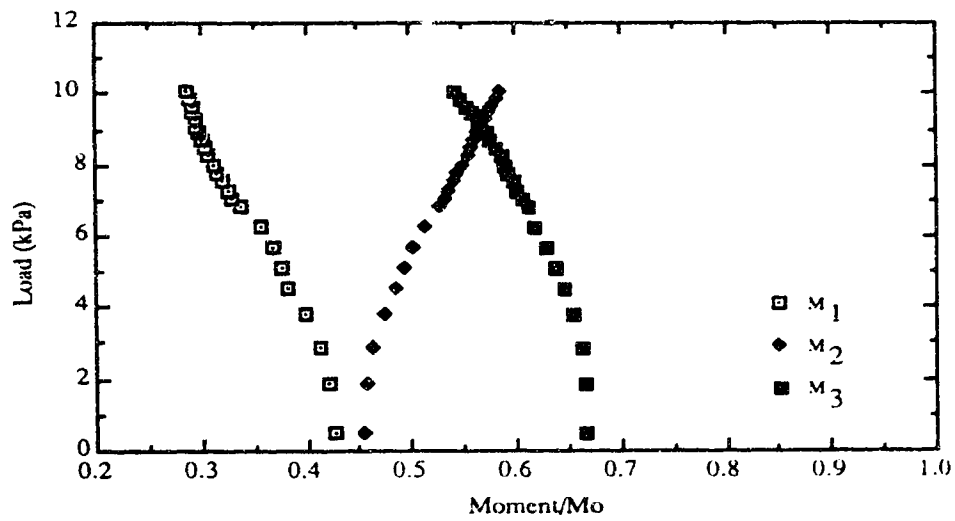
Fig 5.24b: Load vs Moment ratio (N7B6.4)
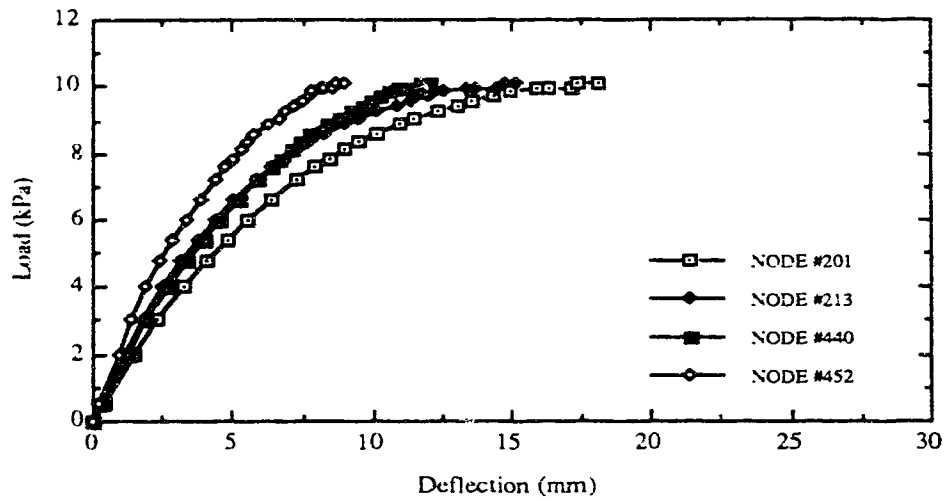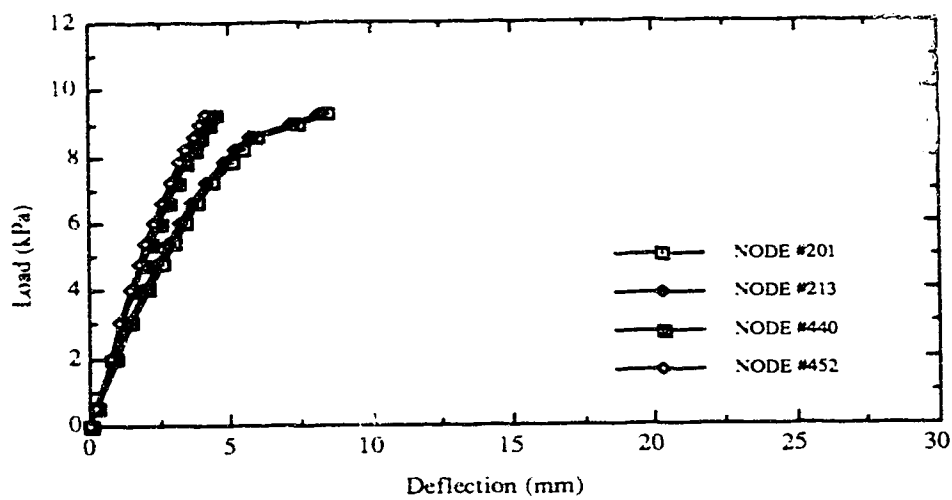
Fig 5.25a: Load vs Deflection (N13B9.2)
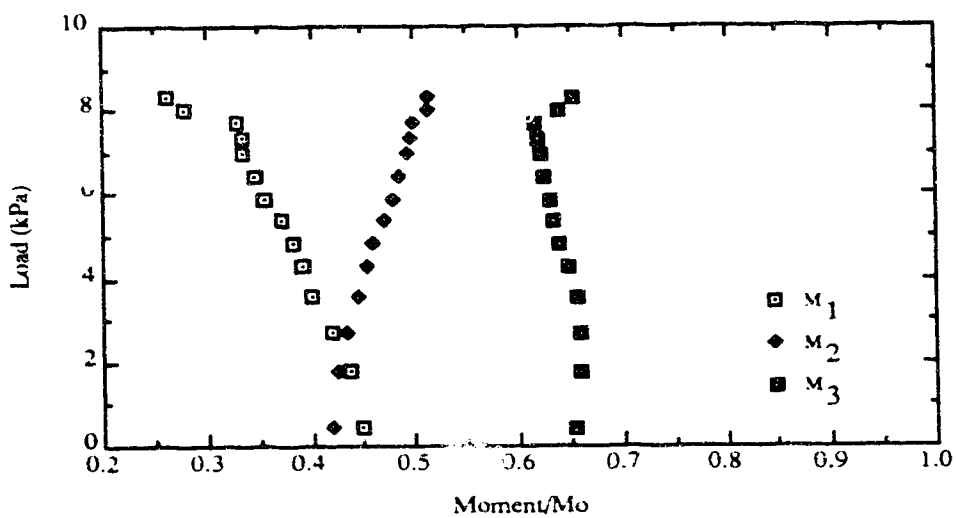
Fig 5.25b: Load vs Moment ratio (N13B9.2)
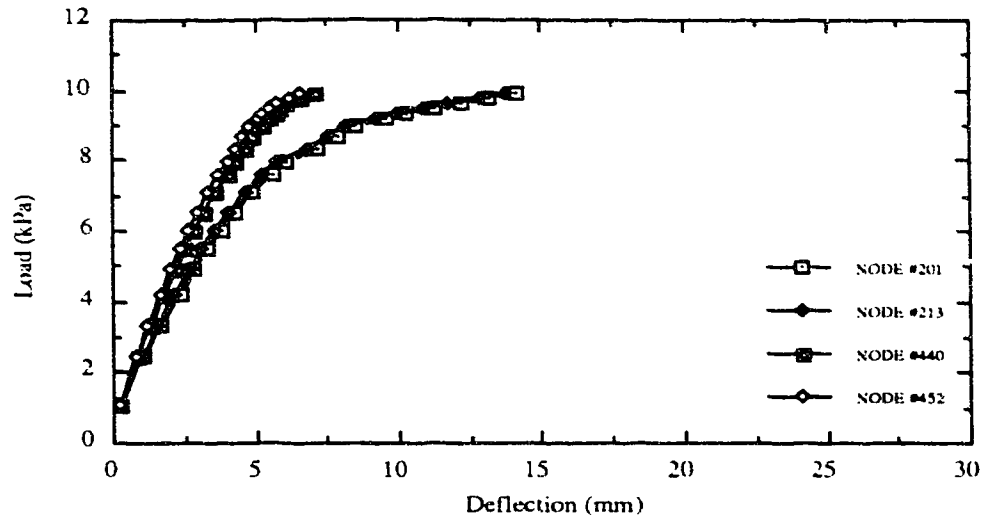
Fig 5.26a: Load vs Deflection (N13B9.4)
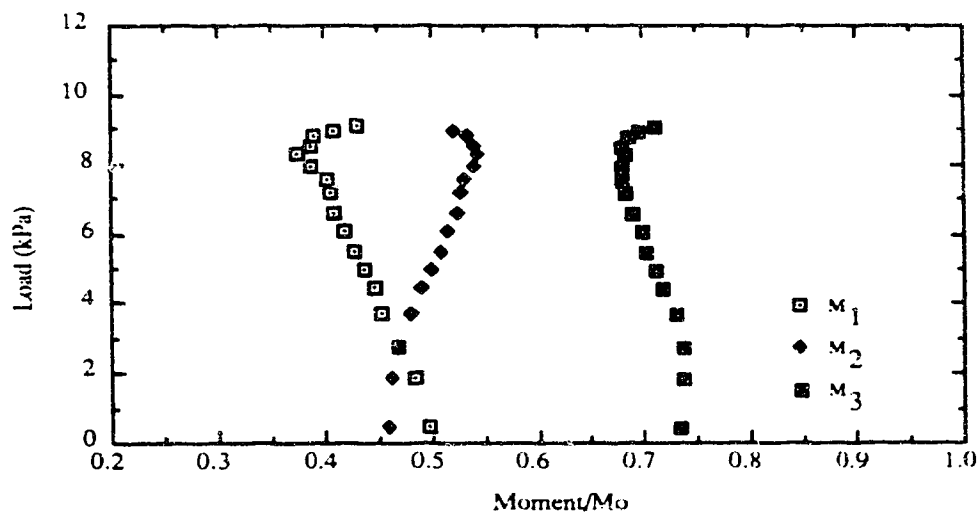
Fig 5.26b: Load vs : . .: : . :?: : (N13B9.4)
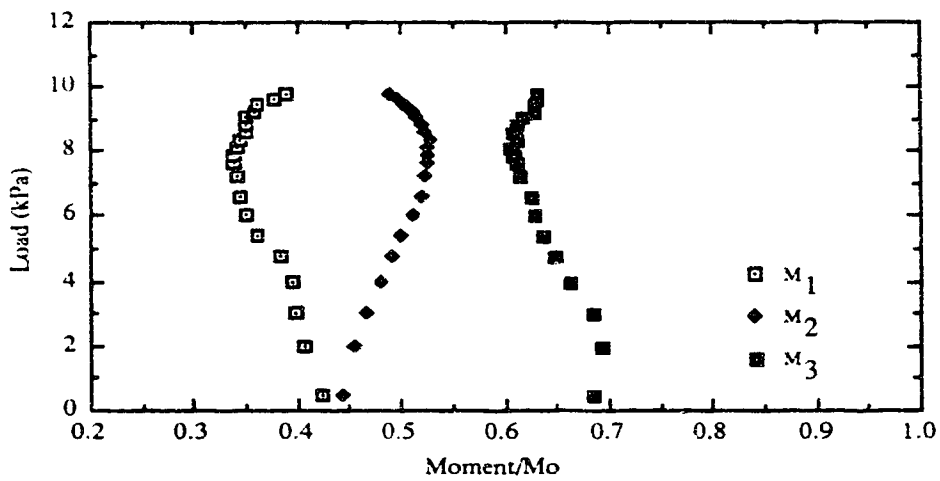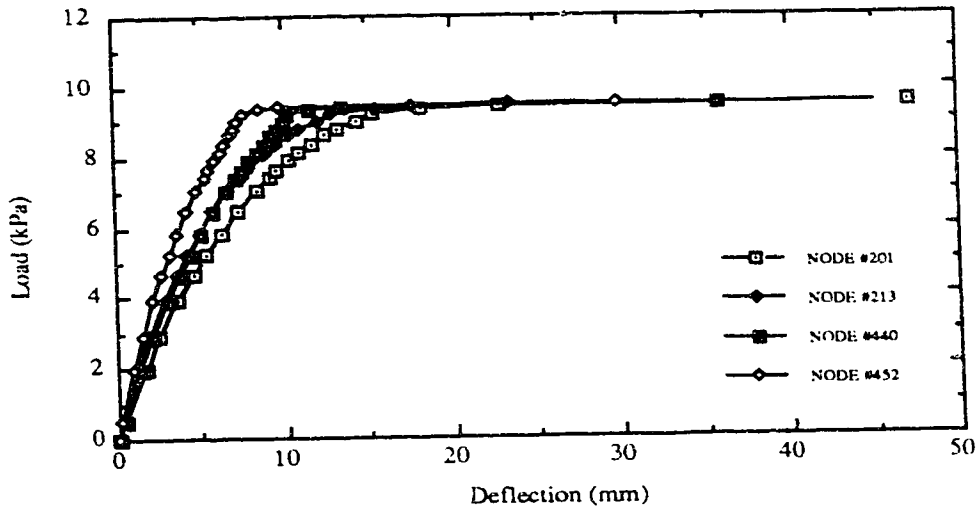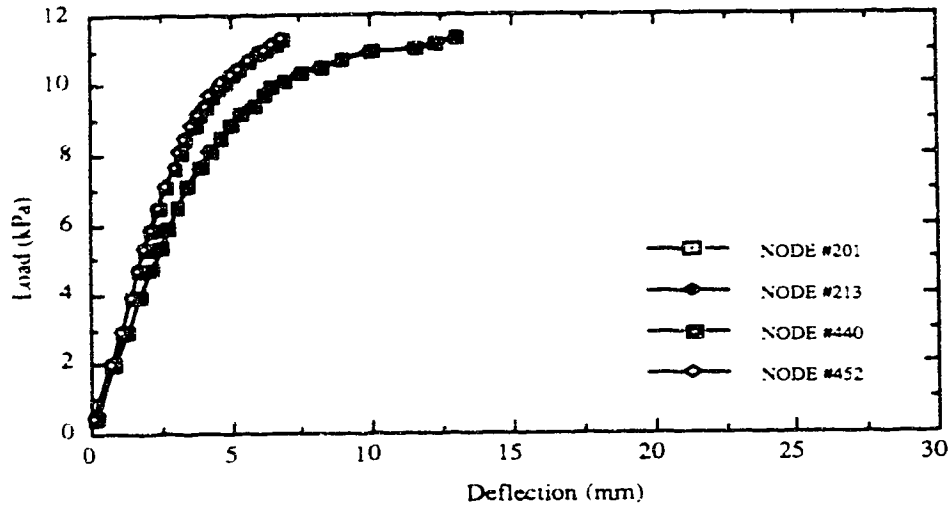
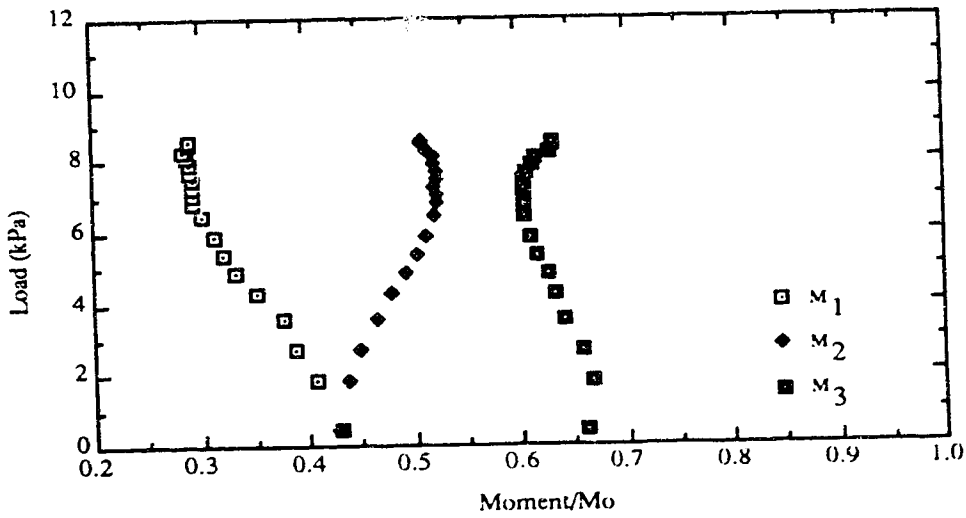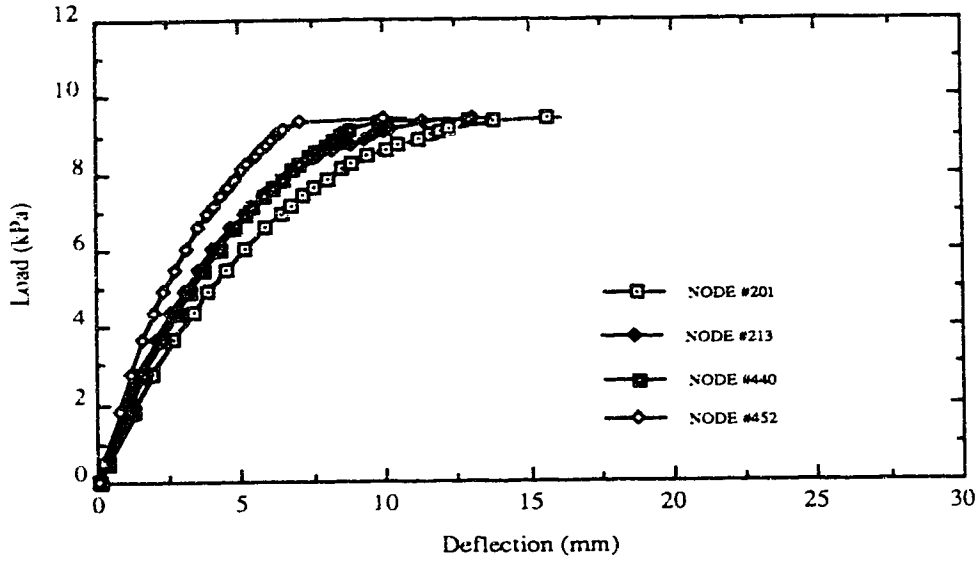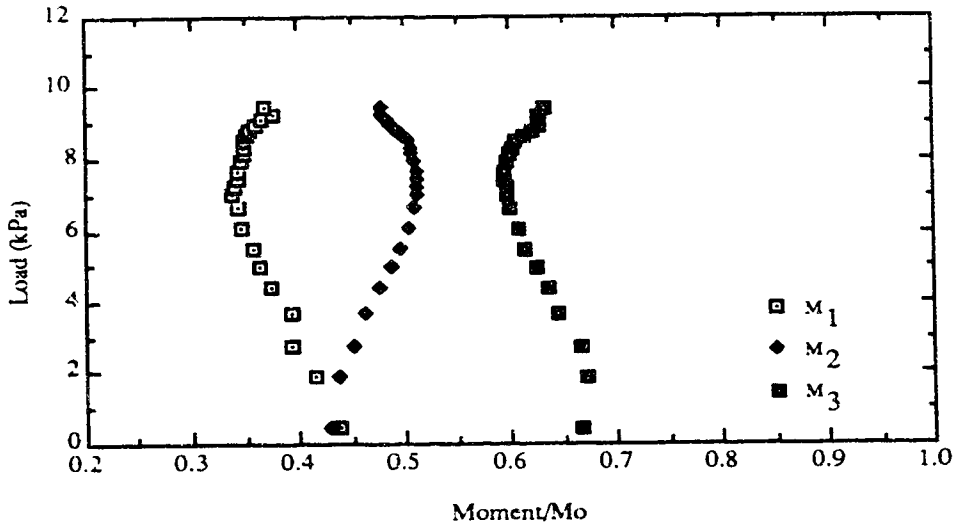Fig 5.27a: Load vs Deflection (N20B12.2)
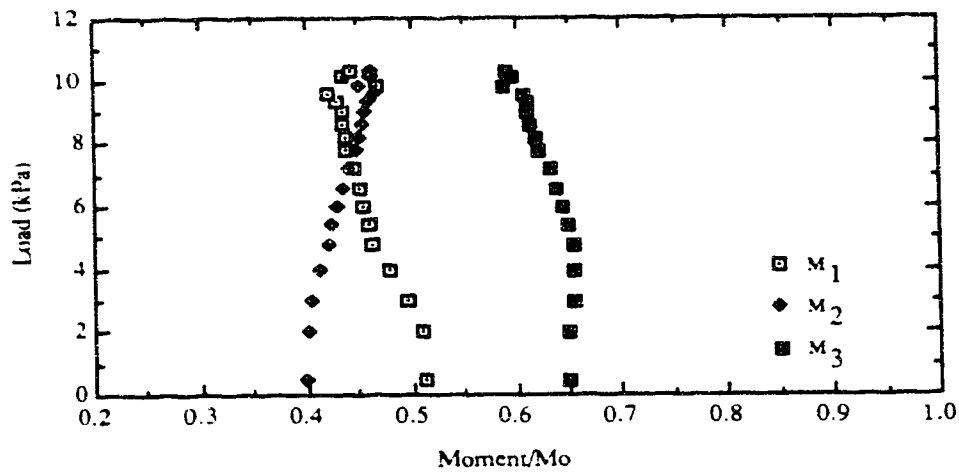
Fig 5.27b: Load vs Moment ratio (N20B12.2)
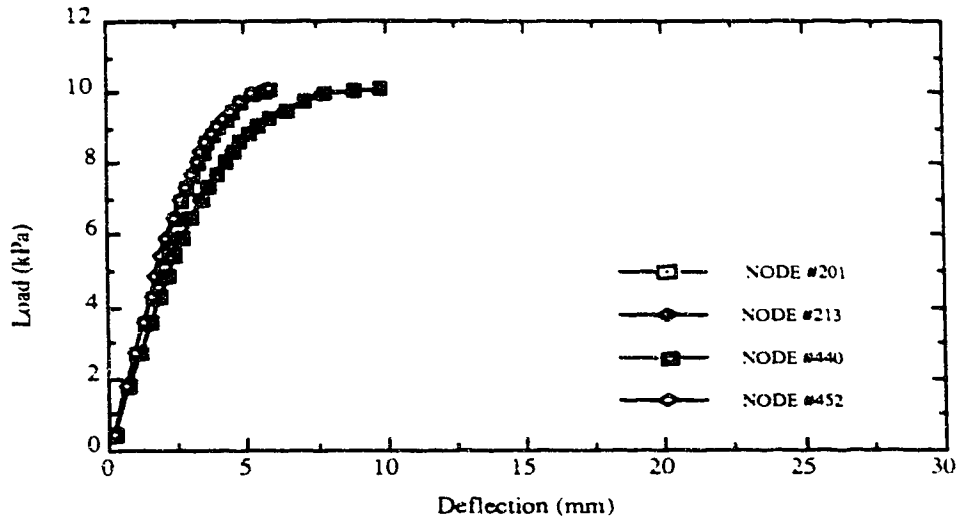
Fig 5.28a: Load vs Deflection (N20B12.4)
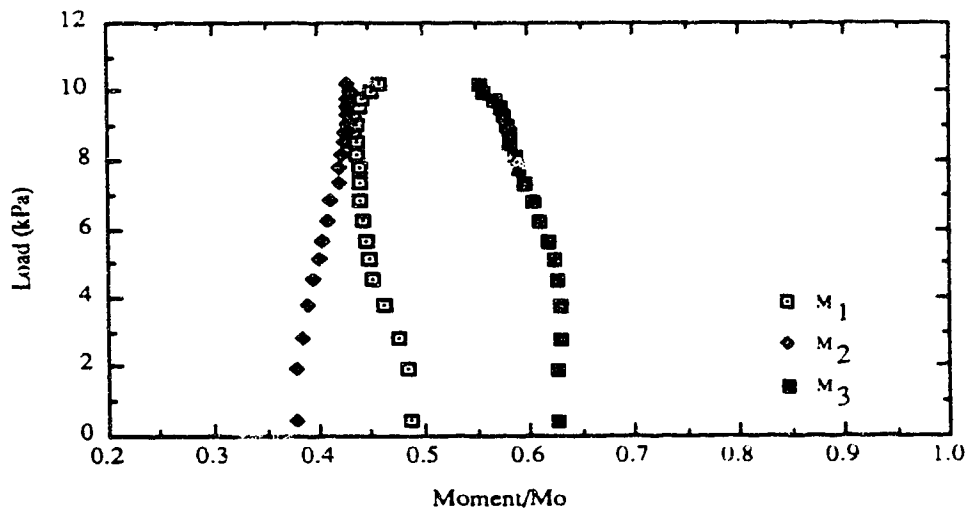
Fig 5.28b: Load vs Moment ratio (N20B12.4)

Chapter 6

Evaluation of DDM' and EFM

6.1 Introduction

The purpose of this chapter is to evaluate the results from the code procedures by using solutions obtained using the non-linear finite element program NISA80.

6.2 Comparison of moment ratios

Design moment ratios obtained from NISA80 are compared to corresponding values from the DDM' and EFM, at the service and factored load levels. Moment ratios are presented in Tables 6.1a to e, corresponding to Sections 1 to 5, respectively. In these tables, when moment ratios from NISA80 are presented as a range, they correspond to the two exterior support reinforcement ratios used which are the likely minimum and maximum values in practice. When a single moment ratio is presented, it corresponds to the single value for reinforcement provided at the exterior support for that design strip. Moment ratios obtained for the code procedures are presented as individual values since they are independent of the reinforcement provided at the design sections. When design strips could not be loaded to the full factored load, an asterisk (*) is used, instead of the moment ratio.

For square panels, there is reasonable agreement in design moment ratios between code design procedures and NISA80 at Section 1, although the EFM gives lower design moment ratios at

156

this section. The DDM' tends to give larger moment ratios for larger column to slab stiffness ratios. This is not surprising because the DDM' is based on the α_{ec}, a function of the exterior column cross section. At Section 3, there is reasonable agreement in design moment ratios, although the DDM' and EFM tend to give larger moment ratios compared to NISA80. This results in lower design moment ratios at Section 2 for the DDM' and EFM compared to those from NISA80. In the interior span, there is reasonable agreement between all procedures at Sections 4 and 5, but NISA80 indicates slightly lower and higher design moment ratios at Sections 4 and 5, respectively.

For panel aspect ratios less than 1.0, the EFM gives much smaller moment ratios at the exterior support (Section 1), as the panel aspect ratio reduces. There is reasonable agreement in design moment ratios between the DDM' and NISA80, at Section 1, but the DDM' gives lower moment ratios. At Section 3, as for square panels, the DDM' and EFM give higher moment ratios. This results in lower moment ratios for the code procedures and higher values at Section 2 for NISA80. In the interior span, there is reasonable agreement between procedures but the EFM tends to give higher moment ratios at Section 4 and lower values at Section 5.

For panel aspect ratios greater than 1.0, there is much better agreement in design moment ratios obtained from the different procedures at Section 1. At Section 3, the code procedures give slightly higher moment ratios compared to NISA80, so that NISA80 gives slightly higher moment ratios at Section 2,

compared to the code procedures. In the interior span, there is much better agreement between the DDM' and EFM, both of which give slightly higher moment ratios at Section 4 compared to NISA80. Correspondingly, NISA80 gives higher moment ratios at Section 5, compared to the code procedures.

6.3 Reasons for the differences

The causes for the differences in the design moment ratios obtained for NISA80 and the code procedures are dealt with in this section. As the DDM' gives design moments only at the critical sections, the discussion of the DDM' is in terms of the design moments only. The EFM, on the other hand, gives both the centreline moments at supports and design moments at critical sections, and the discussion involves both these moments. As major differences were observed at Section 1, the discussion will focus on the exterior support and Section 1, for selected design strips.

The comparison of centreline moments and the corresponding reductions to obtain design moments at the exterior support (Section 1) are presented in Table 6.2, for NISA80 and the EFM. For the DDM', only design moment ratios at Section 1 are presented, for reasons mentioned above. Centre to centre moments are presented as ratios of the centre to centre static moment, M_1. Design moment ratios are also presented, but as ratios of the static moment, M_0.

For square panels (panel aspect ratios greater or equal to 1.0), there is good agreement on design moment ratios between

those obtained using NISA80 for a reinforcement ratio of 0.20 M_O at the exterior support (Section 1) and those obtained using the code procedures DDM' and EFM. When a reinforcement ratio of 0.4 M_O is used at Section 1, moments ratios obtained at Section 1 for NISA80 are greater. Since 0.4 M_O is an unusually large reinforcement ratio, it is concluded that the code procedures give excellent results for the prototype slab.

For panel aspect ratios greater than 1.0, there is reasonable agreement between the methods but the DDM' tends to overestimate the moment ratios at Section 1 when the panel aspect ratio approaches 2.0.

For panel aspect ratios less than 1.0, approaching 0.5, there are substancial differences between the methods as mentioned previously. The differences in design moment ratios between the DDM' and NISA80 are much less compared to the differences between the EFM and NISA80. For the DDM', design moment ratios are about half those for NISA80 whereas for the EFM they are about 1/15 th of the NISA80 values.

It is observed from Table 6.2 that the reduction in centreline moments, $\Delta M/M_1$, for NISA80 and the EFM for small panel aspect ratios are remarkably close which would indicate that the method of reducing centreline moment to Section 1 using Eqn 2.6 is satisfactory. However, the centreline moment ratios from the EFM are only about half those obtained for NISA80. The extremely low values of design moment ratios at Section 1 for the EFM result for moment reduction ratios approaching the centreline moment ratios. This would suggest that the EFM does

not model the exterior stiffness satisfactorily for small panel aspect ratios. These differences may be attributed to the transverse torsional member, employed in the EFM.

The transverse torsional member model over-softens the exterior column, especially for small panel aspect ratios, leading to smaller values for the equivalent column stiffness, K_{ec}. Some researchers (Vanderbilt and Corley, 1983) have observed this and proposed limiting the torsional member length, l_t, to a length equal to the smaller of l_1 and l_2.

In order to investigate the effect of the length of the transverse torsional member on the exterior column stiffness, the equation for computing the torsional stiffness, K_t, is recast as follows:

$$K_t = \Sigma \frac{9 E_c C}{l_t \left(1 - \frac{c_2}{l_t}\right)^3}$$

(6.1)

For various design strips (T series) with size B columns of height 3500 mm, the variation in the stiffness ratio, $K_{ec}/\Sigma K_c$, and the moment ratios M_{cl}/M_1 and M_e/M_o, with the torsional member length ratio, l_t/l_2, are presented in Table 6.3 for the EFM. For the DDM', only the stiffness ratio α_{ec} and moment ratio M_e/M_o are presented. It can be seen that, both the equivalent column stiffness and the corresponding centreline moments are sensitive to the length of the torsional member for panel aspect ratios less than 1.0. In order to obtain centreline moments for the EFM similar to the

values obtained using NISA80 for panel aspect ratios less than 1.0, the torsional member length has to be reduced to less than half the width of the design strip, l_2. The DDM' however gives design moment ratios that compare reasonably well with those obtained for NISA80 if the length of the torsional member is kept equal to l_2 but excellent agreement when the recommendation of limiting the torsional member length to the lesser of the two panel dimensions is applied. For the EFM, on the other hand, although considerable improvement is made, it may not be sufficient, especially for panel aspect ratio less than 1.0. For panel aspect ratios greater than 1.0, using a torsional member length of l_2 for the EFM may lead to larger exterior column stiffnesses and hence larger design moment ratios than the values obtained using NISA80.

Thus, it may be concluded that both code design procedures give reasonable design moments for panel aspect ratios greater or equal to 1.0. For panel aspect ratios less than 1.0, the DDM' gives better design moments compared to the EFM. The recommendation of limiting the torsional member length improves solutions obtained for both code procedures, but not sufficiently for the EFM, especially for panel aspect ratio less than 1.0.

Table 6.1a: Exterior column support design moment ratio (Section 1)

Design strip	NISA80 (service)	NISA80 (factored)	DDM	EFM
N5C1	0.283-0.284	0.242-*	0.112	0.016
N5A2.3	0.3.3	0.321	0.145	0.023
N5B3	0.394-0.395	0.319-0.320	0.205	0.029
N5D6.3	0.416	0.288	0.270	0.012
N7C1	0.227-0.255	*	0.162	0.098
N7A3.3	0.308	*	0.196	0.136
N7B6	0.311-0.337	0.261-0.295	0.275	0.185
N7D9.3	0.349	0.302	0.335	0.190
N10B6	0.306-0.341	0.281-0.378	0.312	0.259
N10B12	0.308-0.349	0.297-0.361	0.332	0.281
N10I12	0.353-0.416	*-0.427	0.365	0.312
N10I24	0.356-0.404	*	0.379	0.326
N10L6	0.342-0.364	0.333-*	0.405	0.250
N10L12.2	0.363	*	0.439	0.285
N10L48	0.267-0.399	*-0.382	0.472	0.318
N13B9	0.355-0.387	*-0.370	0.406	0.362
N20B12	0.454-0.470	0.430-0.466	0.510	0.475

Table 6.1b: Exterior span positive moment ratio (Section 2)

Design strip	NISA80 (service)	NISA80 (factored)	DDM	EFM
N5C1	0.543	0.624-*	0.582	0.650
N5A2.3	0.532	0.590	0.587	0.632
N5B3	0.523-0.506	0.587-0.560	0.542	0.648
N5D6.3	0.487	0.603	0.514	0.633
N7C1	0.573-0.563	*	0.737	0.579
N7A3.3	0.553	*	0.545	0.563
N7B6	0.537-0.527	0.584-0.569	0.612	0.550
N7D9.3	0.530	0.577	0.487	0.538
N10B6	0.537-0.523	0.524-0.496	0.496	0.506
N10B12	0.535-0.519	0.525-0.503	0.487	0.497
N10I12	0.530-0.506	*-0.506	0.473	0.485
N10I24	0.523-0.518	*	0.467	0.478
N10L6	0.517-0.510	0.526-*	0.456	0.514
N10L12.2	0.511	*	0.441	0.496
N10L48	0.543-0.498	*-0.503	0.427	0.479
N13B9	0.500-0.489	*-0.498	0.455	0.463
N20B12	0.450-0.440	0.474-0.457	0.411	0.418

Table 6.1c: Interior support design moment ratio (Section 3)

Design strip	NISA (service)	NISA (factored)	DDM'	EFM
N5C1	0.631-0.630	0.510-*	0.733	0.716
N5A2.3	0.557	0.498	0.728	0.713
N5B3	0.560-0.594	0.507-0.560	0.718	0.675
N7D6.3	0.610	0.505	0.709	0.759
N7C1	0.627-0.619	*	0.725	0.745
N7A3.3	0.586	*	0.720	0.738
N7B6	0.615-0.610	0.572-0.566	0.708	0.715
N7D9.3	0.591	0.545	0.698	0.751
N10B6	0.621-0.612	0.671-0.630	0.702	0.729
N10B12	0.623-0.612	0.653-0.634	0.699	0.725
N10I12	0.586-0.572	*-0.506	0.694	0.719
N10I24	0.552-0.557	*	0.697	0.717
N10L6	0.624-0.616	0.624-*	0.688	0.740
N10L12.2	0.615	*	0.682	0.737
N10L48	0.648-0.605	*-0.613	0.677	0.738
N13B9	0.645-0.636	*-0.633	0.687	0.713
N20B12	0.646-0.649	0.622-0.621	0.672	0.688

Table 6.1d: Interior support design moment ratio (Section 4)

Design strip	NISA(service)	NISA(factored)	DDM	EFM
N5C1	0.614-0.615	0.501-*	0.650	0.708
N5A2.3	0.627	0.611	0.650	0.704
N5B3	0.587-0.588	0.540-0.542	0.650	0.648
N5D6.3	0.559	0.459	0.650	0.672
N7C1	0.611-0.607	*	0.650	0.708
N7A3.3	0.644	*	0.650	0.705
N7B6	0.594-0.596	0.531-0.557	0.650	0.659
N7D9.3	0.578	0.536	0.650	0.677
N10B6	0.595-0.591	0.581-0.599	0.650	0.664
N10B12	0.593-0.591	0.545-0.570	0.650	0.659
N10I12	0.614-0.609	*-0.561	0.650	0.660
N10I24	0.563-0.561	*	0.650	0.656
N10L6	0.578-0.574	0.532-*	0.650	0.665
N10L12.2	0.574	*	0.650	0.655
N10L48	0.586-0.570	*-0.552	0.650	0.644
N13B9	0.608-0.605	*-0.583	0.650	0.646
N20B12	0.612-0.611	0.587-0.586	0.650	0.635

Table 6.1e: Interior span positive moment ratio (Section 5)

Design strip	NISA (service)	NISA (factored)	DDM'	EFM
N5C1	0.386-0.385	0.499-*	0.350	0.292
N5A3.3	0.373	0.389	0.350	0.296
N5B6	0.413-0.412	0.460-0.485	0.350	0.352
N5D9.3	0.441	0.541	0.350	0.328
N7C1	0.389-0.393	*	0.350	0.292
N7A3.3	0.356	*	0.350	0.295
N7B6	0.406-0.404	0.469-0.443	0.350	0.348
N7D9.3	0.422	0.464	0.350	0.323
N10B6	0.405-0.409	0.419-0.441	0.350	0.336
N10B12	0.407-0.409	0.455-0.429	0.350	0.341
N10I12	0.386-0.391	*-0.404	0.350	0.340
N10I24	0.438	*	0.350	0.344
N10L6	0.422-4445	0.468-*	0.350	0.335
N10L12.2	0.426	*	0.350	0.345
N10L48	0.414-0.430	*-0.448	0.350	0.356
N13B9	0.392-0.395	*-0.417	0.350	0.354
N20B12	0.388-0.389	0.413-414	0.350	0.365

Table 6.2: Comparison of NISA80, DDM and EFM at the exterior support (factored load level)

Design Strip Ratio	Stiffness ratio α_{cs}	NISA80			DDM	EFM		
		M_{cl}/M_1	$\Delta M/M_1$	M_e/M_o	M_e/M_o	M_{cl}/M_1	$\Delta M/M_1$	M_e/M_o
N5C1.2	0.83	0.329	0.133	0.242	0.112	0.144	0.131	0.016
N5A2.3	1.66	0.440	0.201	0.321	0.145	0.177	0.159	0.023
N5B3.2	3.00	0.468	0.234	0.319	0.205	0.247	0.226	0.029
N5B3.4	3.00	0.473	0.238	0.320	0.205	0.247	0.226	0.029
N5D6.3	6.00	0.533	0.324	0.288	0.270	0.325	0.312	0.012
N7B6.2	6.00	0.369	0.156	0.242	0.275	0.310	0.159	0.185
N7B6.4	6.00	0.398	0.157	0.378	0.275	0.310	0.159	0.185
N7D9.3	9.00	0.462	0.218	0.302	0.335	0.378	0.224	0.190
N10B6.2	6.00	0.363	0.121	0.281	0.312	0.345	0.122	0.259
N10B6.4	6.00	0.437	0.111	0.378	0.312	0.345	0.122	0.259
N10B12.2	12.00	0.368	0.116	0.297	0.332	0.365	0.123	0.281
N10B12.4	12.00	0.427	0.116	0.361	0.332	0.365	0.123	0.281
N10I12.4	12.00	0.478	0.110	0.427	0.365	0.393	0.124	0.312
N10L6.2	6.00	0.	0.232	0.333	0.405	0.443	0.225	0.250
N10L48.4	48.00	0.539	0.234	0.399	0.468	0.499	0.249	0.315
N13B9.4	9.00	0.406	0.087	0.370	0.406	0.438	0.126	0.312
N20B12.2	12.00	0.485	0.114	0.430	0.504	0.535	0.140	0.469
N20B12.4	12.00	0.516	0.114	0.466	0.504	0.535	0.140	0.469

Table 6.3: Effect of the torsional member length on code procedures (T series)

Design Strip	Geometry		EFM				DDM'	
	l_1/l_2	l_t/l_2 ($N\text{-}mm \times 10^{10}$)	ΣK_{ec}	$K_{ec}/\Sigma K_c$	M_{cl}/M_1	M_e/M_o	α_{ec}	M_e/M_o
T5B20	0.50	0.25	25.37	0.67	0.44	0.27	1.57	0.40
T5B20	0.50	0.50*	14.03	0.37	0.35	0.16	0.91	0.31
T5B20	0.50	0.75	9.48	0.25	0.29	0.09	0.62	0.25
T5B20	0.50	1.00	7.12	0.19	0.25	0.03	0.47	0.21
T7B20	0.75	0.25	25.37	0.67	0.50	0.40	2.35	0.46
T7B20	0.75	0.50	14.03	0.37	0.41	0.30	1.36	0.38
T7B20	0.75	0.75*	9.48	0.25	0.35	0.23	0.94	0.31
T7B20	0.75	1.00	7.12	0.19	0.31	0.18	0.71	0.27
T10B20	1.00	0.25	25.37	0.67	0.53	0.46	3.14	0.49
T10B20	1.00	0.50	14.03	0.37	0.45	0.38	1.81	0.42
T10B20	1.00	0.75	9.48	0.25	0.39	0.31	1.25	0.36
T10B20	1.00	1.00*	7.12	0.19	0.35	0.26	0.95	0.32
T13B20	1.33	0.25	30.51	0.81	0.57	0.51	4.93	0.54
T13B20	1.33	0.50	18.26	0.42	0.52	0.46	3.10	0.49
T13B20	1.33	0.75	12.54	0.33	0.48	0.41	2.17	0.45
T13B20	1.33	1.00*	9.48	0.25	0.44	0.36	1.66	0.41
T20B20	1.00	0.25	35.91	0.95	0.62	0.56	8.54	0.58
T20B20	1.00	0.50	25.37	0.67	0.59	0.53	6.28	0.56
T20B20	1.00	0.75	18.26	0.48	0.57	0.50	4.64	0.54
T20B20	1.00	1.00*	14.03	0.37	0.54	0.48	3.63	0.51

*Recommended l_t/l_2 values by Vanderbilt and Corley (1983)

Chapter 7

Prismatic Equivalent Frame Method (PEFM)

7.1 Introduction

The EFM simplifies the analysis of three-dimensional column-slab systems to that of two-dimensional frames. It was found that, despite the computational effort involved in obtaining stiffnesses for use in the EFM, it does not give reasonable design moments for some geometries. Furthermore, for slabs without beams studied in Chapter 3, consideration of the variation in the cross section was found to be unwarranted. This suggests that a plane frame analysis procedure, using prismatic members with appropriately assigned stiffnesses, may lead to comparable and even more reasonable design moments compared to those obtained using the EFM. This chapter examines such a procedure.

Since most of the differences in moment ratios were observed at the exterior support, the procedure for obtaining the effective moment of inertia for columns to be input for the plane frame program is aimed mainly at the exterior support. The purpose of the torsional member in the EFM is to soften the column stiffness by making use of the equivalent column stiffness, K_{ec}, rather than the gross stiffness, ΣK_c. With the PEFM, the reduction in column stiffness is achieved by making use of a reduction factor, γ. This factor is applied to the gross moment of inertia of the column, I_g, to obtain the effective column moment of inertia, I_{eff}, as follows:

$$I_{eff} = \gamma I_g \qquad (7.1)$$

Although the stiffness of the exterior column support is the major cause for the differences in design moments, for simplicity, the computed reduction factor is applied to the gross moment of inertia of each interior column.

7.2 Modelling of the design strip

When using the PEFM, the design strip is modelled as a series of prismatic slab-beam elements and supporting columns, as shown in Figs 7.1 and 7.2. The boundary conditions are the same as those used by the EFM. Columns, of centre to centre heights equal to floor to floor heights, are assumed fixed at the extreme ends. All other nodes are left free to deform. It should be mentioned that there are other possibilities for boundary conditions but this configuration was chosen because it conforms to the positions of joints in the frame.

Cantilever spans of lengths equal to half the exterior column dimension, $c_1/2$, or the actual length of the cantilever, if different, must be included. Use of cantilever spans is to account for the total applied load and to obtain realistic moments for the exterior columns. Solutions obtained using the EFM and NISA80 also took into account cantilever spans.

As for any plane frame analysis, the PEFM gives centreline moments at the supports. Therefore, the computed centreline moments have to be reduced to obtain design moments at the critical sections. In Chapter 5, it was clearly demonstrated that the

equilibrium reduction procedure (Eqn 2.6), employed in the EFM, gave reductions that compared very well with those obtained from NISA80. Therefore, the same procedure is used in the PEFM.

While the basic modelling for PEFM requires nodes at the intersection of members only, if desired, additional nodes may be placed along the axes of the members so that moments at these locations may be obtained directly from the output. This technique gives identical design moments as would be obtained using the equilibrium procedure for reducing centreline moments as given by Eqn 2.6 and was used in the study. Nodes were also provided at the clear in.   s of slab-beam members.

7.3   Geometry and major variables of design strips

In general, the same series as used in Chapters 3 but with column designations of Chapter 5 (Table 5.1) are considered. For all design strips, the nominal column height is 3.5 m (support to support), the slab thickness is 200 mm and the concrete strength is 30 MPa. The design strips from the C and P series, are used to study the effects of column and panel aspect ratios on the design moment ratios. The PEFM was also applied to design strips from the S series and to slabs with beams (PB and PE series). For the PB, PE and S series, design moment ratios are compared to those obtained by the code procedures DDM' and EFM as there are no NISA80 solutions for these design strips.

The primary variables for the C, P and S series are; exterior column aspect ratio, panel aspect ratio and successive span length ratio, respectively. For the PB and PE series, the primary variables

are the beam widths and depths, respectively. For slabs with edge beams only, the total depth of edge beams was 500 mm, but beam web thicknesses ranged from 200 to 500 mm. For slabs with beams between all supports, beam dimensions in the longitudinal direction were selected to give beam to slab stiffness ratios in the longitudinal direction (α_1) of 0.5, 1.0, 1.5, 2.0, 3.0 and 4.0. The same beam dimensions were used for beams in the transverse direction.

The other variable for all design strips is the relative or 'effective' moment of inertia for columns, γ. Interior columns for all design strips were square and of sizes either B (500x500) or C (350x350), corresponding to the smaller exterior column dimension.

7.4 Prediction of the reduction factor, γ

From the discussion in Chapter 6, it was felt that the effective moment of inertia of columns for use in the PEFM will be a function of the panel aspect ratio. A trial and error approach is used in obtaining the required reduction factors. Selection of values for the reduction factor in slabs without beams is based on comparing solutions obtained using NISA80 to those obtained from the code procedures (DDM' and EFM). For the S series and slabs with beams (PB and PE series), the selection of reduction factors is based on solutions obtained using the code procedures.

Panel aspect ratio as defined in this study is the ratio l_1/l_2 whereas in A23.3, it is defined as the inverse of this ratio or l_2/l_1. It was therefore decided to use the ratio l_2/l_1 in proposing equations for determining the reduction factors to be used when reducing the

column moment of inertia. However, in all discussions panel aspect ratio is still the ratio l_1/l_2.

7.4.1 C and P series

For a start, a linear expression for the reduction factor to obtain effective column stiffness for use in the PEFM was tried, as follows:

$$\gamma = 0.15 + 0.35 \frac{l_2}{l_1} \qquad (7.2)$$

The above equation is shown graphically in Fig 7.3.

Moment ratios obtained using the PEFM are compared to those obtained for the DDM', EFM and NISA80 at each critical section in Tables 7.1a to c. Moment ratios for the PEFM, using the reduction factors given by Eqn 7.2 are presented under column P1. At Section 1, it may be observed that for panel aspect ratios less than 1.0, the proposed equation for reduction factor leads to moment ratios for the PEFM that are much closer to the DDM' and NISA80 values than to those obtained from the EFM. For a panel aspect ratio of 2.0, the PEFM gives moment ratios that are just smaller than those obtained for NISA80, in contrast with the code procedures which give much larger values. For panel aspect ratios of about 1.0, use of Eqn 7.2 leads to larger design moment ratios at Section 1 compared to those obtained from either the code procedures or NISA80. At Section 3, the PEFM in general gives moment ratios that are lower than those obtained for the code procedures and closer to those obtained using

NISA80. As pointed out earlier, this is desirable, as the code procedures tend to give higher negative moment ratios. In the interior span (Sections 4 and 5), there is better agreement in design moments obtained using NISA80 and the PEFM than those from the code procedures for all panel aspect ratios.

To improve the agreement between the PEFM and NISA80 at Section 1 for panel aspect ratios between the extremes, a bilinear form of an equation was tried as follows:

when $l_2/l_1 \leq 1.0$, $\gamma = 0.2 + 0.2\ l_2/l_1$

when $l_2/l_1 > 1.0$, $\gamma = -0.1 + 0.5\ l_2/l_1$ (7.3)

Eqn 7.3 is also presented graphically in Fig 7.3. Moment ratios obtained using the PEFM with reduction factors determined from Eqn 7.3 are presented in Tables 7.1a, b and c under column P2, at each critical section. Moment ratios from the code procedures and NISA80 remain the same.

Using Eqn 7.3 for the PEFM, it is observed that there is generally better agreement in design moment ratios at Section 1 compared to the previous case although for panel aspect ratios of about 1.0, PEFM still gives greater moment ratios compared to those obtained for the code procedures and NISA80. As mentioned earlier, for stiff exterior columns, moment ratios at Section 1 are sensitive to the amount of reinforcement provided across this section. It is observed that although the moment ratios based on Eqn 7.3 are generally larger than those obtained using NISA80, comparison should be to the lower reinforcement ratios as these are the ratios

preferred in practice. At Section 3, the design moment ratios from the PEFM have increased slightly but are still in between NISA80 and the code values. The change in design moment ratios for the PEFM in the interior span is small but it leads to even better agreement with NISA80.

To improve agreement in design moments further, the bilinear reduction factor equation was adjusted as follows:

$$\text{when } l_2/l_1 \leq 1.0, \ \gamma = 0.3$$
$$\text{when } l_2/l_1 > 1.0, \ \gamma = -0.3 + 0.6 \ l_2/l_1 \qquad (7.4)$$

Eqn 7.4 is also presented graphically in Fig 7.3.

Using this equation, moment ratios obtained for the PEFM are presented in Tables 7.1a, b and c under column P3 for each critical section. At Section 1, for panel aspect ratios of about 1.0, it is observed that moment ratios given by the PEFM agree very closely with those for the DDM' and fall between the values given by the EFM and NISA80 in some cases. Values for extreme panel aspect ratios are not significantly different from those obtained using Eqn 7.3. At Section 3, the change in moment ratios is small but agreement between procedures is better. In the interior span, again the change in moment ratios for the PEFM is small and for all panel aspect ratios, the moment ratios fall between the code values and NISA80 moment ratios. Therefore, Eqn 7.4 is recommended for slabs without beams.

7.4.2 S series

The reader is reminded that for the S series, the width of the design strip is kept constant at 7 m and the span ratio is defined as the ratio, l_1/l'_1 (see Fig 7.2). So, when the span ratio is greater or equal to 1.0, the exterior panel is square (panel aspect ratio equal to 1.0) whereas for span ratios less than 1.0, the exterior panel aspect ratio is less than 1.0.

Eqns 7.2, 7.3 and 7.4 were again used to determine reduction factors for use in the PEFM for the S series. Moment ratios obtained for the code procedures are compared to those obtained by the PEFM when the different equations for reduction factor are used in Tables 7.2a to c. Moment ratios for the PEFM corresponding to Eqns 7.2, 7.3 and 7.4 are presented under columns P1, P2 and P3, respectively, at each critical section.

Moments in the exterior span are compared in Table 7.2a. For all span ratios, the use of Eqn 7.4 is seen to provide the most consistent agreement with the code procedures. For equal spans, $l_1/l'_1 = 1.0$, the design moment ratios at Section 3 fall between the code values and at Section 1 is equal to the DDM' values. For small values of l_1/l'_1, say equal to 0.5, the unrealistically small centreline moment leading to positive moment at Section 1 that is obtained using the EFM does not occur with the PEFM although the moment is smaller than that obtained for the DDM'. Similarly at Section 3, a design moment of 1.3 M_O is more likely than the 2.1 M_O obtained using the EFM.

In interior spans, Table 7.2b, when the first interior span is only half the exterior span, the negative moments at midspan are

reduced. While a definite conclusion cannot be made without say, finite element solutions, it is felt that the moment distribution obtained using PEFM and Eqn 7.4 are equally as acceptable as those obtained using the EFM.

7.4.3 PB series (Slabs with beams between all supports)

Using the moment of inertia reduction factors given by Eqn 7.3, PEFM moment ratios were obtained for the PB series (slabs with beams between all supports) and are compared to moment ratios obtained for the EFM in Table 7.3. It can be seen that the PEFM gives consistently lower design moment ratios at Section 1 compared to the EFM, especially for larger beam to slab stiffness ratios and larger panel aspect ratios. Moreover, the moment ratios in some cases are unrealistically low. It is inferred that use of Eqn 7.4 would lead to even lower design moment ratios at Section 1, especially for panel aspect ratios near 1.0. From Table 7.3, it is clear that the required reduction factors are a function of both the beam to slab stiffness ratio and the panel aspect ratio. Also, when beams are present, a larger effective column stiffness is required to lead to larger design moment ratios at Section 1.

For slabs with beams, it was felt that regardless of the panel aspect ratio, the maximum moment of inertia for columns is the gross moment of inertia. This led to the development of Table 7.4. In this table, the reduction factors for slabs without beams are based on Eqn 7.4. To take into account both the beam to slab stiffness ratio and panel aspect ratio, the reduction factor was made a function of the parameter $\alpha l_2/l_1$, where α is the beam to slab stiffness ratio.

The value of this parameter at which the gross moment of inertia should be used, ie. $\gamma=1.0$, was set at greater or equal to 1.0. To obtain values of reduction factors for values of $\alpha l_2/l_1$ between 0.0 and 1.0 in Table 7.4, linear interpolation is suggested.

To evaluate Table 7.4, PEFM solutions were obtained for design strips with panel aspect ratios of 0.5, 1.0 and 2.0, and longitudinal beam to slab stiffness ratios (α_1) ranging from 0.25 to 4.0 using reduction factors in Table 7.4 and two definitions of α. The two definitions for α considered were α_1 and α equal to the average of the beam to slab stiffness ratios $(\alpha_1$ and $\alpha_2)$ at the exterior support. These solutions are designated PEFM-α_1 and PEFM-α_a, respectively. Design moment ratios at Section 1 obtained for the PEFM are compared to those obtained using the code procedures (DDM-84, DDM' and EFM) for each panel aspect ratio, in Figs 7.4 to 7.6.

For a panel aspect ratio of 1.0, Fig 7.5, the definition of α affects the column stiffness reduction factor only for values of α_1 less than 1.0. This is because for the same beam dimensions in the each direction, α_2 is much larger than α_1 at the exterior support. It is seen that there is little difference in the design moment ratios between the two definitions of α. For values of α less than 1.0, there is excellent agreement between moment ratios at Section 1 obtained using PEFM and the code procedures DDM' and EFM. For values of α_1 greater than 1.0, the three methods show decreasing moment with increasing α_1 but the rate of decrease is greater with the PEFM. For high values of α_1, the moments from the PEFM fall approximately midway between those using the current code

procedures, DDM-84 and EFM. While not presented, the agreement in moment ratios at other critical sections is excellent.

For panel aspect ratios greater than 1.0, Fig 7.6 the moment ratios at Section 1 are less sensitive to the magnitude of α, and values of moment ratios for the PEFM are consistently about 10% less than for the DDM' and EFM, but are larger than the DDM-84 values. For $l_1/l_2=2.0$, the moments at Section 1 from DDM-84 are much smaller than those from other methods.

For a pane' aspect ratio of 0.5, Fig 7.4, it is obvious that there is considerable variation in design moment from the four procedures. For $\alpha=0.0$, it was shown that the PEFM moment ratios agreed closely with those obtained from NISA80, and that the EFM moment ratios were unrealistically low. There is hardly any difference in design moment ratios for the PEFM if the average of the beam to slab stiffness ratios rather than α_1 is used in obtaining the reduction factors. For $\alpha_1=1.0$, there is close agreement between PEFM, DDM-84 and EFM with DDM' giving moment ratios approximately twice as great. For larger values of α, the rate of moment drop is greater for the PEFM compared to the code procedures. Although not presented, the agreement between moment ratios at other critical sections is good.

From Figs 7.4 to 7.6, the magnitude of α does not have a large influence on the design moments and this may be due to using the same beam dimensions in the two directions. However, this is permitted, as long as the beam to slab stiffness ratios in the two directions do not differ significantly so as to negate two-way behaviour.

It is concluded, that for slabs with beams, the effective column stiffness obtained using Table 7.4 leads to satisfactory design moments.

7.4.4 PE series

For slabs with edge beams (PE series), the reduction factors of Table 7.4 were also applied for the PEFM. Values of α used in the interpolation correspond to either the full or half the edge beam to slab stiffness ratios (α_2) as there are no beams in the longitudinal direction. The corresponding solutions are designated PEFM-α_2 and PEFM-α_a, respectively. Moment ratios for the PEFM at Section 1 are compared to corresponding values from the DDM-84, DDM' and EFM for panel aspect ratios of 0.5, 1.0 and 2.0 in Figs 7.7 to 7.9.

For a panel aspect ratio of 0.5, the effective moment of inertia is close to the gross moment of inertia for all beam to slab stiffness ratios and so moments are not sensitive to the definition of α. In Fig 7.7, moment ratios for the PEFM at Section 1 are nearly constant (between 0.31 and 0.33) and are very close to the DDM-84 values. In contrast, both the DDM' and EFM give significantly lower moment ratios at Section 1 for small values of α_2. For larger values of α_2, the PEFM moment ratios fall in between those obtained for the code procedures but approach the EFM values.

For a panel aspect ratio of 1.0, there is excellent agreement in design moment ratios between the DDM' and PEFM at Section 1, for slabs without beams ($\alpha_2=0.0$) and for larger beam sizes ($\alpha_2=2.5$). Between these values, the PEFM gives larger moment ratios at Section 1 compared to the code procedures. The DDM-84 values

seem reasonable for beam to slab stiffness ratios less than 1.0 but are much lower for larger α_2 values. Defining α_2 as α results in the use of gross moments of inertia in columns which lead to slightly higher moment ratios.

For a panel aspect ratio of 2.0, moment ratios obtained at Section 1 for the PEFM agree well with those obtained for the DDM' and EFM. While using $\alpha=\alpha_2$ results in better agreement between the EFM and PEFM at Section 1, the moment ratios obtained using the average value, in this case $\alpha=\alpha_2/2$, may be considered to lead to more realistic moments as moment ratios obtained for the code procedures do not take into account cracking in the concrete at higher load levels. NISA80 indicated that moment ratios near ultimate were lower than the service values. DDM-84 gives much lower design moment ratios compared to the other procedures.

7.5 Recommendation of reduction factors

It is concluded that the reduction factors for determining effective column stiffness for use in the PEFM given in Table 7.4 are satisfactory for obtaining design moments at critical sections. Values of design moment ratios obtained using the PEFM for slabs without beams are closer to those obtained using the non-linear finite element program, NISA80 than to those obtained using the EFM. The problem of unrealistically low moment ratios at Section 1 observed in the EFM, for small l_1/l_2 ratios, is eliminated. Moment ratios for slabs with beams are equally reasonable and agree closely with the code procedures.

In evaluating Table 7.4, comparisons with the EFM were made with no adjustment to the computed design moments. As indicated in Chapter 2, the design codes permit modifying the design moment obtained using any form of elastic frame analysis by up to 20% provided the total panel moment is satisfied. Hence, this provision can also be applied to the PEFM. Obviously, where such modifications are used, agreement between PEFM and EFM can be made much closer.

It is recognized that the recommendations for column stiffness factors given in Table 7.4 may be improved should an exhaustive study of the PB, PE and S series based on a non-linear finite element analysis be done. However, in the absence of such studies, the proposed reduction factors for use in the PEFM are sufficiently accurate for design purposes.

Table 7.1a: Design moment ratios for C and P series (slabs without beams)

Design Strip	Section 1						Section 2					
Procedure	D'	E	N	P1	P2	P3	D'	E	N	P1	P2	P3
N5C1.2	0.112	0.016	0.242	0.108	0.118	0.118	0.582	0.650	0.624	0.603	0.598	0.598
N5A2.3	0.145	0.023	0.360	0.242	0.253	0.253	0.587	0.632	0.575	0.555	0.550	0.550
N5B3.2	0.205	0.029	0.319	0.280	0.290	0.290	0.542	0.648	0.587	0.551	0.547	0.547
N5B3.4	0.205	0.029	0.320	0.280	0.290	0.290	0.542	0.648	0.560	0.551	0.547	0.547
N5D6.3	0.270	0.012	0.288	0.325	0.316	0.316	0.514	0.633	0.603	0.539	0.509	0.509
N7B6.2	0.275	0.185	0.261	0.390	0.377	0.357	0.612	0.550	0.584	0.474	0.479	0.486
N7B6.4	0.275	0.185	0.295	0.390	0.377	0.357	0.612	0.550	0.569	0.474	0.479	0.486
N7D9.3	0.335	0.190	0.302	0.388	0.377	0.363	0.487	0.538	0.577	0.461	0.464	0.470
N10B6.2	0.312	0.259	0.281	0.384	0.349	0.300	0.496	0.546	0.524	0.384	0.475	0.495
N10B6.4	0.312	0.259	0.378	0.384	0.349	0.300	0.496	0.546	0.496	0.478	0.475	0.495
N10I12.4	0.365	0.312	0.427	0.483	0.458	0.421	0.473	0.485	0.506	0.430	0.439	0.453
N10L48.2	0.472	0.315	0.360	0.467	0.458	0.443	0.427	0.475	0.514	0.429	0.432	0.437
N10L48.4	0.472	0.315	0.406	0.467	0.458	0.443	0.427	0.475	0.500	0.429	0.432	0.437
N13B9.4	0.406	0.362	0.370	0.415	0.391	0.367	0.455	0.463	0.498	0.450	0.459	0.468
N20B12.2	0.510	0.469	0.430	0.421	0.410	0.410	0.411	0.418	0.474	0.447	0.451	0.451
N20B12.4	0.510	0.469	0.466	0.421	0.410	0.410	0.411	0.418	0.557	0.447	0.451	0.451

D'=DDM'; E=EFM; N=NISA80; P1, P2, P3=PEFM (Eqns 7.2, 7.3 and 7.4)

Table 7.1b: Design moment ratios for C and P series (slabs without beams)

Design Strip	Section 3						Section 4					
Procedure	D'	E	N	P1	P2	P3	D'	E	N	P1	P2	P3
N5C1.2	0.733	0.716	0.510	0.686	0.686	0.686	0.650	0.708	0.501	0.655	0.653	0.653
N5A2.3	0.728	0.713	0.489	0.649	0.647	0.647	0.650	0.704	0.611	0.632	0.630	0.630
N5B3.2	0.718	0.675	0.507	0.617	0.615	0.615	0.650	0.648	0.540	0.569	0.567	0.567
N5B3.4	0.718	0.675	0.560	0.617	0.615	0.615	0.650	0.648	0.542	0.569	0.567	0.567
N5D6.3	0.709	0.759	0.505	0.588	0.665	0.665	0.650	0.672	0.459	0.554	0.594	0.594
N7B6.2	0.708	0.700	0.572	0.663	0.666	0.671	0.650	0.659	0.531	0.661	0.609	0.612
N7B6.4	0.708	0.700	0.566	0.663	0.666	0.671	0.650	0.659	0.537	0.661	0.609	0.612
N7D9.3	0.698	0.700	0.545	0.691	0.694	0.697	0.650	0.677	0.536	0.651	0.635	0.638
N10B6.2	0.702	0.729	0.671	0.693	0.701	0.711	0.650	0.664	0.581	0.631	0.638	0.647
N10B6.4	0.702	0.729	0.630	0.693	0.701	0.711	0.650	0.664	0.599	0.632	0.638	0.647
N10I12.4	0.694	0.719	0.506	0.658	0.664	0.672	0.650	0.659	0.561	0.648	0.627	0.634
N10L48.2	0.677	0.738	0.611	0.675	0.678	0.682	0.650	0.644	0.555	0.616	0.617	0.619
N10L48.4	0.677	0.738	0.594	0.675	0.678	0.682	0.650	0.644	0.553	0.616	0.617	0.619
N13B9.4	0.687	0.713	0.633	0.686	0.692	0.698	0.650	0.646	0.583	0.627	0.631	0.634
N20B12.2	0.672	0.688	0.622	0.684	0.687	0.687	0.650	0.635	0.587	0.626	0.628	0.628
N20B12.4	0.672	0.688	0.621	0.684	0.687	0.687	0.650	0.635	0.586	0.626	0.628	0.628

D'=DDM; E=EFM; N=NISA80; P1, P2, P3=PEFM (Eqns 7.2, 7.3 and 7.4)

Table 7.1c: Design moment ratios for C and P series (slabs without beams)

Design Strip	Section 5					
Procedure	D'	E	N	P1	P2	P3
N5C1.2	0.350	0.292	0.499	0.345	0.347	0.347
N5A2.3	0.350	0.296	0.396	0.368	0.370	0.370
N5B3.2	0.350	0.352	0.460	0.431	0.433	0.433
N5B3.4	0.350	0.352	0.485	0.431	0.433	0.433
N5D6.3	0.350	0.328	0.541	0.446	0.406	0.406
N7B6.2	0.350	0.350	0.469	0.339	0.391	0.388
N7B6.4	0.350	0.350	0.443	0.339	0.391	0.388
N7D9.3	0.350	0.464	0.464	0.349	0.365	0.362
N10B6.2	0.350	0.336	0.419	0.368	0.362	0.353
N10B6.4	0.350	0.336	0.441	0.368	0.362	0.353
N10I12.4	0.350	0.350	0.404	0.352	0.373	0.366
N10L48.2	0.350	0.350	0.445	0.384	0.383	0.381
N10L48.4	0.350	0.350	0.447	0.384	0.383	0.381
N13B9.4	0.350	0.354	0.417	0.373	0.369	0.366
N20B12.2	0.350	0.365	0.413	0.374	0.372	0.372
N20B12.4	0.350	0.365	0.414	0.374	0.372	0.372

D'=DDM; E=EFM; N=NISA80; P1, P2, P3=PEFM (Eqns 7.2, 7.3 and 7.4)

Table 7.2a: Design moment ratios for S series (full factored load on all spans)

Design Strip	Section 1					Section 2					Section 3				
Procedure	D'	E	P1	P2	P3	D'	E	P1	P2	P3	D'	E	P1	P2	P3
S5B20*	0.209	-.138	0.101	0.114	0.114	0.540	0.038	0.281	0.288	0.288	0.718	2.062	1.338	1.311	1.311
S7B20	0.270	0.123	0.247	0.178	0.160	0.514	0.441	0.402	0.309	0.308	0.708	0.996	0.948	0.744	0.764
S10B20	0.316	0.260	0.399	0.365	0.317	0.494	0.500	0.454	0.467	0.485	0.701	0.739	0.692	0.702	0.714
S13B20	0.316	0.288	0.425	0.392	0.345	0.494	0.542	0.480	0.480	0.519	0.701	0.627	0.615	0.615	0.616
S15B20*	0.316	0.294	0.431	0.398	0.351	0.494	0.551	0.486	0.496	0.527	0.701	0.602	0.597	0.616	0.594
S20B20*	0.316	0.301	0.439	0.406	0.359	0.494	0.561	0.494	0.512	0.537	0.701	0.576	0.573	0.570	0.567

D'=DDM'; E=EFM; P1, P2, P3=PEFM

* Outside the span limitations for the DDM

Table 7.2b: Design moment ratios for S series (full factored load on all spans)

Design Strip	Section 4					Section 5					Section 6				
Procedure	D'	E	P1	P2	P3	D'	E	P1	P2	P3	D'	E	P1	P2	P3
S5B20*	0.650	0.559	0.574	0.575	0.575	0.350	0.479	0.437	0.435	0.435	0.650	0.484	0.553	0.555	0.555
S7B20	0.650	0.600	0.581	0.580	0.578	0.350	0.439	0.434	0.436	0.440	0.650	0.522	0.552	0.552	0.542
S10B20	0.650	0.683	0.638	0.646	0.658	0.350	0.358	0.379	0.376	0.371	0.650	0.601	0.604	0.603	0.599
S13B20	0.650	0.898	0.753	0.753	0.828	0.350	0.162	0.270	0.270	0.215	0.650	0.777	0.706	0.706	0.743
S15B20*	0.650	1.070	0.850	0.784	0.967	0.350	0.004	0.178	0.247	0.008	0.650	0.921	0.793	0.722	0.864
S20B20*	0.650	1.910	1.354	1.482	1.658	0.350	-.774	-.305	-.416	-.567	0.650	1.638	1.257	1.357	1.475

D'=DDM'; E=EFM; P1, P2, P3=PEFM

* Outside the span limitations for the DDM

Table 7.2c: Design moment ratios for S series (full factored load on all spans)

Design Strip	Section 7					Section 8				
Procedure	D'	E	P1	P2	P3	D'	E	P1	P2	P3
S5B20*	0.650	1.627	1.054	1.034	1.034	0.350	-.627	-.054	-.034	-.034
S7B20	0.650	0.785	0.772	0.604	0.616	0.350	0.215	0.228	0.167	0.154
S10B20	0.650	0.613	0.612	0.611	0.609	0.350	0.387	0.388	0.389	0.391
S13B20	0.650	0.535	0.562	0.562	0.543	0.350	0.465	0.438	0.438	0.457
S15B20*	0.650	0.518	0.551	0.554	0.528	0.350	0.482	0.435	0.446	0.472
S20B20*	0.650	0.498	0.535	0.524	0.509	0.350	0.502	0.465	0.476	0.491

D'=DDM'; E=EFM; P1, P2, P3=PEFM

* Outside the span limitations for the DDM

Table 7.3: Moment ratios for PB series (Eqn 7.3 for reduction factor)

Design Strip Procedure	Section 1		Section 2		Section 3		Section 4		Section 5	
	E	P	E	P	E	P	E	P	E	P
PB5B5 (1.0)	0.175	0.171	0.580	0.602	0.666	0.625	0.609	0.587	0.391	0.413
PB7B5 (1.0)	0.313	0.214	0.495	0.547	0.697	0.692	0.630	0.639	0.370	0.361
PB10B5 (1.0)	0.387	0.232	0.454	0.524	0.704	0.720	0.639	0.661	0.361	0.339
PB13B5 (1.0)	0.437	0.265	0.435	0.510	0.694	0.716	0.635	0.654	0.365	0.346
PB20B5 (1.0)	0.496	0.317	0.411	0.488	0.681	0.708	0.633	0.643	0.367	0.357
PB5B5 (2.0)	0.143	0.083	0.594	0.647	0.669	0.622	0.616	0.603	0.385	0.397
PB7B5 (2.0)	0.285	0.130	0.507	0.586	0.702	0.698	0.636	0.658	0.364	0.342
PB10B5 (2.0)	0.362	0.150	0.464	0.561	0.710	0.727	0.643	0.681	0.357	0.319
PB13B5 (2.0)	0.410	0.181	0.444	0.547	0.701	0.725	0.638	0.674	0.362	0.326
PB20B5 (2.0)	0.471	0.234	0.419	0.523	0.690	0.720	0.635	0.661	0.365	0.339
PB5B5 (3.0)	0.111	0.028	0.609	0.023	0.672	0.615	0.625	0.611	0.384	0.389
PB7B5 (3.0)	0.254	0.077	0.520	0.678	0.707	0.698	0.642	0.671	0.358	0.329
PB10B5 (3.0)	0.330	0.100	0.475	0.612	0.716	0.729	0.648	0.695	0.352	0.307
PB13B5 (3.0)	0.378	0.128	0.455	0.586	0.709	0.728	0.643	0.687	0.357	0.313
PB20B5 (3.0)	0.442	0.178	0.429	0.572	0.698	0.726	0.638	0.674	0.362	0.326
PB5B5 (4.0)	0.082	-.009	0.622	0.701	0.675	0.608	0.633	0.615	0.383	0.385
PB7B5 (4.0)	0.228	0.041	0.531	0.631	0.710	0.697	0.648	0.679	0.352	0.321
PB10B5 (4.0)	0.309	0.066	0.485	0.602	0.721	0.729	0.653	0.695	0.347	0.297
PB13B5 (4.0)	0.357	0.091	0.464	0.590	0.714	0.730	0.647	0.697	0.353	0.303
PB20B5 (4.0)	0.421	0.138	0.437	0.567	0.705	0.728	0.642	0.685	0.358	0.315

E=EFM, P=PEFM

Table 7.4: Values of reduction factors, γ, for PEFM

Panel	l_2/l_1		
Stiffness ratio	0.50	1.00	2.00
$\alpha \dfrac{l_2}{l_1} = 0.0$	0.30	0.30	0.90
$\alpha \dfrac{l_2}{l_1} \geq 1.0$	1.00	1.00	1.00

Note: Linear interpolation between values is suggested
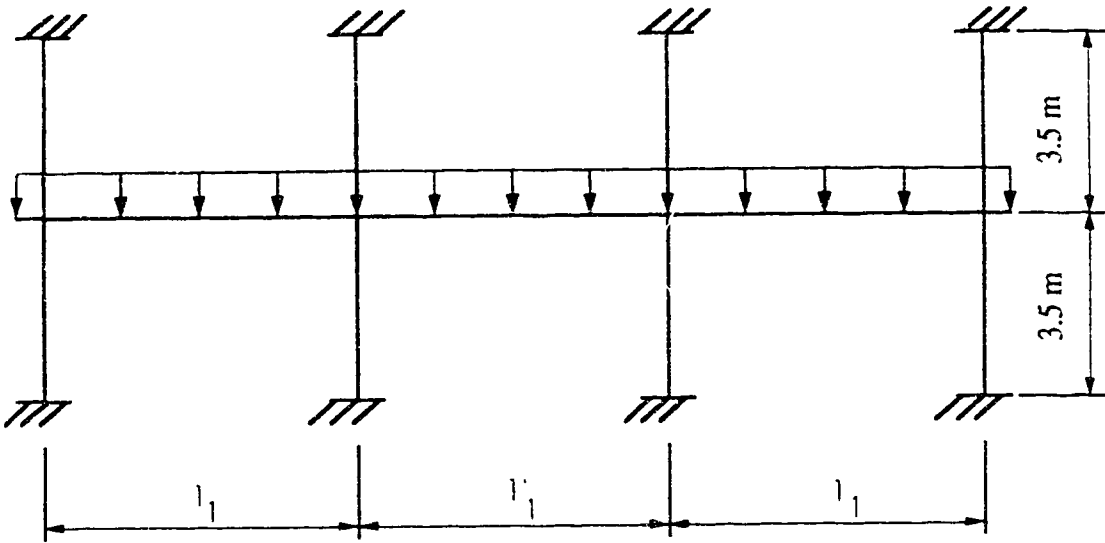
Fig 7.1:Design strip geometry for C and P series
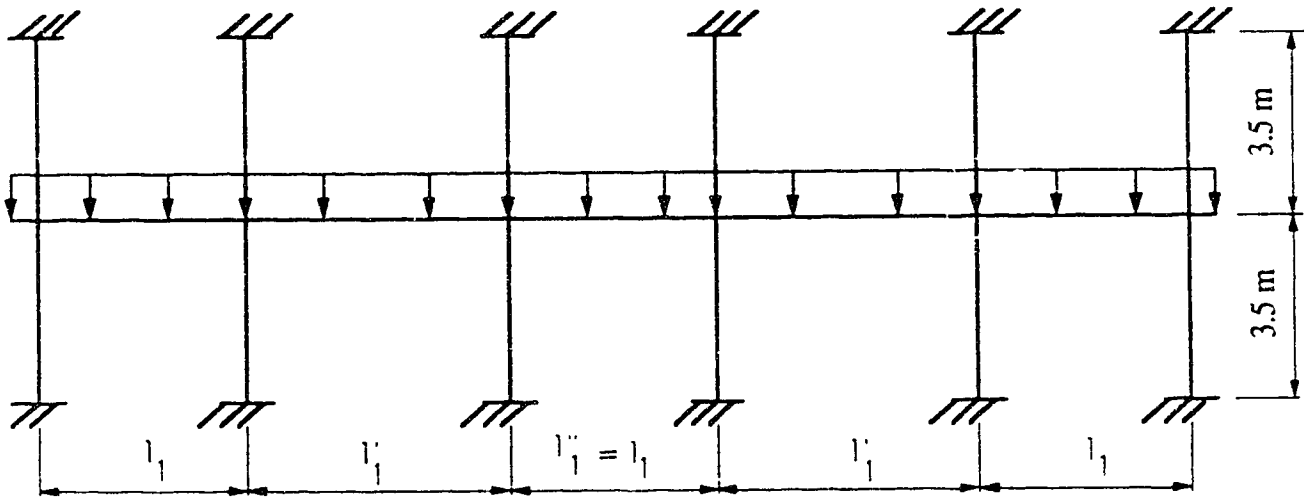
Fig 7.2: Design strip geometry for S series
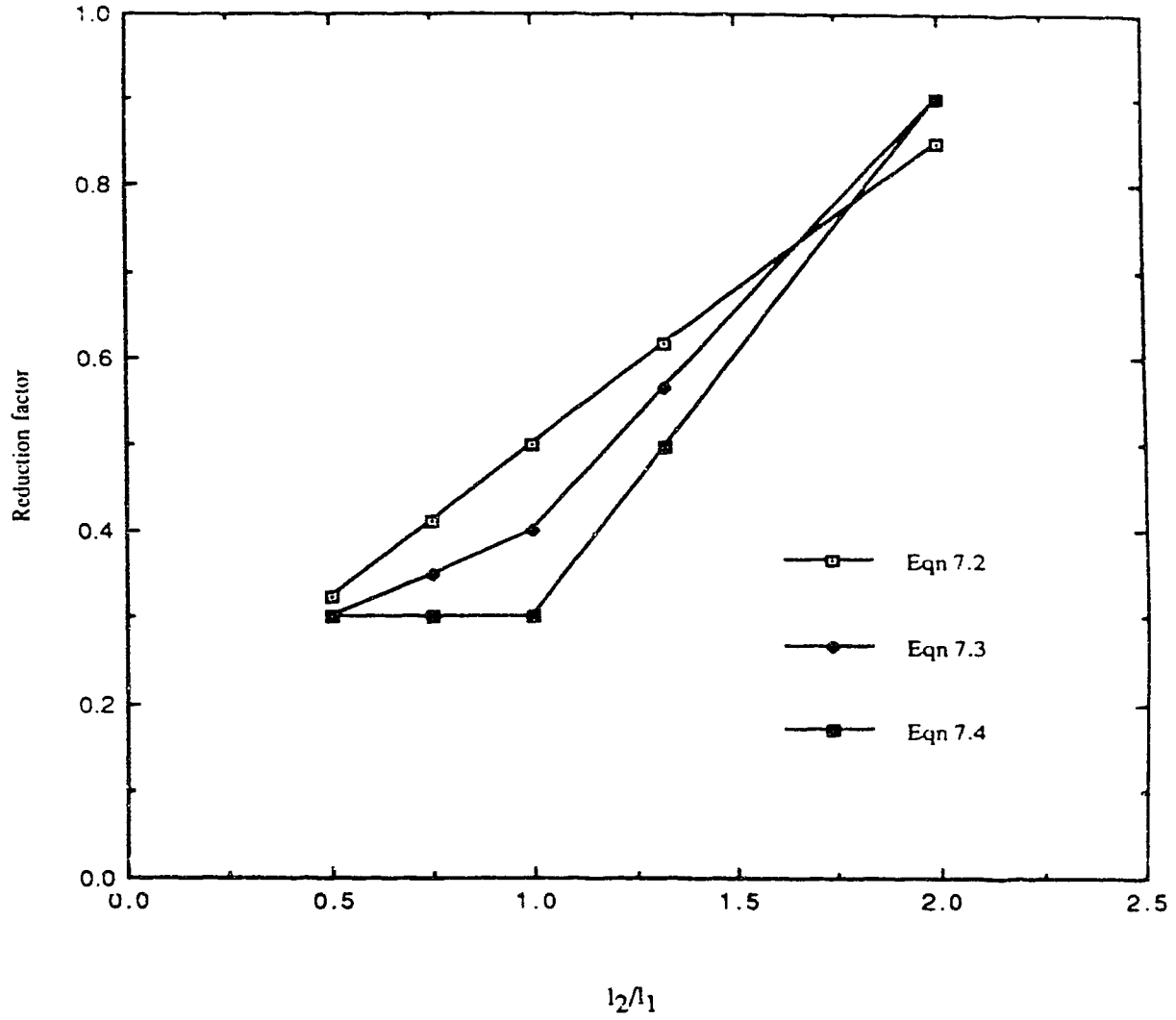
Fig 7.3: Reduction factor vs l_2/l_1
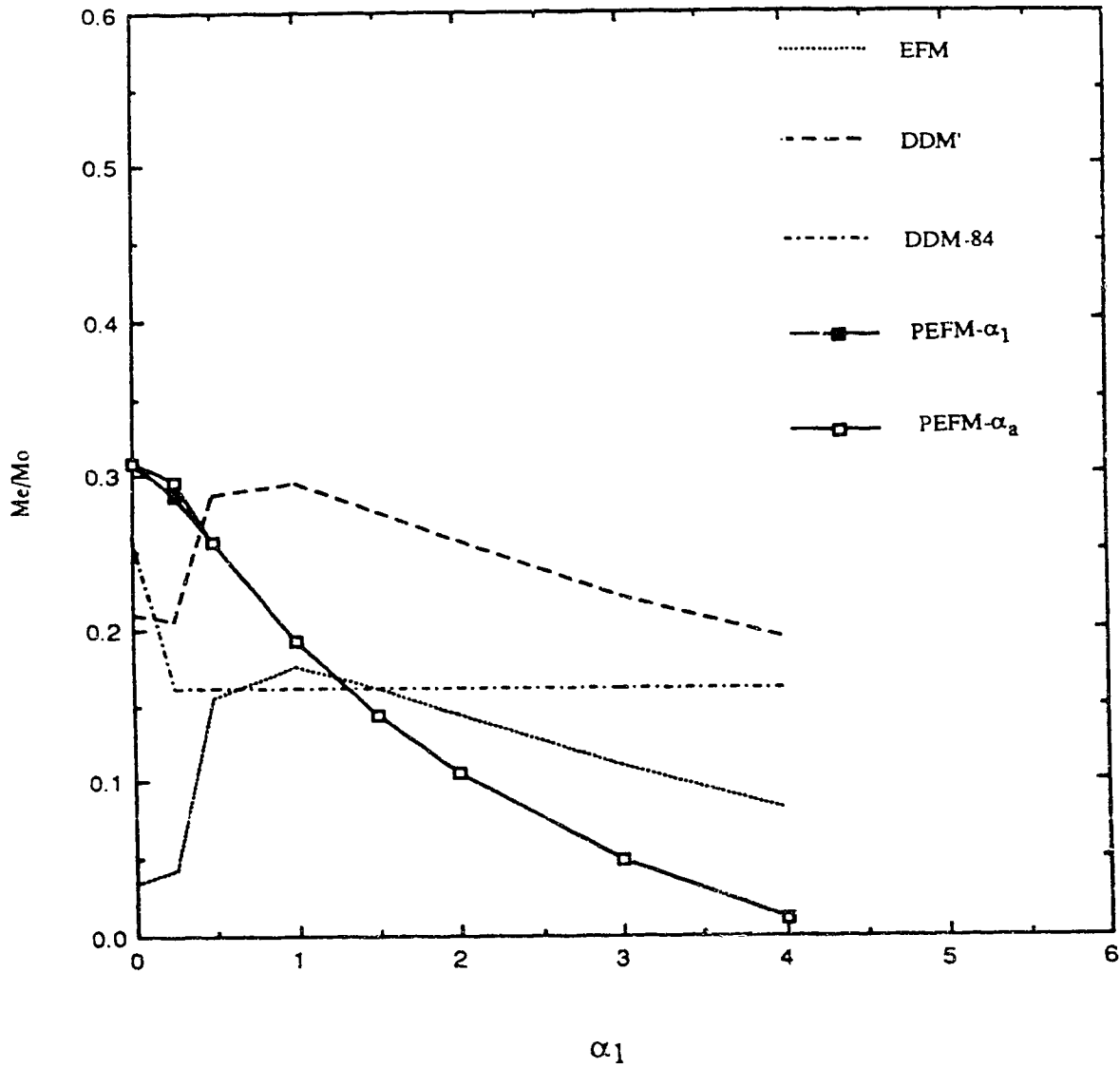
Fig 7.4: Moment ratio at Section 1 (PB series, $l_1/l_2=0.5$)
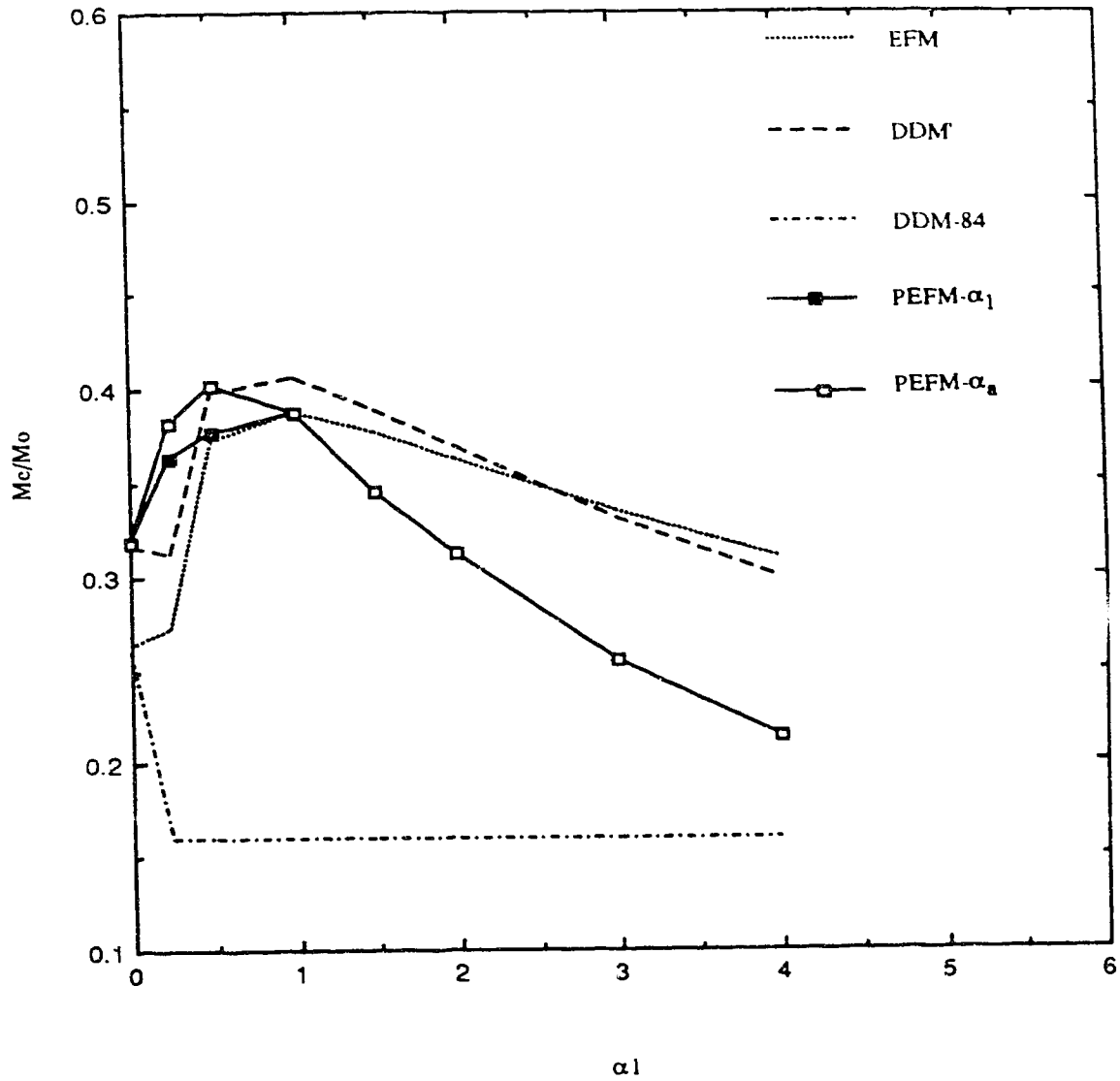
Fig 7.5: Moment ratio at Section 1 (PB series, $l_1/l_2=1.0$)
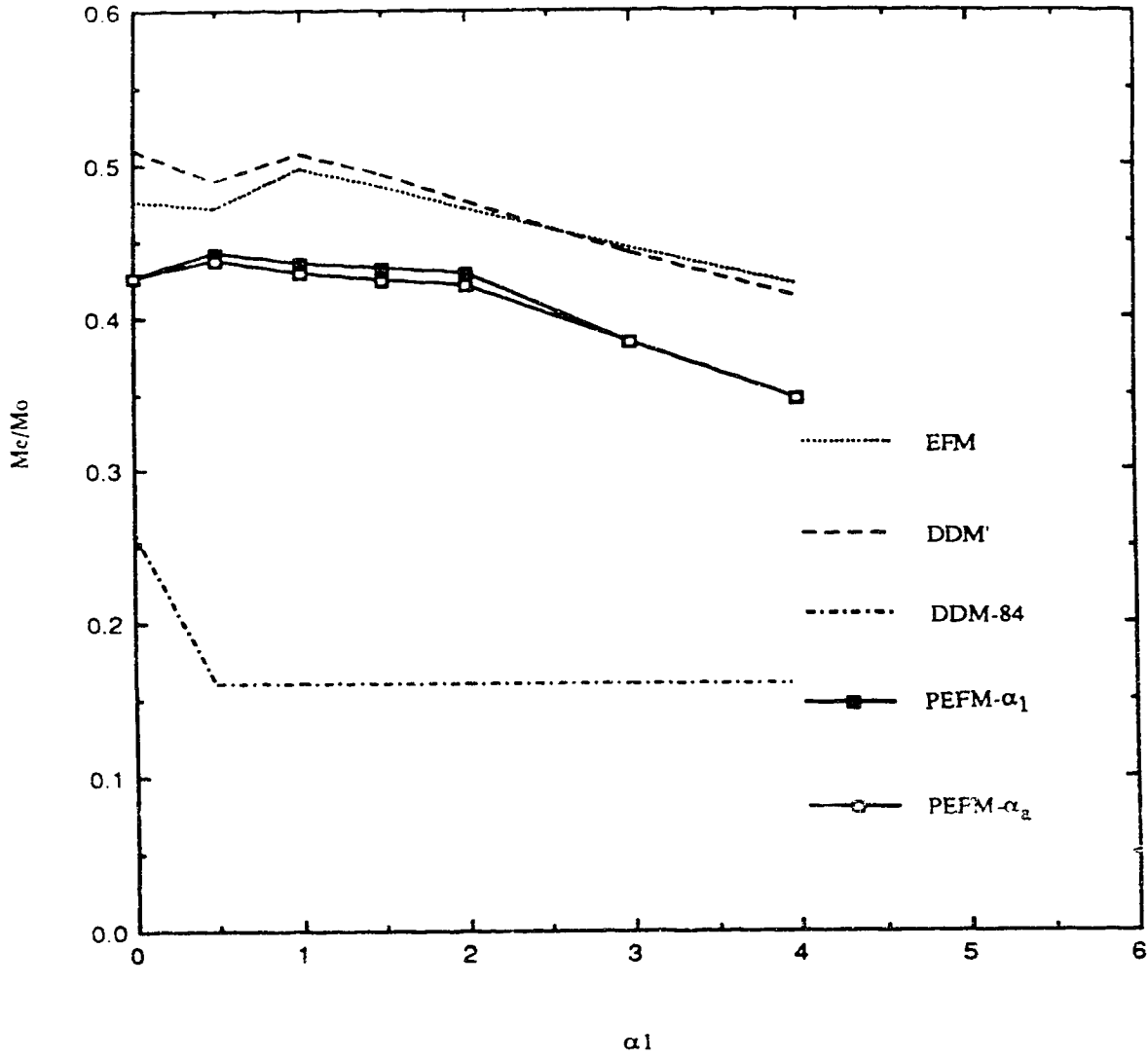
Fig 7.6: Moment ratio at Section 1 (PB series, $l_1/l_2=2.0$)
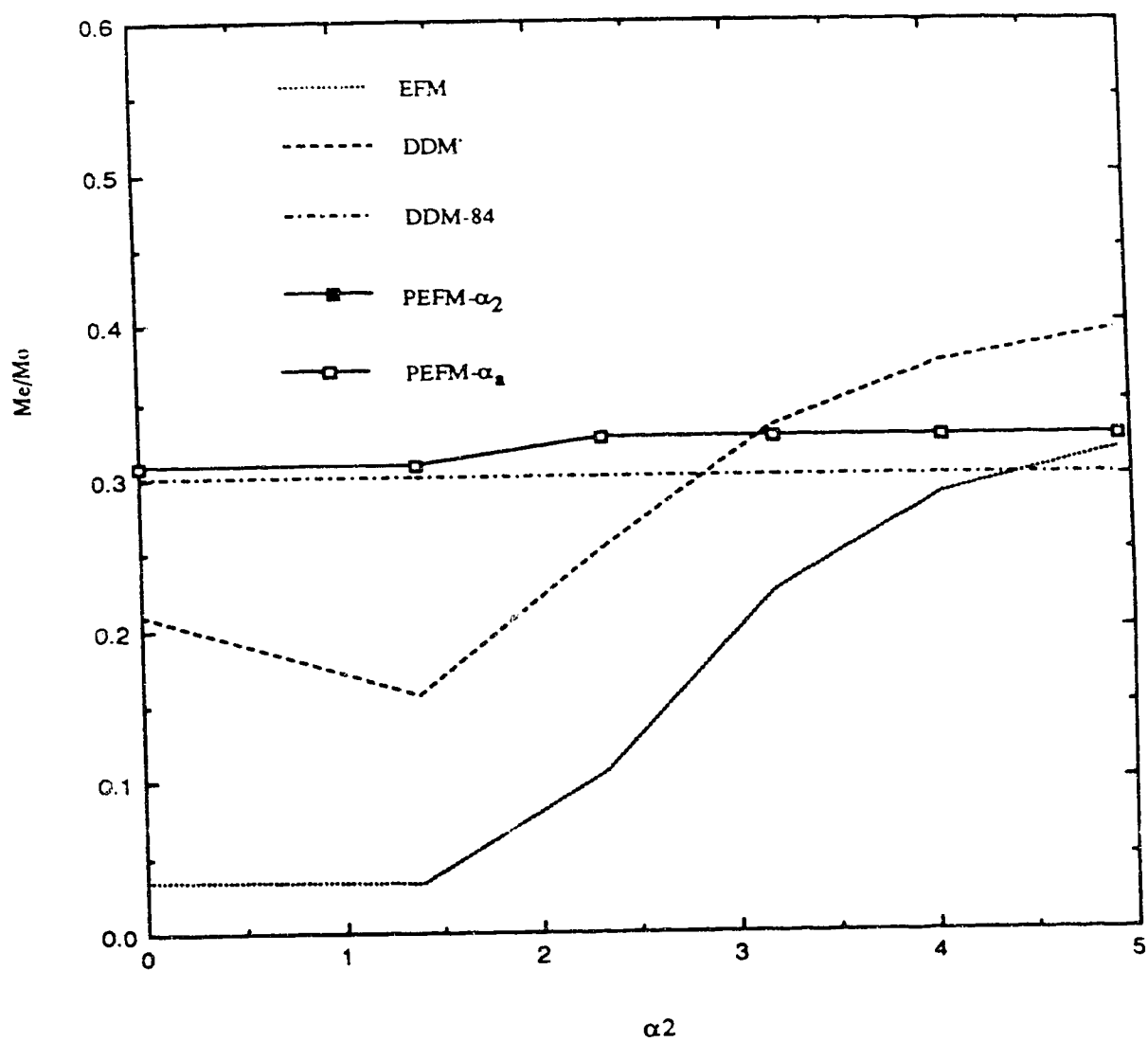
Fig 7.7: Moment ratio at Section 1(PE series, l_1/l_2=0.5)
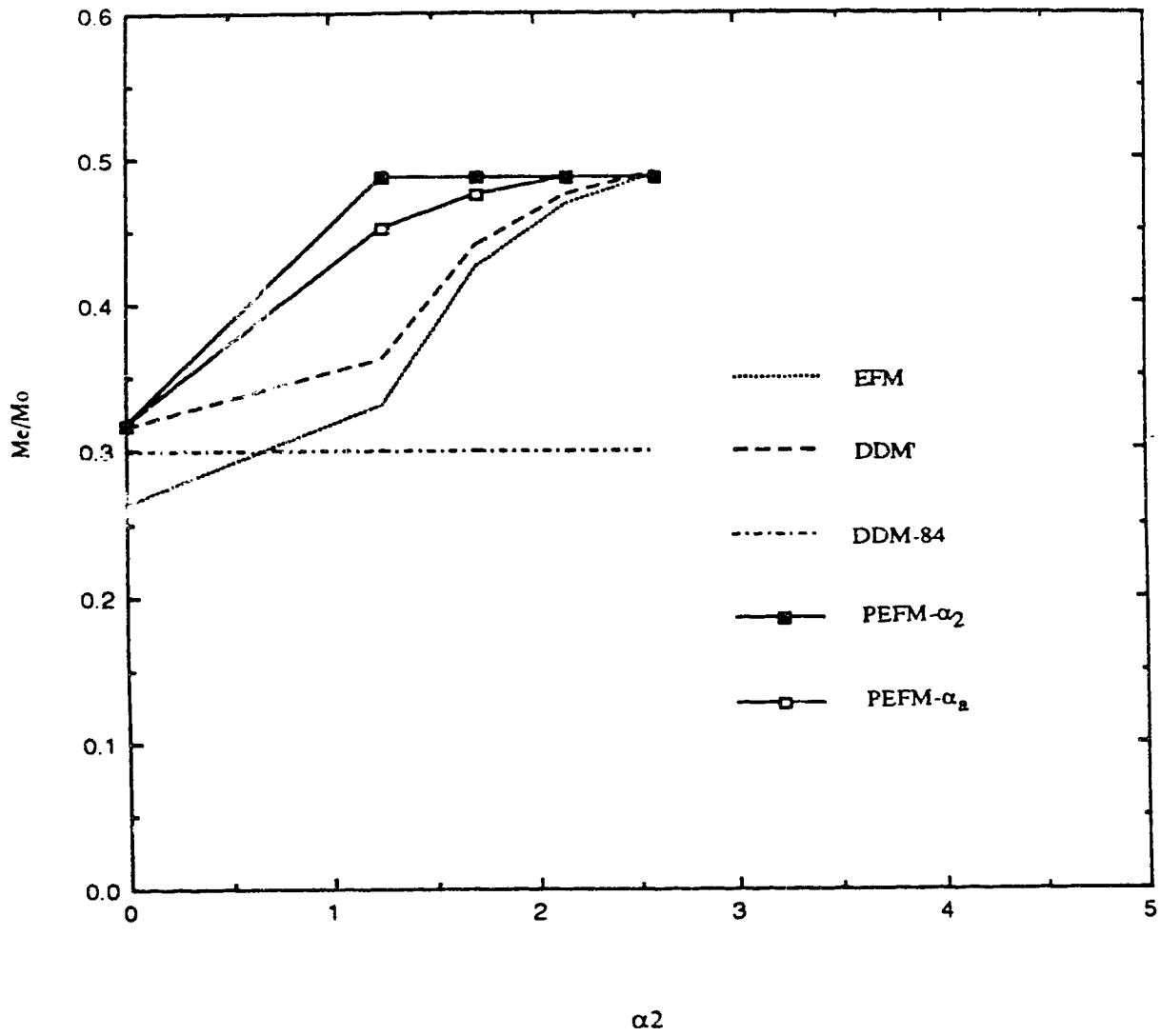
Fig 7.8: Moment ratio at Section 1 (PE series, $l_1/l_2 = 1.0$)
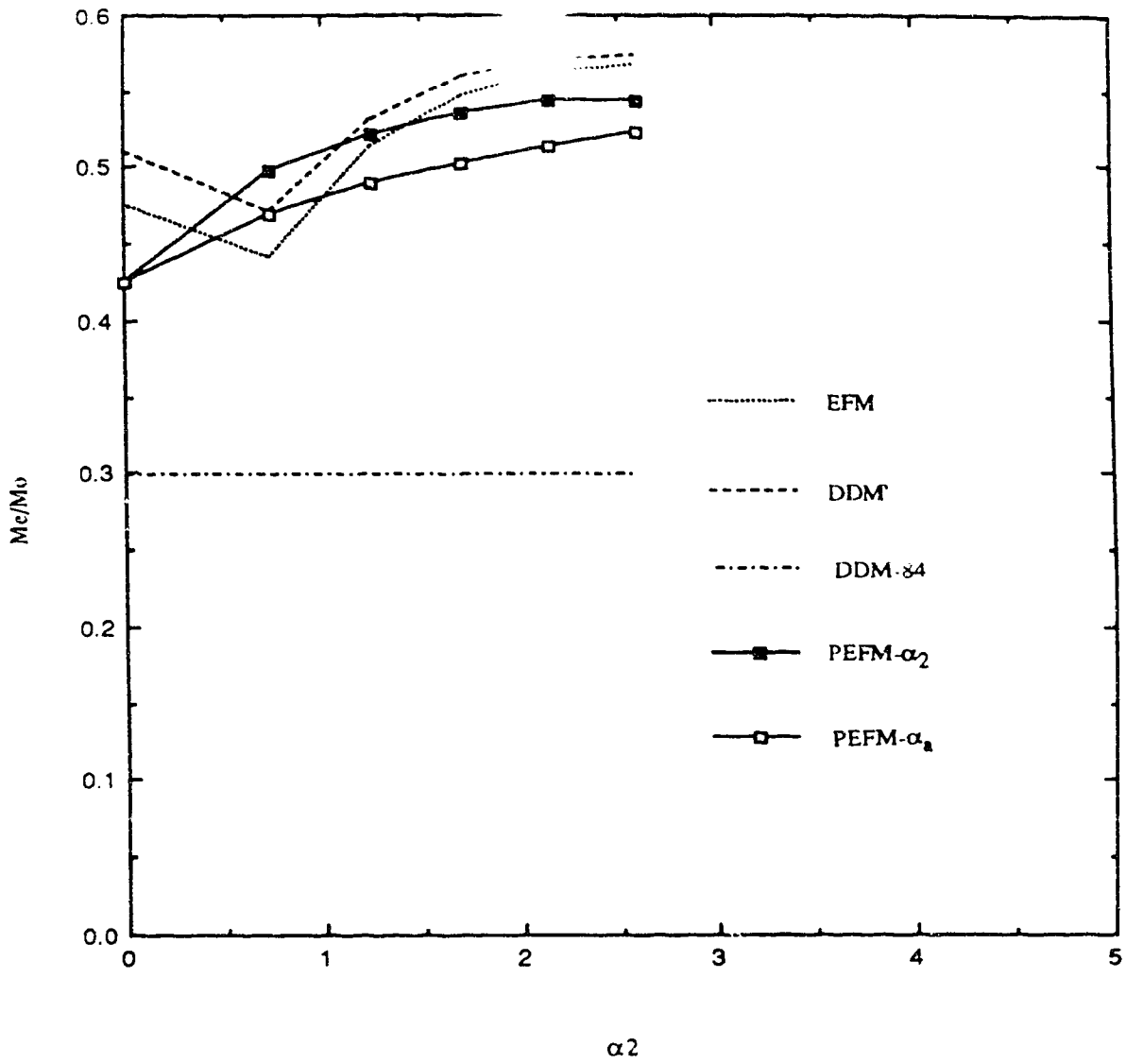
Fig 7.9: Moment ratio at Section i (PE series, $l_1/l_2 = 2.0$)

Chapter 8

Summary, Conclusions and Recommendations

8.1 Summary

Present North American codes contain two design procedures for continuous two-way column supported slab systems that use a two-dimensional frame idealization, namely the Direct Design Method (DDM) and the Equivalent Frame Method (EFM). To facilitate discussion of the DDM in this study, the term DDM' is used when referring to the version employing the stiffness ratio α_{ec} while DDM-84 is used when referring to the table of coefficients. The code design procedures give different design moments for some slab geometries. To evaluate these differences, solutions obtained using the code procedures are compared to those obtained using a non-linear finite element program, NISA80. A simplified procedure for obtaining design moments by using any standard elastic plane frame program, with prismatic members, PEFM, is proposed.

Solutions are first obtained for various panel and column aspect ratios, using DDM-84, DDM' and EFM, for slabs with and without beams. Using a program specifically written to implement the code procedures, SLAB, the effects of panel aspect ratio (l_1/l_2), column size, column aspect ratio and beam size, on design moments, are explored. Using NISA80, only on slabs without beams, the effects of panel and column aspect ratios on design moments are investigated. In addition, the effect of varying the amount of flexural reinforcement provided at the exterior support is

199

addressed. An insight into the transverse distribution of the design moments at the critical sections is obtained. Based on these comparisons, reduction factors for obtaining the effective stiffness factors in columns for use in the PEFM are proposed. These factors are functions of the panel aspect ratio (l_1/l_2) and the beam to slab stiffness ratio.

Using the proposed reduction factors for column stiffness expressions, PEFM solutions are obtained for the slabs used in the non-linear finite element study. These solutions are compared to NISA80 solutions and the code procedures DDM' and EFM. PEFM solutions are also obtained for slabs with beams (PE and PB series) as well as for slabs where the successive span lengths are the primary variables (S series). For the PB, PE and S series, comparison of solutions is made only with the code procedures.

8.2   Conclusions

The following major conclusions may be deduced from this study:

1   For design strips with and without beams, there is good agreement in design moments obtained using the code procedures, for exterior panel aspect ratios (l_1/l_2) equal to or greater than 1.0.

2   For exterior panel aspect ratios (l_1/l_2) less than 1.0, the EFM gives smaller design moments and as the panel aspect ratio approaches 0.5, the design moment ratios for slabs without beams are unreasonably low.

3   At interior supports, design moments obtained using the
     code procedures are higher than those obtained using
     NISA80 and correspond to the uncracked stage.

4   Based on the non-linear finite element analyses for
     slabs without beams, the transverse distribution of
     design moments at critical sections is a function of panel
     aspect ratio. Because this is not accounted for in the
     current code provisions, new procedures for distribution
     are proposed.

5   Limiting the transverse torsional member length to the
     lesser of the panel dimension improves solutions
     obtained using the DDM' and EFM, but not sufficiently
     for the EFM when panel aspect ratios are small.

6   Based on the non-linear finite element study, the
     influence of the amount of reinforcement provided at
     the exterior support critical section can be observed if
     the exterior column is stiff enough to allow
     development of the reinforcement provided at this
     critical section.

7   In the shorter directions of rectangular panels, the magnitudes of design moment ratios are generally controlled by the reinforcement provided to satisfy the code minimum reinforcement requirements.

8   The column stiffness reduction factors for use in the PEFM are a function of both panel aspect ratio and the beam to slab stiffness ratio.

9   The PEFM gives consistently satisfactory design moments for two-way slabs, for all panel aspect ratios and beam stiffnesses.

8.3   Recommendations for future study

Further non-linear finite element studies are required to obtain solutions for slabs with beams and for the cases when successive span lengths are varied (S series). The effect of pattern loads on the behaviour of slab systems should also be investigated.

In the absence of exhaustive laboratory test data on slab systems, non-linear finite element analysis can provide data upon which evaluations and development of code design procedures for slab systems may be based. However, this can only be done if geometric and material models used in the analyses can represent the very complex behaviour of slab systems adequately. The non-linear finite element program chosen should allow modelling all elements of the slab system as non-linear elements. Provision should be made to enable application of pattern loads on the slab.

Finally, the program should have graphic capabilities to substantially facilitate the manipulation of input and output.

With regard to NISA80, the failure criteria, especially in the tension-compression zone, should be improved to allow better representation of moment redistribution as cracking progresses. The program should be modified to allow input of different numbers of layers of concrete over the depth, for various groups of elements. Brick elements should be incorporated in the program, so that columns and beams may be modelled as non-linear elements. The number of load curves should be increased to allow more than one distributed load curve.

After the above studies have been performed, some laboratory tests should be carried out to verify the predicted behavior of slab systems.

REFERENCES

AALAMI, B. N. (1972), Moment Rotation Relation between Column and Slab, ACI Journal, May, pp. 263-269.

ADOSS (1991), Analysis and Design of Slab Systems, CPCA, Version 5.24, Ottawa.

AHMAD, S., IRONS, B. S. and ZIENKIEWICZ, O. C. (1968), Curved Thick Shell Elements and Membrane Elements with particular reference to Axisymmetric problems, Proceedings, 2nd Conference on Matrix Methods in Structural Mechanics, Wright-Patterson A. F. Base, Ohio.

ALLEN, F. H., DARVALL, P. L., GLOVER, R. E. and PECKNOLD, D. A. (1978), Discussion of Pecknold's paper, 'Slab Effective widths for Equivalent Frame Analysis', ACI Journal, October, pp. 583-586.

AMERICAN CONCRETE INSTITUTE (1983), ACI Committee 318, Building Code Requirements for Reinforced Concrete (ACI 318-83), Detroit.

AMERICAN CONCRETE INSTITUTE (1989), ACI Committee 318, Building Code Requirements for Reinforced Concrete (ACI 318-89), Detroit.

AUSRALIAN STANDARD (1988), Concrete Structures, Standards Association of Australia, AS 3600, pp. 32-37.

BALAKRISHNAM, S. and MURRAY, D. W. (1986), Finite Element Prediction of Reinforced Concrete Behaviour, Structural Engineering Report, No. 138, Department of Civil Engineering, University of Alberta, Edmonton, 487p.

BANGASH, M. Y. H. (1989), Concrete and Concrete Structures: Numerical Modelling and Applications, Elsevier Science Publishers Ltd, 668p.

BAZANT, Z. P. and OH, B. H. (1983), Crack Band Theory for Fracture of Concrete, Materials and Structures, Vol. 16, No. 93, pp. 155-177.

BAZANT, Z. P. and OH, B. H. (1984), Deformation of Progressively Cracking Reinforced Concrete Beams, ACI Journal, May-June, pp. 268-278.

BROTCHIE, J. F. (1957), General Method Analysis of Flat Slabs and Plates, ACI Journal, August, pp. 31-50.

BROTCHIE, J. F. (1959), General Elastic Analysis of Flat Slabs and Plates, ACI Journal, August, pp. 127-159.

BROTCHIE, J. F. and RUSSELL, J. J. (1964), Flat Plates Structures, ACI Journal, August, pp. 959-995.

CANADIAN PORTLAND CEMENT ASSOCIATION (1985), Concrete Design Handbook, CPCA, Ottawa.

CANO, M. T. and KLINGNER, R. E. (1988), Comparison of Analysis Procedures for Two-Way Slabs, ACI Structural Journal, November-December, pp. 597-608.

COPE, J. R. (1984), Material Modelling of Real Reinforced Concrete Slabs, Proceedings of the International Conference on Computer-Aided Analysis and Design of Concrete Structures, part I, pp. 85-117.

CORLEY, W. G. and JIRSA, J. O. (1970), Equivalent Frame Analysis for Slab Design, Code Background Paper, ACI Journal, Proceedings, Vol. 67, No. 11, November, pp. 875-884.

CORLEY, W. G. and SOZEN, M. A. and SIESS, C. P. (1961), The Equivalent Frame Analysis for Reinforced Concrete Slabs, University of Illinois Civil Engineering Studies, Structural Research Series No. 218, Urbana, Illinois, June, 166p.

DAMJANIC, F. and OWEN, D. R. J. (1984), Practical Considerations for Modelling on Post-cracking Concrete Behaviour for Finite Element Analysis of Reinforced Concrete, Proceedings of the International Conference on Computer-Aided Analysis and Design of Concrete Structures, Part I, pp. 693-706.

DARWIN, D. (1985), Crack Propagation-A study of Model Parameters, Finite Element Method of Reinforced Concrete Structures, Proceedings of seminar sponsored by the Japan Society for Promotion of Science and the U.S. National Science Foundation, May 21-24, pp. 184-203.

DARWIN, D. and PECKNOLD, A. D. (1977), Nonlinear Biaxial Stress-Strain Law for Concrete, J. Eng. Mech., EM2, April, pp. 229-241.

DARWISH, M. N., GROSSMAN, J. S., CANO, M. T. and KLINGNER, R. E. (1989), Discussion of Cano and Klingner's paper, 'Comparison of Analysis Procedures for Two-way Slabs', ACI Structural Journal, September-October, pp. 624-626.

DISTASIO and VAN BUREN (1970), Transfer of Bending Moment between Flat Plate Floor and Column, ACI Journal, Vol. 57, No. 3, September, pp. 399-314.

FERGUSON, P. M., BREEN, J. E. and JIRSA, J. O. (1988), Reinforced Concrete Fundamentals, Fifth Edition, John Wiley and Sons.

FORIBORZ BARZEGAR-JAMSHIDI and SCHNOBRICH, W. C. (1986), Nonlinear Finite Element Analysis of Reinforced Concrete under Short-term Monotonic Loading, University of Illinois, Urbana, Illinois.

FRASER, D. J. (1977), Equivalent Frame Method for Beam-Slab Structures, ACI Journal, May, pp. 223-228.

GAMBLE (1970), Discussion of Code Procedures, ACI Journal, September.

GILBERT, R. I. and WARNER, R. F. (1978), Tension Stiffening in Reinforced Concrete Slabs, J. Struct. Division, ASCE, ST12, December, pp. 1885-1899.

GROSSMAN, J. S. (1987), Column-Slab Connections-Code Procedures, History and Shortcomings, Paper presented at the ACI Fall Convention, Seattle, Washington, November, 15p.

HAND, F. R., PECKNOLD, D. A. and SCHNOBRICH, W. C. (1973), Nonlinear Layered Analysis of Reinforced Concrete Plates and Shells, J. Struct. Division, ASCE, Vol. 99, ST7, pp. 1491-1505.

HILLERBORG, A. (1985), Numerical Methods to Simulate Softening and Fracture of Concrete, Fracture Mechanics of Concrete: Structural application and numerical calculation, Ed. by SIH, C. C. and TOMASO, D. A., Klumer Academic Publishers, USA.

HU, HSUAN-TEH and SCHNOBRICH, W. C. (1986), Non-linear Analysis of Plane Stress Reinforced Concrete under Short-term Monotonic Loading, University of Illinois, Urbana, Illinois.

HU, HSUAN-TEH and SCHNOBRICH, W. C. (1990), Non-linear Analysis of Cracked Reinforced Concrete, ACI Struct. Journal, V. 87, No. 2, March-April, pp. 199-207.

JIRSA, J. O., SOZEN, M. A. and SEISS, C. P. (1969), Pattern Loadings on Reinforced Concrete Floor Slabs, Proceedings, ASCE, Vol. 95, ST6, June, pp. 1117-1137.

KLINGNER, R. E. (1990), Analysis Procedures for Two-Way Slabs, Paper presented to Middle Tennesse Chapter, ACI, February, 26p.

KUPFER, H. B. and GERSTLE, K. A. (1973), Behaviour of Concrete under Biaxial Stresses, J. Eng. Mechanics, EM4, ASCE, August, pp. 853-866.

LIN, C. S. and SCORDELIS, A. C. (1975), Nonlinear Analysis of Reinforced Concrete Shells of General Form, J. Struct. Division, ASCE, Vol. 101, No. ST3, pp. 523-538.

MacGREGOR, J. G. (1988), Reinforced Concrete Mechanics and Design, First edition, Prentice Hall, 799p.

MASSICOTTE, B., ELWI, A. E. and MacGREGOR, J. G. (1988), Analysis of Reinforced Concrete Panels Loaded Axially and Transversely, Structural Engineering Report No. 161, Department of Civil Engineering, University of Alberta, Edmonton, 254p.

MILFORD, R. V. (1984), Ph.D thesis, University of Illinois at Urbana-Champagne, Illinois.

MISIC, J. and SIMMONDS, S. H. (1970), Comparative Study of Slab-Beam Systems, M. Sc thesis, University of Alberta, Fall, 81p.

PARK, R. and GAMBLE, W. L. (1980), Reinforced Concrete Slabs, John Wiley & Sons, 618p.

RAMM, E. (1977), A plate/shell element for large deflections and rotations, in: BATHE, K. J., ODEN, J. T. and WUNDERLICH, W., eds, 1977, Formulation and computational algorithms, U.S.-Germany Symposium, M.I.T., pp. 264-293.

RAMM, E. (1980), Strategies for Tracing the Non-linear Response near Limit Points, in: WUNDERLICH, W., STEIN, E. and BATHE, K. J. , eds, Nonlinear Finite Element Analysis in Structural Mechanics, Proceeding of the Europe-U. S. Workshop, Ruhr Universitat, Bochum, West Germany, pp. 63-89.

RAPHAEL, J. M. (1984), Tensile Strength of Concrete, ACI Journal, March-April, pp. 158-165.

RAZAGPUR, A. G. and GHALI, A. (1981), Shear Lag Analysis in Reinforced Concrete, IABSE Colloquim on Advanced Mechanics of Reinforced Concrete, Final Report, delft, June, pp. 671-686.

ROTS, J. G., KUSTERS, G. M. A. and BLAAUWENDRAAD, J. (1984), The need for Fracture Mechanics Options in Finite Element Models for Concrete Structures, Proceedings of the International Conference on Computer-Aided Analysis and Design of Concrete Structures, Part I, pp. 19-32.

SHARAN, S. K., CLYDE, D. and TURCKE, D. (1978), Equivalent Frame Analysis Improvement for Slab Design, ACI Journal, February, pp. 55-59.

SIMMONDS, S. H. (1962), Effects of Column Stiffness on Moments in Two-Way Floor Systems, University of Illinois Civil Engineering Studies, Structural Research Series, No. 235, July.

VANDERBILT, M. D. (1979), Equivalent Frame Analysis for Lateral Loads, Journal of the Structural Division, ASCE, ST 10, October, pp. 1981-1997.

VANDERBILT, M. D. and CORLEY, W. G.(1983), Frame Analysis of Concrete Buildings, Concrete International, December, pp. 33-43.

WAHEED, A. (1971), Design Moments by Equivalent Frame Method, M.Eng Report, University of Alberta, Edmonton, 21p.

WANG, C. K. (1983), Intermediate Structural Analysis, McGraw-Hill Book Company, 790p.

WANG, CHIA-KIA. C. and SALMON, C. G. (1979), Reinforced Concrete Design, Third edition, Harper and Row Publishers, 917p.

WONG, Y. C. and COULL, A. (1980), Effective Slab Stiffness in Flat Plate Structures, Proceedings of the Institution of Civil Engineers, Part 2, 69, September, pp. 721-735.

Appendix A

Program SLAB

A.1 Introduction

This program performs the analysis of two-way slab systems using the Direct Design Method (DDM) and Equivalent Frame Method (EFM) as defined in the North American codes, ACI-318-89 and CAN/CSA A23.3-M84, for slabs subjected to gravity loads. The program was written in Fortran 77 to facilitate comparison of solutions obtained for different geometries.

A.2 Input

The first line of the input file is a heading that can be used to describe the design strip being analyzed. This is followed by the designation of the design building code to be used, the system of units and the form of output desired. The geometry of the design strip is then entered and consists of the number and lengths of spans, indication of presence or absence of beams, the position of the design strip (interior or exterior) and the width of the design strip. This width is specified by inputting widths to the left and right of the centreline of the design strip. In addition, storey heights (above and below the slab), cantilever span lengths in both longitudinal and transverse directions and slab thickness are required.

At each column position, column dimensions (above and below the slab), capital, drop panel and beam dimensions, if any,

210

are required. Because moment-shear transfer analysis is carried out for slabs without beams, the amount of cover to reinforcement is also required.

For loading, the program allows only uniformly distributed gravity loading. Both dead and live loads have to be input. Wall loading may be input as an equivalent concentrated load acting at a certain eccentricity from the centreline of the exterior column. Factored loads are computed based on the load factors associated with the design code chosen.

A.3   Output

For output, two options are available. The normal output gives the name of the design strip, echo's all the data input and gives design moments at all critical sections for each of the design procedures (DDM-84, DDM' and EFM). The maximum shear stress resulting from moment-shear transfer is also output at each column that does not have beams framing into it.

The second output option, used to verify manual calculations, consists of the above plus intermediate design parameters such as flexural stiffnesses, torsional stiffnesses and fixed end actions, required to perform the DDM and EFM.

Appendix B

Evaluation of model parameters

B.1 Evaluation of E_1 and E_2 using Massicotte's procedure

The equations for cracking energy, G_f and cracking energy density, W_f were simplified as follows:

$$G_f = K\,w_c \frac{f'^{\,2}_t}{E_c} \qquad\qquad (B.1)$$

or

$$G_f = K\,w_c\,f'_t\,\varepsilon_{cr} \qquad\qquad (B.2)$$

and

$$W_f = \frac{G_f}{w_c} = K\,f'_t\,\varepsilon_{cr} \qquad\qquad (B.3)$$

where K = A constant based on experimental studies

f'_t = Tensile strength of concrete

ε_{cr} = Strain at cracking

Massicotte obtained an average value for K equal to 5.0 and

$$W_f = K\,f'_t\,\varepsilon_{cr} \qquad\qquad (B.4)$$
$$= 5.0\,f'_t\,\varepsilon_{cr}$$
$$= (10.0/2)f'_t\,\varepsilon_{cr}$$

Because the energy density in the ascending branch of the tension stiffening curve, W_{f1}, is the area $(1/2)f'_t\,\varepsilon_{cr}$, it represents

one-tenth the total energy under the curve.

For f'_c of 25 Mpa the ratio E_c/E_1 is 4.96. E_2 can be evaluated from the energy density expression. The energy density, W_{f2}, is the area under the first descending slope, given by:

$$W_{f2} = (f'_t + 0.33f'_t) (\varepsilon_\mu - \varepsilon_{cr})/2 = (1.33/2)f'_t (\varepsilon_\mu - \varepsilon_{cr}) \qquad (B.5)$$

where ε_μ = Strain at end of first slope

Knowing the ratio E_c/E_1, the change in strain under the first descending slope is found to be $3.32(\varepsilon_\mu - \varepsilon_{cr})$. The corresponding area is calculated as:

$$W_{f2} = (1.33/2) f'_t (3.32 \varepsilon_{cr}) = (4.42/2) f'_t \varepsilon_{cr} \qquad (B.6)$$

The energy density under the second branch, W_{f3} is the difference between the total area and the sum of the two areas, as follows:

$$W_{f3} = W_f - (W_{f1} + W_{f2}) = (4.58/2) f'_t \varepsilon_{cr} \qquad (B.7)$$

but also

$$W_{f3} = (\mu f'_t/2) (\varepsilon_{max} - \varepsilon_\mu) \qquad (B.8)$$
$$= (0.33 f'_t/2) (\varepsilon_{max} - \varepsilon_\mu)$$

Equating B.7 to B.8, $(\varepsilon_{max} - \varepsilon_\mu)$ is found to be $13.88\varepsilon_{cr}$ and the second descending slope, E_2 is evaluated from:

$$E_2 = -(\mu \ f'_t)/(\epsilon_{max} - \epsilon_\mu) = -(0.33 \ f'_t)/13.88(\epsilon_{max} - \epsilon_\mu)$$
$$= -E_c/42.06$$

Therefore, the slopes E_1 and E_2 may be taken as $E_1 = -E_c/5.0$ and $-E_c/42.0$, respectively. Knowing these slopes, the tensile strength of concrete, f'_t and assuming a cracking zone width, w_c ($2d_a$ to $3d_a$, where d_a is the maximum size of aggregate), the cracking energy, G_f may be calculated.

Appendix C

Summing of moments at critical sections

C.1   Summing of moments using D3SUMM

Moments output from the program are at positions of gauss points and not at the critical sections. Therefore, interpolation or extrapolation is required to obtain moments at critical sections.

The procedure involves specifying which elements border the required critical section(s) in the X or Y direction. The routine makes use of gauss moments and their corresponding influence widths. Because there are no gauss points at element intersections, the following procedure is used to obtain the sum of moments at required sections:

C.2   Exterior span positive moment critical section

For cases where gauss moments bordering the section are similar in nature, such as at midspans, gauss moments are interpolated to obtain intensities at the required section. The interpolated intensities are then multiplied by the corresponding influence widths and summed, to obtain the total moment across the whole section.

C.3   Negative and interior span positive moment critical sections

For sections bordering both stiffened and unstiffened regions, the gauss moments from the stiffened portion are unrealistic, therefore, the procedure outlined in C.2 is not

appropriate. Also, where there is only one row of gauss points, such as at sections located at the edge, the procedure in C.2 can not work. For these cases, gauss moments in the unstiffened part, closest to the required sections, below or above the section, are made use of to obtain the sum of moments at the position of gauss points. The moments at the required sections are then obtained by extrapolation.

The basic assumption is that the bending moment diagram is a parabolic curve which requires a minimum of three moment values and their corresponding locations. Knowing these quantities and their locations, it is then possible to solve for the unknown constants to define the parabola which is of the form:

$$y = a_1 + a_2 x + a_3 x^2$$

(C.1)

For each span, if the moments at the three sections and the corresponding distances from the face of the left support are known, the unsymmetric system of equations may be written as follows:

$$\begin{bmatrix} 1 & x_1 & x_1^2 \\ 1 & x_2 & x_2^2 \\ 1 & x_3 & x_3^2 \end{bmatrix} \begin{Bmatrix} a_1 \\ a_2 \\ a_3 \end{Bmatrix} = \begin{Bmatrix} M_1 \\ M_2 \\ M_3 \end{Bmatrix}$$

(C.2)

where x_1, x_2 and x_3 = positions of gauss points from face of
column under consideration

M_1, M_2 and M_3 = corresponding moments

Solving the above system of equations gives the values of the constants for each load level. Using these constants, it is then possible to evaluate the extrapolated or interpolated moment at any section. Since x is measured from the face of the left column, the constant 'a$_1$' is equal to the moment at the face of that column.

Because of the large number of load levels, a simple program was written to evaluate the constants and obtain the extrapolated or interpolated moments at the critical sections. The corresponding ratios of the total static moments at the critical sections were also evaluated.

Appendix D

Column-slab stiffness ratio

D.1 Column-slab stiffness ratio, α_{cs}

Because the modelling of columns assumed in NISA80 solutions is different from that used in codes, corresponding column-slab stiffness ratios for analysis of design strips by the code were obtained by adjusting the column Young's modulus. This means that, the column-slab stiffness ratios used in NISA80 analyses correspond to 1.5 times the values obtained using code procedures. Gross dimensions were used in obtaining the other properties.

The column-slab stiffness ratio, α_{cs} for use in NISA80 analyses was obtained using the following relationships:

$$\alpha_{cs} = \frac{\Sigma \, \text{Column Stiffness}}{\text{Slab stiffness}} \qquad (D.1)$$

$$\text{Column Stiffness} = 2 \, \frac{3E_{col}}{l'_{col}} \left(\frac{c_2 c_1^3}{12} \right) \qquad (D.2)$$

where E_{col} = Column Young's modulus

l'_{col} = Length of column from slab center-line to the point of inflection

c_1, c_2 = Column dimensions

$$\text{Slab Stiffness} = 4 \frac{E_{slb}}{l_1} \left(\frac{l_2 h^3}{12} \right) \qquad \text{(D.3)}$$

where E_{slb} = Slab Young's modulus

    h   = Slab thickness

    l_1 = Center to center span length of design strip

    l_2 = Width of design strip

$$\alpha_{cs} = 1.5 \left(\frac{E_{col}}{E_{slb}} \right) \left(\frac{l_1}{l_2} \right) \left(\frac{c_2 c_1^3}{l'_{col} h^3} \right) \qquad \text{(D.4)}$$

Specific stiffness ratios in the analyses were obtained by adjusting the ratio of the column Young's modulus relative to the slab Young's modulus, as the column stub lengths were kept constant.

Appendix E

Reinforcement representation

D.1 Reinforcement

Reinforcement is input as thicknesses at given depths over the slab depth. Actual positions of the reinforcement are given in Table E.1. Reinforcement densities for square and rectangular panels are given in Tables E.2 and E.3.

Table E.1: Reinforcement positions over the depth of the slab

Reinforcement direction and position	Depth from top of slab (mm)
X axis-Top	30.6
X axis-Bottom	158.1
Y axis-Top	41.9
Y axis-Bottom	169.4

X axis: Along the design strip
Y axis: Perpendicular to the design strip axis

Table E.2a: Top reinforcement densities for square panels

Design Strip / Reinforcement	REINFORCEMENT THICKNESS (mm^2/mm)									
	1	2	3	4	5	6	7	8	9	10
N10B6.2	0.000	0.203	0.725	0.315	0.989	0.989	0.989	0.989	0.314	0.989
N10B6.4	0.000	0.405	1.535	0.315	0.989	0.989	0.989	0.989	0.314	0.989
N10B12.2	0.000	0.203	0.725	0.315	0.989	0.989	0.989	0.989	0.314	0.989
N10B12.4	0.000	0.405	1.535	0.315	0.989	0.989	0.989	0.989	0.314	0.989
N10I12.2	0.000	0.253	0.490	0.315	0.989	0.989	0.989	0.989	0.314	0.989
N10I12.4	0.000	0.517	1.107	0.315	0.989	0.989	0.989	0.989	0.314	0.989
N10I24.2	0.000	0.253	0.490	0.315	0.989	0.989	0.989	0.989	0.314	0.989
N10I24.4	0.000	0.517	1.107	0.315	0.989	0.989	0.989	0.989	0.314	0.989
N10L6.2	0.000	0.200	0.725	0.315	0.989	0.989	0.989	0.989	0.314	0.989
N10L6.4	0.000	0.405	1.535	0.315	0.989	0.989	0.989	0.989	0.314	0.989
N10L12.2	0.000	0.200	0.725	0.315	0.989	0.989	0.989	0.989	0.314	0.989
N10L48.2	0.000	0.227	0.571	0.290	0.909	0.909	0.989	0.989	0.314	0.989
N10L48.4	0.000	0.454	1.141	0.290	0.909	0.909	0.989	0.989	0.314	0.989

Table E.2b: Bottom reinforcement densities for square panels

Design Strip Reinforcement	REINFORCEMENT THICKNESS (mm²/mm)											
	11	12	13	14	15	16	17	18	19	20	21	22
N10B6.2	0.428	0.653	0.428	0.653	0.400	0.408	0.400	0.408	0.400	0.400	0.400	0.400
N10B6.4	0.400	0.529	0.400	0.529	0.400	0.408	0.400	0.408	0.400	0.400	0.400	0.400
N10B12.2	0.428	0.653	0.428	0.653	0.400	0.408	0.400	0.408	0.400	0.400	0.400	0.400
N10B12.4	0.400	0.529	0.400	0.529	0.400	0.408	0.400	0.408	0.400	0.400	0.400	0.400
N10I12.2	0.428	0.653	0.428	0.653	0.400	0.408	0.400	0.408	0.400	0.400	0.400	0.400
N10I12.4	0.400	0.529	0.400	0.529	0.400	0.408	0.400	0.408	0.400	0.400	0.400	0.400
N10I24.2	0.428	0.653	0.428	0.653	0.400	0.408	0.400	0.408	0.400	0.400	0.400	0.400
N10I24.4	0.400	0.529	0.400	0.529	0.400	0.408	0.400	0.408	0.400	0.400	0.400	0.400
N10L6.2	0.428	0.653	0.428	0.653	0.400	0.408	0.400	0.408	0.400	0.400	0.400	0.400
N10L6.4	0.428	0.653	0.428	0.653	0.400	0.408	0.400	0.408	0.400	0.400	0.400	0.400
N10L12.2	0.428	0.653	0.428	0.653	0.400	0.408	0.400	0.408	0.400	0.400	0.400	0.400
N10L48.2	0.400	0.400	0.400	0.488	0.269	0.408	0.400	0.408	0.400	0.400	0.400	0.400
N10L48.4	0.400	0.400	0.400	0.488	0.269	0.408	0.400	0.408	0.400	0.400	0.400	0.400

Table E.3a: Top reinforcement densities for rectangular panels

Design Strip / Reinforcement	REINFORCEMENT THICKNESS (mm²/mm)									
	1	2	3	4	5	6	7	8	9	10
N5C1.2	0.000	0.046	0.185	0.073	0.220	0.220	1.039	1.039	0.329	1.039
N5C1.4	0.000	0.092	0.375	.073	0.220	0.220	1.039	1.039	0.329	1.039
N5A2.3	0.000	0.067	0.224	0.073	0.220	0.220	0.924	0.924	0.329	1.039
N5B3.2	0.000	0.042	0.150	0.066	0.200	0.200	1.071	1.071	0.339	1.071
N5B3.4	0.000	0.084	0.300	0.066	0.200	0.200	1.071	1.071	0.339	1.071
N5D6.3	0.000	0.070	0.223	0.065	0.196	0.196	1.039	1.039	0.329	1.039
N7C1.2	0.000	0.111	0.456	0.177	0.545	0.545	1.039	1.039	0.329	1.039
N7C1.4	0.000	0.223	0.943	0.177	0.545	0.545	1.039	1.039	0.329	1.039
N7A2.3	0.000	0.164	0.554	0.177	0.545	0.545	0.924	0.924	0.329	1.039
N7B6.2	0.000	0.106	0.378	0.166	0.511	0.511	0.989	0.989	0.314	0.989
N7B6.4	0.000	0.223	0.756	0.166	0.511	0.511	0.989	0.989	0.314	0.727
N7D9.3	0.000	0.178	0.577	0.165	0.505	0.505	1.039	1.039	0.329	1.039
N13B9.2	0.000	0.236	0.537	0.315	0.989	0.989	0.688	0.688	0.222	0.688
N13B9.4	0.000	0.480	1.117	0.315	0.989	0.989	0.688	0.688	0.222	0.688
N20B12.2	0.000	0.373	0.353	0.315	0.989	0.989	0.199	0.199	0.066	0.199
N20B12.4	0.000	0.767	0.725	0.315	0.989	0.989	0.199	0.199	0.066	0.199

Table E.3b: Bottom reinforcement densities for rectangular panels

Design Strip Reinforcement	REINFORCEMENT THICKNESS (mm^2/mm)											
	11	12	13	14	15	16	17	18	19	20	21	22
N5C1.2	0.400	0.400	0.400	0.400	0.400	0.400	0.400	0.400	0.428	0.400	0.428	0.400
N5C1.4	0.400	0.400	0.400	0.400	0.400	0.400	0.400	0.400	0.428	0.400	0.428	0.400
N5A2.3	0.400	0.400	0.400	0.400	0.400	0.400	0.400	0.400	0.400	0.400	0.400	0.400
N5B3.2	0.400	0.400	0.400	0.400	0.400	0.400	0.400	0.400	0.400	0.400	0.400	0.400
N5B3.4	0.400	0.400	0.400	0.400	0.400	0.400	0.400	0.400	0.400	0.400	0.400	0.400
N5D6.3	0.400	0.400	0.400	0.400	0.400	0.400	0.400	0.400	0.428	0.400	0.428	0.400
N7C1.2	0.400	0.400	0.400	0.400	0.400	0.400	0.400	0.400	0.428	0.400	0.428	0.400
N7C1.4	0.400	0.400	0.400	0.400	0.400	0.400	0.400	0.400	0.428	0.400	0.428	0.400
N7A2.3	0.400	0.400	0.400	0.400	0.400	0.400	0.400	0.400	0.400	0.400	0.400	0.400
N7B6.2	0.400	0.400	0.400	0.400	0.400	0.400	0.400	0.400	0.408	0.400	0.408	0.400
N7B6.4	0.400	0.400	0.400	0.400	0.400	0.400	0.400	0.400	0.408	0.400	0.408	0.400
N7D9.3	0.400	0.400	0.400	0.400	0.400	0.400	0.400	0.400	0.428	0.400	0.428	0.400
N13B9.2	0.400	0.400	0.400	0.605	0.400	0.400	0.400	0.400	0.400	0.400	0.400	0.400
N13B9.4	0.400	0.400	0.400	0.489	0.400	0.400	0.400	0.400	0.400	0.400	0.400	0.400
N20B12.2	0.400	0.400	0.400	0.605	0.400	0.400	0.400	0.400	0.400	0.400	0.400	0.400
N20B12.4	0.400	0.400	0.400	0.491	0.400	0.400	0.400	0.400	0.400	0.400	0.400	0.400